Intra-tumoural regulatory T cells:

a potential new target for anti-cancer immunotherapy

Demelza Jane Ireland B.Sc. (Hons.)

This thesis is presented for the degree of Doctor of Philosophy of

The University of Western Australia
School of Biomedical, Biomolecular and Chemical Sciences
Discipline of Microbiology and Immunology

2006

THE UNIVERSITY OF
WESTERN AUSTRALIA

Declaration for theses containing published work and/or work prepared for publication

3

This thesis contains **published work and/or work prepared for publication, some of which has been co-authored**. The bibliographic details of the works and where they appear in the thesis are set out below. (The candidate must attach to this declaration a statement detailing the percentage contribution of each author to the work. This must been signed by all authors. Where this is not possible, the statement detailing the percentage contribution of authors should be signed by the candidate's Coordinating Supervisor).

Publications associated with this thesis

1. **Needham DJ, Lee JX and Beilharz MW.** 2006. Intra-tumoural regulatory T cells: a potential new target for anti-cancer immunotherapy. *Biochemical and Biophysical Research Communications* 343(3):684-691.
    a. DJ Needham designed experiments, conducted 70% of the experimental work and wrote the paper
    Signature _____ Date _____
    b. JX Lee conducted 30% of the experimental work
    Signature _____ Date _____
    c. MW Beilharz co-ordinated experimental design and revision of the paper prior to submission
    Signature _____ Date _____

2. **Ireland DJ*, Kissick HT* and Beilharz MW.** 2006. Alpha-tocopheryl succinate: toxicity and lack of anti-tumour activity in immuno-competent mice. *Food and Chemical Toxicology* (under review). *Authors contributed equally to this work.
    a. DJ Ireland designed experiments, supervised HT Kissick, assisted in the experimental work (20%) and wrote the paper
    Signature _____ Date _____
    b. HT Kissick conducted 80% of the experimental work
    Signature _____ Date _____
    c. MW Beilharz co-ordinated experimental design and revision of the paper prior to submission
    Signature _____ Date _____

3. **Ireland DJ*, Kissick HT* and Beilharz MW.** 2006. Intra-tumoural T_{reg} cells act via TGF-β secretion to inhibit anti-tumour immune responses in murine mesothelioma. (in preparation). *Authors contributed equally to this work.
    a. DJ Ireland designed and conducted 40% of the experiments and wrote the first draft of the paper
    Signature _____ Date _____
    b. HT Kissick designed and conducted 60% of the experiments and provided critical review of the paper
    Signature _____ Date _____
    c. MW Beilharz co-ordinated experimental design and revision of the paper prior to submission
    Signature _____ Date _____

Declaration and Signatures

This thesis was submitted as the requirement for the degree of Doctor of Philosophy (Microbiology and Immunology) at The University of Western Australia and has not been submitted elsewhere as part of another degree.

All work presented in this thesis was performed by myself, unless stated otherwise

Candidate

_____

Demelza J Ireland

Supervisor

_____

Dr Manfred W Beilharz

Secondary supervisor

_____

Dr Leanne M Sammels

Table of Contents

Acknowledgements

I would like to thank my principal supervisor Dr Manfred Beilharz for his guidance, support and encouragement throughout this PhD candidature. I would also like to thank him for other learning opportunities such as grant writing, animal ethics applications, teaching and supervision roles that he has entrusted me with. Thanks also to my secondary supervisor Dr Leanne Sammels for critical review of this thesis during the writing stage.

I would like to thank colleagues of the Beilharz laboratory particularly Dr Erika Bosio, Dr Andrea Paun, Mrs Kathryn Shaw, Mr Clayton Fragall, Mrs Tracey Lee-Pullen, Miss Alayne Bennett and Mr Andrew Lim for technical advice and discussions. Thanks also to several Honours students who have worked on this project particularly Mr Desmond Yang for help with experiments conducted as part of Chapter 3, Miss Andrea Lee for help with experiment conducted as part of Chapters 4 and 5 and Mr Haydn Kissick for help with experiments conducted as part of Chapters 5, 6 and 7.

Thanks to several collaborators and their respective research groups. Prof. Bruce Robinson (UWA) for discussions and reagents relating to the murine model of mesothelioma and human mesothelioma sections, Dr Phil Stumbles (UWA) for collaborating on the Vb pilot study, Dr Cheryl Johansen (UWA) for the anti-ross river virus mAb, Assoc. Prof. Jiri Neuzil (Griffith University) for discussions and reagents relating to alpha-tocopheryl succinate, Dr Christine Carson (UWA) for discussion and reagents relating to terpinen-4-ol and Dr Deon Ventnor (Mater Medical Research Institute) for conducting the gene-chip microarray analysis.

Thanks to essential research support services and staff such as Ms Simone Ross and Miss Helen Moulder of the UWA L and M block animal houses, Mrs Kathryn Heel-Miller of BIAF, Miss Melissa Andrade of UWA Microbiology and Immunology teaching, general staff members Mr John Devlin, Mrs Gillian Walters and Mrs Glynis Rowland and the post-graduate co-ordinator Assoc. Prof. Barbara Chang..

Thanks to funding bodies that have supported me personally and the research in general. I am thankful for an Australian Postgraduate Award and a University of Western Australia Completion Scholarship. The Cancer Council of WA and Genetic Technologies Ltd have financially supported the cancer research of the Beilharz Laboratory.

Thanks finally to my family and friends, particularly my very supportive husband, Greg and our growing baby who spared me morning sickness during the writing and submission of this thesis.

Abstract

Previous studies in the field of tumour immunology had identified regulatory T (T_{reg}) cells as important suppressors of the anti-tumour immune response as the presence of T_{reg} cells in the peripheral blood of cancer patients was correlated with worse disease outcomes. Other studies had identified T_{reg} cells to be active at sites of immune regulation such as the gut of colitis patients. It was therefore hypothesised that T_{reg} cells would be present and active within tumours to suppress the cellular anti-tumour immune response. Malignant mesothelioma (MM), the slowly developing, asbestos induced pleural cavity cancer is a growing world-wide problem and at the present there is no effective treatment. The need to develop new approaches to MM therapy raised the central issues of this PhD project: (1) to investigate the involvement of T_{reg} cells in the tumourigenesis of MM in a characterised murine model and (2) to develop an effective strategy based on the manipulation of T_{reg} cells as an anti-cancer therapy.

It was found using the murine model of mesothelioma that T_{reg} cells were involved in the development of solid tumours. This discovery was based on specifically timed treatments with Vinblastine (Vb) coinciding with T_{reg} cell expansion resulting in tumour growth inhibition. Although timed Vb treatment resulted in significant tumour growth inhibition in the murine mesothelioma studies of this thesis, timed Vb treatments are not clinically relevant as people do not receive a tumour cell inoculum at a known time-point. Focus then turned to exploring the involvement of T_{reg} cells within established sub-cutaneous 9 mm^2 solid murine mesothelioma tumours themselves. It was clearly shown that T_{reg} cells are present within small but established tumours and that as tumours grow the intra-tumoural percentage of T_{reg} cells also increases. It followed therefore that if T_{reg} cells were present and active within tumours that T_{reg} cell manipulating therapies should be targeted specifically to the tumour. A novel therapy for solid tumours was developed involving the intra-tumoural administration of an anti-CD25 mAb (CD25 is a marker of T_{reg} cells) which resulted in significant tumour growth inhibition. Further characterisation of the intra-tumoural T_{reg} cells in the murine model of mesothelioma was conducted and revealed transforming growth factor-β (TGF-β) as an important cytokine for mediating T_{reg} cell function. A second therapy was therefore developed involving the intra-tumoural administration of a TGF-β soluble

receptor to block T_{reg} cell function. These intra-tumoural therapies are clinically relevant as they avoid (i) the systemic side-effect of general T_{reg} cell depletion leading to autoimmunity and (ii) the systemic immune dysfunction which would result from a systemic TGF-β depletion. The T_{reg} cell inactivating therapies investigated in this thesis did result in tumour growth inhibition but not complete tumour regression. To improve treatment efficacy, a combination of intra-tumourally administered anti-CD25, anti-CTLA-4 and anti-GITR mAbs was trialled. This treatment targeting multiple pathways of T_{reg} cell mediated immuno-suppression and resulted in tumour regression in 50% of treated animals.

Finally, the anti-tumour immune response is complex and a potentially synergistic multi-modality treatment designed to inactivate intra-tumoural T_{reg} cells but to also induce apoptosis in tumour cells themselves was investigated. Alpha-tocopheryl succinate (α-TOS), an analogue of vitamin E, had previously been shown to induce apoptosis in human MM xenografts implanted into immuno-deficient (nude) mice. Administration of α-TOS was therefore examined as a potentially synergistic treatment to be coupled with T_{reg} cell inactivation. At the previously published doses used to treat immuno-deficient mice, α-TOS was found to be toxic to the immuno-competent mice used in this study. A marked depleting effect on total T cells was seen in the treated animals.

The results of this thesis demonstrated the high potential for an adjunct immunotherapy of MM. They did however also highlight the importance of future studies into anti-cancer therapies to be conducted using clinically relevant tumour models and clinically relevant treatment regimes. The need to consider synergistic multi-modal therapies was also emphasised.

List of Figures

List of Tables

List of Equations

List of Abbreviations

Abbreviation	Definition
2-ME	2-mercaptoethanol
A	absorbance
AIDS	acquired immunodeficiency syndrome
APC	antigen presenting cell
APC-conjugated	allophycocyanin-conjugated
α-TOS	alpha-tocopheryl succinate
BSA	bovine serum albumin
CCR2	chemokine (C-C motif) receptor 2
CpG-ODN	cytosine-phosphorothiote-guanine-rich oligodeoxynucleotides
CRP	C-reactive protein
CTL	cytotoxic T lymphocyte
CTLA	cytotoxic T lymphocyte associated antigen
DC	dendritic cell
ddH_2O	distilled, deionised water
DMEM	Dulbeccos's modified eagle meadium
DMSO	dimethyl sulphoxide
EAE	Experimental autoimmune encephalomyelitis
EDTA	ethylenediaminetetraacetic acid
FACS	fluorescent activated cell sorting
FCS	foetal calf serum
FGFR	Fibroblast growth factor receptor
Fgl2	Fibrinogen like protein 2
FITC	fluorescein isothiocyanate
G	gauge
(x) g	gravity
GITR	glucocorticoid induced tumour necrosis factor receptor
GrzB	Granzyme B
HA	hyaluronan
HCV	hepatitis C virus
HIV	human immunodeficiency virus
HPRT	hypoxanthine -phosphoribosyl transferase

Abbreviation	Definition
HRP	horseradish peroxidase
IDO	indoleamine 2,3-dioxygenase
i.p.	intraperitoneal
i.t.	intra-tumoural
i.v.	intravenous
IFN	interferon
Ig	immunoglobulin
IL	interleukin
LAK	lymphocyte activated killer cell
Lck	lymphocyte protein tyrosine kinase
LN	lymph node
mAb	monoclonal antibody
MAIDS	murine acquired immunodeficiency syndrome
MHC	major histocompatibility complex
MOBS	mouse osmolarity buffered saline
MM	malignant mesothelioma
NF-κB	nuclear factor-kappa B
NK	natural killer cell
Nrp-1	neuropilin-1
OD	optical density
OVA	ovalbumin
PD-1	programmed cell death-1
p.i.	post infection
PBS	phosphate buffered saline
PCR	polymerase chain reaction
PE	phycoerythrin
ROS	reactive oxygen species
rpm	revolutions per minute
RRV	ross river virus
RT	reverse transcriptase
SAA	serum amyloid A
s.c.	subcutaneous

Abbreviation	Definition
SEM	standard error of the mean
SPF	specified pathogen free
STAT	signal transducer and activator of transcription
SV40	Simian virus 40
T	treatment time-point
TAA	tumour associated antigen
TCR	T cell receptor
TGF	transforming growth factor
TIL	tumour infiltrating lymphocyte
TMB	tetramethylbenzidine
TNF	tumour necrosis factor
Tol	tolerogenic
TRAIL	tumour necrosis factor-related apoptosis-inducing ligand
T_{reg} cell	regulatory T cell
U	unit
Vb	vinblastine
VitE	vitamin E

Chapter 1:
Literature Review

1.1 Introduction: malignant mesothelioma and its murine model

The mesothelium is a single layer of cells that covers the entire surface of the pleura aiding in the smooth movement of the lungs during respiration (1). Malignant mesothelioma (MM) is a relatively rare cancer of the pleura but also less commonly of the peritoneum, tunica vaginalis and pericardium (2-4). Typically, a patient presents with symptoms of pleural effusion and chest wall pain. The final diagnosis of MM is however complicated due to a difficulty in distinguishing MM from adenocarcinoma (5). The recent discovery of a serum marker, mesothelin, for MM may improve diagnosis in the future (6). Unfortunately, even after making improvements in the diagnosis of MM, MM remains a universally fatal cancer with median survival from presentation being only 9-12 months (reviewed in (5)).

Despite MM being a relatively rare cancer, its incidence is increasing steadily and not expected to peak world wide until approximately 2020 (7). The Comparative Risk Assessment project of the World Health Organization assessed worldwide mortality and morbidity in the year 2000 resulting from exposures to selected occupational hazards. In 2000, the specific occupational risk factor, namely asbestos in the case of mesothelioma was found to be responsible worldwide for almost 100% of mesothelioma cases (8). The correlation between asbestos exposure and the incidence of asbestos disease, particularly MM, is clear. By the late 1990s, governments in many developed countries, including Australia, banned or seriously restricted the use of asbestos. Unfortunately, as a result, it has been reported that global asbestos producers have engaged in selling asbestos to developing countries including countries of Asia and Latin America (9). In most of these countries, it has been found that there is little control on asbestos exposures from occupational, environmental and domestic sources. It is likely that the high incidence of MM currently seen in the US, UK and Australia will be reproduced in the developing world in the near future.

In a recent Lancet review of MM by a leading MM research group in Western Australia (a collaborative laboratory for parts of this thesis), the management and treatment options for MM were discussed (5). Diagnostic surgery, palliative surgery and potentially curative surgery options exist for MM. Essentially the authors recommended the combination of surgery with adjunct therapies to remove residual

disease. At present chemotherapy can be used successfully for palliation but not cure. Chemotherapy treatments often not only reduce the tumour burden but can also reduce the debilitating symptoms of this cancer. Pemetrexed, cisplatin and gemcitabine are the current gold standards for chemotherapy. Overall the results of radiotherapy for MM have been reported to be disappointing except for radiotherapy as an adjunct to surgery. Novel therapies, such as immunotherapy and gene therapy, have received much research focus over the last 10 years as traditional therapies have proven largely ineffective. Suicide gene therapy, for example, involves the transfer into tumour cells of the herpes simplex virus thymidine kinase which by itself does not have any effect on tumour development. When combined with ganciclovir treatment, the sucide gene construct is activated and results in the destruction of the transformed tumours cells and neighbouring tumour cells also (10). Finally, MM seems to be responsive to immunotherapy. MM patients are known to mount an anti-tumour immune response and some cases of spontaneous regression have been reported (11, 12). Early experiments investigating local cytokine therapy such as intra-pleural interleukin (IL)-2 or interferon (IFN)-γ were suggested to be effective at inducing an anti-tumour response in patients with early stage but not late stage tumours. Murine pre-clinical studies have continued to explore the potential for immunotherapy to treat MM.

In the early 1990s an asbestos induced model of MM was developed by the previously mentioned collaborating laboratory (13). In this initial study, BALB/c and CBA mice were injected intra-peritoneally with crocidolite asbestos. Between 7 and 25 months later, approximately one third of the mice had developed mesotheliomas as determined by standard cytological and histological parameters. From these primary tumours, continuously growing cell lines were established in culture which were later also confirmed as mesothelioma by cytological and ultrastructural (electron microscopy) analyses. As in the human MM, the murine mesothelioma cell lines were shown to vary in their morphology and growth rates with doubling times ranging from 14 to 30 hrs. All cell lines were capable of producing tumours when injected s.c. or i.p. into syngeneic mice. The murine C57BL/6J (AE17) mesothelioma model was established later in the same laboratory by the same techniques. The AE17 cell line used in this study, has been reported to grow slower than other well-studied tumour cell lines (including the B16 melanoma cell line), allowing the study of later treatment time points (14). The ability to study later treatment time-points and also to examine the

effect of treatments over a longer course of tumour development is more relevant to the clinical situation. The murine mesothelioma cell lines are commonly implanted s.c. for the pre-clinical investigations of potential therapies for MM. Tumours implanted s.c. develop into hard encapsulated solid tumours which are readily palpable and easily measured using microcallipers. Alternately, to more closely mimic the human disease, murine mesothelioma tumour cells can be implanted i.p. where they develop a more aggressive cancer typified by more nodule like tumour lesions (15). Tumours developed i.p. may be more clinically relevant to human MM but are much harder to monitor both in terms of tumour growth rate and the efficacy of treatments.

1.2 Tumourigenesis

An early hypotheses of tumourigenesis suggested that tumours developed as clones from a single cell. This hypothesis of clonal tumour evolution was described by Professor Nowell in Science in 1976 and is presented in Figure 1.1C and inset D (16). It was proposed that tumour initiation occurs following an induced change in a single and previously normal cell which makes it "cancerous" and provides it a selective advantage over adjacent normal cells such as loss of cell cycle regulation. Unrestrained cell division then occurs for this cell but from time to time, due to genetic instability in the expanding tumour cell population, other mutant cells are produced. Nearly all of these mutant cells would be cleared because of either a metabolic disadvantage or immune destruction but occasionally a mutant cell with an additional selective advantage with respect to the other tumour cells or the original normal cells will become a precursor for further tumour development.

The cancer stem cell hypothesis evolved from the same very early suggestions that cancers may arise from a progenitor or stem cell. Advances in stem cell biology have resulted in the recent reactivation of interest in cancer stem cells and the revived cancer stem cell hypothesis is also depicted in Figure 1.1B. The cancer stem cell hypothesis makes two major points (1) that tumours may originate from tissue stem cells (cells that have the ability to develop into any cell type required for organogenesis) through a process of dysregulated self-renewal and (2) as a result of this tumours may continually contain a population of cells with key stem cell like properties (such as self-renewal, the ability to differentiate, active telomerase expression, anti-apoptotic properties and the

ability to migrate and metastasize) ensuring continued tumour growth. Further aspects of the cancer stem cell hypothesis are reviewed by Wicha, Liu and Dontu in a recent review (17).

A second novel mechanism of tumourigenesis was also proposed in the last two years. The chromosomal basis of cancer hypothesis was proposed by Duesberg and colleagues (18) and was suggested to help explain the reasons why cancer (1) is not usually a heritable disease, (2) can be caused by non-mutagenic carcinogens, (3) develops only years after exposure to a carcinogen (such as mesothelioma following asbestos exposure) and (4) is aneuploid (a chromosomal state where the number of chromosomes is not a multiple of the haploid set). The chromosomal basis of cancer hypothesis suggests cancer is a chromosomal disease such that tumourigenesis is initiated by random aneuploides which can be induced by a carcinogen or may arise spontaneously. Aneuploidy unbalances thousands of genes and results in chromosomal variations from which traditional Darwinian selection encourages evolution and malignant progression of cancer cells (Fig. 1.1D). Continuing the evolution analogy, cancer cells then become a new "species" of cell with an unstable karyotype explaining the long latency period following exposure to a carcinogen as overall there is a low probability of species evolution.

Central to all three hypotheses of tumour induction is genetic or chromosomal changes. These changes and downstream effects were reviewed by Loeb and Loeb (19). Normal cells undergo regular DNA damage and repair in a counterbalanced manner without error. In tumour cells, DNA damage and repair are out of balance resulting in the accumulation of multiple mutations. Mutations occur in genes resulting in a selective advantage and cell survival in adverse conditions but genetic changes may also occur in genes that stabilise the genome. Genetic instability as a result of mutations in genes required for chromosomal segregation may result in the aneuploid phenotype observed in cancer cells and bring together the above tumourigenesis hypotheses.

Malignant mesothelioma is an unusual cancer as its major aetiological agent, asbestos, is known. MM will be used as an example in the following sections as the murine model of mesothelioma was the focus for this research. A recent review in Lancet summaries the pathogenesis of this cancer (5). Basically, the asbestos fibre is of a

perfect size and shape to cause repeated damage and inflammation to the pleura following inhalation. Specifically, the fibre can interfere with mitosis by severing the mitotic spindle which can result in aneuploidy and other chromosomal changes common to all cancers including MM. Asbestos damage also results in the release of toxic oxygen radicals which are known to result in DNA damage such as strand breaks while persistent kinase-mediated signalling induced by asbestos can elevate the expression of early response proto-oncogenes in mesothelial cells. Although asbestos is the major cause of MM, Simian Virus 40 (SV40) which contaminated the Salk polio vaccine in the 1950s and 1960s has also been linked with MM but no direct association between SV40 infection and MM has been confirmed. SV40 is known to block tumour suppressor genes and is a potent oncogenic virus for both human and rodent cells. On a molecular level, most malignant mesotheliomas have abnormal karyotypes often with extensive aneuploidy and structural rearrangements. The most common chromosomal abnormality is the complete loss of chromosome 22, while the most common genetic changes are a loss of $P16^{INK4A}$, $P14^{ARF}$ and *NF2* all of which suggest that tumour suppressor gene loss is essential for mesothelioma development.

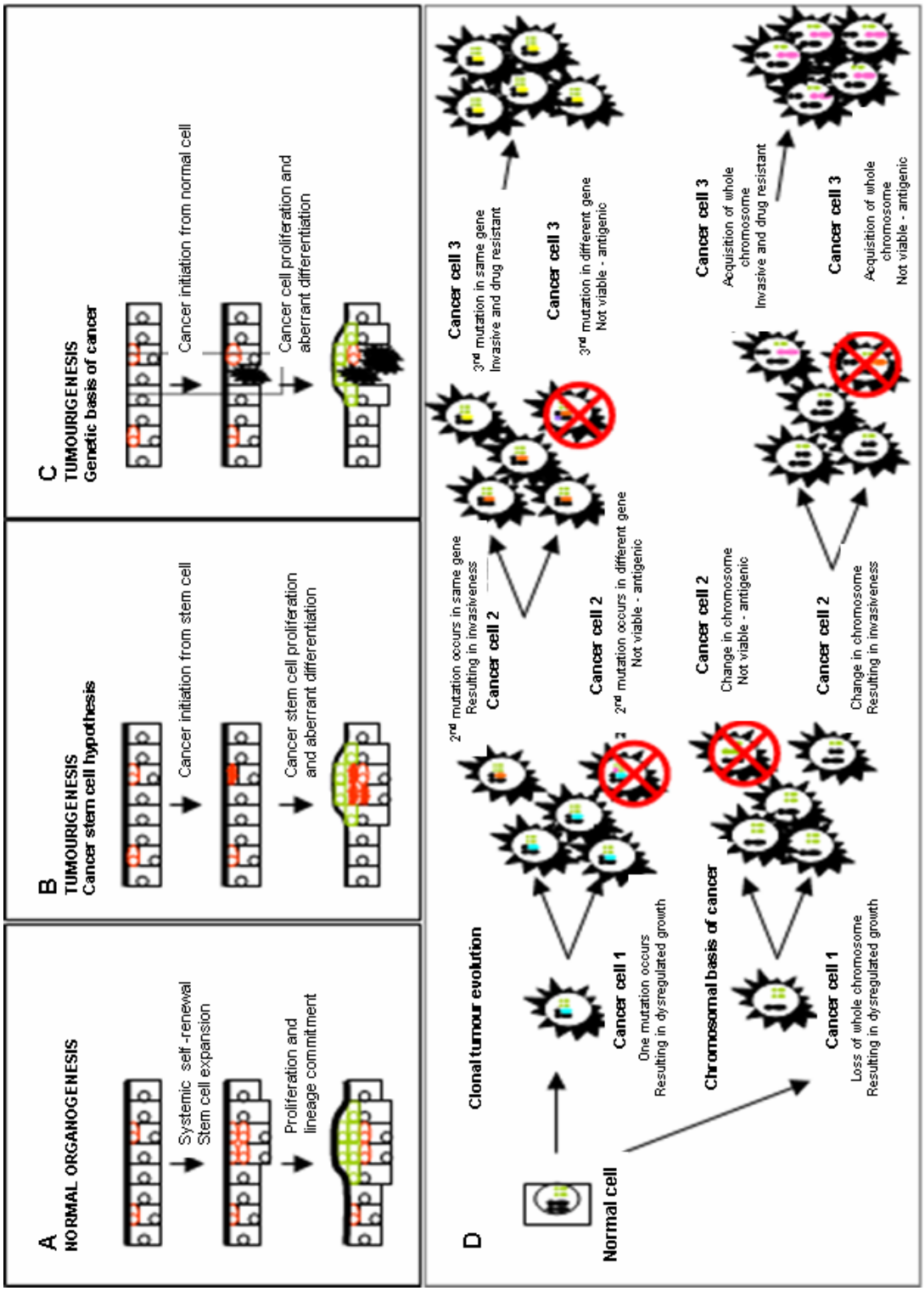
A
NORMAL ORGANOGENESIS
Systemic self-renewal
Stem cell expansion
Proliferation and
lineage commitment
B
TUMOURIGENESIS
Cancer stem cell hypothesis
Cancer initiation from stem cell
Cancer stem cell proliferation
and aberrant differentiation
C
TUMOURIGENESIS
Genetic basis of cancer
Cancer initiation from normal cell
Cancer cell proliferation and
aberrant differentiation
D
Clonal tumour evolution
Normal cell
Cancer cell 1
One mutation occurs
Resulting in dysregulated growth
2nd mutation occurs in same gene
Resulting in invasiveness
Cancer cell 2
2nd mutation occurs in different gene
Not viable - antigenic
Cancer cell 3
3rd mutation in same gene
Invasive and drug resistant
3rd mutation in different gene
Not viable - antigenic
Chromosomal basis of cancer
Cancer cell 1
Loss of whole chromosome
Resulting in dysregulated growth
Cancer cell 2
Change in chromosome
Not viable - antigenic
Cancer cell 2
Change in chromosome
Resulting in invasiveness
Cancer cell 3
Acquisition of whole
chromosome
Invasive and drug resistant
Cancer cell 3
Acquisition of whole
chromosome
Not viable - antigenic

Figure 1.1: Proposed mechanisms of tumourigenesis

(A) In normal organogenesis, systemic stem cells (red) undergo tightly regulated expansion, differentiation, lineage commitment (green). This is then followed by cell migration, terminal cell differentiation and then apoptosis of the fully differentiated cell. (B) During tumourigenesis under the cancer stem cell hypothesis, systemic stem cells (red) proliferate but undergo aberrant differentiation resulting in cancer cells (solid red). (C) Under the chromosomal (genetic) basis of cancer hypothesis, normal cells undergo mutations resulting in a cancer cell (solid black) that then undergoes further proliferation and aberrant differentiation. (D) is an inset of (C) and demonstrates two methods by which a normal cell can become cancerous. Clonal tumour evolution suggests that mutations are acquired and those cells with mutations conferring increased survival or resistance will proliferate. The chromosomal basis of cancer suggests whole chromosomes are gained or loss which again may confer increased survival or resistance in the cancer cell. (Adapted from (16-18))

1.3 Immunosurveillance and immunoediting

Tumourigenesis is the outgrowth of the "fittest" transformed cells or specific cancer stem cells as outlined in the previous section. However as tumours evolve, they do not do it in isolation, but within a host equipped with an immune response capable of eliminating foreign cells such as bacteria or transformed cells such as those that are virally infected. The immunosurveillance hypothesis, first proposed by Paul Ehrlich in 1909 but which much later (mid 1990s) gained acceptance thanks to the cancer research groups of Burnet and Thomas, who suggested that sentinel thymically derived cells constantly survey the body for transformed/tumour cells. The immunosurveillance hypothesis has since been revised in the early 2000s to also include a role for cells of the innate immune response (reviewed in (20)). Immunosurveillance can be broken into two arms, the innate and adaptive immune responses (Fig. 1.2A). In the adaptive response, immunogenic, tumour-derived and tumour-associated antigens (TAAs) are captured and presented by antigen presenting cells (APCs) such as dendritic cells (DCs). APCs need to be activated by death signals, to express the costimulatory molecule B7 in order to present antigen to T cells. Activated APCs then migrate to the draining lymph node of the tumour where they present, following B7-CD28 interactions, TAA peptides via MHC class I molecules to $CD8^+$ T cells and via MHC class II molecules TAA peptides to $CD4^+$ T cells. Activated $CD4^+$ T cells express CD40L which further stimulates $CD40^+$ APCs. TAA-specific, activated $CD8^+$ effector T cells and $CD4^+$ helper T cells can migrate back to the tumour and mount an anti-tumour immune response which involves both subsets of activated T cells but also local APCs.

The innate response is triggered by signals which are likely to be a result of the same initial malignant transformation of the cell, such as the expression of the stress-induced ligands MICA and Rae-1. These ligands interact with the NKG2D-DAP10 receptor complex expressed on the surface of several innate cells including macrophages, γδ-T cells and natural killer (NK) cells (NKT cells are also involved in the innate response by providing interferon (IFN)-γ to NK cells) resulting in cell activation which triggers degranulation by the cells, the release of perforin and hence mediates the apoptosis of the tumour cell.

The fact that spontaneous regression of malignant mesothelioma has been documented (11) suggests that immunosurveillance is active in MM. Regression in such cases was associated with mononuclear cell infiltration into the tumour and serological evidence of anti-MM reactivity. Early studies of tumour infiltrating lymphocytes (TILs) in human mesothelioma patients suggested a positive correlation between TIL numbers and survival time (reviewed in (21)) while *in vitro* studies of both human and murine mesothelioma cells demonstrated killing of mesothelioma cells by lymphokine-activated killer (LAK) cells and γδ-T cells but not NK cells supporting the notion that mesothelioma cells are susceptible to destruction by immunological means (22).

The clinical presence of a tumour however, suggests that immunosurveillance based on innate and adaptive anti-tumour immune responses is either not sufficient, not efficient or both. This analysis led to the 3 phase immunoediting hypothesis (reviewed in (23)). The first phase of the immunoediting process, known as the elimination phase, corresponds to the original immunosurveillance hypothesis (Fig. 1.2A). This is where normal cells or cancer stem cells are transformed to tumour cells and express TAAs and generate danger signals that initiate the innate and adaptive anti-cancer immune responses. During an efficient elimination phase the tumour cells may be completely cleared. However, if this process is not successful, the tumour cell may enter the equilibrium phase of the immunoediting process. The equilibrium phase is the second phase of the immunoediting process and is a period of latency, which probably also occurs before any symptoms are experienced by the host (Fig. 1.2B). This is where those cells not destroyed during the elimination phase undergo further transformation resulting in tumour variants carrying mutations which increase resistance to the anti-tumour immune response. Edited tumour cells which survive the equilibrium phase may enter the final escape phase of immunoediting where unrestrained tumour growth occurs (Fig. 1.2C). This is likely to be the stage at which tumours become clinically detectable. Immunoediting, or the development of tumour variants with increased resistance to the anti-tumour immune response appears to be a passive process on behalf of the tumour. More active mechanisms of escape have also been proposed and are discussed in the following sections.

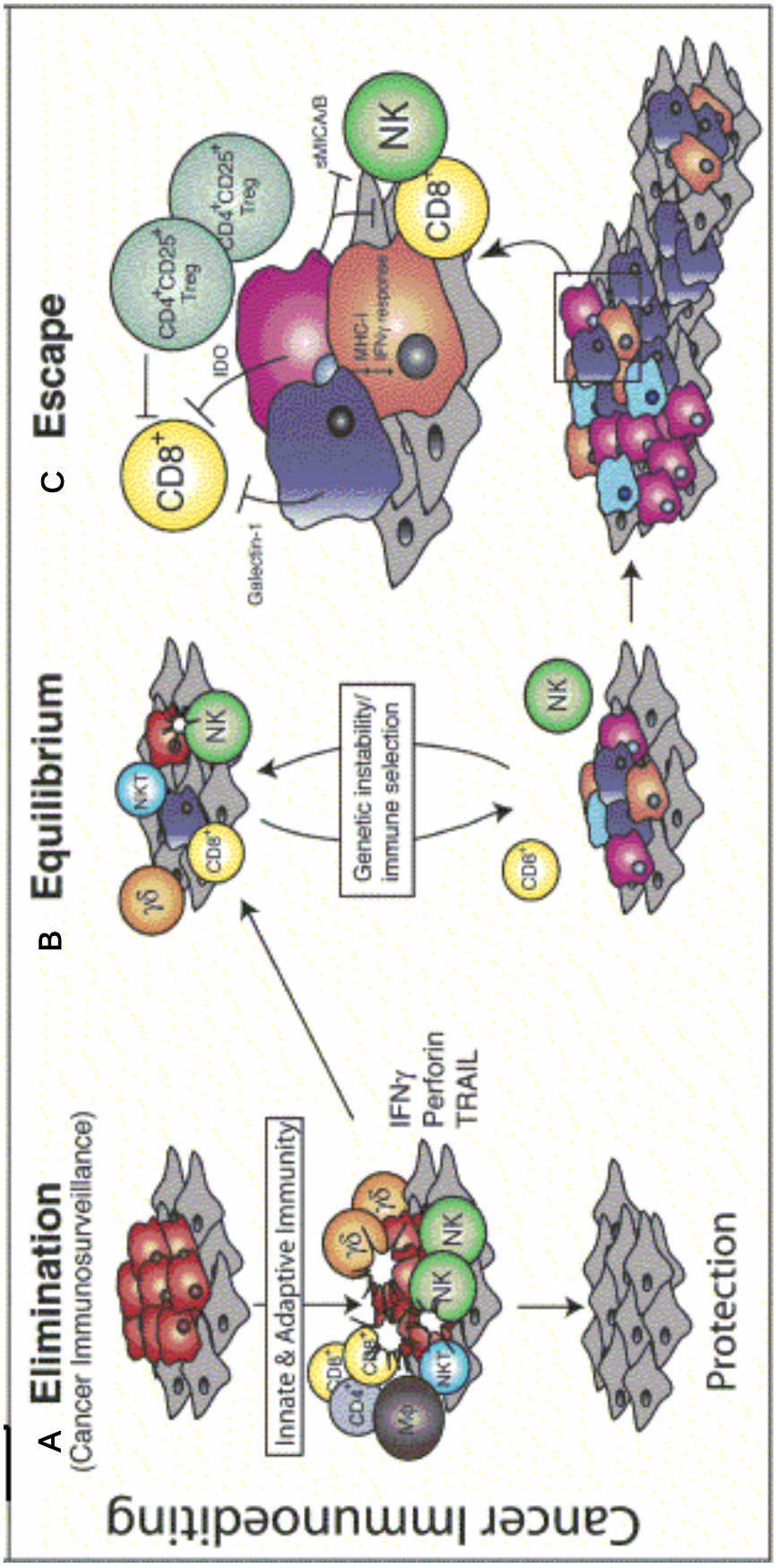
Cancer Immunoediting
A Elimination
(Cancer Immunosurveillance)
Innate & Adaptive Immunity
IFNγ
Perforin
TRAIL
Protection
B Equilibrium
Genetic instability/
immune selection
C Escape
CD8+
IDO
Galectin-1
CD4+CD25+ Treg
CD4+CD25+ Treg
sMICA/B
NK
CD8+
MHC-I
IFNγ response

Figure 1.2: The three phases of the cancer immunoediting process

(A) Normal cells (grey) subject to common oncogenic stimuli ultimately undergo transformation and become tumour cells (red). Even at early stages of tumourigenesis, these cells may express distinct tumour-specific markers and generate proinflammatory "danger" signals that initiate the cancer immunoediting process. In the first phase of elimination, cells and molecules of innate and adaptive immunity, which comprise the cancer immunosurveillance network, may eradicate the developing tumour and protect the host from tumour formation. (B) However, if this process is not successful, the tumour cells may enter the equilibrium phase where they may be either maintained chronically or immunologically sculpted by immune "editors" to produce new populations of tumour variants. (C) These variants may eventually evade the immune system by a variety of mechanisms and become clinically detectable in the escape phase. (Taken from (23)).

1.4 Tumour Immune Evasion

The inability of most cancer patients to develop an effective immune response, despite evidence of immunogenicity in the tumours, implies the existence of tumour specific immune evasion strategies. Several tumour immune evasion mechanisms have been defined and were reviewed in (24). MHC class I restricted CTLs are considered to be the major anti-tumour effector cells so the downregulation of MHC antigens by tumours cells is a powerful way to avoid CTL lysis. However, tumours lacking MHC class I expression end up more susceptible to NK cell killing. To compensate for this, tumours cells can also upregulate the expression of MHC molecules such as HLA-E, which ligates to the NKG2A inhibitory receptors on NK cells and CTLs. Tumour antigen presentation to DCs is necessary for CTL activation and is dependent on the expression of several adhesion and costimulatory molecules. Tumour-infiltrating DCs have been shown to lack CD80 and CD86 expression resulting in T cell anergy while tumour cells themselves have been shown to downregulate the expression of ICAM-1 necessary for the adhesion of CTLs to their target (tumour cell). Tumours can secrete immunosuppressive substances such as gangliosides and defensins but also cytokines in order to induce immune escape. IL-10 and TGF-β are the most common tumour secreted cytokines with known immunosuppressive effects. Also IL-6 secretion in tumours has been associated with poor survival in patients. The most direct mechanism of immune escape would have to be T cell destruction or inactivation. Secreted proteins from tumours may be presented in the thymus and cause clonal deletion of newly generated T cells, while in the periphery, the expression of FasL by tumour cells can induce apoptosis in T cells expressing CD95 (Fas). Loss of ζ chains and other CD3 compartments by T cells has been correlated with a decline in anti-tumour immune response in patients and may be a result of tumour infiltrating macrophages inducing a decreased expression of CD3ζ or as a result of oxidative stress. Much of the above evidence supports a tumour "turning off" the immune response, but tumours may also be able to harness the immune response to their advantage. IL-10 usually secreted by T cells can also support tumour growth in some cancers e.g. melanoma. Melanoma tumour cells can also secrete IL-10 themselves making it an autocrine growth factor. Tumour infiltrating lymphocytes can secrete angiogenic factors of benefit to the tumour. Tumour cells themselves can also mop up IL-2 which is required by T cells for proliferation leaving the TIL anergic. IL-2 can be a promoter of tumour cell growth.

Finally, tumours have been shown to recruit, selectively proliferate and/or convert regulatory T (T_{reg}) cells. T_{reg} cells play important roles in the natural host immune response to prevent autoimmunity but are also important in controlling the immune response and hence immunological tolerance. In the case of tumour immunity, T_{reg} cells have been identified in the peripheral blood of cancer patients and were associated with worse disease outcomes, but more recently have been found within tumours themselves (25-29). Recent data, including the work presented in this thesis, suggests that tumours actively recruit T_{reg} cells or convert T cells into T_{reg} cells in order to suppress the anti-tumour immune response in situ. The rest of this review will focus on the role of T_{reg} cells in tumour immune evasion and methods for manipulating T_{reg} cells for therapeutic advantage.

In terms of MM it has been shown that MM cells can secrete immunomodulatory factors such as TGF-β which has the ability to downregulate the expression of MHC class I (30-32). In a separate study, MM cells were shown by direct immunofluorescence and northern blotting to constitutively express MHC class I but not MHC class II. MHC class II molecules are required for the presentation of tumour antigens to $CD4^+$ T cells (33). By *in vitro* experimentation, MM cells were shown to be resistant to NK cell mediated lysis (34) while finally, MM tumours have been shown to comprise T_{reg} cells. Late last year, T_{reg} cells were identified in the peripheral blood and pleural effusions associated with MM (31, 35). This year it was shown that MM tumours themselves comprise T_{reg} cells (32).

1.5 T_{reg} cells as a mechanism of tumour immune evasion

T_{reg} cells constitute an active and dominant mechanism of immunological tolerance. Together with clonal deletion, anergy and antigen ignorance, T_{reg} cells act to achieve the task of preserving immunological tolerance to self while allowing immunity to the foreign. T_{reg} cells may also serve to modulate the intensity and duration of the immune response in general. So why do we need T_{reg} cells? One potential explanation is that if the immune system had to rely solely on elimination or functional inactivation of self-reactive lymphocytes to preserve self tolerance it would erase a significant fraction of its repertoire of antigen recognition specificities. This could expose the immune system to the hazard of reducing the diversity of the antigen receptor repertoire to an extent that

could impair its capacity to embrace all potential foreign antigenic diversity and make the host vulnerable to attack. Such risks could be avoided if a proportion of self-reactive lymphocytes were to be maintained in a flexible state of unresponsiveness.

1.5.1 The history and re-emergence of T_{reg} cells

The idea of T cell immunosuppression of autoimmune disease was first described by Nishizuka and Sukakura in the late 1960s when it was found that the thymectomy of mice on the third day of life results in organ specific autoimmunity (36). Specifically, the animals lost their ovaries as a result of a massive invasion of the ovaries with immune cells. Not long after that, Gershon became the first to propose the existence of a specific T cell population with the capacity to dampen immune responses, especially autoreactive ones, and was instrumental in giving these cells the name of suppressor T cells (37). Due to the inability of these early researchers to purify a population of these T cells or to define specific markers of these cells for subsequent analyses, the research into suppressor T cells mostly fell by the wayside. With an array of sophisticated and highly effective means of controlling immunological tolerance already defined by other researchers, it is not surprising that many doubted the existence of suppressor T cells.

During the mid to late 1980s a few small research groups were still investigating the idea of suppressor T cell involvement in autoimmunity and also in cancer development. North and Awwad, for example successfully mapped the timing of the anti-tumour immune response to implanted cancers using murine Meth A fibrosarcoma and P815 mastocytoma models. Based on the expression of the CD8 cell surface molecule, North and Awaad defined anti-tumour effector T cells as $CD8^+$ while suppressive T cells were $CD8^-$ (38). It was shown that T cells capable of causing tumour regression were generated first on about day 6 post tumour challenge. These cells reached a peak at about day 9 post tumour challenge but then were progressively lost until day 15 when their presence could no longer be detected. This decay in immunity was believed to be caused by the negative immunoregulatory function of suppressor T cells that were progressively acquired from day 9 onwards. It was therefore seen that effector T cells did not disappear suddenly but were progressively lost as T_{reg} cells were acquired.

It was not until later in the 1990s that more serious consideration was given to suppressor T cells and they underwent a resurgence and a name change to T_{reg} cells. Sakaguchi *et al* (1995) identified an approximately 10% subpopulation of $CD4^+$ T cells that co-expressed the IL-2 receptor alpha chain (CD25) to be T_{reg} cells (39). The depletion of these cells from adult splenocytes prior to adoptive cell transfer into immuno-compromised hosts resulted in a range of autoimmune diseases similar to those seen following the day 3 thymectomy outlined above. Since the characterisation of these cells as $CD4^+CD25^+$ T cells in 1995 much work has focussed on functionally analysing these cells both *in vitro* and *in vivo* in relation to tumour development.

1.5.2 General characterisation of T_{reg} cells

Functionally and phenotypically similar cells to the murine $CD4^+CD25^+$ T_{reg} cells identified by Sakaguchi have also been found in humans (40). In general $CD4^+CD25^+$ T_{reg} cells are considered anergic because they do not proliferate or produce IL-2 in response to TCR stimulation *in vitro*. Upon TCR stimulation they do however suppress the proliferation of $CD4^+$ and $CD8^+$ T cells by inhibiting the production of IL-2 and the upregulation of IL-2 receptors including CD25 (41).

1.5.2.1 Natural versus induced T_{reg} cells

A specialised population of $CD4^+CD25^+$ T_{reg} cells, known as natural T_{reg} cells, are generated in the thymus by a process of positive selection of self-reactive T cells. Natural T_{reg} cells develop early in the neonatal thymus and are exported to the periphery competent to suppress the activation of other self-reactive T cells (42, 43). In addition to these naturally suppressive, thymically derived T_{reg} cells, other types of induced T_{reg} cells have been described. T_R1 cells are generated by activation in the presence of IL-10 (44), Th3 cells have been shown to be activated by the administration of oral antigen and are hence involved in the process of oral tolerance (45) while a third, possibly distinct, population of T_{reg} cells was induced by repeated stimulations with immature dendritic cells (46). This suggested a role for environmental factors in the periphery (as opposed to the thymus) in the generation of T_{reg} cells. The origin of $CD4^+CD25^+CD103^+$ T_{reg} cells also seems to differ from the natural thymically derived $CD4^+CD25^+$ T_{reg} cells in that they were found only in the thymus during adulthood and

numbers increased with age (47). $CD4^+CD25^+CD103^-$ T cells on the other hand emerged from the thymus within the first days after birth and did not change in number during aging. The expression of CD103 is a hallmark of T cells residing in or near epithelial sites. TGF-beta is also abundant at such sites and is able to induce CD103 (48). Concurrently TGF-β has been proposed to be involved in the development of T_{reg} cells (49) so CD103 expression may suggest that the T_{reg} cells have developed in a TGF-β rich environment or that CD103 and TGF-β may be involved together in the development of T_{reg} cells.

Tr1 cells were identified during studies using ovalbumin (OVA) TCR-transgenic mice (44). T_{reg} cell clones with an inability to proliferate in response to TCR stimulation and with a distinct cytokine profile of high IL-10 and IL-5 secretion with or without TGF-β secretion but with little to no IL-2, IL-4 or IFN-γ secretion were generated by culturing T cells from the OVA TCR-transgenic mice with OVA and IL-10. Although Tr1 cells have mostly been shown to prevent autoimmune diseases there is also a suggested role for Tr1 cells in tumour development, specifically murine glioma (50). Th3 cells that secrete high levels of TGF-β have been identified in studies of oral tolerance including the role of oral treatment with myelin basic protein in multiple sclerosis and experimental autoimmune encephalomyelitis (EAE) (51, 52). The *in vivo* significance of these Th3 cells and the role of TGF-β in their induction as well as effector function is interesting in light of the finding that some tumour cell lines actively produce TGF-β (53). The induction of these Th3 type T_{reg} cells may therefore represent a mechanism of tumour immune evasion. Natural $CD4^+CD25^+$ T_{reg} cells were originally defined based on cell surface marker expression rather than cytokine secretion profile, specifically the expression of CD25 which is also expressed by Tr1 and Th3 cells. Following initial *in vitro* experiments it was found that these T_{reg} cells acted via cell-to-cell contract and the expression of the CTLA-4 costimulatory molecule (54, 55). The role of cytokines in the immunosuppression exerted by these cells is controversial. Cell surface TGF-β expression has been implicated in the cell-to-cell contact dependent mechanism of immunosuppression but is contested by the finding that T_{reg} cell suppression can be independent of membrane bound TGF-β (56, 57). The use of IL-10 by these T_{reg} cells has also been disputed. To explain this situation it may in fact be the case that these T_{reg} cells are made up of distinct populations utilising different mechanisms of suppression. T_{reg} cells may also have the ability to utilise alternate mechanisms of

immunosuppression depending on which situation of immune regulation they find themselves in.

1.5.2.2 Markers of T_{reg} cells

Much attention has focussed on the identification of specific cell surface markers for T_{reg} cells. Although both a $CD8^+$ T_{reg} cell and a B cell with regulatory properties have been described (58-60) this review of T_{reg} cell markers will focus on $CD4^+$ T_{reg} cells as these cells were the original impetus for this PhD project and $CD4^+$ T_{reg} cells strongly dominate much of this field at present. Since the beginning of the T_{reg} cell resurgence, studies have focussed on CD25 as the best marker for $CD4^+$ T_{reg} cells in both mice and humans (61). The function of CD25 as an activation induced cytokine receptor (IL-2 receptor alpha chain) and the role of $CD25^+$ T cells as T_{reg} cells is not clear and does not allow the distinction of T_{reg} cells from activated $CD4^+$ T cells. In mice, natural T_{reg} cells are commonly identified as $CD4^+CD25^+$ T cells. Unfortunately, in humans it is much more difficult to characterise T_{reg} cells based simply on the co-expression of both CD4 and CD25 as the higher incidence of activated $CD4^+$ T cells that express CD25 consequently contaminate the $CD4^+CD25^+$ T_{reg} cell populations (62). CD25 is also an early activation marker on other T cells and it is important to note that the mere acquisition of CD25 expression does not confer suppressive ability (54, 63).

The forkhead transcription factor Foxp3 is specifically expressed in $CD4^+CD25^+$ T_{reg} cells and is required for their development (64). The lethal autoimmune syndrome observed in Foxp3-mutant scurfy mice and Foxp3-null mice results from a $CD4^+CD25^+$ T_{reg} cell deficiency. Foxp3 expression can also be shown to confer suppressor function on peripheral $CD4^+CD25^-$ T cells thus Foxp3 is a critical regulator of $CD4^+CD25^+$ T_{reg} cell development and function. Foxp3 as a marker of T_{reg} cell development and function in both mice and humans is reviewed in (65). Unfortunately, although Foxp3 is one of the most specific markers of T_{reg} cells, the nuclear localisation of Foxp3 precludes the use of Foxp3 as a direct tool for T_{reg} cell isolation (62).

There is increasing evidence that T_{reg} cells are in fact a heterogenous population (66, 67). Several groups have subdivided $CD4^+CD25^+$ T_{reg} cells into two groups based on

the expression of L-selectin/CD62L or integrin $\alpha_E\beta_7$/CD103. $CD4^+CD25^+$ T_{reg} cells found to express high levels of CD62L have been shown to be more suppressive *in vivo* (68-70) and to have a superior capacity to home to lymph nodes (71, 72). CD62L has now also been suggested as a marker capable of delineating activated effector cells from T_{reg} cells in tumour-draining lymph nodes (73). CD103 was initially described as a marker of intraepithelial T cells residing in the gut wall, skin or lung (74, 75). While initial experiments suggested the ligand for CD103, E-cadherin, was expressed only on epithelial cells but not on endothelium (76) there is increasing evidence for a role of CD103 in homing via a ligand on endothelial cells (77). The finding that CD103 may act to retain T cells in the epithelium and may also be involved in the costimulation of T cells led to the investigation of CD103 on T_{reg} cells (78, 79). An early study of the expression of CD103 by T_{reg} cells found that the expression of CD25 and CD103 can distinguish 2 sub-populations of T_{reg} cells with distinct properties, the $CD25^+CD103^+$ and the $CD25^+CD103^-$. The $CD25^+CD103^+$ T_{reg} cells were found to comprise 4% of total $CD4^+$ T cells and 25% of the $CD4^+CD25^+$ T cells in the periphery and in *in vitro* assays were found to be the most potent suppressors as they were active at a higher T_{reg} cell:target cell ration when compared to the $CD25^+CD103^-$ T_{reg} cells. One argument proposed from this research was that the $CD4^+CD25^+$ T_{reg} cells are a heterogeneous population of multiple subsets of T_{reg} cells while it may also be argued that the low percentage of $CD25^+CD103^+$ T_{reg} cells may represent an activated form. The latter may not be the case as unlike CD25, CD103 is not induced upon activation (47). CD103 may thus act to predispose T_{reg} cells for retention within epithelial tissues or may have a unique function in the homing of T_{reg} cells from lymphoid sites to the sites of inflammation. A subsequent global gene expression study found that the $CD25^+CD103^-$ T_{reg} cells displayed a naïve-like phenotype with high expression of CD62L while both the subsets of $CD25^+CD103^+$ T_{reg} cells showed an activated phenotype as they expressed lower levels of CD103 and high levels of CD44 (72). In terms of migratory ability, the expression of CD103 was necessary for the homing of T_{reg} cells to the site of Leishmania major infection in mice (80).

In separate studies to delineate subpopulations of $CD4^+CD25^+$ T_{reg} cells the expression of CD44 was examined (81). The adhesion (rolling) of lymphocytes is mediated by the activated form of CD44 ($CD44^{act}$) on peripheral T cells and its ligand hyaluronan (HA) on endothelial cells (82). Beyond the adhesion activity on endothelia, CD44 has been

suggested to be involved in the specific migration of T cells in the microvasculature during an immune response from the peripheral lymphoid organs to the inflamed site where extravasation of activated T cells occurs. CD44 is highly expressed on resting lymphocytes but in an inactive form. The binding of HA can only occur once CD44 has been conformationally activated (82-84). The activation of CD44 is achieved via TCR stimulation (82, 85). After TCR stimulation CD44 is highly expressed by T cells but its conversion to the active form occurs relatively late and only in a small subset of activated T cells under full TCR stimulation (81). Similarly, CD44 was suggested as a means of subtyping $CD4^+CD25^+$ T_{reg} cells. *In vitro*, $CD4^+CD25^+$ T cells could be induced to express $CD44^{act}$ but more importantly *in vivo* the expression of $CD44^{act}$ by T_{reg} cells was correlated with more potent suppressor function (81). Further examination of $CD4^+CD25^+$ T_{reg} cells expressing the $CD44^{act}$ has found them to be more suppressive compared to $CD4^+CD25^+$ T_{reg} cells expressing CD44 in the unactivated form. Although the association between $CD44^{act}$ expression and suppression is clear from these studies it is still unclear what role this marker plays in the suppressive response (81). The expression of $CD44^{act}$ may simply leave the cell armed and ready with a trafficking molecule so it is primed to execute suppressor function at any time. Interestingly, mesothelioma cells but not normal mesothelial cells have been shown to express HA receptors while a subset of TIL in MM have been shown to express CD44 (15).

A further novel marker of T_{reg} cells which has not seen much further investigation is Neuropilin-1 (Nrp-1). Nrp-1, a receptor involved in axon guidance, angiogenesis, and the activation of T cells was shown to be constitutively expressed on the surface of $CD4^+CD25^+$ T_{reg} cells independently of their activation status (86). $CD4^+Nrp\text{-}1^+$ T cells were shown to express high levels of Foxp3 and suppress $CD4^+CD25^-$ T cells. Nrp-1 expression is down-regulated in naive $CD4^+CD25^-$ T cells after TCR stimulation thus Nrp-1 may constitute a useful surface marker to distinguish T_{reg} cells from both naive and recently activated $CD4^+CD25^+$ non-regulatory T cells. Although Nrp-1 appears to be expressed on freshly isolated T_{reg} cells but down-regulated on activated $CD4^+CD25^+$ T cells the utility of Nrp-1 for the isolation of T_{reg} cells from activated T cells has not been ascertained (62).

$CD4^+CD25^+$ T_{reg} cells have also been distinguished from recently activated T cells by the expression of cytotoxic T lymphocyte-associated antigen-4 (CTLA-4) (87, 88), while glucocorticoid induced tumour necrosis factor receptor (GITR) has been proposed to have a functional role in the suppression mechanisms of T_{reg} cells, as stimulation through GITR on $CD4^+CD25^+$ cells abrogates the suppressive function of these cells (89). CTLA-4 has been shown to be expressed constitutively by T_{reg} cells at levels between 10% and 50% (45, 55, 90, 91). GITR has also been shown to be constitutively expressed on T_{reg} cells (92, 93). CTLA-4 and GITR are both also expressed by activated $CD4^+$ T cells and are thus not delineating markers for T_{reg} cells.

Finally, programmed cell death-1 (PD-1; CD279) a receptor molecule which is upregulated on activated $CD4^+$ T cells was recently suggested as a negative selective marker for T_{reg} cells (62). The ligands PDL-1 (CD274) and PDL-2 (CD273) are expressed by various haemopoetic cells and have been suggested to be involved in the maintenance of peripheral tolerance. While investigating the role of these molecules in peripheral tolerance, Raimondi *et al* (2006) observed that in contrast to activated $CD4^+$ T cells, T_{reg} cells expressed very limited surface PD-1. Further investigation showed that although freshly isolated T_{reg} cells did not express cell surface PD-1 they did retain PD-1 intra-cellularly allowing for the ready distinction of the two cell populations. This work suggested a method for the distinction and negative selection of resting T_{reg} cells which are $CD4^+CD25^+PD\text{-}1^-$ from T_{reg} cells that have been recently activated by TCR stimulation resulting in the translocation of PD-1 to the cell surface.

1.5.3 T_{reg} cell involvement in tumour development

T_{reg} cells may represent a mechanism of tumour escape from the immune response. The following sub-sections outline the evidence for T_{reg} cell involvement in tumour immune evasion.

1.5.3.1 T_{reg} cells in the periphery of tumour bearing hosts

There are several examples for the presence of increased peripheral T_{reg} cells in patients with cancer suggesting a correlation between peripheral T_{reg} cells and worse disease outcomes. Patients with epithelial malignancies show an increase of

$CD4^+CD25^+$ T_{reg} cells in the peripheral blood (94). The prevalence of T_{reg} cells was also shown to be increased in the peripheral blood of patients with invasive breast or pancreatic cancers (26). The prevalence of peripheral blood $CD4^+CD25^+$ T_{reg} cells in both gastric (n = 20; 14.2 ± 4.9%) and oesophageal cancer patients (n = 10; 19.8 ± 6.9%) was also significantly higher than that in healthy donors (n = 16; 7.2 ± 2.1%) (95).

1.5.3.2 Intra-tumoural T_{reg} cells

Reflecting the ubiquitous role of T_{reg} cells, populations have been found in many locations in the body suggesting these cells may play different roles in different locations. But as T_{reg} cells of differing phenotypes and specificities have been described it is difficult to know if there are many types of T_{reg} cells or if T_{reg} cells change depending on the environment in which they are located (96, 97)

The earliest indication that T_{reg} cells were active at the site of immune regulation came from the work by Powrie and others in auto-immune gastritis models (44, 98-100). The gastrointestinal tract is exposed to many different antigens, including food and commensal bacteria, and it is therefore important that the intestine has a mechanism for inducing tolerance. Evidence suggests that one such mechanism is the presence of T_{reg} cells in the gut mucosa. T_{reg} cells were then identified in the lungs of both normal and *Pneumocystis carinii* and *Bordatella pertussis* infected mice (101, 102) and also associated with rodent models of asthma where airway constriction is seen as a result of too few active T_{reg} cells (103-105). In a retroviral model (Friends Leukaemia virus) the Hasenkrug laboratory demonstrated an important role for T_{reg} cells in establishing the chronicity of infection (106). The presence of an induced population of splenic T_{reg} cells in mice with murine AIDS (MAIDS) was later reported by our group (107). In HIV infected patients there is a poor correlation between peripheral blood T_{reg} cells and viral load (as published by independent research in our laboratory (108). However, a good correlation was found between viral load and T_{reg} cell populations in the tonsils (109). T_{reg} cells were detected in the synovial fluid of patients with rheumatoid and juvenile idiopathic arthritis (110, 111), the islets of Langerhans in diabetes models (112-114), the uteri of pregnant mice (115), skin grafts (116) and periodontal disease tissues (117).

During the time these thesis studies were undertaken, $CD4^+CD25^+$ T_{reg} cells have been implicated in cancer studies of both mice and humans (25-29, 94, 95, 118-120). $CD4^+CD25^+$ T_{reg} cells have been described within murine melanomas, fibrosarcomas and mammary tumours (28, 53, 121). In humans, $CD4^+CD25^+$ T_{reg} cells have been identified inside lung, ovarian, colorectal, breast, pancreatic and gastric tumours (25, 27, 95, 118, 122, 123). Only a few of these studies have however characterized changes in this intra-tumoral T_{reg} cell population. In a mouse fibrosarcoma model it was most recently found that although there is no change in the $CD4^+CD25^+$ T cell population within the spleen and draining-LN of tumour-bearing mice, there is an increase in the $CD4^+CD25^+$ T cells in tumours at day 16 post tumour challenge (~65%) compared to tumours at day 7 (~30%) (28). Curiel *et al* (2004) found a much larger percentage of T_{reg} cells in late stage human ovarian carcinomas ($CD4^+CD25^+$ T cells represented ~30% of total tumour-located $CD4^+$ T cells) compared to early stage tumours ($CD4^+CD25^+$ T cells represented ~12% of total tumour-located $CD4^+$ T cells) and showed that $CD4^+CD25^+$ T cells were undetectable in normal ovarian tissue. Ichihara *et al* (2003) found that there is an increase in $CD4^+CD25^+$ cells as a percentage of all TIL in advanced gastric cancer ($19.8 \pm 4.5\%$) as compared to the percentage in early gastric cancer ($4.8 \pm 2.1\%$) and the percentage of intraepithelial $CD4^+CD25^+$ cells of normal gastric mucosa ($4.0 \pm 1.2\%$). Lastly, it has been shown that although there is no significant difference between the prevalence of $CD4^+CD25^+$ cells in normal breast and pancreatic tissue donors ($8.6 \pm 0.71\%$) and patients with benign breast and pancreatic lesions, there is a significant increase in $CD4^+CD25^+$ cells in the tumours of patients with malignant breast cancer ($16.6 \pm 1.22\%$) and malignant pancreatic cancer ($13.2 \pm 1.13\%$) (122).

1.5.4 Accumulation/induction of intra-tumoural T_{reg} cells

There are several hypotheses about the origin and movement of intra-tumoural T_{reg} cells. The first theory is that T_{reg} cells preferentially move to and accumulate in tumours as they progress. These T_{reg} cells are presumed to originate in the periphery and be induced to migrate to the tumour. At the time this work was being conducted it had been hypothesised that the intra-tumoural accumulation of T_{reg} cells resulted from a migration of peripheral $CD4^+$ T cells consistent with the findings of Curiel *et al* (2004).

The chemokine CCL22 was implicated in this migration of T_{reg} cells and was shown to be secreted by the tumour cells themselves and also by tumour-located macrophages (27). Others suggested markers of T_{reg} cell migration are CD62L and CD103. CD62L is suggested to be involved in the homing of lymphocytes to the lymph nodes (73) while CD103 is proposed to be involved in the migration of lymphocytes to inflamed sites (47). The role of CCL22 and the cell surface markers CD62L and CD103 on the migration of T_{reg} cells into murine mesotheliomas were investigated as part of this thesis.

In general it has been suggested that TGF-β is involved in the generation and expansion of human $CD4^+CD25^+$ T_{reg} cells (124) while in murine systems a role for IL-10 in the differentiation but not proliferation of these cells has been proposed (102). Moreover human $CD4^+$ T cells primed in the presence of IL-10 and IFN-α can be differentiated into Tr1 cells, and murine T cell precursors cultured with TGF-β can be induced to form Th3 cells (49, 125). These findings prompted McGuirk and Mills (2002) to ask the question whether a distinct subtype of APC exists which promotes the differentiation of T_{reg} cells from naïve T cells. Specific DC1 or DC2 maturation is induced depending on the foreign stimulus and results in the specific activation of the Th1 or Th2 pathways respectively. It was therefore proposed that the specific activation of a DC that can secrete IL-10 (DCr) could direct naive T cells down the Tr1 pathway (102, 126,McGuirk, 2002 #392).

A third explanation for the intra-tumoural presence and activity of T_{reg} cells is that T_{reg} cells are induced within tumours via the immunosuppressive cytokine TGF-β (127, 128). It has been suggested that TGF-β within tumours can induce the conversion of $CD4^+CD25^-$ T cells into $CD4^+CD25^+Foxp3^+$ T_{reg} cells (127, 128). As it was known that mesothelioma tumour cells are secretors of TGF-β (129) it was further hypothesised that TGF-β secreted by the tumour cells themselves may induce the conversion of naïve $CD4^+$ T cells into T_{reg} cells in order to provide an environment of immunosuppression thus allowing unrestrained tumour growth.

Finally, it has been proposed recently that the accumulation of intra-tumoural T_{reg} cells results from the selection and proliferation of naturally occurring

$CD4^+CD25^+Foxp3^+$ T_{reg} cells and requires signalling through the TGF-β receptor II (130). More specifically it was shown using two rodent tumour models that during tumour development tumour cells themselves convert a population of immature dendritic cells into a regulatory type DC that secrete TGF-β. These DCs are then recruited to tumour draining LN where they selectively promote the proliferation of T_{reg} cells in a TGF-β dependent manner.

1.5.5 Immunosuppression by T_{reg} cells

Pioneering *in vitro* experiments found that T_{reg} cells needed to be in close proximity to their cellular target for suppression to occur (54). However, triggering of GITR has been shown to extinguish this contact dependent suppressive activity of T_{reg} cells (92, 131). Recent studies have revealed a functional role for CD25 expression in T_{reg} cells such that the interruption of the IL-2R/IL-2 signalling pathway blocks T_{reg} cell function potentially via alterations in the expression of GITR (132, 133). Tr1 cells (inducible T_{reg} cells) suppress predominantly by a cytokine dependent mechanism characterised by IL-10 and TGF-β secretion. Similarly natural T_{reg} cells have been suggested to work by TGF-β dependent mechanism but also via contact-dependent mechanisms (134).

DCs can present self-antigens in addition to foreign antigens to T cells. These foreign antigens may also be cross-reactive toward self. It may therefore be the case that self-reactive T cells and also T_{reg} cells are continuously engaged in interactions with DCs during different phases of an immune response. The suppressive activity of T_{reg} cells is sensitive to the presence of DC co-stimulation and on the production of IL-2 by activated effector T cells (135, 136). Thus mature DCs bearing high levels of costimulatory molecules are believed to off-set the suppressive activity of T_{reg} cells allowing effector T cells to proliferate. The well documented cell-dose dependence for suppressive activity of T_{reg} cells suggests that as the response progresses T_{reg} cells may expand and eventually catch-up with and down-regulate effector T cells as per the original suggestion of North (opcit (38, 137). During the immune response T_{reg} cells are actively involved in regulating the immune response. Specifically, since T_{reg} cells are highly activated it is possible that the elevated levels of CD25 expression results in increased IL-2 consumption and increased suppression (ie. there is a level of competition for IL-2 between T_{reg} cells and effector T cells) (41).

Initially T_{reg} cells were described to have a particular pattern of cytokine expression showing reduced IL-2, IL-4, IFN-γ and TNF-α but high IL-10 expression (47, 135, 138). The cytokine profile of T_{reg} cells on a single cell level is not well documented (47). Cytokine profiling of T_{reg} cells is notoriously difficult as low cytokine production has been associated with T_{reg} cells (135, 139). The $CD25^{+}CD103^{+}$ T_{reg} cells described earlier have also been cytokine profiled and were found to secrete the lowest levels of cytokines except IL-10 (47). Finally, Mills and colleagues suggested that unstimulated T_{reg} cells could be characterised on the basis of their secretion of high levels of IL-10 and/or TGF-β, some IL-5 and little to no IL-4 (personal communication: Prof. K. Mills, Trinity College, Dublin). Seo *et al* (2001) utilised this notion of high IL-10 secretion by T_{reg} cells and hence IL-10 as a mechanism of T_{reg} cell action in their intra-tumoural anti-IL-10 mAb treatment experiments. The intra-tumoural administration of anti-IL-10 mAb resulted in B16 melanoma tumour growth inhibition while the intra-tumoural treatment of tumours with recombinant IL-10 resulted in more vigorous tumour growth (53). Further investigation of the effects of cytokine blockade as a means of inactivating T_{reg} cells is warranted in the future.

Granzyme B (GrzB) is a serine protease secreted mainly by CTLs and NK cells and upon secretion induces apoptosis in the target cells (140). Recently, human $CD4^{+}$ T cells, more specifically T_{reg} cells, were also shown to synthesize GrzB (141-144). In 2005 GrzB was suggested as one of the key components of T_{reg} cell mediated suppression as the induction of regulatory activity was correlated with the up-regulation of GrzB expression (134). Proof of a functional involvement of GrzB in contact-mediated suppression by T_{reg} cells was shown by the reduced ability of T_{reg} cells from $GrzB^{-/-}$ mice to suppress as efficiently as T_{reg} cells from WT mice. GrzB mediated immuno-suppression was also shown to be perforin independent as suppression by T_{reg} cells from $perforin^{-/-}$ and WT was indistinguishable. More specifically the T_{reg} cell mediated suppression appeared to be mediated by the induction of apoptosis in the $CD4^{+}CD25^{-}$ effector T cells.

1.5.6 Antigen specificity of T_{reg} cells

$CD4^+CD25^+$ T_{reg} cells have been shown to have a polyclonal TCR specificity similar to that of helper T cells suggesting a broad range of antigen specificities (139). Although there are some tumour specific antigens, the vast majority of antigens expressed by tumours are also expressed on normal cells. This is interesting as there is some evidence that T_{reg} cells have an increased specificity for self antigens (145, 146). There are now several studies of the roles of T_{reg} cells in the response to infectious pathogens (102, 147, 148). Together these studies suggested that T_{reg} cells may also have a specificity for foreign antigens. It is unclear how specificity for these foreign antigens arises but it has been suggested that molecular mimicry, foreign peptides with a similar structure to self peptides, may provide a signal for pathogen specific-T_{reg} cells and in the context of tumour immunology, also specific TAAs. The LAGE1 protein, for example, has been shown to be a ligand for tumour-specific T_{reg} cell clones generated from the TILs of melanoma patients (89). LAGE1 is expressed in cancer cells and normal testis, but not in other human normal tissues. Finally, the same research group was found T_{reg} cells clones from human patients that could specifically recognise peptides derived from tumour specific ARTC-1 (149).

1.6 T_{reg} cell manipulation for the treatment of cancer

If the recruitment or induction of T_{reg} cells is required by tumours to create part of their immunological protection and hence evade the anti-tumour immune response, therapies targeting these T_{reg} cells should be useful in restricting tumour growth.

1.6.1 Systemic T_{reg} cell inactivation

The seminal publications of North and Awwad in the late 1980s and early 1990s investigating the timing of the anti-tumour immune response were the original empirical observations of the therapeutic benefit of T_{reg} cell depletion (150-153). North and Awwad furthered this work in 1990 by showing that it was possible to overcome dominant immunosuppression at a late stage of tumour development and cause an immunologically mediated tumour regression when tumour-bearing mice were treated with a single injection of the anti-mitotic drug Vinblastine (Vb) (154). These results were consistent with their interpretation that at a late stage of tumour development,

functionally suppressed anti-tumour $CD8^+$ CTLs were non-cycling and co-existed with a functionally active and dominant population of expanding $CD4^+$ T_{reg} cells that could be selectively destroyed by the anti-mitotic nature of Vb. Whilst similar experiments in the present study showed similar effects, they were limited and perhaps more importantly they lack clinical relevance. Patients presenting with MM have established tumours so treating at a specific time-point post tumour challenge (for example day 15) is not a possibility. Therefore, the treatment of established tumours with T_{reg} cell inactivating therapies was undertaken.

On its own, the systemic depletion of T_{reg} cells via the administration of an anti-CD25 mAb had significant success (155-157) without resulting in any significant autoimmune side-effects. It must be noted however that such pre-treatments are also clinically irrelevant. In combination with vaccination strategies or further mAb treatments systemic T_{reg} cell depletion has also had success but these treatments (described below) were also administered prior to tumour challenge or within only 1 or 2 days of tumour implantation. Pre-treatment of mice with anti-CD25 mAb has been shown to hinder B16 murine melanoma growth but can also enhance the immunogenicity of a tumour cell based vaccine against B16 melanoma (87). Survival of mice was even further improved by the treatment of mice with a combination of anti-CD25 mAb to deplete T_{reg} cells and anti-CTLA-4 mAb to block T cell costimulation (87). There is sufficient evidence to suggest that the immune response raised against tumour-expressed antigens may cross react with normal tissue, due to shared self antigens, resulting in both tumour regression but also autoimmunity (158-160). Although the early studies with systemic anti-CD25 mAb depletion did not report any serious autoimmune side-effects, the combination of strong TCR stimulation with the absence of T_{reg} cells has been shown to result in multi-organ specific autoimmune disease (161).

1.6.2 Intra-tumoural T_{reg} cell inactivating therapies

Many groups have targeted CD25 as a mechanism of depleting T_{reg} cells and studying the resultant effects on T cell activation, trafficking, and/or effector functions. Until recently it was widely believed that treatment with anti-CD25 mAb resulted in the rapid and efficient depletion of $CD4^+CD25^+$ T_{reg} cells as determined by secondary staining

with FACS mAbs against a different CD25 epitope (132). A recent concise study by Kohm *et al* (2006) found that the administration of anti-CD25 mAb did not result in the depletion of the $CD25^+$ T_{reg} cells but a shedding of the CD25 molecule from the surface of cells. This conclusion was supported by the findings that anti-CD25 mAb treatment decreased the number of $CD4^+CD25^+$ T cells but not $CD4^+Foxp3^+$ T cells and as the vast majority of $CD4^+CD25^+$ T cells are Foxp3 in the study it was concluded CD25 was lost from the cells only. This very recent data suggests that inactivation rather than depletion is occurring. In these PhD thesis studies the use of anti-CD25 mAb in a novel treatment regime involving intra-tumoural treatments into established tumours was investigated. During the time of these thesis studies it was also revealed by two international research groups that the intra-tumoural inactivation of T_{reg} cells based on CD4 and GITR expression can also result in tumour growth inhibition. The intra-tumoural depletion of total $CD4^+$ T cells via the administration of an anti-CD4 mAb inside the murine fibrosarcomas resulted in tumour growth inhibition of established tumours (28). A low dose of the intra-tumoural mAb was titrated in this experiment in order to ensure that the observed tumour growth inhibition was a direct result of the local depletion of $CD4^+$ T cells and not a systemic effect. Although these results were positive, it is assumed that as most intra-tumoural $CD4^+$ T cells are T_{reg} cells in established tumours that the treatment selectively targeted T_{reg} cells and not $CD4^+$ helper T cells which have also been shown to be required for the anti-tumour immune response. Perhaps a more specific approach to the intra-tumoural inactivation of T_{reg} cells was the intra-tumoural administration of anti-GITR mAb in a further murine tumour model (29). Intra-tumoural anti-GITR mAb treatment was shown to again result in tumour growth inhibition most likely due to the inactivation of intra-tumoural T_{reg} cells. As mentioned above, these contemporary PhD thesis studies investigated the efficacy of intra-tumoural inactivation of T_{reg} cells via the administration of anti-CD25 mAb. These studies also furthered this work to include the administration of anti-CTLA-4 and anti-GITR mAbs intra-tumourally to inhibit tumour development. In light of current knowledge, that the T_{reg} cell response to tumours is complex and may involve multiple pathways of T_{reg} cell mediated immunosuppression, a novel combination of intra-tumoural anti-CD25, anti-CTLA-4 and anti-GITR mAbs was also trialled.

1.6.3 Combination therapies to target multiple aspects of anti-tumour immune response

Malignant mesothelioma, like many invasive solid tumours is difficult to treat. Surgery is often a preferred first treatment for MM but is complicated by the fact that tumour deposits often remain (5). On its own immunotherapy has met with some success in the treatment of cancers, including MM, but may be boosted by combination with other approaches including surgery, chemotherapy, vaccination or apoptosis induction. In a recently published study using a murine model of mesothelioma it was found that chemotherapy induced apoptosis (gemcitabine) of residual tumour deposits following surgical debulking improves tumour clearance and is required for the induction of long-term immunologic memory (162). In a similar way, this thesis proposed the combination of intra-tumoural T_{reg} cell inactivation via anti-CD25 mAb treatment with the induction of apoptosis in the tumour cells. Alpha-tocopheryl succinate (α-TOS) is an analogue of Vitamin E which has been shown in *in vitro* experiments to specifically induce apoptosis in human mesothelioma cells but to be mostly non-toxic to normal mesothelial cells (163). In a model of human mesothelioma involving the xenograft of human MM cells into nude mice it was shown that α-TOS can also induce apoptosis in tumour cells *in vivo* while being largely non-toxic (164). α-TOS has been shown to synergise with tumour necrosis factor-related apoptosis-inducing ligand (TRAIL) dependent apoptosis in cancer cells (165). The activation of nuclear factor-kappaB (NF-κB) has been shown to interfere with induction of apoptosis triggered by TRAIL so an agent that can suppress NF-κB activation may sensitise tumour cells to TRAIL-dependent apoptosis. α-TOS has been shown to sensitise cells to TRAIL mediated apoptosis and further supports the possibility that this semisynthetic analogue of vitamin E is a potential adjuvant in cancer treatment. A further example of the potential synergy between apoptosis induction and immunotherapy in murine tumours was demonstrated by very recent experiments using the lewis lung model (166). The chicken anaemia virus-derived Apoptin protein was shown to induce apoptosis in tumour cells but not in normal diploid cells. IL-18 is a Th1-type cytokine that has demonstrated potential as a biological adjuvant in murine tumour models as it induces high levels of IFN-γ secretion from both NK and T cells. In this study it was reported that the growth of established tumours in mice immunized with the Apoptin protein in conjunction with IL-18 was significantly inhibited as a result of this synergistic

treatment compared with the growth of tumours in mice treated with either modality alone.

Chapter 2:
Materials and Methods

2.1 Materials

2.1.1 Mice

Female C57BL/6J mice between 6 and 8 wks of age were obtained from the Animal Resources Centre (Perth, Australia) and maintained under SPF housing conditions (Discipline of Microbiology and Immunology, University of Western Australia). All animal work was carried out in accordance with the guidelines of The National Health and Medical Research Council of Australia and the approval of The University of Western Australia's Animal Ethics Committee.

2.1.2 Human malignant mesothelioma biopsies

Human tissue biopsy array slides comprising human malignant mesothelioma, pleural effusion associated with MM and control tissue samples were kindly provided by Prof. Bruce Robinson. Prof. Robinson's group developed this tissue biopsy slide array which can be used for the immunohistochemical analysis of multiple biopsy samples at the one time with a concurrent comparison to multiple organ control tissues. These slides are paraffin embedded and hold approximately 35 MM biopsy samples plus approximately 35 pleural effusion samples and 35 control tissues samples such as tonsil and appendix (Fig. 2.1).

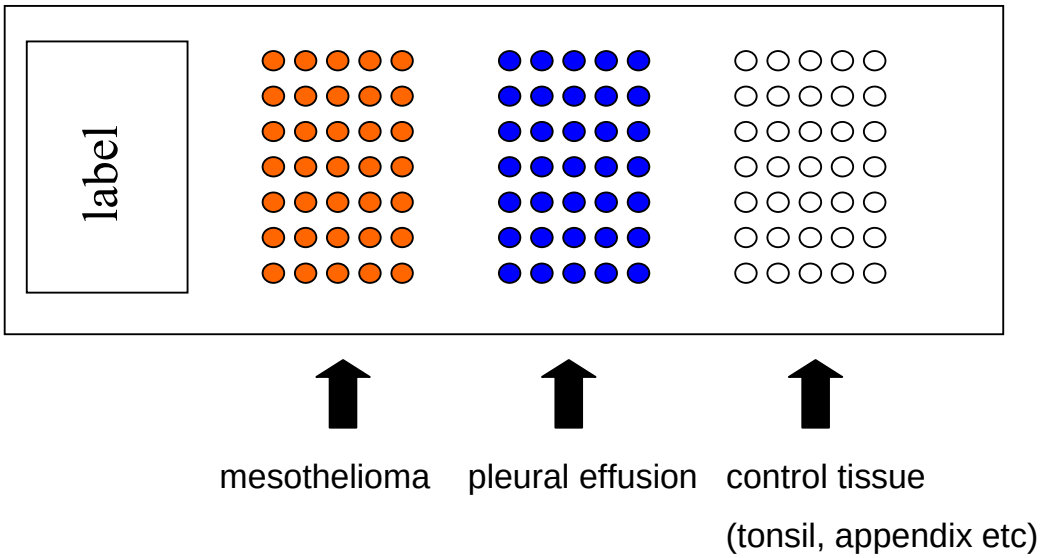

Figure 2.1: Representation of human MM tissue array slide

Multiple frozen human MM biopsy samples along with pleural effusions samples and normal control tissue samples were paraffin embedded on tissue array slides.

2.1.3 Reagents, recipes and equipment used for cell culture, tumour implantation, antibody preparation and the preparation of single cell suspensions.

Table 2.1 presents the hybridoma and tumour cell lines used in these studies. Table 2.2 outlines reagents used while Table 2.3 describes the required equipment for the above techniques. Below are the recipes for all required solutions.

10 mM calcium chloride

1.47 g $CaCl_2$ was dissolved in 100 ml ddH_2O. 20 ml aliquots were made and sterilised by autoclaving. Aliquots were stored at room temp.

RPMI-1640

Dissolve 10.4 g RPMI-1640 in 900 ml ddH_2O with 2 g $NaHCO_3$. pH to 7.2 (0.2 below the desired 7.4 as pH rises upon filtration). Make up to 1 L and filter sterilise using Gelman vacuum filter (0.2 μm). RPMI-1640 was stored at 4°C.

10% FCS RPMI-1640

In a laminar flow hood, 500 ml of sterile RPMI-1640 was supplemented with 5 ml of sterile L-glutamine, 5 ml of sterile antibiotics for media solution, 50 ml of sterile FCS and 40 μl of sterile 0.5 M 2-mercaptoethanol. Supplemented RPMI-1640 was stored at 4°C. L-glutamine has a short half-life in media, add fresh L-glutamine to media if more than 1 month old.

0.1 M EDTA

3.72 g EDTA was dissolved in 40 ml ddH_2O. pH to 8 as EDTA will not dissolve unless at pH 8. Make up to 100 ml with ddH_2O and autoclave to sterilise. Store at room temp

0.5 M EDTA

18.61 g EDTA was dissolved in 40 ml ddH_2O. pH to 8 as EDTA will not dissolve unless at pH 8. Make up to 100 ml with ddH_2O and autoclave to sterilise. Store at room temp

0.5 M 2-mercaptoethanol

Dissolve 1.74 ml 2-mercaptoethanol in 50 ml ddH_2O. Filter sterilise using a 2 µm syringe filter and make 500 µl aliquots. Store at -20°C and add 40 µl to 500 ml RPMI-1640 when required.

1 x PBS

Add one tablet of PBS to 100 ml ddH_2O. Autoclave to dissolve and sterilise. Store at room temp.

2% Dextran-T500 in PBS

Add 4 g Dextran-T500 to 200 ml 1 x PBS. Make 10 ml aliquots and autoclave to sterilise. Store at room temp.

1 mM EDTA in PBS

Add 0.0327 g EDTA to 100 ml 1 x PBS. pH to 7.2 and make 10 ml aliquots. Autoclave to sterilise and store at room temp.

Antibiotics for tissue culture media

Reconstitute 1 x 600 mg vial of benzyl penicillin in 5 ml ddH_2O. Add to a beaker containing 5 x 40 mg/ml vials of gentamicin. Make volume up to 100 ml with ddH_2O. Filter sterilise using a 0.2 µm syringe filter and make 5 ml aliquots. Store at -20°C and add a 5 ml aliquot to 500 ml RPMI-1640 when required.

Heat inactivated FCS

Defrost 500 ml FCS in 37°C water bath for approximately 1 hr. Heat inactivate FCS by incubating for 30 min at 60°C. Make 50 ml sterile aliquots in laminar flow hood and store at -20°C.

Saturated ammonium sulphate

Weigh out 761 g ammonium sulphate. Make up volume to 1 L with ddH_2O. Autoclave to dissolve and sterilise. Store at room temp (some crystal will drop out of solution).

Collagenase/dispase solution

Make to a concentration of 200 U/ml by dissolving 200 mg collagenase and 200 mg dispase in 200 ml sterile DMEM. Filter sterilise through a 0.2 µm filter. Solution is stored in 50 ml aliquots at -20°C for a maximum of 6 months.

3 mg/ml EDTA in PBS

0.6 g EDTA is dissolved in 200 ml 1 x PBS. Make 10 ml aliquots and autoclave to sterilise. Store at room temp.

DNase I

Dissolve 23 mg DNase I in 1 ml of ddH_2O and 1.3 ml 10 mM $CaCl_2$. Filter sterilise using a 0.2 µm syringe filter and store at -20°C in 100 µl aliquots.

Liberase blendzyme 3

Resuspend 7 mg vial in 2 ml injection quality H_2O. Swirl on ice for 30 min to dissolve. Filter sterilise using a 0.2 µm syringe filter and make 100 µl aliquots. Store at -20°C.

L-glutamine

Dissolve 7.3 g L-glutamine in 250 ml ddH_2O. Stir using a magnetic stirring flea for 5-10 min to dissolve. Filter sterilise using a 0.2 µm syringe filter and make 5 ml aliquots. Store at -20 °C and add 5 ml to 500 ml RPMI-1640 when required.

Freezing medium

Comprises 90% (v/v) FCS and 10% (v/v) DMSO. Make fresh or store for short term (2 weeks) at 4°C.

Red cell lysis buffer

8.3 g NH_4Cl is dissolved in 1 L ddH_2O. 4.12 g Tris is dissolved in 200 ml ddH_2O. Add 9 parts NH_4Cl solution to 1 part Tris solution. Filter sterilise using a Gelman vacuum filter (0.2 µm) and make 100 ml aliquots to be stored at room temp.

Supplemented CD hybridoma media

Add to 1 L CD hybridoma media 10 ml of sterile L-glutamine and 10 ml of sterile antibiotics for media. Store at 4°C.

Trypan blue

Dissolve 0.1 g trypan blue in 100 ml 1 x PBS. Filter sterilise using a 0.2 µm syringe filter. Make 5 ml aliquots and store at room temp.

Table 2.1: Tumour and hybridoma cell lines

A description of tumour cell lines, hybridoma cell lines and cytokine positive control cells.

Cell line	Description/mAb production	Obtained from/supplier
43B2	Anti-ross river virus IgG1 mAb	Dr C. Johansen, University of Western Australia, Australia
9H10	Anti-CTLA-4 mAb	Dr. D Cooper, Clinical Cell Culture C3, Australia
AE17	C57BL/6J murine mesothelioma	Prof. B Robinson, University of Western Australia, Australia
B16	C57BL/6J murine melanoma	Laboratory stocks
EL4	C57BL/6J murine lymphoma	Laboratory stocks
DTA-1	Anti-GITR mAb	Prof S Sakaguchi, Institute for Frontier Medical Science, Japan
JES52A5	Anti-IL-10 mAb	Dr Dale Godfrey, University of Melbourne
MICK-2	IL-4/IL-10 positive control cells for intra-cellular flow cytometry	BD Pharmingen, USA
PC61	Anti-CD25 mAb	Prof J Allison, University of California, USA

Table 2.2: Reagents used for cell culture, tumour implantation, antibody preparation and the preparation of single cell suspensions

Reagent	Product number	Supplier
2-Mercaptoethanol	44143	BDH
Ammonium chloride (NH_4Cl)	10017	AnalaR, BDH
Ammonium sulphate $(NH_4)_2SO_4$	A56-500g	Univar, Ajax Finechem
Benzyl penicillin 600 mg	R10329	CSL
Calcium chloride ($CaCl_2$)	960	Ajax, Unilab
CD Hybridoma media	11279	Gibco
Collagenase Type 1A	C2674	Sigma
Dextran T-500	17.0320.01	Amersham Pharmacia
Dimethyl sulphoxide (DMSO)	10323.4L	BDH
Dispase II	165859	Roche Diagnostics
Fetal calf serum (FCS)	10099-141	Gibco BRL
Gentamicin 80mg/2ml	509641	David Bull Laboratories
L-glutamine	G3126-100g	Sigma
Liberase blendzyme 3	11824184001	Roche Diagnostics
Phosphate buffered saline Dulbecco A tablets (PBS)	BR0014G	Oxoid
RPMI medium-1640	31800-089	Gibco BRL
Triton X-100	161-0407	Biorad
Trypan Blue	-	Hopkins and Williams
Trypsin-EDTA	T4049	Sigma

Table 2.3: Equipment used for cell culture and antibody preparation

Equipment	Product number	Supplier
Centrifuge tubes 15 ml 50 ml	 352099 352098	 BD Falcon, USA BD Falcon, USA
CO_2 incubator	-	Forma Scientific
Cryotubes	375418	Nalge Nunc International, USA
Dialysis membrane (20 mm)	453103	Selby, USA
Needles N25/500 for Hamilton	 N1531	 SGE, Australia
Neubauer chamber	B.5.748	Hawksley, England
Syringes 100 µl Hamilton	 005250	 SGE, Australia
Tissue culture flasks 75 cm^2 225 cm^2	 156499 159934	 Nalge Nunc International, Denmark Nalge Nunc International, Denmark
Tissue culture hood	-	Gelman Sciences
Vernier microcallipers	-	Kaiser, Australia

2.1.4 Reagents, recipes and equipment used for flow cytometry, immunoassays and cell sorting.

Table 2.4 lists all antibodies and conjugates used in these studies. Table 2.5 details all reagents required and Table 2.6 all equipment required for the above mentioned techniques. Below are recipes for all required solutions.

Cell staining buffer

0.0352 g Sodium azide was dissolved in 100 ml 1 x PBS. pH to 7.4, autoclave to sterilise and store at room temp. 5 ml sterile FCS is added prior to use. After addition of FCS, cell staining buffer should be stored at 4°C.

FACS sort buffer

1 x PBS was supplemented with 1 mM EDTA and 1% FCS (heat-inactivated). Filter sterilise using a 0.2 μm syringe filter and store at 4°C.

1 mM EDTA

Add 0.0327 g EDTA to 100 ml ddH_2O. pH to 7.2 and make 10 ml aliquots. Autoclave to sterilise and store at room temp.

Cell lysis buffer

To make 500 ml add 0.605 g Tris-HCl (10 mM), 0.690 g NaH_2PO_4 (10 mM), 0.710 g Na_2HPO_4 (10 mM), 3.790 g NaCl (130 mM), 1.33 g Sodium pyrophosphate (10 mM) to 495 ml ddH_2O with stirring. pH to 7.5 and add 5 ml 1% (v/v) Triton X-100. Filter sterilise and store at 4°C. Add 5 μl/ml of protease inhibitor cocktail prior to use.

1% (v/v) Triton X-100

Add 1 ml Triton X-100 to 99 ml ddH_2O. Filter sterilise and store at room temp.

Carbonate ELISA coating buffer

Add 1.325 g Na_2CO_3 (0.025 M) and 1.05 g $NaHCO_3$ (0.025 M) to 400 ml ddH_2O. pH to 9.6 and then make up to 500 ml. Autoclave to sterilise and store at room temp.

Phosphate ELISA coating buffer

Add 5.9 g Na_2HPO_4 and 8.05 g NaH_2PO_4 to 500 ml ddH_2O. pH to 6.5 and autoclave to sterilise. Store at room temp.

Cytokine ELISA antibody diluent

Sterile 1 x PBS was supplemented with 10% (v/v) FCS. Make fresh and store in the short term at 4°C.

TBST ELISA wash buffer

To 1 L ddH_2O add 3.032 g Tris and 8.776 g NaCl. pH to 7.76 and sterilise. Store at room temp. Add 0.05% Tween-20 prior to use.

Cytokine ELISA wash buffer

Sterile 1 x PBS was supplemented with 10% (v/v) sterile FCS and 0.05% (v/v) Tween-20. Make fresh and store in the short term at 4°.

Mouse osmolarity buffered saline (MOBS)

In ddH_2O, make a solution containing 6.46 mM $NaHPO_4$, 1.47 mM KH_2PO_4, 2.68 mM KCl and 1.68 mM NaCl. pH to 7.4 and autoclave to sterilise. Store at room temp.

Neutralising antibody ELISA antibody diluent buffer

Sterile MOBS was supplemented with 1% (w/v) BSA and 0.05% Tween-20. Store at 4°C.

Neutralising antibody ELISA antibody binding buffer

A 0.159% (w/v) Na_2CO_3 and 0.293% (w/v) $NaHCO_3$ solution was made in ddH_2O. pH to 9.6 and autoclave to sterilise. Store at room temp.

Neutralising antibody ELISA blocking buffer

Sterile MOBS buffer supplemented with 1% (w/v) BSA. Store at room temp.

Neutralising antibody ELISA wash buffer

Sterile MOBS was supplemented with 0.05% Tween-20 and stored at room temp.

p-nitrophenyl phosphate

Dissolve a 5 ng tablet in 5 ml ddH_2O. Make fresh.

Dialysis tubing wash buffer

Make a 1 mM solution of EDTA and supplement with 2% (w/v) $NaHCO_3$. Autoclave and store at room temp.

Table 2.4: Antibodies and conjugates

Antibody	Specificity	Clone	Conjugate	Supplier	Product Number
CCL22	mouse	158113	purified	R&D systems	MAB439
CD103	mouse	M290	PE	BD Pharmingen	557495
CD25	human	4C9	purified	Novocastra	NCL-CD25-305
CD25	mouse	PC61	FITC	Ebioscience	11-0251
CD25	mouse	7D4	FITC	BD Pharmingen	553072
CD25	mouse	PC61	PE	Ebioscience	12-0251-83
CD3	mouse	145-2C11	PE-Cy5	Ebioscience	15-0031-81
CD4	mouse	RM4-5	APC	Ebioscience	17-0042-82
CD62L	mouse	MEL-14	PE-Cy5	Ebioscience	15-0621-81
CD69	mouse	H1.2F3	PE	Ebioscience	12-0691
CD8	mouse	53-6.7	PE	Ebioscience	12-0081
CTLA-4	mouse	UC10-4F10-11	PE	BD Pharmingen	553720
Foxp3	human	236A/E7	affinity purified	Ebioscience	14-4777
Foxp3 (staining kit)	mouse	FJK-16s	PE	Ebioscience	72-5775-40
Goat anti-rabbit IgG	rabbit	-	FITC	BD Pharmingen	554020
IgG	mouse	A3562	alkaline phosphatase	Sigma,	A3562
IL-10	mouse	JES5-16E3	PE	BD Pharmingen	554467
IL-10	mouse	JES5-2A5	capture antibody for ELISA	BD Pharmingen	551215
IL-10	mouse	JES5-16E3	biotinylated detection antibody for ELISA	BD Pharmingen	29934
IL-4	mouse	11B11	PE	BD Pharmingen	554435
IL-4	mouse	11B11	capture antibody for ELISA	BD Pharmingen	554434
IL-4	mouse	BVD6-24G2	detection antibody for ELISA	BD Pharmingen	554390
Nrp-1	human	H-286	purified	Santa Cruz Biotechnology	Sc-5541
Rabbit anti-goat IgG	goat	-	alkaline phosphatase	Cappel	59292
TGF-β1	mouse	A75-2	Capture antibody for ELISA	BD Pharmingen	555052
TGF-β1	mouse	A75-3	Biotinylated detection antibody for ELISA	BD Pharmingen	555053

Table 2.5: Reagents used for flow cytometry, immunoassays and cell sorting

Reagent	Product number	Supplier
Bovine serum albumin (BSA)	85040	JRH Biosciences
Cytofix/Cytoperm solution set	554722;554723	BD Pharmingen
Ficoll-paque Plus	17-144-03	Amersham Biosciences
Goat anti-serum to rat serum	56005	Cappel
Imag anti-mouse PE particles	557899	BD Pharmingen
Imag Buffer	552362	BD Pharmingen
Imag mouse CD4 T lymphocyte enrichment set	558131	BD Pharmingen
osmosol	LP-A64296	Lab Aids
Phase murine serum amyloid A immunoassay	TP802-M	Tridelta
Protease inhibitor cocktail	P8340	Sigma
Recombinant IL-10 standard	550070	BD Pharmingen
Recombinant IL-4 standard	550067	BD Pharmingen
Recombinant TGF-beta standard	Component of 559119	BD Pharmingen
Streptavidin-HRP for ELISA	554066	BD Pharmingen
Tetramethylbenzidine (TMB) liquid substrate system	T0440	Sigma

Table 2.6: Equipment used for flow cytometry, immunoassays and cell sorting

Equipment	Supplier	Product number
Concentration columns		
Microconcentrator 100	Amicon	4211
Centricon plus-20	Amicon Millipore	UFC28HK08
FACS columns/round bottom test tubes	BD Falcon	352054
Flow cytometers		
FACS Calibur	Becton Dickenson	343023
FACS Vantage	Becton Dickenson	343268
Cell Quest analysis software	Becton Dickenson	342182
FlowJo analysis software	FlowJo	v7.1.3
Imag cell separation magnet	BD Pharmingen	552311
Maxisorp ELISA plates	Nalge Nunc	44-2404
Polytron tissue homogeniser	Janke and Kunkel	Ultra-turrax T25

2.1.5 Reagents, recipes and equipment for RNA extraction, RT-PCR and agarose gel electrophoresis

Table 2.7 outlines primers used for real-time RT-PCR. Table 2.8 details reagents required and Table 2.9 the equipment required for the above techniques. Below are the recipes of all required solutions.

1% Agarose (w/v)

5 g agarose was added to 500 ml 1 x TAE buffer. Make 30 ml aliquots and autoclave to allow dissolution and to sterilise. Store at room temp. Microwave on low for 5 min to melt and add 2 µl ethidium bromide prior to use.

10 mg/ml ethidium bromide

Dissolve 1 g of ethidium bromide in 100 ml ddH_2O by stirring for several hours. Store at 4°C in the dark.

SEB

Make in 0.1 M EDTA a 50% sucrose solution. pH to 8 to aid dissolution of EDTA and add 0.1% bromophenol blue. Make 5 ml aliquots and store at room temp.

40 x TAE buffer

Dissolve 193.6 g Tris and 14.9 g EDTA in 1 L ddH_2O. pH to 8, autoclave and store at room temp. Dilute 1:40 with ddH_2O prior to use.

$T_{10}E$ buffer

A solution of 10 mM Tris and 1 mM EDTA was made in ddH_2O. pH to 8.0 to aid dissolution of EDTA. Autoclave and store at room temp.

Table 2.7:Primers

Primers for real-time RT-PCR were resuspended at the appropriate concentration in $T_{10}E$ buffer and stored at -20°C.

Primer	Sequence (5'-3')	Genbank accession number	Final concentration in PCR
HPRT-forward	TGA AGA GCT ACT GTA ATG ATC AGT CAA C	HPRT:NM_013556	0.4 mM
HPRT-reverse	AGC AAG CTT GCA ACC TTA ACC A		
TGF-β-forward	CGC CAT CTA TGA GAA AAC C	TGF-β1:NM_011577	0.3 mM
TGF-β-reverse	GGT AGA GTT CCA CAT GTT GC		

Table 2.8: Reagents for RNA extraction, RT-PCR and agarose gel electrophoresis

Product	Product number	Supplier
100bp DNA ladder	M-DNA-100bp	Axygen Biosciences
Agarose, LE	V312B	Promega
Bromophenol blue	B-6131	Sigma
Ethidium bromide	E-8751	Sigma
iTaq SYBR green supermix with Rox	170-8850	Biorad
Oligo dT(15) primer	C1101	Promega
QIAshredder columns	79656	Qiagen
RNAlater	76106	Qiagen
RNase free DNase set	79254	Qiagen
RNaseZap	9780;9782	Ambion
RNasin plus RNase inhibitor	N2611	Promega
RNeasy mini kit	74106	Qiagen
Sensiscript RT kit	205211	Qiagen
Sucrose	A530-500g	Univar

Table 2.9: Equipment for RNA extraction, Genechip, and real-time RT-PCR

Equipment	Supplier	Product number
GelDoc imaging system	Kodak	-
Filter tips		
1000 µl	Axygen	TF-1000-R-S
200 µl	Sarstedt	70.76.211
10 µl	Sarstedt	70.1130.210
Gene-amp 5700 PCR machine	Applied Biosystems	-
Heater block	Grant	-
Mini-sub DNA cell	Biorad	-
PCR optical caps	Applied Biosystems	4323032
PCR optical tubes	Applied Biosystems	N801-0933

2.1.6 Reagents and recipes used to prepare non-antibody treatments for tumour growth inhibition.

Table 2.10 details the non-antibody treatments used in these PhD studies. Below are recipes for the preparation of such reagents and any associated solutions.

200 mM α-Tocopheryl succinate

1.6 g α-TOS was dissolved in 15 ml sterile DMSO with slight warming to 37°C. 1 ml aliquots were made and stored at 4°C. Aliquots freeze at 4°C and as such were warmed to 27°C to ensure dissolution of α-TOS prior to use.

5 µg/ml anti-CCL22 mAb

500 µg stock of anti-CCL22 mAb was resuspended in 1 ml sterile 1 x PBS. 750 µl of this stock solution was stored at -20°C. 250 µl was further diluted by the addition of 24.75 ml 1 x PBS. 500 µl aliquots were made and stored at -20°C.

100 µg/ml TGF-β soluble receptor

5o µg stock of TGF-β soluble receptor was resuspended in 500 µl of sterile l x PBS + 0.1% (w/v) BSA. Further dilutions to 25 µg/ml and 5 µg/ml were made in sterile 1 x PBS as required and stored at -20°C.

Nucolox

7.5 g nucolox was dissolved in 200 ml sterile ddH_2O. 500 µl aliquots were made and stored at 4°C.

Table 2.10: Non-antibody treatments for tumour growth inhibition

Product	Catalogue number	Supplier
Alpha-tocopheryl succinate	95255	Sigma
Nucolox	63980	Sigma Pharmaceuticals
Recombinant mouse TGF-β soluble receptor II/Mouse Fc	1600-R2-C	R&D Systems
Vinblastine	461049	DBL

2.1.7 General reagents, recipes and equipment

Table 2.11 details general reagents required for multiple techniques. General equipment is presented in Table 2.12. Recipes for general solutions are presented below. Table 2.13 list URLs for selected suppliers of reagents and equipment.

10 x PBS

22.75 g Na_2HPO_4, 5.53 g NaH_2PO_4 and 2.87 g NaCl were dissolved in 900 ml ddH_2O. pH to 7.4 and make up to 1 L. Make 500 ml aliquots, autoclave and store at room temp.

1M NaOH

10 ml 10M NaOH added to 90 ml ddH_2O. Store at room temp away from any acids.

1M HCl

Add 8.4 ml 37% HCl to 91.6 ml ddH_2O. Store at room temp away from any bases.

Table 2.11: General reagents

Product	Catalogue number	Supplier
Disodium hydrogen orthophosphate (Na_2HPO_4)	10249.4C	AnalaR, BDH
Ferric chloride	UN2582	Pharmo Scope
DNase 1, type II	D4527	Sigma
Ethanol, absolute	90144.9020	Merck
Ethylenediaminetetraacetic acid (EDTA)	10093.5V	AnalaR, BDH
H_2O, injection quality	221343	Astra Zenica
Hydrochloric acid (HCl)	101256J	AnalaR, BDH
Methoxyfluorane (Penthrane)	R43144	Medical Developments
Polyoxyethylene sorbitol monolaurate (tween-20)	10245	Sigma
Potassium chloride (KCl)	10198	AnalaR, BDH
Sodium azide (NaN_3)	1222	Labchem
Sodium bicarbonate ($NaHCO_3$)	44143	BDH
Sodium carbonate (Na_2CO_3)	10240	AnalaR, BDH
Sodium chloride (NaCl)	10241	AnalaR, BDH
Sodium dihydrogen orthophosphate (NaH_2PO_4)	10245	AnalaR, BDH
Sodium hydroxide (NaOH)	10252	AnalaR, BDH
Sodium pyrophosphate ($Na_4P_2O_7$)	30208	AnalaR, BDH
Tris	15504-020	Gibco BRL
Tris-HCl	T3253-500g	Sigma

Table 2.12: General Equipment

Equipment	Supplier	Product number
Blood collection tubes		
Uncoated	Microtainer BD	365957
EDTA coated	Microtainer BD	365974
Filters		
Micropore syringe		
0.2 µm	Acrodisk Pall Gelman	4612
0.4 µm	Acrodisk Pall Gelman	4614
Vacuum filter (0.2 µm)	Pall Life Sciences	4622
Microfuge tubes		
0.5 ml	Sarstedt	72.699
1.5 ml	Treff lab	96.07246.9.01
2.0 ml	Sarstedt	72.695
Needles		
26 ½ G	Terumo	NN2613R
Syringes		
1 ml tuberculin	Becton Dickenson	302100
2 ml	Becton Dickenson	302204
10 ml	Becton Dickenson	302143
60 ml	Becton Dickenson	300142
pH strips		
2.5-4.5	Merck	1.09541
0-6	Merck	1.09531
6.5-10	Merck	1.09543
Spoon sieve	-	-

Table 2.13: URLs of suppliers

Supplier	URL
Ajax Finechem	www.ajaxfinechem.com
Ambion	www.ambion.com
Amersham Pharmacia	www.apbiotech.com
Axygen Biosciences	www.axygenbio.com
BD Pharmingen	www.bdbiosciences.com/pharmingen
BDH	www.merck.com.au
Becton Dickenson	www.bd.com
Biorad	www.bio-rad.com
Cappel	www.mpbio.com
Corning Costar	www.corning.com/lifesciences
CSL	www.csl.com
Difco	www.corptech.com
Ebioscience	www.ebioscience.com
Flowjo	www.flowjo.com
Gelman	www.pall.com
Geneworks	www.geneworks.com.au
Gibco BRL	www.lifetech.com
Hawksley	www.hawksley.co.uk
JRH Biosciences	www.sigmaaldrich.com
Labchem	www.labchem.net
Merck	www.merck.com
Nalge Nunc International	www.nalgenunc.com
Novocastra	www.novocastra.co.uk
Oxoid	www.oxoid.com.uk
Promega	www.promega.com
Qiagen	www.qiagen.com
R&D systems	www.rndsystems.com
Roche Diagnostics	www.roche.com
Santa Cruz Biotechnology	www.scbt.com
Sarstedt	www.sarstedt.com
Sigma	www.sigma-aldrich.com
Trefflab	www.anachem.com.uk
Tridelta	www.trideltaltd.com

2.2 Methods

All tissue culture was carried out in a laminar flow hood using aseptic techniques.

2.2.1 Murine tumour cell culture, maintenance and tumour cell implantation

The AE17, B16 and EL4 cell lines were maintained in RPMI 1640 media supplemented with 10% FCS, 2 mM L-glutamine, 50 mg/L gentamicin, 60 mg/L benzyl penicillin and 0.05 mM 2-mercaptoethanol. Cells were cultured at 37°C in a 5% CO_2 incubator and passaged when 70% confluent or every 3 days.

2.2.1.1 Resuscitation of cells

A cryovial of cells was thawed by hand and then added dropwise to 10 ml of prewarmed supplemented media in a 15 ml centrifuge tube. Cells were pelleted by centrifugation at 500 x g (1500 rpm) for 5 min and then washed once in 10 ml media. Cells were then resuspended in 15 ml media and transferred to a 75 cm^2 tissue culture flask. The following day the media was replaced with 15 ml fresh media to remove any cells not surviving the freeze/thaw process.

2.2.1.2 Cell passage

Tumour cells are adherent and begin to adhere within 3 hours. Cells were considered ready for passage when the cell monolayers were 70-80% confluent (approximately 1 x 10^7 cells in a large flask and approximately 1 x 10^6 cells in a small flask) or every three days. The cell monolayer was washed once by adding 10 ml PBS to the tissue culture flask. The PBS was then removed and 1 ml trypsin/EDTA added and flasks incubated at 37°C for 2 min in CO_2 incubator. Cells were dislodged from the base of the flask by vigorous tapping. Cells were resuspended in 10 ml media and placed into a 15 ml centrifuge tube and pelleted by centrifugation at 500 x g (1500 rpm) for 5 min. Cell pellets were washed once with 10 ml supplemented media. For a 1/10 split, cells were resuspended in 10 ml media and 1/10 (1 ml) of cells added to a fresh flask containing 14 ml fresh supplemented media. Passage numbers were always noted and AE17 cells not allowed to pass passage 15.

2.2.1.3 Cryopreservation of cells

Cells were only harvested for frozen stocks from flasks that were 70-80% confluent. Cells were detached and washed as per 2.2.1.2 then pelleted, counted by trypan blue exclusion using a neubauer chamber and resuspended in freezing medium at 1-2 x 10^6 cells/ml. 1 ml cells was then transferred to a 1.8 ml cryovial and stored at -20°C overnight prior to relocation to -80°C for short term storage or for long term storage after 24 hours at -80°C the cells were transferred to -180°C.

2.2.1.4 Cell counts by trypan blue exclusion

Cell suspensions were diluted in trypan blue solution and mixed gently. 10 µl of stained cell suspension was transferred to a neubauer chamber and viable cells counted. Dead cells stain blue. Between 30 and 300 cells were counted within a total of 25 squares and each count was repeated 3 times. Cell concentration was calculated as described in equation 1.

Equation 1: Cell counting by trypan blue exclusion

$$\frac{\text{Number of viable cells counted}}{\text{Number of squares counted}} \times 25 \times \text{dilution factor} \times 10^4 = \text{cells/ml}$$

2.2.1.5 Harvesting cells for in vivo implantation

Cells were only harvested from flasks that were 70-80% confluent (approximately 1 x 10^7 cells in a large flask) as per Section 2.2.1.2. Cells were washed twice in 10 ml PBS and were then counted by trypan blue exclusion. Cells were resuspended at the appropriate concentration for implantation and taken on ice to the Animal Care Unit.

2.2.1.6 In vivo tumour cell implantation and growth monitoring

For the subcutaneous growth of tumour, mice were injected s.c. onto the right-hand side of the back of the ribcage at day 0 with the appropriate number of tumour cells in

100 µl PBS using a 100 µl Hamilton syringe (Fig 2.2). For s.c. development of AE17 tumours either 1 x 10^6 or 1 x 10^7 tumour cells were implanted. 1 x 10^6 EL4 cells and 5 x 10^5 B16 cells were implanted s.c for the analysis of other s.c. solid tumours. Tumour growth was monitored daily and tumour areas calculated by multiplying two, right-angled tumour diameters measured using microcallipers as shown in Equation 2. For i.p. implantation of AE17 tumours, 1 x 10^6 tumours cells were resuspended in 100 µl PBS and administered by a single i.p. injection. Tumour development was monitored daily by light palpation of the abdomen, checks for overall loss of condition, such as hunching and ruffling of coat, and the comparison of animal body weight to tumour-free control mice. Hamilton syringes and specially designed needles were washed immediately after tumour cell implantation to avoid blocking. The syringes and needles were washed internally 3 times with 100 µl 1% triton X-100, then 3 times in ddH_2O and 3 times in 70% ethanol and autoclaved with the barrel of the syringe removed.

Equation 2: Tumour area calculation

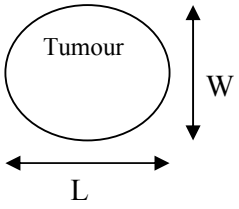

Tumour area (mm^2) = L x W

Figure 2.2: Mesothelioma tumour implantation site.

Mice are implanted s.c. with tumour cells in a 100 µl volume of PBS. Solid tumours develop and are allowed to reach the humane end-point of 100 mm^2 as pictured in the figure.

2.2.2 Euthanasia of mice

Mice were humanely culled, when tumours reached the humane endpoint measurement of 100 mm^2 or if mice had undergone a significant loss of condition as defined by the Animal Ethics Committee by hunching, ruffled fur, slowed movements etc. Mice were anaesthetised by inhalation of methoxyfluorane by placing the animal in a rubber sealed anaesthetic jar containing 1 ml methoxyfluorane for up to 5 min. Mice were considered fully anaesthetised when breathing had slowed and no flinch reaction was observed upon gently squeezing footpads. Mice were then euthanased by cervical dislocation.

2.2.3 Preparation of single cell suspensions

Several methods for the dissociation of solid tissues such as spleen, LN and tumours were trialled.

2.2.3.1 Mechanical dissociation of solid tissues

Tumours, spleens or LN were removed from mice and placed into 1.5 ml microfuge tubes containing 1 ml supplemented media. Tissues were minced inside the microfuge tubes into fine pieces using scissors for approximately 5 min. The tissue homogenate was then transferred to a fine wire mesh spoon sieve resting in a petri dish and forced through using the barrel of a 3ml syringe. Single cell suspensions were collected into a new microfuge tube. The spoon sieves were then washed with a further 0.5 ml media and this media also transferred into the microfuge tube containing the single cell suspension. Cells were then pelleted by centrifugation at 2000 x g (6000 rpm) for 2 min and washed twice in 1 ml PBS by the same centrifugation process. Single cell suspensions of spleens underwent a further red cell lysis step. Cells were resuspended in 1 ml red cell lysis buffer and incubated at room temp with gently inversion for 5 min. 0.5 ml of supplemented media was then added and the cells pelleted by centrifugation as outlined above. Cells were washed a further 2 times with PBS.

2.2.3.2 Collagenase/dispase enzymatic digestion

This method for the digestion of tumours was modified from the murine muscle digestion protocol used in the Beilharz laboratory (167). Tumours were removed from

mice and collected into a 1.5 ml microfuge tube containing 1 ml unsupplemented media. The whole tumour was washed twice with 1 ml PBS by centrifugation at 2000 x g (6000 rpm) for 2 min. The tumour was then transferred to a petri dish containing 5 ml collagenase/dispase solution (200U/ml) and the tumour minced using a scalpel for 10 min or until the slurry could be pipetted with a blunt 10 ml pipette into a 250 ml conical flask containing a magnetic stirring flea. The petri dish was washed with a further 20 ml collagenase/dispase solution which was also transferred to the conical flask. The tumour homogenate was placed on a prewarmed magnetic stirrer at 37°C for 45 min with the stirring flea only just allowing the circulation of the solution. The tumour homogenate was then transferred to a 50 ml Falcon tube and cells pelleted by centrifugation at 500 x g (1500 rpm) for 10 min. Cells were washed twice in 5 ml PBS by centrifugation at 500 x g (1500 rpm) for 5 min. Cells were resuspended in 20 ml trypsin/EDTA and transferred to a clean 250 ml conical flask for further stirring at 37°C for 10 min. 1 ml cell staining buffer was added after 10 min to inactivate trypsin and the tumour homogenate transferred to a 15 ml Falcon tube and remaining clumps allowed to settle out for 10 min. The supernatant containing the well digested single cell suspension was removed, transferred to a clean tube and the cells washed twice with 1 ml PBS.

2.2.3.3 Mechanical dissociation and enzymatic digestion with Liberase blendzyme 3/ DNase

Small tumours (<50 mm^2), spleens and LN were surgically removed and collected into a 1.5 ml microfuge tube containing 500 µl unsupplemented media. Large tumours (>50 mm^2) were collected into a 2 ml microfuge tube containing 1 ml unsupplemented media. Tumours, spleens and LNs were minced finely using scissors for up to 1 min at room temperature before enzymatic digestion for 40 min at room temperature by the addition of 1.4 U (12.5 µl) Liberase blendzyme 3 and 1000 kU (13.5 µl) DNase 1 with mixing on a rotating wheel (all volumes were doubled for large tumours). The digestion was stopped by the addition of 75 µl of 0.1 M EDTA and 5 min incubation at room temp with mixing on a rotating wheel. The tumour cell homogenate was pushed through a fine wire mesh spoon sieve using the plunger of a 3 ml syringe to break down any remaining clumps. The single cell suspension was washed twice with 500 µl PBS and centrifuged at 2000 x g (6000 rpm) for 2 min in a microcentrifuge before staining

with fluorochrome-conjugated antibodies for flow cytometric analysis. Red blood cells were lysed in the spleen preparations as outlined in section 2.2.3.1

2.2.3.4 Preparation of lymphocytes from whole blood.

Blood was collected by two methods depending on the amount required. For small volumes of blood (<200 µl) a nick in the tail vein of mice was made using a scalpel. Blood was collected into an EDTA-coated blood collection tube to prevent clotting. The bleeding was halted by the dabbing of ferric chloride onto the nick and the application of pressure for approximately 2 min. For the collection of up to 1 ml of blood, mice were anaesthetised by the inhalation of methoxyfluorane and then pinned out on a cork board. A 26 ½ gauge needle attached to a 1 ml syringe was inserted into the heart of the mouse and the blood collected in the syringe transferred to an EDTA coated blood collection tube. Mice were then euthanased by cervical dislocation (Section 2.2.2). The whole blood was then added to a tube containing an equal volume (to the amount of blood collected) of 3 mM EDTA in PBS. An equal volume (to the amount of blood collected) of 2% Dextran-T500 was then added and gently mixed with the blood/EDTA solution. Blood was incubated at 37°C for 30 min to allow separation of lymphocytes. The clear upper layer containing lymphocytes was then transferred to a new tube and cells pelleted by centrifugation at 2000 x g (6000 rpm for 2 min. Cells were resuspended in 1 ml red cell lysis buffer to lyse any remaining red blood cells as outlined in section 2.2.3.1. Lymphocytes were washed twice in 1 ml PBS by centrifugation at 2000 x g (6000 rpm) for 2 min.

2.2.4 Flow cytometry

Flow cytometric data for stained cell populations were acquired on a FACS Calibur flow cytometer and analysed using CellQuest or FlowJo software. Instrument settings were set by an experienced operator using unstained cells as negative controls. Single stained cells were used to set initial positive settings and then double stained cells for setting compensations.

2.2.4.1 Cell surface staining for flow cytometry

Single cell suspensions for flow cytometric staining of cell surface markers were washed twice in 1 ml cell staining buffer prior to resuspension at a concentration of approximately 1 x 10^7 cells/ml. Approximately 1 x 10^6 cells were then stained in a 100 µl volume of cell staining buffer in a 1.5 ml microfuge tube by the addition of 1 µl (1/100 dilution, usually equivalent to 200 µg antibody) of fluorochrome conjugated antibody. Cells were incubated at 4°C in the dark for 20 min. Cells were flooded by the addition of an additional 200 µl cell staining buffer and pelleted by centrifugation at 2000 x g (6000 rpm) for 2 min. Cells were then washed a further 2 times with 200 µl cell staining buffer prior to resuspension in 200 µl cell staining buffer for acquisition.

2.2.4.2 Intra-cellular staining for flow cytometry

In general, intra-cellular staining is damaging to cells and so works best on a large starting population of cells and requires very gentle handling of the cell pellets as they become very fragile. For intra-cellular staining of Foxp3 or cytokines, single cell suspensions were initially stained for cell surface markers as described in section 2.2.4.1. Intra-cellular staining for Foxp3 was conducted using the PE-conjugated anti-mouse Foxp3 staining set as per the manufacturer's protocol (eBioscience, USA). The manufacturer suggests fixation/permeabilisation can be performed for 2 to 18 hours. 2 hours was preferred for these experiments. Cells were fixed/permeabilised in a lower volume of fixation/permeabilisation buffer (500 µl) and also only washed in a 500 µl volume of permeabilisation buffer. For intra-cellular staining of cytokines, single cell suspensions which had been previously stained for cell surface markers were pelleted by centrifugation at 2000 x g (6000 rpm) for 2 min and then resuspended in 500 µl Cytofix/Cytoperm solution. Cells were fixed and permeabilised by incubation at 4°C for 20 min. Cells were washed with 200 µl Perm wash buffer and then resuspended in 100 µl perm wash buffer for intracellular staining of cytokines. 2 µl (1/50 dilution, 400 µg of antibody) of fluorochrome conjugated anti-cytokine antibody was then added and cells incubated at 4°C for 30 min. Cells were flooded with 200 µl Perm wash buffer and pelleted prior to two more washes in 200 µl Perm wash buffer and resuspension in 200 µl perm wash buffer for acquisition. Mick-2 IL-4/IL-10 positive control cells were aliquotted and stored as per the manufacturer's protocol. Cells were resuscitated and washed in cell staining buffer prior to staining in the same manner as

test samples. Mick-2 positive control cells were used to set gating criteria on the flow cytometer.

2.2.5 Immunohistochemical analysis of T_{reg} cells

Human tonsil, benign lymphocytic effusions and malignant mesothelioma biopsy sections were analysed for T_{reg} cell presence by immunohistochemistry in the laboratory of our collaborator Prof Bruce Robinson.

2.2.6 Vinblastine treatment

Mice were weighed and a dosage of 6 mg/kg body weight of Vb was administered by i.p. injection at the appropriate time post tumour challenge. Mice were monitored regularly for side effects such as bloating and colitis. Mice treated with Vb (and also any control animals) showing signs of colitis were treated daily with a murine equivalent dose (weight dependent, approximately 30 µl/day) of a natural fibre supplement, Nucolox, by the oral route. Mice were culled if their overall condition had deteriorated to the humane end-point as defined by the Animal Ethics Committee as weight loss, hunching and ruffled fur.

2.2.7 Monoclonal antibody preparation and treatment

Anti-CCL22 mAb was purchased in a purified form. Anti-CD25, anti-CTLA-4, anti-IL-10 and anti-GITR mAbs were purified from the supernatant of hybridoma cell lines and then concentrated for *in vivo* administration to mice.

2.2.7.1 Preparation of and treatment with anti-CCL22 mAb solution

The 500 µg stock of anti-CCL22 mAb was resuspended in 1 ml PBS. 750µl of stock solution was stored at -20°C. 250 µl was further diluted by the addition of a further 24.75 ml of PBS to give a final concentration of 5 µg/ml. Aliquots were stored at -20°C. Mice were treated with 500 ng i.p. or 200 ng i.t. anti-CCL22 mAb.

2.2.7.2 Hybridoma cell culture

Hybridoma cells were stored in freezing media at -180°C. Frozen vials were thawed by hand and added dropwise to 10 ml supplemented CD hybridoma media. Cells were washed once by centrifugation at 500 x g (1500 rpm) for 5 min and then resuspended in 1 ml supplemented CD hybridoma media and transferred to a 75 cm^2 tissue culture flask containing a further 14 ml supplemented CD hybridoma media. Hybridoma cells were cultured in supplemented CD hybridoma media for up to three days prior to passage. Cells are semi-adherent and therefore did not require trypsinisation when harvesting. The media containing non-adherent cells was removed from the tissue culture flasks, transferred to a 15 ml Falcon tube and cells pelleted by centrifugation. Cells (approximately 1 x 10^6) were transferred to a fresh 225 cm^2 flask with supplemented CD hybridoma media containing 40 ml CD hybridoma media for a further 4 days of culture to collect mAb.

2.2.7.3 Harvesting mAb from tissue culture supernatant.

Antibodies were harvested from the supernatant of the hybridoma cell line at the same time as cell splitting. Cells were considered ready for harvesting once the semi-adherent cells had started coming off the bottom of the flasks (approximately 4 days). The CD hybridoma media containing the cells was removed from the flask, transferred to a 50 ml centrifuge tube and centrifuged at 500 x g (1500 rpm) for 5 min to pellet the cells and debris present in the media. The supernatant containing the antibody was then transferred to fresh tubes and stored at 4°C for ammonium sulphate precipitation of antibodies

2.2.7.4 Ammonium sulphate precipitation of antibodies

Hybridoma supernatant (500 ml) was transferred to a large conical flask containing a stirring flea and placed on a magnetic stirrer. While the antibody was gently being stirred, an equal volume of saturated ammonium sulphate solution (not crystals) was added in a slow stream over approximately 1 hr. The mixture was then gently stirred overnight at 4°C. Upon completion, the mixture was transferred to 500 ml centrifuge flasks and spun at 3000 rpm for 30 min to pellet the precipitated antibody. The pellet was retained and resuspended in PBS to 10% of the starting supernatant volume (50 ml)

being careful to avoid bubbles and frothing. The antibody solution was then transferred to dialysis tubing and dialysed overnight in 1 L 1x PBS with stirring. Overnight dialysis was repeated 3 times against three changes of 1 L 1x PBS. The antibody solution was then removed from the tube and centrifuged to remove any remaining debris and then quantified, aliquotted and stored at -20°C until required.

2.2.7.5 Preparation of dialysis tubing

Lengths of dialysis tubing were boiled in dialysis tubing wash buffer for 10 min. The tubing was rinsed in ddH_2O and autoclaved in 1mM EDTA. Tubing was rinsed again in ddH_2O immediately prior to use.

2.2.7.6 Quantification, concentration and storage of mAbs

The concentration of mAb solution was determined by spectrophotometry. The absorbance of neat and 1/10 dilution of antibody was read against a PBS control at 280 nm. The approximate protein concentration was calculated using Equation 3. Antibodies were prepared in serum free media to reduce contaminating proteins. When required, the mAb solution was concentrated using antibody concentration columns as per the manufacturer's protocol. Small Centricon microconcentrator columns were used for small volumes of antibody solution (<2 ml) while the large Centricon plus-20 columns were used for larger volumes (<20 ml) Concentrated antibodies were quantitated again, aliquotted and stored at -20°C.

Equation 3: Calculation of protein concentration

The standard absorbance (A) at 280 nm for 1 mg/ml IgG is 1.35

$$\frac{A(\text{ mAb solution})}{1.35} = \text{mg/ml}$$

2.2.7.7 mAb treatment

mAb solutions were thawed on ice and transported to the Animal Care Unit for *in vivo* treatments. For systemic treatments, the appropriate amount of mAb solution was administered i.p. by a single injection at the appropriate time-point. For intra-tumoural treatments, mice received a maximum of 40 µl mAb solution (depending on the mAb and concentration) administered into and around tumours of 9 mm^2 in size. 10 µl of mAb solution was injected directly into the tumour followed by injections of 10 µl s.c. at 120° intervals around the base of the tumour (see individual results sections for specific details on the mAb concentrations tested and the volumes injected). Control mice were left either untreated, treated with an equivalent volume of PBS or treated with an unrelated isotype-matched IgG1 mAb. The anti-IgG1 mAb (43B2 anti-RRV mAb, gift of Dr C. Johansen, The University of Western Australia) was purified using the same ammonium sulphate precipitation method and resuspended in PBS. A higher protein content was chosen for the isotype control treatment because it was prepared in media containing FCS, whilst the mAbs prepared in the Beilharz laboratory were prepared in serum-free media.

2.2.7.8 Neutralising antibody ELISA

An ELISA for the detection of neutralising antibodies to the rat anti-mouse CD25 mAb was developed. Flat-bottomed Nunc Maxisorp plates were coated with 50 µl of the PC61 anti-CD25 mAb solution (1 mg/145 µl) diluted 1/50 using antibody binding buffer. The plates were sealed and incubated O/N at 4°C. The PC61 coating antibody was flicked out and plates washed once with 200 µl blocking buffer for 3 min. The blocking buffer was then flicked out and the plate tapped on absorbent towel to remove any remaining blocking buffer. A further 100 µl blocking buffer per well was then added and the plates sealed and blocked at 37°C for 2 hours. Samples were prepared by diluting mouse serum, collected from "escape" or control mice, 1:2 using antibody diluent buffer. After 2 hours of blocking, the block buffer was flicked out and the plates washed once for 3 min with 200 µl wash buffer and excess buffer removed by tapping the plates on absorbent towels. 50 µl per well of diluted serum (in triplicate) was added to the wells making sure no air bubbles remain. Dilution buffer only was used as a blank. Plates were again sealed and incubated at 37°C for 2 hours. Serum was then flicked out and plates washed 3 times for 3 min with 200 µl wash buffer and any excess

removed by tapping. 50 µl of 1/1000 dilution (in dilution buffer) of alkaline phosphatase-conjugated anti-mouse IgG (whole molecule) was then added to each well and incubated at 37°C for a further 2 hours. The secondary antibody was then flicked out and the plates washed 3 times for 3 min with 200 µl wash buffer and any excess removed by tapping. Finally, 100 µl of P-nitrophenyl phosphate substrate was added to each well and incubated at room temp for 30 min prior to reading the absorbance at 405 nm using a plate reader. As a positive control, goat anti-serum to rat was used together with an alkaline-phosphatase conjugated rabbit anti-goat IgG as the detection antibody.

2.2.8 Preparation and administration of α-TOS

All α-TOS experiments were based on the published protocols of collaborator Assoc. Prof. Jiri Neuzil.

2.2.8.1 Preparation of α-TOS solution

α-TOS was resuspended in DMSO with slight warming to 37°C for approximately 5 min. For a 200 mM solution, 1.6 g α-TOS was dissolved in 15 ml DMSO while 0.8 g and 0.4 g were added to 15 ml DMSO for a 100 mM or 50 mM solution respectively. Prepared α-TOS solutions were stored at 4°C between treatments. DMSO freezes at 4°C and as such solutions needed to be thawed at 37°C prior to injection.

2.2.8.2 In vitro analysis of apoptosis induction

Apoptosis induction in AE17 cells was determined by Annexin V staining as previously described (164) in the laboratory of Assoc. Prof. Jiri Neuzil, Griffith University, Australia.

2.2.8.3 Treatment with α-TOS

Mice were treated i.p. with 100 µl of a 50 mM, 100 mM or a 200 mM α-TOS solution. Control mice received an equivalent volume of DMSO vehicle alone. Mice were monitored closely for tumour growth inhibition with behavioural side effects

documented. Upon humane culling by methoxyfluorane inhalation followed by cervical dislocation, mice were autopsied and internal abnormalities documented.

2.2.9 TGF-β Soluble receptor preparation and treatment

2.2.9.1 Preparation of TGF-β soluble receptor solution

The 50 µg of TGF-β soluble receptor stock was resuspended in 500 µl PBS to give a concentration of 100 µg/ml. BSA was then added to the solution to a final concentration of 0.1% w/v to prevent non-specific binding of the receptor to the tube. Further dilutions were made and aliquots of 5 µg/ml and 25 µg/ml were stored at -20°C.

2.2.9.2 Treatment with TGF-β soluble receptor

Mice with tumours measuring 9 mm^2 received a total of 20 µl of TGF-β soluble receptor solution, of the appropriate concentration, injected directly intra-tumourally with a 26 ½ gauge needle every third day. Control mice were left untreated. Tumour growth was monitored daily.

2.2.10 T_{reg} cell sorting

Two methods for isolating T_{reg} cells were optimised. FACS was used when very high purity was required but is a long process (up to 9 hours) and resulted in reduced cell viability. Imag sorting was used when a reduced purity was acceptable but cells were required quickly and at a high viability.

2.2.10.1 Ficoll separation of lymphocytes

Tumours are comprised of a wide range of cells including lymphocytes. To aid in the isolation of a pure population of T_{reg} cells, ficoll-paque plus was used to enrich the lymphocyte population. Tumour cell suspensions were made as previously described (Section 2.2.3.3). The tumour cell suspensions were made up to a volume of 4 ml and under-laid with 3 ml ficoll-paque plus gently to ensure no mixing of the interface. Ficoll separation was performed by centrifugation at 500 x g (1500 rpm) for 10 min

with no brake. The lymphocyte enriched population was found at the interface of the original cell suspension and the ficoll layer. This layer was carefully removed and washed three times with cell staining buffer prior to any further cell sorting.

2.2.10.2 Fluorescence activated cell sorting (FACS)

Ficoll enriched lymphocytes were resuspended in 1 ml FACS sort buffer. 20 µl (1/50 dilution) of fluorochrome conjugated antibodies (CD4-APC and CD25-FITC) were added to the cells and incubated at 4°C for 20 min. Cells were washed 3 times and resuspended in 3 ml FACS sort buffer for sorting. FACS was conducted by an experienced operator at The Biomedical Imaging and Analysis Facility, UWA, using the FACS Vantage flow cytometer with a 70 µm nozzle and a pressure of 14 psi. For FITC staining, samples were excited with a 488 nm (blue) laser and the signal collected with a 530/30 band pass filter (which means it collects all light between 515-545nm). APC excitation was with the 635 nm (red) laser and the signal collected with a 660/20 band pass filter. Cells were diluted in osmosol as required to prevent clumping and were collected into 500 µl supplemented RPMI media and later transferred to RNAlater. Alternatively, cells were collected directly into 500 µl RNAlater.

2.2.10.3 Imag sorting

When cells were required quickly, Imag magnetic bead sorting was performed. Imag bead sorting was conducted initially, as per the manufacturer's protocol, to isolate a $CD4^+$ T cell enriched population using the $CD4^+$ T cell enrichment set. The negatively selected enriched $CD4^+$ T cells were then stained for the secondary CD25 marker by standard cell surface marker staining for flow cytometry. CD25-PE labelled cells were then positively isolated based on the expression of CD25-PE using anti-PE beads by the manufacturer's protocol. Round bottom 5 ml tubes were used with a maximum cell volume of 1.5 ml. Following some optimisation it was found that triple rather than double purifying cells is preferred at both the CD4 enrichment step and the CD25 positive selection step. To confirm purity of sorted cells, cells were stained again post-sort with CD4-APC and CD25-PE as per the standard flow cytometry staining protocol and sorting efficiency confirmed using the FACS Calibur flow cytometer.

2.2.11 ELISA sample preparation and protocols

2.2.11.1 Preparation of serum

Blood was collected via the tail vein or by cardiac puncture into uncoated blood tubes. When bleeds were taken from the same mouse for a time-course experiment, mice were bled at 3 day intervals and only 50 µl collected each time. Blood was allowed to clot and settle at 4°C overnight. The upper layer was then transferred to a fresh microfuge tube for storage at -20°C. Multiple freeze/thaws were avoided for serum samples.

2.2.11.2 Preparation of tumour lysates for ELISA

Tumours were removed and weighed prior to resuspension in 500 µl cell lysis buffer. Tumours were then homogenised using a polytron homogeniser at 13500 rpm for 1 min. The homogenised tumour sample was then centrifuged at 500 x g (1500 rpm) for 5 min. The supernatant was then collected and stored at -20°C for future ELISA analysis.

2.2.11.3 Cell culture of T_{reg} cells for ELISA

T_{reg} cells were sorted as previously described by Imag magnetic bead selection. 5 x 10^4 T_{reg} cells or control cells were plated in 200 µl supplemented RPMI media per well in a 96 well tissue culture plate and incubated overnight at 37°C. The cell suspension was then removed and cells pelleted by centrifugation at 2000 x g (6000 rpm) for 2 min. Supernatant was then collected and stored if required at -20°C for ELISA. Cells were stained by standard flow cytometry staining protocol using CD4-APC and CD25-PE to confirm purity.

2.2.11.4 Acidification of T_{reg} cell culture supernatant for TGF-β ELISA

To convert the TGF-β produced *in vitro* by T_{reg} cells into its bio-active form found *in vivo*, the supernatant needed to be acidified. To 200 µl of supernatant, 8µl 1M HCl was added to reduce the pH to 3. The supernatant was incubated for 15 min with HCl before 6 µl of 1M NaOH was added to bring the pH back to 7.6 for ELISA analysis.

2.2.11.5 Il-4 and IL-10 ELISA

All reagents were warmed to room-temp prior to use. IL-10 and IL-4 ELISAs were conducted using Nunc Maxisorp plates coated with 100 µl capture antibody diluted in phosphate coating buffer (4 µg/ml) and incubated at 4°C overnight. Plates were washed 3 x with 200 µl ELISA wash buffer. Recombinant IL-10 and IL-4 were used as a standard. 200 µg/ml stock of rIL-10 or rIL-4 was diluted to 10 µg/ml in sterile PBS containing 5 mg/ml BSA and stored in aliquots of 10 µl at -80°C. Standards were serially diluted 1:2 in antibody diluent from 1000 pg/ml to 15.625 pg/ml with antibody diluent used as a blank and plated in duplicate. Serum samples were diluted 1:4 in antibody diluent and either 50 µl or 100 µl of diluted serum or test supernatant (neat) plated out and incubated at room temp for 1 hr. Plates were washed 3 x with 200 µl ELISA wash buffer prior to the addition of 100 µl detection antibody diluted in antibody diluent (1 µg/ml) and incubated at room temp for 1 hr. Plates were washed 3 x with 200 µl ELISA wash buffer to remove all excess detection antibody. 100 µl horseradish peroxidase (HRP) diluted in antibody diluent was added to each well and incubated at room temp for 30 min. Excess/unbound HRP was removed by 3 washes using 200µl ELISA wash buffer. 100 µl tetramethylbenzidine (TMB) substrate was added to each well and incubated in the dark for 30 min. The colour reaction was stopped by the addition of 50 µl 1M HCl and absorbances read at 450 nm within 30 min.

2.2.11.6 TGF-β ELISA

TGF-β ELISA was also conducted using Nunc Maxisorp plates coated with 100 µl capture antibody diluted in carbonate ELISA coating buffer (2 µg/ml) and incubated at 4°C overnight. Plates were washed once with 200 µl TBST wash buffer. A recombinant human TGF-β standard was used. The 2 µg standard stock was diluted to 1 µg/ml in 2 ml of 4 mM HCl containing 1 mg/ml BSA and stored at -20°C. Standards were serially diluted 1:2 in antibody diluent from 1000 pg/ml to 15.625 pg/ml with antibody diluent used as a blank and plated in duplicate. Serum, tumour lysates and supernatant test samples were diluted in antibody diluent and either 50 µl or 100 µl added per well and incubated at room temp for 1 hr. Plates were washed 5 x with 200 µl TBST wash buffer prior to the addition of 100 µl detection antibody diluted in

antibody diluent (1 µg/ml) and incubated at room temp for 1 hr. Plates were washed 5 x with 200 µl TBST wash buffer to remove all excess detection antibody. 100 µl HRP diluted in antibody diluent was added to each well and incubated at room temp for 30 min. Unbound HRP was removed by 3 washes with 200 µl TBST wash buffer. 100 µl TMB substrate was added to each well and incubated in the dark for 30 min. The colour reaction was stopped by the addition of 50 µl 1M HCl and absorbances read at 450 nm within 30 min.

2.2.11.7 SAA ELISA

SAA ELISA was carried out according to the manufacturer's protocol. SAA ELISA was conducted on serum samples from mice implanted with either i.p. or s.c. murine mesothelioma tumours. Pooled serum samples from all ten mice of a group were also analysed by SAA ELISA.

2.2.12 RNA extraction, Reverse transcription and real-time PCR

RNA was extracted from AE17 cells for down-stream RT-PCR analysis.

2.2.12.1 RNA extraction

If RNA could not be immediately extracted from sorted cells, the cells were placed in RNAlater at a concentration of 1 x 10^6 cells/ml and stored at -20°C until RNA extraction. The RNeasy mini kit together with QIAshredder columns were used to extract RNA from a minimum of 1 x 10^6 cells as per the manufacturer's protocol. If reverse transcription could not be carried out immediately, RNA was stored at -20°C

2.2.12.2 Agarose gel electrophoresis

RNA and final PCR products were checked by agarose gel electrophoresis using a 1% agarose gel containing Ethidium Bromide (40 µl agarose gel plus 2 µl of 10 mg/ml Ethidium Bromide). 2 µl RNA was mixed with 5 µl SEB dye and loaded into the gel. RNA was electrophoresed for 30 min at 100 volts. Gel photographs were taken using the Kodak Gel Doc system.

2.2.12.3 Global genechip analysis

Cells were sorted for global genechip analysis by FACS and stored at -20°C in RNAlater for RNA extraction. Cells were shipped in RNAlater at room temp to Mater Medical Research Institute, Qld, Australia for genechip analysis by collaborators Dr Gareth Price and Dr Deon Ventnor. Affymetrix GeneChip Mouse Genome 430 2.0 Arrays were used to profile the cells. The genechips allow for the analysis of over 39,000 transcripts. All samples were prepared using the Affymetrix Two-cycle Labelling Kit and were analysed on the multi-species Test3 genechip to confirm sample integrity and labelling efficiency prior to analysis using the Mouse Genome 430 2.0 Array. Relative expression levels were calculated using Equation 4.

Equation 4: Calculation of relative gene expression

$$\text{Relative expression} = \log_2\left(\frac{\text{tumour gene expression}}{\text{naïve spleen gene expression}}\right)$$

2.2.12.4 Reverse transcription

RNA was reversed transcribed using the Sensiscript RT Kit and a separate Oligo dT primer and RNase inhibitor as outlined in Table 2.15. All reagents were thawed on ice and samples prepared on ice using filter tips, powder free gloves and equipment that had been cleaned with RNaseZap. A master mix of all reagents except the template RNA was made. RNA template was added last and samples incubated at 37°C for 60 min. If real-time PCR was not prepared immediately, cDNA was stored at -20°C.

2.2.12.5 Real-time PCR

A master mix was set up on ice in a room separate from the room used for RNA extraction or the analysis of PCR products using specifically dedicated pipettes and filter tips. Optical tubes and caps were used for PCR analysis. RT negative controls (RNA only) were run for each test sample with a no template control (H_2O only) also analysed. The cycling conditions used are outlined in Table 2.17.

Table 2.14 RT sample preparation

Component	Volume/reaction	Final Concentration
10 x buffer RT	2 µl	1 x
dNTP mix (5 mM each dNTP)	2 µl	0.5 mM each dNTP
Oligo-dT primer	1 µl	500 ng
RNase inhibitor (40 units/µl) (diluted ¼ in buffer RT)	1 µl	10 units
Sensiscript reverse transcriptase	1 µl	
RNase free water	3 µl	
Template RNA	10 µl	
Total volume	**20 µl**	

Table 2.15: PCR set-up

Component	**Volume/reaction**
SYBR green	25 µl
RNase free-H_2O	18µl
Forward primer	1µl
Reverse primer	1 µl
Template cDNA	5 µl

Table 2.16: PCR cycling conditions

Number of cycles	Temperature	Time	Stage
1	95°C	10 min	Hot start
40	95°C	30 sec	Denaturation
40	58°C	30 sec	Annealing
40	72°C	1 min	Extension
1	72°C	10 min	Final elongation

2.2.13 Statistical analysis

All data are presented as the mean ± SEM. Statistical analysis was conducted by Student's t test, assuming unequal variance of the means of the populations being examined and all values cited are two-tailed at a 95% confidence interval. P-values < 0.05 are represented by a single asterisk. All graphs are plotted using Prism Graphpad software

Chapter 3:

T_{reg} cells in the periphery of murine mesothelioma-bearing mice

3.1 Introduction

The publications of North and Awwad in the late 1980s and early 1990s investigating the timing of the cellular anti-tumour immune response were the original empirical observations that led to the work described in this PhD thesis. North hypothesised in 1985, based on several empirical studies (168, 169), that the immune response evoked by tumours failed to develop to a level required to induce tumour regression because it is down-regulated by regulatory T (T_{reg}) cells (at the time known as suppressor T cells) (38). Using Meth A fibrosarcomas and P815 mastocytomas North and colleagues showed that cytotoxic T lymphocytes (CTLs) capable of causing tumour regression are first generated in immuno-competent mice on about day 6 of tumour growth (Fig. 3.1). This was shown by transferring T cells from spleens of tumour bearing mice at days 3, 6, 9, 12, 15 or 18 post tumour challenge into irradiated tumour bearing hosts and checking for the regression of the host tumour. The CTLs reach a peak at about day 9 but then are progressively lost until day 15. This day 6 generation, day 9 peak and day 15 loss of detection was also confirmed by an *in vitro* cytolytic activity assay where tumour cells were used as targets and spleen cells from day 3, 6, 9, 12, 15 and 18 post tumour challenge immuno-competent mice were used as effector cells in a chromium release assay. This decay in anti-tumour immunity was believed to be caused by the negative immuno-regulatory function of T_{reg} cells that are acquired progressively from day 9 onwards. It was seen that CTLs do not disappear suddenly but are progressively lost as T_{reg} cells are acquired.

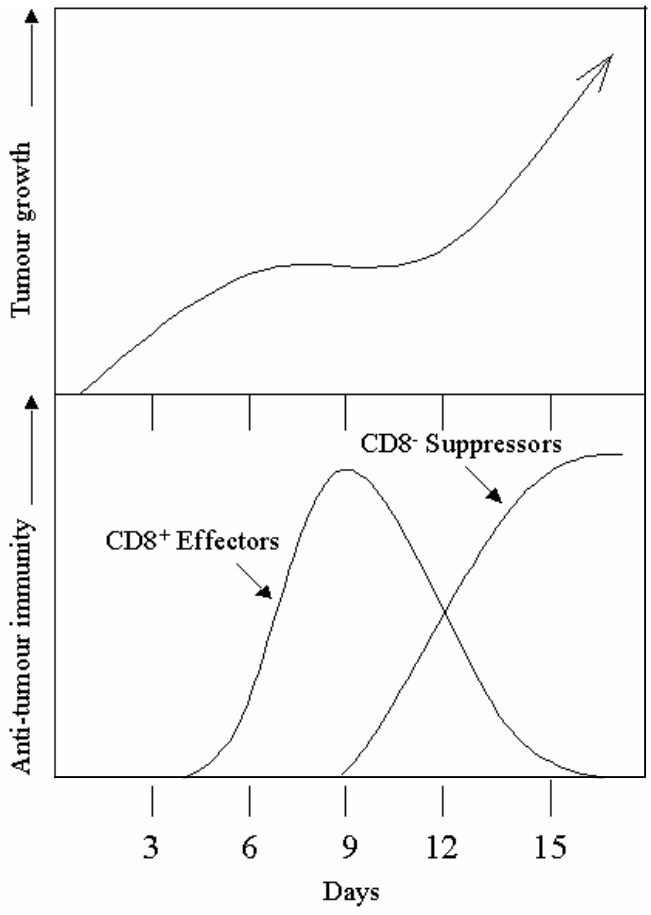

Figure 3.1: The kinetics of the anti-tumour immune response (adapted from (38))

The upregulation of effector T cells at about day 6 of tumour growth leads to an inhibition of tumour growth. Effector T cells are, however, negatively regulated by T_{reg} cells (suppressor T cells) which are expanding from day 9 onwards and which cause the progressive loss of effector T cells and the subsequent continued growth of the tumour.

North and Awwad furthered this work in 1990 by showing that it was possible to overcome dominant immunosuppression at a late stage of tumour development and cause an immunologically mediated tumour regression when a tumour-bearing mouse is treated with a single but carefully timed injection of the anti-mitotic drug Vinblastine (Vb) (154). These results were consistent with their interpretation that at a particular stage of tumour development (days 13–15 post tumour challenge in Fig. 3.1), functionally suppressed anti-tumour $CD8^+$ CTLs were non-cycling and co-existed with a functionally active and dominant population of expanding $CD4^+$ T_{reg} cells that could be selectively destroyed by the anti-mitotic nature of Vb. Vb is a plant derived, anti-mitotic drug that acts as an inhibitor of cellular proliferation by irreversibly depolymerising microtubules, an important part of the cytoskeleton and mitotic spindle, resulting in mitotic arrest at metaphase, the dissolution of the mitotic spindle and interference with chromosome segregation (170).

On initiation of this PhD project, all reviews of chemotherapy for Malignant Mesothelioma (MM) reported poor response rates typically in the range of 15% to 20% (171, 172). As the incidence of MM was rapidly increasing and not expected to peak until approximately 2020 in Australia there was, and still is, a need for the development of novel therapeutics for this aggressive cancer (173). The Beilharz laboratory, where this PhD work was conducted, had experience with timed Vb treatment in the murine AIDS model and for the first time, in a viral model, had confirmed North and Awwad's observations that Vb could be used to specifically target expanding T_{reg} cells (107). The central aim of this chapter was thus to examine the effect of a single, timed dose of Vb on the development of tumours in mice challenged with murine mesothelioma. By correctly timing a single dose of Vb to coincide with the T_{reg} cell response in the murine model of mesothelioma, the T_{reg} cells could be destroyed. Under these circumstances the anti-tumour immune response would be freed from suppression and tumour growth would be impaired.

The study of Vb treatment efficacy conducted by North and Awwad also definitively showed the suppressive cells in the murine T cell lymphoma model to be a subset of $CD4^+$ T cells (154). These studies by North and Awwad were instrumental to the resurgence of interest in T_{reg} cells in the early to mid 1990s. One of the most important

results of this resurgence in T_{reg} cell research was the discovery by Sakaguchi's group that the IL-2 receptor alpha chain, CD25, was a useful marker of T_{reg} cells (39). Sakaguchi showed that approximately 10% of peripheral $CD4^+$ T cells and 1% of peripheral $CD8^+$ T cells in naïve, adult mice express CD25. The $CD4^+CD25^+$ T cells were shown to be suppressive in nature as the adoptive transfer of $CD4^+CD25^-$ T cells into athymic mice resulted in the induction of autoimmune diseases such as thyroiditis, and gastritis. The subsequent reconstitution of the same mice with the missing $CD4^+CD25^+$ T cell subset prevented autoimmune disease development in a dose dependent manner suggesting that $CD4^+CD25^+$ T cells contribute to the maintenance of self tolerance by down-regulating autoimmune response. The common link between $CD4^+CD25^+$ T_{reg} cells in autoimmunity and tumour development was also made by Sakaguchi's group in 1999 when it was found, in a murine tumour model, that the removal of $CD4^+CD25^+$ T cells by anti-CD25 mAb resulted in tumour regression (155). As T_{reg} cells were proposed by North and Awwad to be the targets of Vb therapy, the initial experiments presented in this chapter were designed to show that T_{reg} cells arose in the periphery of tumour-bearing mice in response to a tumour challenge.

Flow cytometry was used to determine the presence and percentage of $CD4^+CD25^+$ T_{reg} cells in the peripheral blood, spleen, draining and non-draining LNs of mesothelioma-bearing mice. By examining the presence of T_{reg} cells at various times post tumour challenge it was found that an increase in the percentage of T_{reg} cells in the blood occurs between days 14 and 21 post tumour challenge. Vb treatment administered to coincide with this T_{reg} cell expansion was then examined as a means to modulate the effect of T_{reg} cells on tumour development. Vb treatment administered to coincide with the T_{reg} cell expansion slowed tumour development but did not result in complete tumour regression. As the initial experiments had identified cells of the $CD4^+CD25^+$ T_{reg} cell phenotype in the spleen, blood and lymph nodes of the tumour bearing mice, anti-CD25 mAb was used to target T_{reg} cells more specifically. Anti-CD25 mAb had previously been used in tumour models to successfully inactivate peripheral T_{reg} cells prior to tumour challenge (156, 157). Using the murine model of mesothelioma, anti-CD25 mAb administered prior to tumour challenge was found to be effective at inhibiting tumour development when mice were challenged with a low inoculum of tumour cells. By using a larger tumour cell inoculum this pre-treatment

with anti-CD25 mAb was rendered ineffective. Systemic treatment with anti-CD25 mAb was also found to be ineffective against established tumours.

3.2 Results

The AE17 murine mesothelioma cell line was used to develop subcutaneous tumours in syngeneic C57BL/6J mice. The AE17 cell line was derived from a primary asbestos induced tumour and is considered a good model for MM (13, 14).

3.2.1 $CD4^+CD25^+$ T_{reg} cells are present in the periphery of mesothelioma-bearing mice.

C57BL/6J mice were implanted subcutaneously (s.c.) with 1 x 10^6 AE17 cells resulting in the development of solid tumours. Spleen, blood, draining LN (inguinal, axillary and brachial from the same side of the mouse as the tumour implant) and non-draining LN (from the opposite side of the mouse to the tumour implant) were removed from tumour-bearing mice at weekly intervals over a 5 week time-course of AE17 tumour development. The $CD4^+CD25^+$ T_{reg} cell subset was determined as a percentage of total $CD4^+$ T cells by flow cytometry with dual-colour staining. A significant increase in the percentage of $CD4^+$ T cells expressing the CD25 T_{reg} cell marker was seen in the blood between days 14 (10.8 ± 1.0%) and 21 (19.8 ± 3.7%) post tumour challenge ($p < 0.05$) (Fig. 3.2A, orange bars). The T_{reg} cell percentage in the blood remained at the higher level for the rest of the time-course of tumour development. This same increase in the percentage of T_{reg} cells between days 14 and 21 post tumour challenge was not seen in the spleen or lymph nodes (both draining and non-draining) of the tumour-bearing mice. In these cases after averaging the data of all combined time-points of tumour development, a similar percentage of $CD4^+$ T cells expressed CD25 in the spleen (Fig. 3.2A, white bars, 14.1 ± 0.3%) while in the draining and non-draining LN an average of 13.2 ± 0.6% (Fig. 3.2B, blue bars) and 15.1 ± 0.5% (Fig. 3.2B, white bars) of $CD4^+$ T cells expressed CD25 respectively. In fact, the percentage of $CD4^+$ T cells expressing CD25 in the spleens and lymph nodes of tumour-bearing mice over all time-points was consistent with the levels seen in naïve, tumour-free (day 0) mice.

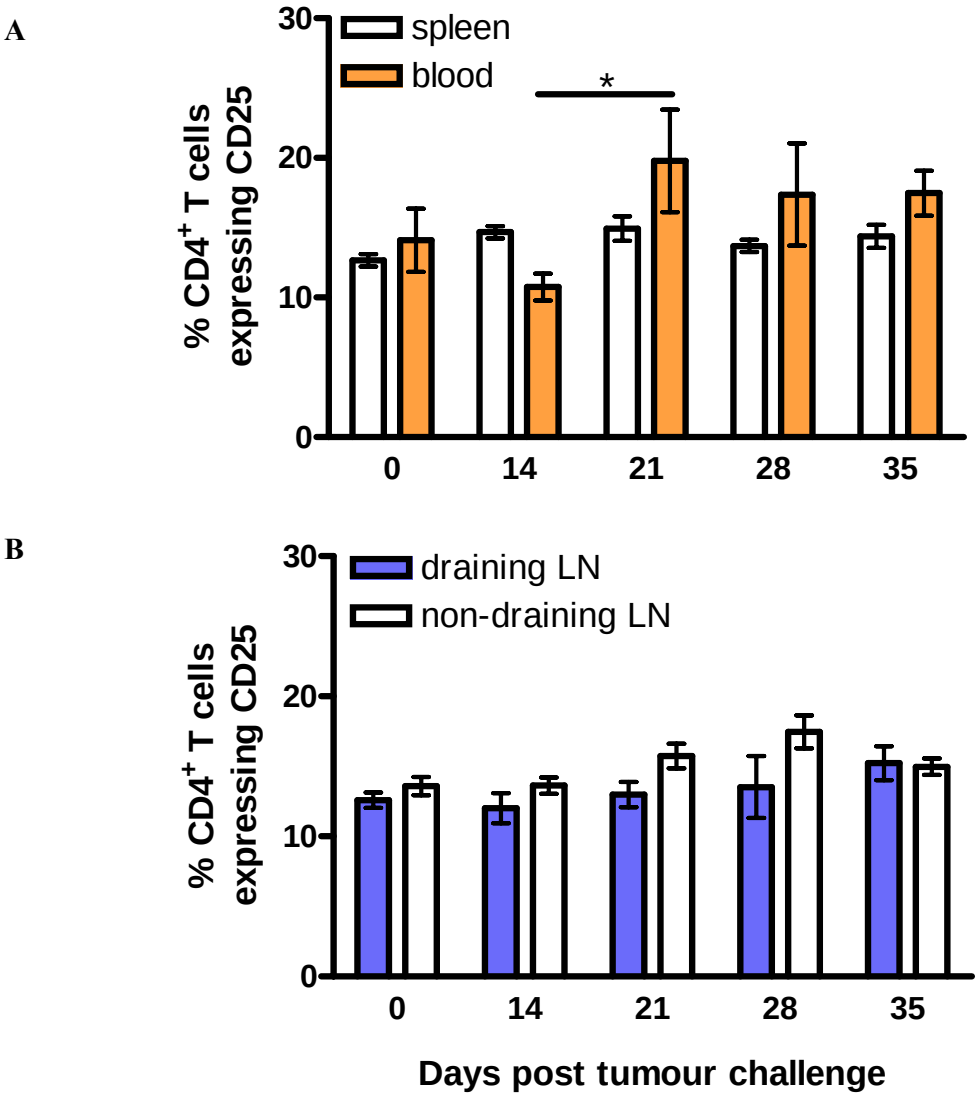

Figure 3.2: $CD4^+CD25^+$ T cells in the periphery of murine mesothelioma-bearing mice.

Mice were implanted s.c. at day 0 with 1 x 10^6 AE17 tumour cells. Mice were culled at days 14, 21, 28 and 35 post tumour challenge and spleens, blood and LNs (both tumour draining and non-draining) removed and single cell suspensions made which were analysed by flow cytometry for the presence of $CD4^+CD25^+$ T_{reg} cells. $CD4^+CD25^+$ T_{reg} cells were calculated as a percentage of total $CD4^+$ T cells located in (A) the spleen (□) and blood (■) and (B) draining (■) and non-draining LNs (□) over the 5 week time-course of tumour development. Day 0 calculations were taken from tumour-free, naïve mice. Data are the mean ± SEM of 8 mice per time-point. A single asterisk represents a p-value < 0.05.

3.2.2 Vinblastine: a potential immunotherapy for mesothelioma.

The standard protocol for the administration of Vb to cancer patients involves weekly intravenous (i.v.) doses ranging from 0.1-0.2 mg/kg given over several months (174). Vb has been used clinically for the treatment of MM but with only limited success (171). The modified Vb treatment regime proposed by North and Awwad in their murine studies involved only a single 6 mg/kg intra-peritoneal (i.p.) dose of Vb administered once between days 13 and 15 post tumour challenge (154). This single, precisely timed dose (administered between days 13 and 15 post tumour challenge) was considered more successful as it acted to specifically target the expanding population of tumour-specific T_{reg} cells rather than killing all dividing cells which often results in severe side-effects. The modified Vb treatment regime of North and Awwad was therefore investigated in the murine mesothelioma model. Interestingly, the Vb treatment time used by North and Awwad post tumour challenge correlated well with the spike in T_{reg} cells observed in the blood of tumour-bearing mice between days 14 and 21 post tumour challenge (see Fig. 3.2A).

3.2.2.1 Vb pilot study: precisely timed, systemic treatment with Vb results in tumour growth inhibition.

A pilot study of the efficacy of a single Vb treatment for murine mesothelioma was conducted in collaboration with the laboratory of Dr Phil Stumbles of The University of Western Australia. Three groups of 5 mice were implanted s.c. on day 0 with 1 x 10^6 AE17 cells. Two groups of mice were used to test the efficacy of Vb. One group was treated i.p. with a single 6 mg/kg body weight dose of Vb 14 days post tumour challenge. This day 14 post tumour challenge time point for the administration of a single dose of Vb was chosen on the basis of the North and Awwad data (154) and the present study which showed an increase in blood located T_{reg} cells beyond day 14 post tumour challenge. A second group of mice was treated in the same manner except the single dose of Vb was administered 15 days post tumour challenge. The final group of mice was left untreated as controls for normal tumour growth. Mice were monitored regularly for tumour development and tumour areas calculated by multiplying two right-angled tumour diameters measured using microcallipers. As a result of a single treatment with Vb, four of the five mice receiving Vb treatment on day 14 post tumour

challenge did not develop tumours (Figure 3.3). In contrast, tumours grew at a normal rate (as compared to untreated controls) in mice treated only one day later (day 15) with the same dose of Vb.

3.2.2.2 The efficacy of Vb to inhibit tumour development is limited to administration within a small "window of treatment opportunity".

Several attempts were made to replicate the positive observations of the collaborative pilot study that tumour development from 1 x 10^6 AE17 cells can be inhibited by a single dose of Vb administered 14 days post tumour challenge. Figure 3.4A represents the data from three combined experiments involving a total of 25 mice per treatment group. Mice were implanted with 1 x 10^6 AE17 tumour cells on day 0. The control group received no further treatment. The day 14 treatment group received a single 6 mg/kg body weight i.p. dose of Vb 14 days post tumour challenge while the day 15 treatment group received the same treatment administered one day later on day 15 post tumour challenge.

In these repeat experiments it was found that a single treatment of Vb administered on day 14 or on day 15 post tumour challenge resulted in tumour growth inhibition. Treatment with Vb 14 days post tumour challenge was slightly more effective than Vb treatment administered one day later (day 15 post tumour challenge) with the tumours of mice treated on day 15 reaching the humane end-point of 100 mm^2 at approximately day 26 while on the same day (day 26 post tumour challenge) the tumours of mice treated on day 14 were only averaging 56.8 ± 7.2 mm^2. Although a statistically significant difference ($p < 0.001$) was seen at day 20 post tumour challenge between the tumour areas of the treated mice (both day 14 and day 15 Vb treated) and the control tumours, complete tumour regression was not observed.

The efficacy of Vb had previously been shown to be timing dependent. As the tumour growth rate was faster in these experiments compared to the pilot study it was decided to try some earlier treatment time-points. Figure 3.4B depicts the combined results of experiments conducted to test the efficacy of Vb administered on days 10, 12 and 13 post tumour challenge. Again, all mice were implanted on day 0 with 1 x 10^6 AE17 cells and treated with a single 6 mg/kg body weight i.p. dose of Vb at the designated

time-point. In total, 25 mice comprised the untreated control group while 5 mice were treated with Vb on day 10, 20 mice were treated with Vb on day 12 and 25 mice were treated with Vb on day 13 post tumour challenge. In these combined experiments only the Vb treatments administered on days 12 and 13 post tumour challenge resulted in significant tumour growth inhibition ($p < 0.001$ at day 20). In mice treated on days 12 and 13 post tumour challenge tumours developed at a rate comparable to the rate at which tumours developed in mice treated with Vb 14 days post tumour challenge (compare Fig. 3.4A and Fig. 3.4B). Treatment with Vb 10 days post tumour challenge inhibited tumour development to a lesser degree than Vb treatments administered on days 12, 13 or 14 post tumour challenge and resulted in tumour sizes that were not statistically different from those of the untreated control tumours ($p=0.08$ at day 20).

It appeared that there was a "window of treatment opportunity" within which treatment with a single dose of Vb significantly inhibited tumour development. The window appeared to open at day 12 post tumour challenge, but it was not yet entirely clear as to the latest time-point at which Vb treatment could result in tumour growth inhibition. Two later treatment time-points were trialled in order to determine the closure of the "window of treatment opportunity". Mice were implanted s.c. on day 0 with 1×10^6 AE17 tumour cells. These experiments were run alongside the treatments administered at days 10, 12 and 13 post tumour challenge and so the untreated control tumours were the same 25 untreated controls shown in Figures 3.4A and 3.4B. Twenty mice were treated with a single 6 mg/kg i.p. dose of Vb on day 16 post tumour challenge while 5 mice were treated in the same manner on day 20 post tumour challenge. Figure 3.4C depicts these combined results.

Treatment with a single dose of Vb on day 16 post tumour challenge was also sufficient to significantly inhibit tumour development. Vb treatment administered 20 days post tumour challenge was, however, not sufficient to induce tumour growth inhibition with tumours developing at a rate comparable to the untreated controls. When the day 20 post tumour challenge treatment was administered the tumours were already very large (83.8 ± 13.5 mm^2). The apparent "window of treatment opportunity" for single dose Vb treatment was therefore between days 12 and 16 post tumour challenge. During this time murine mesothelioma development arising from an inoculum of 1×10^6 AE17 cells could be significantly inhibited with a single 6 mg/kg body weight i.p. dose of Vb.

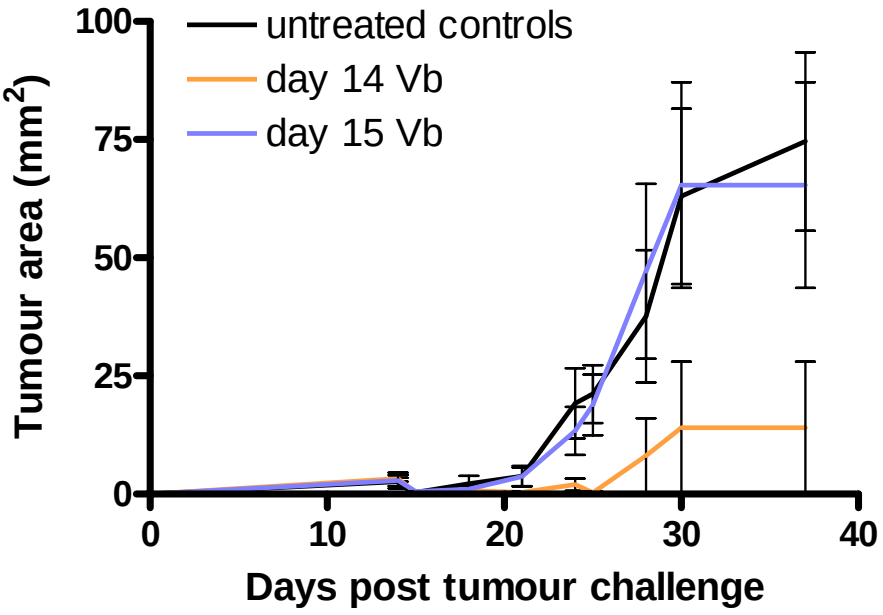

Figure 3.3: Pilot study: A single dose of Vb inhibits murine mesothelioma tumour development.
15 mice were implanted s.c. at day 0 with 1 x 10^6 AE17 murine mesothelioma cells. A single dose of 6 mg/kg body weight Vb was given i.p. to mice at either day 14 or day 15 post tumour challenge. Control mice were left untreated. Tumour areas were calculated by multiplying two, right-angled tumour diameters measured using microcallipers. Data are the mean ± SEM for 5 mice per time-point per treatment group.

A

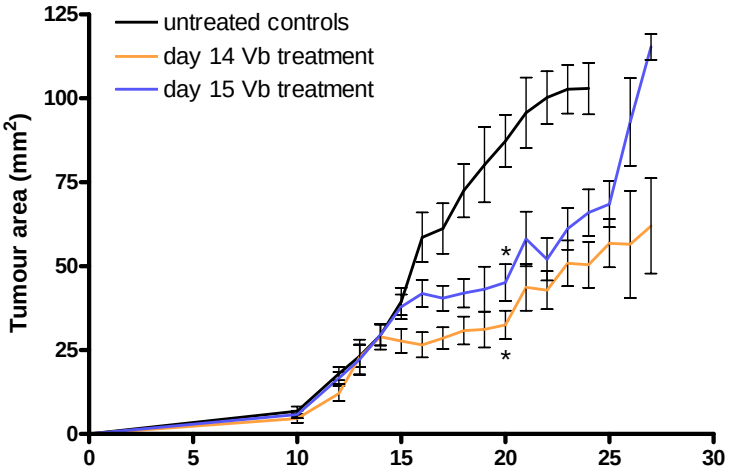
untreated controls
day 14 Vb treatment
day 15 Vb treatment
Tumour area (mm2)
125
100
75
50
25
0
0
5
10
15
20
25
30
*
*

B

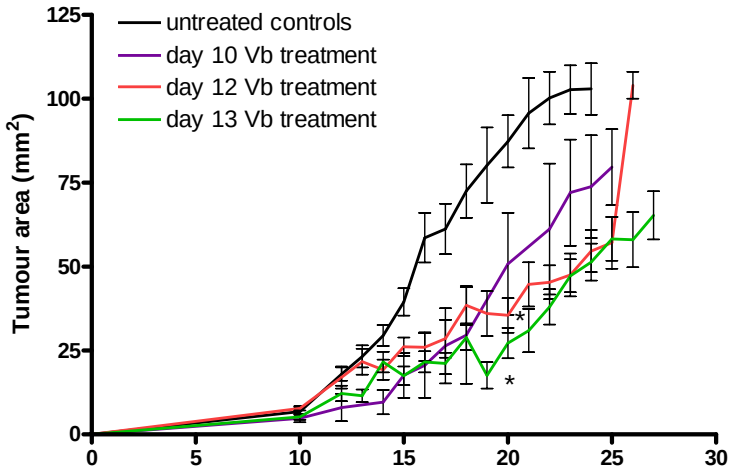
untreated controls
day 10 Vb treatment
day 12 Vb treatment
day 13 Vb treatment
Tumour area (mm2)
125
100
75
50
25
0
0
5
10
15
20
25
30
*
*

C

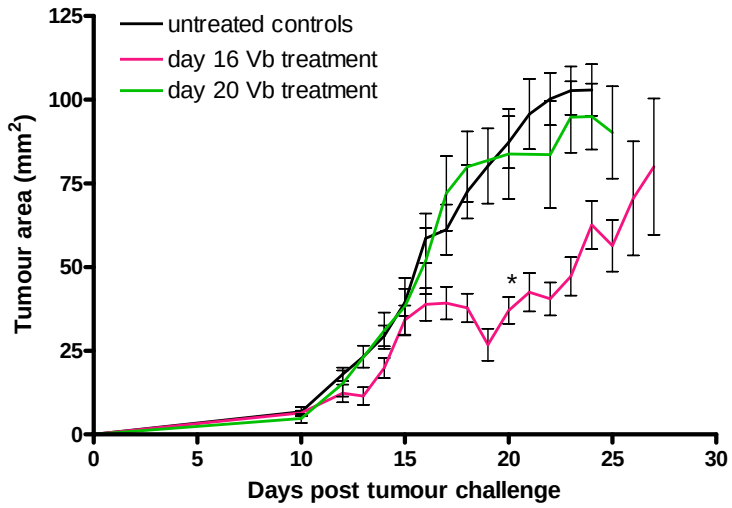
untreated controls
day 16 Vb treatment
day 20 Vb treatment
Tumour area (mm2)
125
100
75
50
25
0
0
5
10
15
20
25
30
Days post tumour challenge
*

Figure 3.4: A single dose of Vb inhibits murine mesothelioma development when administered between days 12 and 16 post tumour challenge.

Mice were implanted s.c. at day 0 with 1 x 10^6 AE17 murine mesothelioma tumour cells. A single 6 mg/kg body weight dose of Vb was given i.p. to mice at either (A) day 14 or day 15 post tumour challenge, (B) day 10, day 12 or day 13 post tumour challenge or (C) day 16 or day 20 post tumour challenge. Control mice were left untreated. Tumour areas were calculated by multiplying two right angled tumour diameters measured using microcallipers. Data are the mean ± SEM for (A) 25 mice per time-point per treatment group, (B) 5 mice treated on day 10, 20 mice treated on day 12, 25 mice treated on day 13 and 25 untreated controls and (C) 5 mice treated on day 20, 25 mice treated on day 16 and 25 untreated controls. A single asterisk represents a p-value < 0.05.

3.2.3 Systemic administration of anti-CD25 mAb

Although it was proposed by North and Awwad that Vb could act to selectively target expanding T_{reg} cells, it is an anti-mitotic drug and so may also be affecting other proliferating cells such as cycling anti-tumour CTLs or the tumour cells (154, 170, 175-178). Since the work of North and Awwad, T_{reg} cells were identified to not only express the CD4 cell surface marker but also to co-express the IL-2 receptor alpha chain, CD25 (155, 156). Anti-CD25 mAb could therefore be administered to mice to more specifically target and inactivate T_{reg} cells (155, 156, 179). Anti-CD25 mAb has previously been administered systemically as an anti-tumour therapy (29, 155-157) and has since been shown to result in the shedding of the CD25 molecule from the surface of cells (132). These early, successful attempts to inactivate $CD4^+CD25^+$ T_{reg} cells and hence induce tumour regression involved the systemic administration of anti-CD25 mAb prior to tumour challenge (29, 156, 157) rather than the timed approach of North and Awwad to target T_{reg} cells that were expanding in response to the tumour. This study therefore undertook both approaches, the pre-treatment of mice with anti-CD25 mAb prior to tumour challenge but also attempted, for the first time, to time the systemic anti-CD25 mAb treatment to coincide with the expansion of T_{reg} cells in mice with established tumours.

3.2.3.1 Pre-tumour challenge, systemic administration of anti-CD25 mAb inactivates T_{reg} cells and results in tumour growth inhibition.

The administration of a single i.p. dose of 0.5 mg anti-CD25 mAb (PC61 clone) four days prior to the implantation of 1 x 10^6 AE17 tumour cells inhibited murine mesothelioma growth (Fig. 3.5A). The single dose systemic treatment with anti-CD25 mAb resulted in the shedding of the CD25 cell surface marker (and hence inactivation) in 87.4 ± 5.5% of $CD4^+CD25^+$ T_{reg} cells in the blood within 24 hrs while 88.5 ± 7.4% of T_{reg} cells were still inactivated after 7 days. This single dose treatment inhibited tumour development for up to 40 days in the 8 treated mice compared to the 6 untreated control mice. All mice that were successfully treated by the single dose of anti-CD25 mAb eventually developed palpable tumours that reached the humane endpoint of 100 mm^2 after approximately 100 days.

3.2.3.2 Systemic inactivation of T_{reg} cells by anti-CD25 mAb is limited by the size of initial tumour cell inoculum.

In contrast to the successful inhibition of tumour development arising from 1 x 10^6 AE17 tumour cells, the administration of a single 0.5 mg dose of anti-CD25 mAb four days prior to tumour challenge with 1 x 10^7 tumour cells (i.e. a ten-fold higher inoculum) did not significantly inhibit tumour development (Fig. 3.5B). The 8 treated mice developed tumours at the same rate as the 6 untreated control mice.

3.2.3.3 Systemic treatment of established tumours with anti-CD25 mAb does not result in tumour growth inhibition.

It was found that a threshold of tumour burden exists which limits the pre-tumour challenge treatment of mice with anti-CD25 mAb. It has also previously been shown that the anti-tumour effect of anti-CD25 mAb is not evident if the treatment is given on day 0 or shortly thereafter (179). Based on our own successful Vb studies we tested the ability of anti-CD25 mAb administered on day 13 post tumour challenge to inhibit tumour development. Treatment at day 13 should result in the significant inactivation of T_{reg} cells at day 14 which was identified earlier in this chapter to be the time-point at which T_{reg} cells were expanding (see Fig. 3.2A) and the middle time-point of the Vb "window of treatment opportunity" (Fig. 3.4). Mice were implanted with 1 x 10^6 AE17 tumour cells at day 0 and treated with 0.5 mg anti-CD25 mAb i.p. 13 days later when tumours were small but established (Fig. 3.6). The 5 mice treated with anti-CD25 mAb developed tumours at the same rate as the 5 untreated control mice. The experiment was terminated early (tumours had only reached ~60 mm^2) as no tumour growth inhibition had been seen by day 30 post tumour challenge.

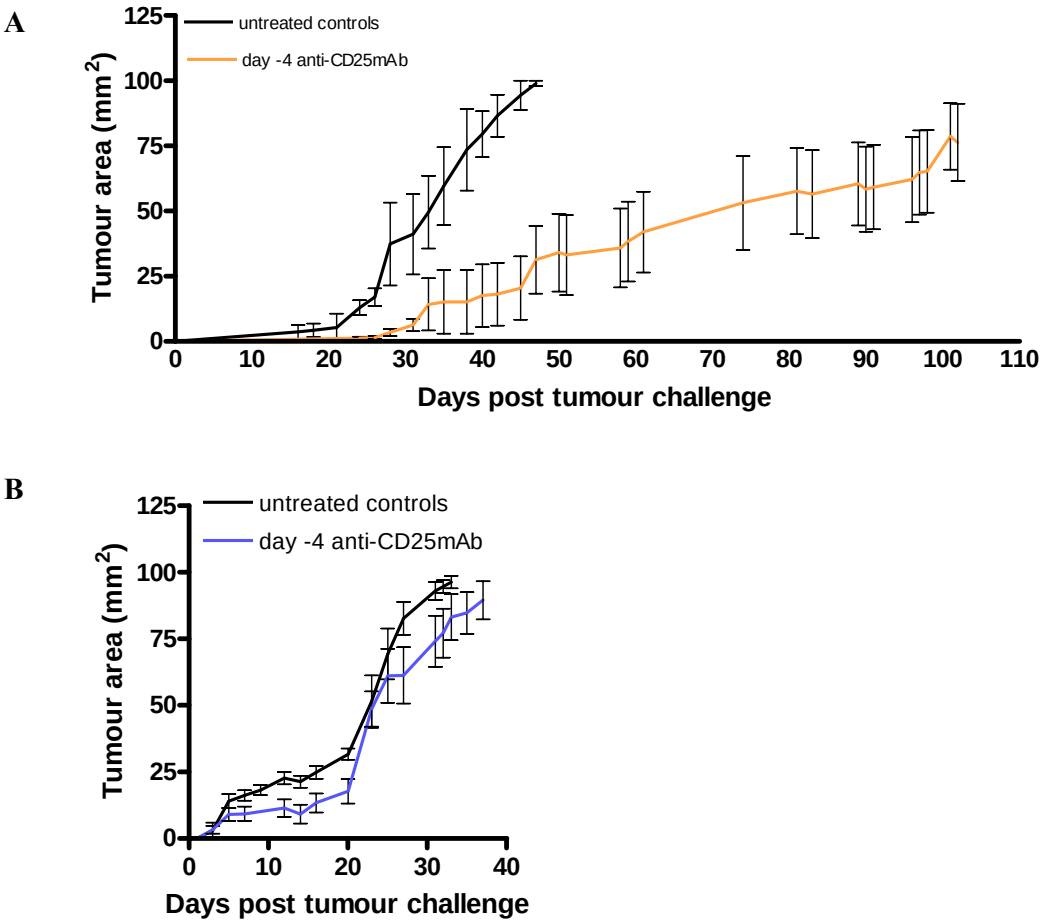

Figure 3.5: A single dose of anti-CD25 mAb administered 4 days prior to tumour challenge no longer inhibits murine mesothelioma development when mice are challenged with a 10-fold higher initial tumour cell inoculum.

A single dose of 0.5 mg of anti-CD25 mAb was given i.p. to mice 4 days prior to tumour challenge. Control mice were left untreated. Mice were then implanted s.c. at day 0 with (A) 1 x 10^6 and (B) 1 x 10^7 AE17 murine mesothelioma cells. Tumour areas were calculated by multiplying two, right-angled tumour diameters measured using microcallipers. Data are the mean ± SEM for 8 treated mice and 6 untreated control mice for each experiment.

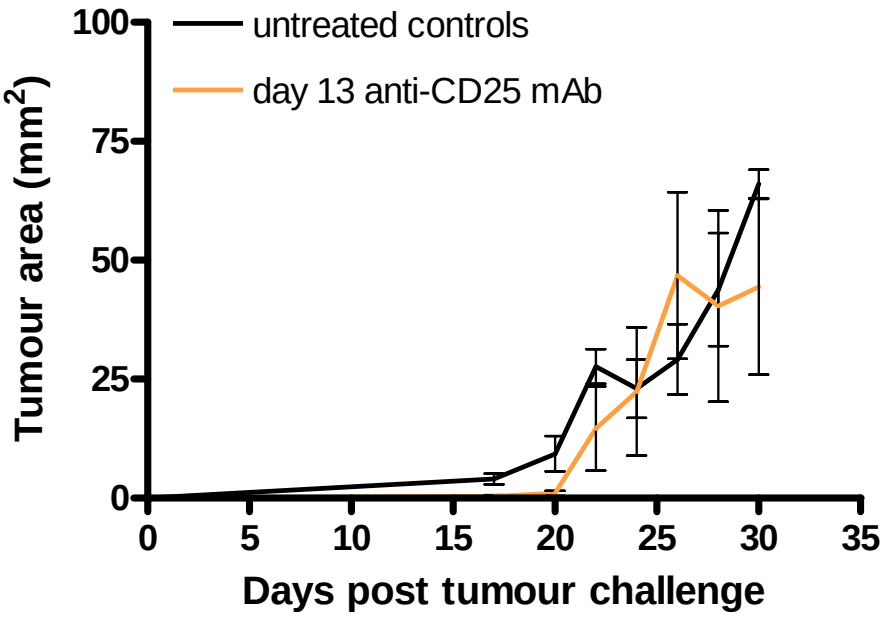

Figure 3.6: A single, systemic dose of anti-CD25 mAb timed to coincide with T_{reg} cell expansion does not inhibit the development of established murine mesotheliomas.

Mice were implanted s.c. at day 0 with 1 x 10^6 AE17 murine mesothelioma tumour cells. A single dose of 0.5 mg of anti-CD25 mAb was given i.p. to mice 13 days post tumour challenge. Control mice were untreated. Tumour areas were calculated by multiplying two, right-angled tumour diameters measured using microcallipers. Data are the mean ± SEM for 5 treated mice and 5 untreated controls.

3.3 Discussion

The clinical presence of a tumour implies that it has evaded the immune response. It was hypothesised that a population of T_{reg} cells down-regulates the immune response to MM resulting in tumour growth. By flow cytometry, $CD4^+CD25^+$ T cells were identified in the spleen, blood and LN of mesothelioma-bearing mice. If these $CD4^+CD25^+$ T cells were of the T_{reg} cell phenotype their selective inactivation would result in improved clearance of the tumour. Of seminal importance to this study was the discovery of T_{reg} cell involvement and inactivation in the murine model of advanced T cell lymphoma by North and Awwad (154). North and Awwad found that the treatment of tumour-bearing mice with a single i.p. dose of Vb at either day 13 or 15 post tumour challenge resulted in tumour regression. In a further series of experiments they demonstrated using selective inactivations of $CD4^+$ and $CD8^+$ T cells that the T_{reg} cells eliminated by Vb treatment were of the $CD4^+$ phenotype. Further studies into the involvement of T_{reg} cells in cancer identified $CD4^+CD25^+$ T cells as regulators of tumour immunity (155, 156, 179).

These studies by North and Awwad formed the basis of this PhD project and the hypothesis that T_{reg} cells are acting in MM to suppress the natural, anti-tumour immune response thus promoting tumour growth. A pilot study was conducted that found a single dose of Vb administered 14 days but not 15 days post tumour challenge significantly inhibited tumour development. This remarkably clear result was somewhat modified by further experiments. In support of the pilot study, follow-up experiments confirmed that a single dose of Vb administered on day 14 or 15 post tumour challenge resulted in significant tumour growth inhibition but not tumour regression. In comparison to the pilot study, the tumour growth rate in these experiments was much faster although the mice were implanted with the same number of tumour cells. The faster growth rate seen in these repeat experiments may have had an effect on the overall anti-tumour immune response and as such the time at which T_{reg} cells were expanding. In case T_{reg} cells were expanding earlier due to an increased tumour growth rate, it was decided to target the Vb treatment to earlier time-points. Further experimentation identified a "treatment window of opportunity" (days 12-16 post tumour challenge) within which a single dose of Vb can result in tumour growth inhibition. Based on the hypothesis that Vb targets expanding T_{reg} cells, it could now be

argued that in the murine model of mesothelioma T_{reg} cells expand in the periphery between days 12 and 16 in response to the tumour. In fact, the timing of the immune response to tumours proposed by North in 1985 suggested that T_{reg} cells were expanded between days 12 and 14 post tumour challenge (38) while this study found that T_{reg} cells expand in peripheral blood from day 14 onwards. The slight difference between the timing of T_{reg} cell expansion in these two studies may be dependent on the differing growth kinetics of the tumours studied. Tumour growth kinetics may also explain the difference in Vb efficacy seen between the pilot study and the follow-up studies in this project. If T_{reg} cells were ablated by the Vb treatment hence releasing anti-tumour CTLs from suppression and allowing them to respond to and act on the tumour, it is possible that the larger tumours at the time of treatment were not as susceptible to Vb treatment and instead were only inhibited in development by the anti-tumour CTLs. A second mechanism by which Vb may be resulting in tumour growth inhibition is, by virtue of the anti-mitotic nature of Vb, that it directly targets the highly proliferative tumour itself (170, 180, 181). *In vitro* studies showed that the murine mesothelioma tumour cells were in fact susceptible to Vb (data not shown) but the fact that Vb treatment efficacy did appear to be timing dependent (only effective when administered during the "window of treatment opportunity") suggested that Vb was not solely acting directly on the tumour.

As the targets of Vb action could include many growing cell types and the tumours could only be inhibited in tumour development and not completely regressed, a more specific T_{reg} cell inactivating treatment was investigated. T_{reg} cells had since been identified as both $CD4^+$ and $CD25^+$ and so the effect of anti-CD25 mAb administration in this tumour model was examined. In support of other published data, it was found that the systemic administration of anti-CD25 mAb, four days prior to tumour challenge with a low inoculum of tumour cells, can inhibit tumour development. In comparison, the same treatment was ineffective at inhibiting tumour development when mice were challenged with a ten-fold higher initial tumour cell inoculum. This suggested some threshold of tumour burden may exist whereby the CTLs released from suppression by the anti-CD25 mAb treatment may not be in high enough numbers to induce the clearance of an increased number of implanted tumour cells. The first hint that tumour size or tumour burden were implicated in the immuno-suppression of tumour development came from the original works of North and Awwad. They found during

their early studies of the anti-tumour effects of cyclophosphamide, γ-irradiation, anti-CD4 mAb and Vb that in all cases regression failed to occur if at the time of treatment the tumour burden was large enough to have induced dominant immuno-suppression (150-154). In addition to this, it was found in these murine mesothelioma studies and several other published studies that the anti-tumour effect of anti-CD25 mAb administered before tumour inoculation was no longer seen if the treatment was given on day 0 or thereafter. These studies were attempting to systemically inactivate all T_{reg} cells in the mice, be they tumour-specific or not, but at the same time may have targeted other cell populations which can express the CD25 molecule, such as activated $CD8^+$ CTLs, which are essential to the clearance of tumours (182-184).

This potential non-specificity of systemic anti-CD25 mAb administration has complicated the interpretation of these results, as was also the case for Vb. The observation that timed anti-CD25 mAb treatment (d13 post tumour challenge) had no effect on tumour development when given systemically probably reflects the tumour inoculum being too large (established tumours) and/or the low bioavailability of the mAb at the tumour site following systemic delivery. Inoculum size in these experiments, established tumours evading the immune system and the variable rate of tumour growth are all suggesting that systemic treatments (Vb or anti-CD25 mAb) are going to fail or at the very least be difficult to apply clinically.

At this time there was some published evidence for the presence of T_{reg} cells within tumours themselves, specifically murine melanoma (53) and human lung, ovarian and colorectal tumours (25, 118). As only a small but significant upregulation of T_{reg} cells was seen in the blood of mesothelioma-bearing mice over the time-course of tumour challenge it was possible that T_{reg} cells would be found within murine mesotheliomas. T_{reg} cells had not yet been identified in either human or murine mesotheliomas and so Chapter 4 describes for the first time the intra-tumoural discovery of $CD4^+CD25^+$ T_{reg} cells in murine mesotheliomas.

Chapter 4:
Intra-tumoural T_{reg} cells in murine mesothelioma

4.1 Introduction

Although our research group and others had evidence for T_{reg} cell involvement in cancer (see Chapter 3), there was only a very limited understanding of whether T_{reg} cells existed and acted within tumours themselves (26, 120). T_{reg} cells had been shown to constitute a component of tumour infiltrating lymphocytes (TILs) in murine melanomas (53) and human lung, ovarian and colorectal tumours (25, 118) but there was little published evidence for any changes in the intra-tumoural T_{reg} cell population with tumour development. One study showed that there was no significant difference between the prevalence of $CD4^+CD25^+$ T_{reg} cells in normal breast and pancreatic tissue donors and patients with benign breast and pancreatic lesions but that there was a significant increase in $CD4^+CD25^+$ T_{reg} cells in the tumours of patients with malignant breast or pancreatic cancer (122). Ichihara *et al* (2003) had similarly found that there was an increase in $CD4^+CD25^+$ T_{reg} cells as a percentage of all TIL in advanced gastric cancer as compared to the percentage in early gastric cancer or normal gastric mucosa (95).

To begin the investigation of intra-tumoural T_{reg} cells in murine mesothelioma it was important to develop a method for the dissociation of solid tumours for the preparation of single cell suspensions for flow cytometric analysis. This chapter provides the first flow cytometric evidence for intra-tumoural T_{reg} cell involvement in murine mesothelioma and supports the hypothesis that intra-tumoural T_{reg} cells within tumours allow the evasion of the host anti-tumour immune response leading to increased tumour growth. In addition to this, by analysing tumours of varying sizes it was found that there is a strong correlation between tumour size and the percentage of intra-tumoural $CD4^+CD25^+$ T_{reg} cells in murine mesotheliomas.

The co-expression of CD4 and CD25 by T cells was used to identify T_{reg} cells in the early studies of T_{reg} cell involvement in tumour immunity but was hindered, as outlined in Chapter 3, by the expression of CD25 by other cell types including activated CTLs, activated B cells and some DCs (182-184). The discovery in 2003 of the forkhead transcription factor Foxp3 as a specific marker of $CD4^+CD25^+$ T_{reg} cells markedly improved the understanding of T_{reg} cell development and function but also allowed for a more thorough examination of T_{reg} cell involvement in tumour immunity (64, 185, 186).

Intra-cellular flow cytometric staining for Foxp3 was used in this chapter to confirm the regulatory phenotype of the intra-tumoural $CD4^+CD25^+$ T cells in murine mesotheliomas.

Curious as to whether the correlation between increasing tumour size and an increase in the percentage of intra-tumoural T_{reg} cells in murine mesothelioma was a mesothelioma specific phenomenon, murine B16 melanomas and EL4 lymphomas (both of which are syngeneic to C57BL/6J mice) were also analysed for intra-tumoural T_{reg} cells. Interestingly, a lower percentage of T_{reg} cells was observed in both B16 melanomas and EL4 lymphomas.

Finally, the translation of this data to the clinic and any follow up studies investigating the immuno-modulation of T_{reg} cells as an immunotherapy for MM would be improved by a concurrent identification of T_{reg} cells in human MM tumours. The initiation of this work into the identification of T_{reg} cells in human MM is reported in this chapter however during the early experimental development three manuscripts (31, 32, 35) detailing T_{reg} cell levels associated with human MM were published and this laboratory's work on human MM sections was terminated.

4.2 Results

4.2.1 Intra-tumoural T_{reg} cells in murine mesothelioma.

The same 5 week time-course of AE17 tumour development described in Chapter 3 was used here to examine intra-tumoural T_{reg} cells in murine mesothelioma and any changes in this population with respect to tumour development.

4.2.1.1 The dissociation of solid murine mesotheliomas for flow cytometric analysis.

To begin the investigation of intra-tumoural T_{reg} cells, several months were spent developing a suitable protocol for the dissociation of tumours for flow cytometric analysis. The analysis of solid tumours by flow cytometry can be difficult due to the highly heterogeneous populations of cells that comprise tumours including TILs,

endothelial cells and the tumour cells themselves. Several protocols for the dissociation of tumours and the preparation of single cell tumour suspensions were compared. Mechanical dissociation alone involved the mincing of solid tumours with scissors and/or a scalpel prior to the passing of the tumour homogenate through a fine wire mesh to remove any remaining large clumps of cells. This method for the preparation of a single cell homogenate for the flow cytometric analysis of intra-tumoural T_{reg} cells was found to be sub-optimal as both a very "sticky" preparation resulted which blocked the flow cytometer but also a distinct population of $CD4^+$ T cells was difficult to resolve. A combination of mechanical dissociation as outlined above and enzymatic digestion by the addition of the enzymes collagenase and dispase, as used by the Beilharz laboratory for the dissociation of murine muscles (167), was also trialled but again resulted in sup-optimal preparations for flow cytometric analysis of solid tumours for the same reasons as outlined for mechanical dissociation alone.

The final protocol tested for solid tumour dissociation, which was also chosen for all future experiments, again involved a combination a mechanical dissociation and enzymatic digestion. Specifically, and as described in full detail in Chapter 2, Section 2.2.3.3, tumours were surgically removed and collected into unsupplemented RPMI-1640. Tumours were then minced finely using scissors and then enzymatically digested for 40 min at room temperature by the addition of Liberase blendzyme 3 and DNase 1. Finally the tumour cell homogenate was pushed through a fine wire mesh spoon sieve using the plunger of a syringe to break down any remaining clumps and resuspended in FACS buffer for staining with fluorochrome-conjugated antibodies for flow cytometric analysis. This method for the dissociation of solid tumours resulted in the preparation of tumour cell suspensions that both flowed well through the flow cytometer and also allowed the resolution of a distinct population of intra-tumoural $CD4^+$ T cells as shown in Figure 4.1.

The $CD4^+CD25^+$ T_{reg} cell subset was determined as a percentage of tumour-located $CD4^+$ T cells by flow cytometry with dual-colour staining. An example of the original flow cytometric data obtained from dissociated AE17 tumours is presented in Figure 4.1 to illustrate the gating criteria used in the following experiments. An obvious $CD4^+$ T cell population was seen when comparing side-scatter and expression of CD4-APC (Fig. 4.1A). These $CD4^+$ T cells were then analysed for the expression of

CD25-FITC (Fig. 4.1B). In this example of an advanced tumour, a high proportion of these tumour-located $CD4^+$ T cells (approximately 60%) co-expressed CD25.

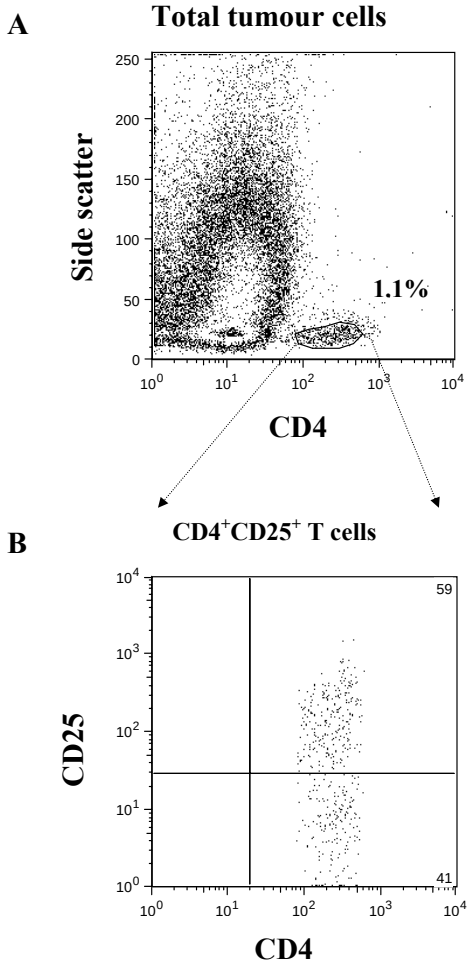

Figure 4.1: Identification of T_{reg} cells within murine mesothelioma tumours by flow cytometry.
(A) An example of original flow cytometric data of a dissociated AE17 tumour illustrating gating criteria for the isolation of $CD4^+$ T cells. Side scatter is represented on the vertical axis while the expression of CD4 is represented on the horizontal axis. (B) The distinct intra-tumoural population of $CD4^+$ T cells was then examined for the co-expression of CD25. Again CD4 expression is represented on the horizontal axis while the vertical axis represents CD25 expression.

4.2.1.2 $CD4^+CD25^+$ T_{reg} cells are resident within murine mesothelioma tumours.

For the intra-tumoural analysis of T_{reg} cells in murine mesothelioma, tumours were removed from mice at weekly intervals over a 5 week time-course of AE17 tumour development (1 x 10^6 AE17 tumour cell inoculum). The combined data showing the intra-tumoural percentages of T_{reg} cells from two, 5 week time-course experiments are presented in Figure 4.2A with a total of 8 tumour-bearing mice analysed per time-point. There is a highly significant increase ($p < 0.001$) in the percentage of $CD4^+CD25^+$ T_{reg} cells from 21.3 ± 2.4% to 54.7 ± 3.2% of tumour-located $CD4^+$ T cells between days 21 and 28 post tumour challenge. This increase is not due to a simultaneous increase in $CD4^+$ T cells within the tumour as over the same time period, intra-tumoural $CD4^+$ T cell percentages remained essentially constant at 1.9 ± 0.2% of the total tumour cells (Fig. 4.2B).

4.2.1.3 The intra-tumoural T_{reg} cell percentage increases with tumour size.

As discussed in Chapter 3 there is a significant amount of variability in tumour growth rate with AE17 tumours capable, from experiment to experiment, of having quite different tumour areas at particular time-points post tumour challenge. To improve the analysis of intra-tumoural $CD4^+CD25^+$ T_{reg} cell population changes, the data presented in Figure 4.2A were re-analysed with respect to tumour size rather than time post tumour challenge (Fig. 4.3). There is an initial sharp increase in the percentage of $CD4^+CD25^+$ T_{reg} cells observed within tumours up to a size of approximately 9 mm^2. In tumours greater than 9 mm^2 a slower increase in T_{reg} cell percentage with tumour size is seen with most tumours greater than 30 mm^2 showing approximately 60% T_{reg} cell content.

To confirm this correlation between tumour size and T_{reg} cell percentage a further set of tumours were removed at either 9 mm^2 or 80 mm^2 from mice challenged with a ten-fold higher tumour cell inoculum (1 x 10^7 AE17 cells) and compared to tumours developed from the original 1 x 10^6 AE17 tumour cell inoculum. With this 10-fold larger tumour cell inoculum, tumours grow at a significantly faster rate. Even with the higher initial tumour cell inoculum, and faster growth rate, small tumours (9 mm^2) have a significantly lower percentage ($p < 0.05$) of $CD4^+CD25^+$ T_{reg} cells than large tumours (80 mm^2) (Fig. 4.4). Moreover, 9 mm^2 and 80 mm^2 tumours developed from 1 x 10^7

AE17 cells contain a similar percentage of T_{reg} cells to tumours of the same size developed from 1 x 10^6 tumour cells despite the 10-fold variation in initial tumour cell inoculum and hence the time it takes to reach the particular tumour size.

4.2.1.4 Confirmation of T_{reg} cell phenotype in murine mesothelioma: Foxp3 expression.

CD25 is also an activation marker and can therefore be expressed not only by T_{reg} cells but other activated T cells (182-184). Although $CD4^+CD25^+$ T cells had been the commonly accepted phenotype of T_{reg} cells, the expression of Foxp3, a transcription factor involved in both T_{reg} cell development and function, had become, at this time, a newer and more definitive marker of the T_{reg} cell phenotype (27, 185-187). It was therefore important to assess whether or not the intra-tumoural $CD4^+CD25^+$ T_{reg} cells found to increase in percentage inside murine mesotheliomas were also Foxp3 expressing. An intra-cellular flow cytometric analysis of 22 dissociated tumours revealed the distinct population of tumour-located $CD4^+CD25^+$ T_{reg} cells to express high levels of Foxp3 in tumours of all sizes (Fig. 4.5). Regardless of tumour size, 81.5 ± 2.5% of intra-tumoural $CD4^+CD25^+$ T_{reg} cells expressed this marker confirming their regulatory phenotype.

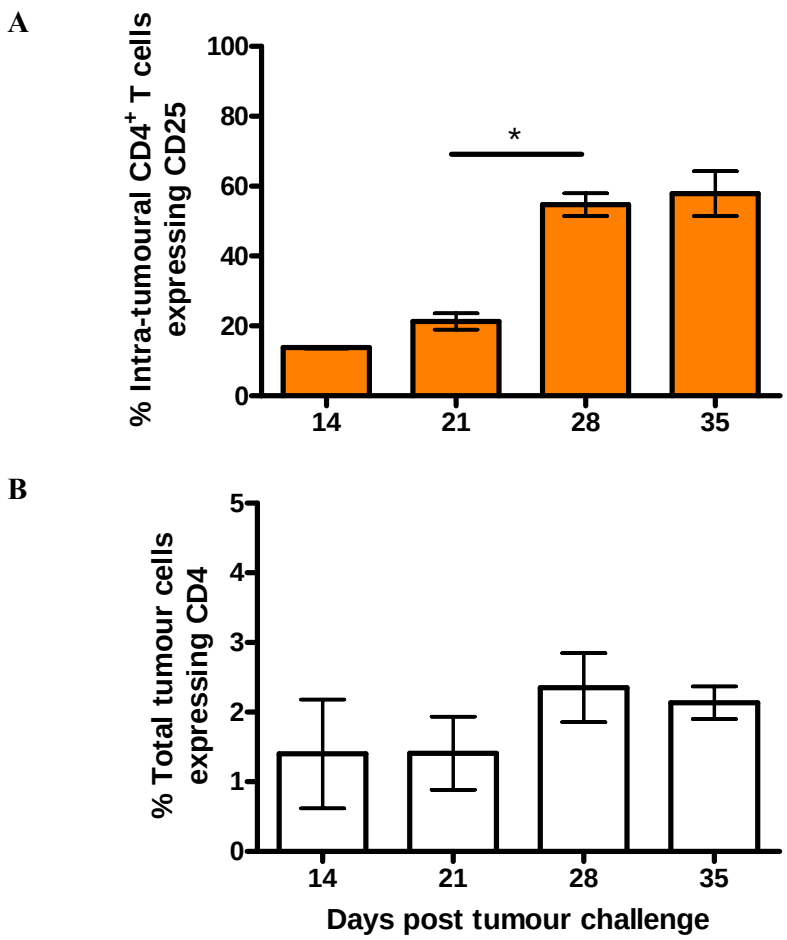

Figure 4.2: $CD4^+CD25^+$ T_{reg} cell upregulation within murine mesotheliomas.

Mice were implanted s.c. at day 0 with 1 x 10^6 AE17 tumour cells. Mice were culled at days 14, 21, 28 and 35 post tumour challenge and tumours removed, dissociated and analysed by flow cytometry for the presence of (A) $CD4^+CD25^+$ T_{reg} cells and (B) $CD4^+$ T cells. (A) $CD4^+CD25^+$ T_{reg} cells were calculated as a percentage of tumour-located $CD4^+$ cells while (B) $CD4^+$ T cells were calculated as a percentage of total tumour cells over a 5 week time-course of tumour development. Data are the mean ± SEM of 8 mice per time-point. A single asterisk represents a p-value < 0.05.

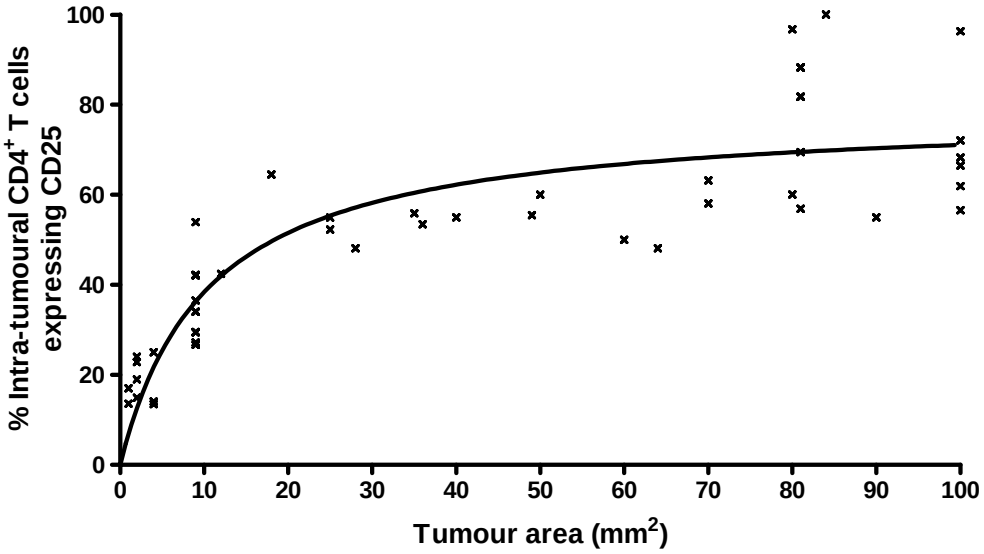

Figure 4.3: Intra-tumoural $CD4^+CD25^+$ T_{reg} cell increase correlates with tumour size.

Mice were inoculated s.c. with 1 x 10^6 AE17 cells at day 0. Tumour areas were calculated by multiplying two right-angled tumour diameters measured using microcallipers. Tumours were removed at the appropriate sizes and single cell suspensions made for flow cytometric analysis with CD25 expression presented as percentage of tumour-located $CD4^+$ T cells. 45 mice were analysed in this experiment and a line of regression plotted.

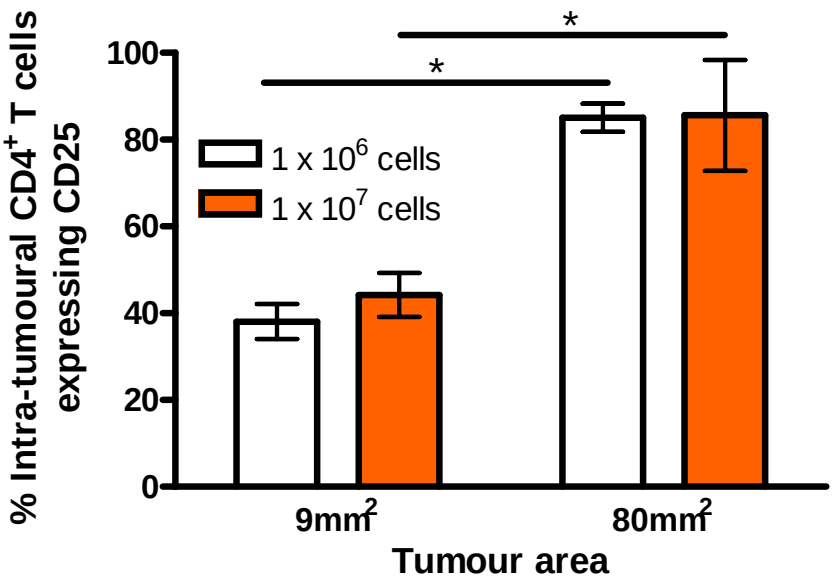

Figure 4.4: Intra-tumoural $CD4^+CD25^+$ T_{reg} cell increases correlate with tumour size irrespective of initial tumour cell inoculum.

Mice were inoculated s.c. with 1 x 10^6 (□) or 1 x 10^7 (■) AE17 cells at day 0. Tumour areas were calculated by multiplying two right-angled tumour diameters measured using microcallipers. Tumours were removed at the appropriate sizes and single cell suspensions made for flow cytometric analysis. The expression of CD25 was presented as a percentage of tumour-located $CD4^+$ T cells. Data are the mean ± SEM of 3 mice per time-point. A single asterisk represents a p-value < 0.05.

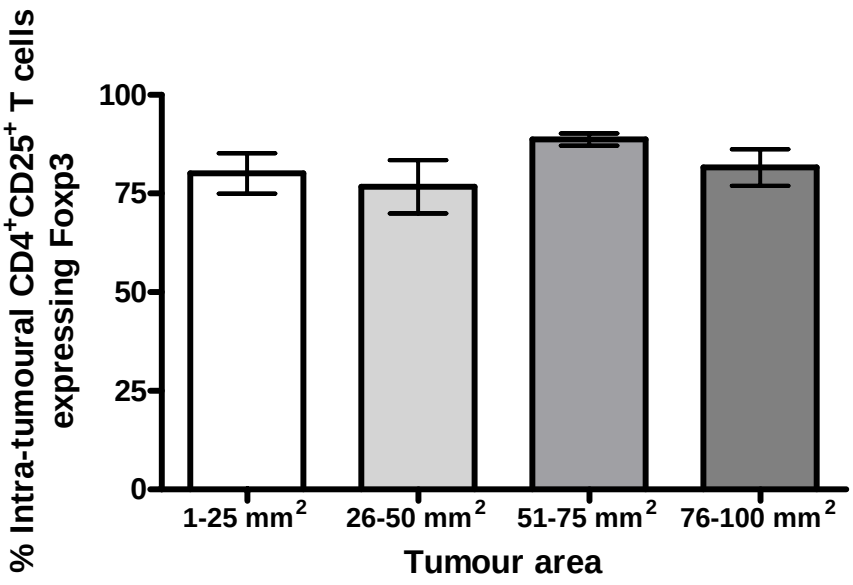

Figure 4.5: Foxp3 expression confirms regulatory phenotype of intra-tumoural $CD4^+CD25^+$ T_{reg} cells.

Mice were implanted s.c. with 1 x 10^7 AE17 tumour cells. 7 mice with tumours between 1 and 25 mm^2, 4 mice with tumours between 26 and 50 mm^2, 4 mice with tumours between 51 and 75 mm^2 and 7 mice with tumours between 76 and 100 mm^2 were analysed. Tumours were removed, dissociated and analysed by intra-cellular flow cytometry for the presence of $CD4^+CD25^+Foxp3^+$ T cells. $CD4^+CD25^+Foxp3^+$ T cells were calculated as a percentage of tumour-located $CD4^+CD25^+$ T cells. Data are the mean ± SEM.

4.2.2 Intra-tumoural T_{reg} cells in other murine tumour models

The discovery of $CD4^+CD25^+Foxp3^+$ T_{reg} cells within murine mesotheliomas and the correlation of a large increase in intra-tumoural T_{reg} cell percentage with increasing tumour size was novel. It was of interest to determine if this was a general feature of other tumour types by testing two further murine models of melanoma (B16) and lymphoma (EL4).

4.2.2.1 Murine B16 melanoma

Eight mice were implanted s.c. with 5 x 10^5 B16 melanoma cells. Four tumours were harvested from mice when tumours were between 9 and 20 mm^2 while the remaining 4 tumours were grown to between 80 and 100 mm^2. Tumours were then dissociated as per the murine mesothelioma protocol and analysed for the percentage of $CD4^+$ T cells co-expressing CD25. Figure 4.6 shows the statistically significant difference in the percentage of intra-tumoural $CD4^+$ T cells expressing CD25 observed between small ($19.2 \pm 3.4\%$) and large ($31.2 \pm 2.6\%$) tumours ($p = 0.03$). Again, there was no difference in intra-tumoural $CD4^+$ T cells as a percentage of total tumour cells between small ($0.4 \pm 0.2\%$) and large ($0.3 \pm 0.1\%$) tumours ($p = 0.5$). Foxp3 analysis of the intra-tumoural $CD4^+CD25^+$ T_{reg} cells in large B16 melanoma revealed that only $43.4 \pm 1.4\%$ co-expressed Foxp3.

4.2.2.2 Murine EL4 lymphoma

Four mice were implanted s.c. with 1 x 10^6 EL4 lymphoma cells. Tumours were harvested from mice when tumours were 100 mm^2 in size. Tumours were then dissociated as per the murine mesothelioma protocol and analysed for the percentage of $CD4^+$ T cells co-expressing CD25. Again, only a very low percentage of total $CD4^+$ T cells were found within EL4 lymphomas ($0.4 \pm 0.1\%$). Of these intra-tumoural $CD4^+$ T cells within large tumours the percentage expressing CD25 was $41.8 \pm 2.8\%$. Foxp3 analysis of the intra-tumoural $CD4^+CD25^+$ T_{reg} cells in EL4 lymphoma revealed that only $5.0 \pm 2.5\%$ co-expressed Foxp3.

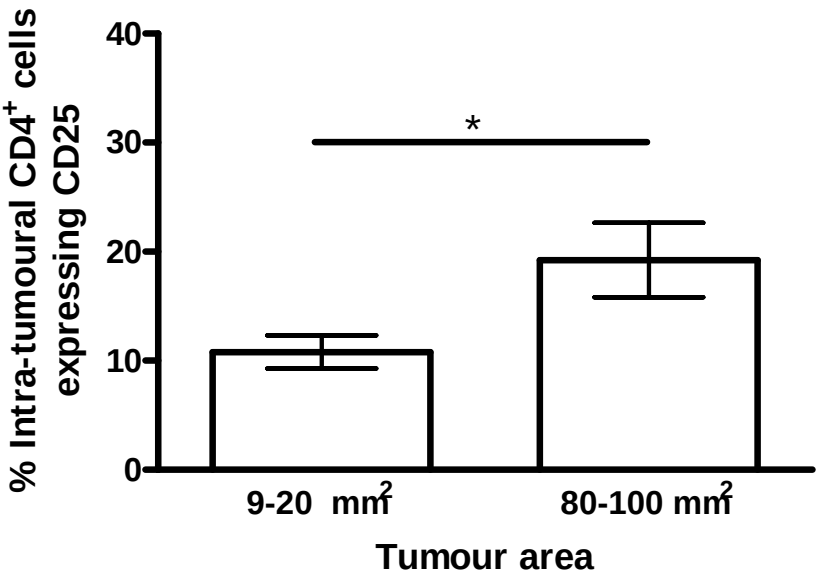

Figure 4.6: Intra-tumoural T_{reg} cells in murine B16 melanoma.

Mice were implanted s.c. at day 0 with 5 x 10^5 B16 melanoma cells. Mice were culled when tumours were between 9 and 20 mm^2 or between 80 and 100 mm^2. Tumours were removed, dissociated and analysed by flow cytometry for the presence of $CD4^+CD25^+$ T_{reg} cells. $CD4^+CD25^+$ T_{reg} cells were calculated as a percentage of tumour-located $CD4^+$ T cells. Data are the mean ± SEM of 4 mice per size range. A single asterisk represents a p-value < 0.05.

4.2.3 Intra-tumoural T_{reg} cells in human MM

After seeing some differences in intra-tumoural T_{reg} cell percentages between murine mesothelioma, melanoma and lymphoma it was important to determine the relevance of this mouse work to human MM. We therefore collaborated with Professor Bruce Robinson's group to investigate the intra-tumoural presence of $CD4^+CD25^+Foxp3^+$ T_{reg} cells in human MM biopsies. Prof. Robinson's group have developed a tissue biopsy slide array which can be used for the immunohistochemical analysis of multiple biopsy samples at the one time with a concurrent comparison to multiple organ control tissues. These slides are paraffin embedded and hold approximately 35 replicates/patient MM biopsy samples plus approximately 35 pleural effusion samples and 35 control tissue samples such as tonsil and appendix (Fig. 2.1). The objective of this experiment was to conduct three colour immunohistochemistry to determine the percentage of intra-tumoural $CD4^+CD25^+Foxp3^+$ T_{reg} cells. As Foxp3 is the most specific indicator of T_{reg} cells (and estimated to be expressed by approximately 1% of sectioned cells) it was used in the initial experiments to optimise staining prior to including a CD25 co-stain and a triple stain for CD4 was to follow, if technically possible.

Initially, control experiments staining human tonsil sections and a benign lymphocytic effusions with the individual antibodies (Ebioscience, anti-human Foxp3 and Novocastra, anti-human CD25) were performed. Figures 4.7 and 4.8 depict good membrane staining of $CD25^+$ cells and nuclear staining of $Foxp3^+$ cells when the antibodies are used separately. Careful examination of figures 4.7B and 4.8B shows the central stained cell to have a circular staining pattern (darker stain at edges of the cells) consistent with membrane staining of CD25. The central cells in figures 4.7D and 4.8D show punctate central staining consistent with the nuclear localisation of the Foxp3 stain. Many attempts to perform double staining were unsuccessful. When punch biopsy specimens of MM tissue were stained with the antibodies individually very few positive cells were observed. 14 from 25 MM samples were negative for CD25, 9 MM biopsies had occasional $CD25^+$ cells while only 2 could convincingly be said to be $CD25^+$. In terms of Foxp3 expression, 23 from 25 MM biopsy samples were negative for Foxp3 staining while only two MM samples were found to contain Foxp3 positive cells.

No more time was devoted to the optimisation of this immunohistochemical technique and the subsequent determination of intra-tumoural T_{reg} cells percentages in human MM tumours as publications appeared at this time with evidence for the presence of T_{reg} cells in human pleural effusions associated with MM, the peripheral blood of MM patients and MM tumours themselves (31, 32, 35). These publications found that $CD4^+CD25^+$ T_{reg} cells were present in the pleural effusions secondary to mesothelioma (7.8% ± 6.8%,) but were significantly lower in prevalence than in non-small cell lung or breast cancer patients (15.0% ± 5.9% and 15.9% ± 3.2%, respectively). In the peripheral blood of MM patients the prevalence of $CD4^+CD25^+$ T_{reg} cells was found to be 13.6% ± 6.4% (188). A significant increase in percentages and absolute counts of the total $CD4^+CD25^+$ T_{reg} cell subset was observed in the peripheral blood of pleural mesothelioma patients (approximately 450 cells/µl blood, n = 10) with respect to healthy donors (approximately 300 cells/µl blood, n = 40) (35). Finally, mesothelioma tissue sections have been analysed by fluorescence microscopy for the phenotypic evidence of $CD4^+CD25^+$ T cells. $CD4^+CD25^+$ T cells were particularly detected at the rim of tumour areas and were confirmed to be Treg cells by staining for Foxp3 (32).

(A) CD25 (20x)

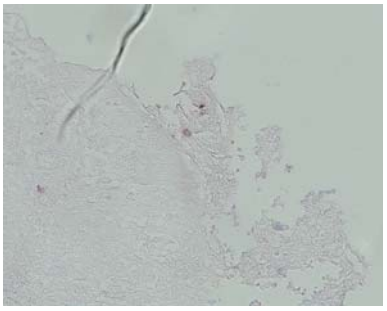

(B) CD25 (40x)

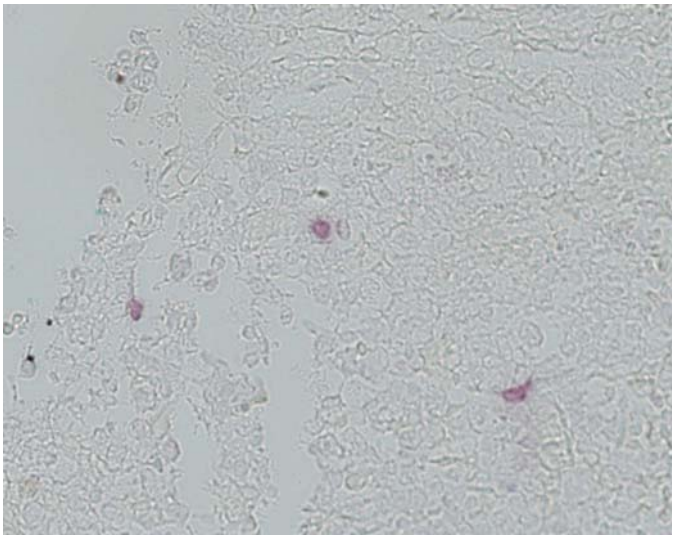

(C) FOXP3 (20x)

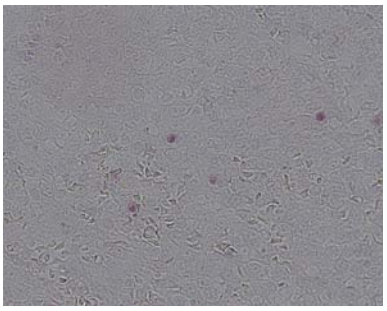

(D) FOXP3 (40x)

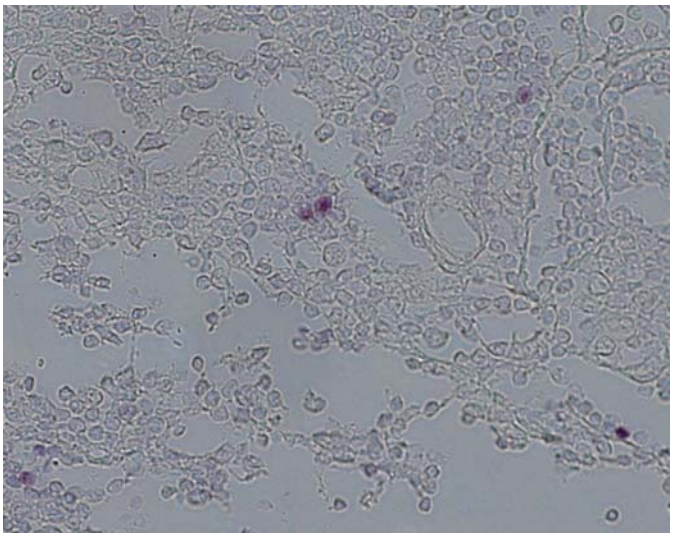

Figure 4.7: Human tonsil sections used for optimising immunohistochemical staining for CD25 and Foxp3

Paraffin embedded human tonsil sections were used to optimise the immunohistochemical staining procedure for T_{reg} cells. (A and B) CD25 cell surface staining (dark pink) at 20x and 40x magnification. (C and D) Foxp3 nuclear staining (dark pink) at 20x and 40x magnification.

(A) CD25 (20x)

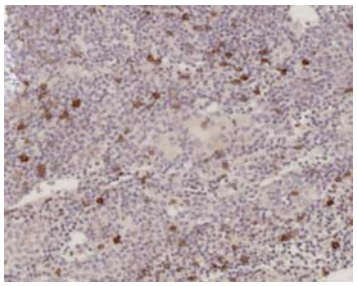

(B) CD25 (40x)

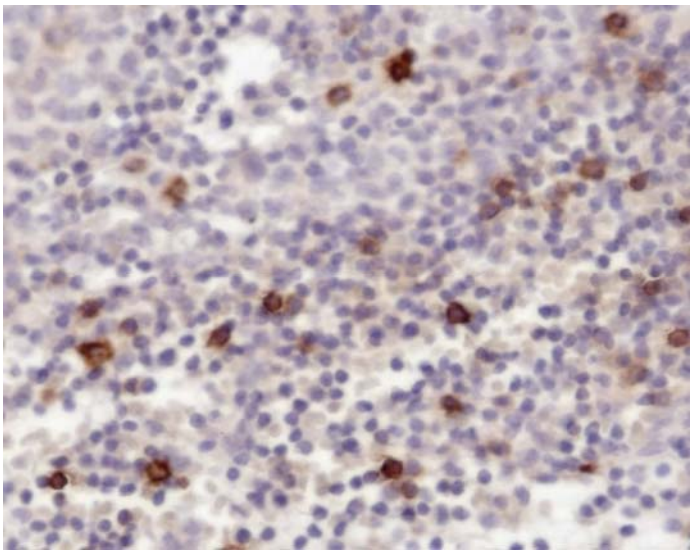

(C) FOXP3 (20x)

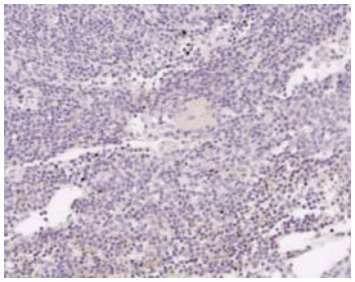

(D) FOXP3 (40x)

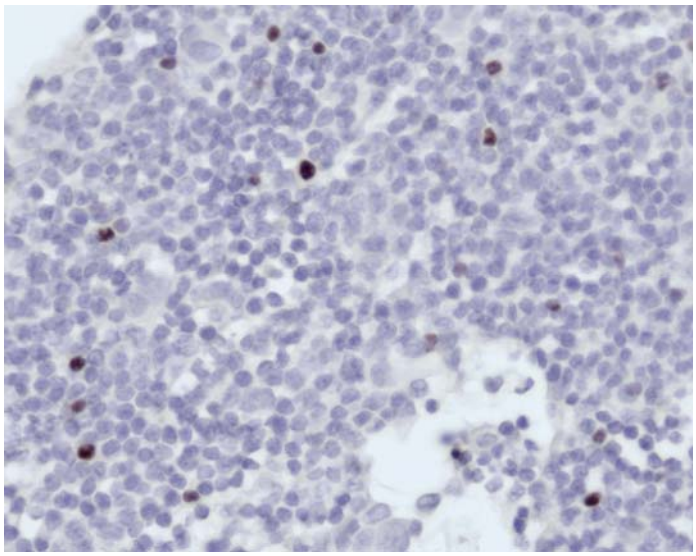

Figure 4.8: Benign lymphocytic effusion used for optimising immunohistochemical staining for T_{reg} cells

Paraffin embedded human benign lymphocytic effusions were also used to optimise the immunohistochemical staining procedure for T_{reg} cells. (A and B) CD25 cell surface staining (brown) at 20x and 40x magnification. (C and D) Foxp3 nuclear staining (brown) at 20x and 40x magnification.

4.3 Discussion

Active and specific immunotherapy of cancers has long been an elusive goal in medicine. While a rare case of spontaneous mesothelioma regression has been reported (11), most attention has been focussed on effector cell "boosting" strategies which have been trialled with limited success to induce mesothelioma growth inhibition (14, 189-193). Evaluations into the presentation of tumour antigens in murine mesothelioma models demonstrated clearly that tumour antigens are constitutively presented in the tumour-draining LN and that they can stimulate T cell proliferative responses (194, 195). It can be concluded from these studies that ignorance to tumour antigens is not an explanation for the failure of the host immune response. As it is known that tumour antigens are being presented, efforts have turned to increasing CTL activity in order to induce tumour regression. Endogenous tumour-specific CTL responses have been enhanced following the treatment of murine mesotheliomas with intra-tumoural IL-2 (14). This treatment strategy however, was only successful at regressing tumours that were small (<13 mm^2) at the time of treatment but not large tumours (>30 mm^2). This suggests that an efficient anti-tumour immune response can be invoked, but that at later stages of tumour development this anti-tumour immune response is being suppressed. It is hypothesised that T_{reg} cells actively suppress the anti-tumour immune response thus inhibiting the efficacy of many trialled immunotherapies and may explain the above mentioned findings of a limited response by large tumours to intra-tumoural IL-2 treatment.

In this chapter the intra-tumoural upregulation of $CD4^+CD25^+Foxp3^+$ T_{reg} cells as a tumour immune evasion mechanism in the murine model of mesothelioma was examined. A strong correlation between tumour size and percentage of $CD4^+CD25^+Foxp3^+$ T cells within the murine mesotheliomas was demonstrated and formed part of our group's recent publication (196). This suggested that the increase in T_{reg} cells within the small murine mesotheliomas allows the evasion of the host anti-tumour effector immune response leading to increased tumour growth. In addition, it was shown that tumours of the same size have similar percentages of T_{reg} cells regardless of the initial inoculum used to create the tumours. Together these results suggested that as a tumour reaches a particular size (~9 mm^2) T_{reg} cells are recruited to

and/or induced within tumours resulting in the suppression of the anti-tumour immune response and rapid tumour growth.

Previous knowledge of T_{reg} cells suggested they had a role to protect against autoimmune disease and hence self-antigens. It was therefore initially hard to understand the reason behind the involvement of T_{reg} cells in tumour immunity. One hypothesis is that T_{reg} cells were directed against self antigens expressed by tumour cells and so were acting to protect against "self" destruction (197, 198). Other work in the field of tumour immunity suggested that tumours had the ability to actively evade the anti-tumour immune response (199, 200). Anti-tumour immune evasion mechanisms include down-regulation of MHC class I, loss of tumour antigen expression, down-regulation of adhesion/accessory molecules by tumour and/or APC, induction of anergy or clonal deletion of responding T cells and changes in T cell signal transduction molecules. We therefore proposed that T_{reg} cells were recruited to tumours or induced within tumours as an anti-tumour immune evasion mechanism. Together, the results presented in this chapter suggest that as a tumour reaches a particular size, T_{reg} cells are upregulated and the anti-tumour immune response is suppressed resulting in rapid tumour growth.

Concurrent with and subsequent to these murine mesothelioma studies characterising the changes in intra-tumoural $CD4^+CD25^+Foxp3^+$ T_{reg} cells other groups have described T_{reg} cells within murine tumours such as melanoma, fibrosarcoma and mammary tumours (28, 53, 121) and in human mesothelioma, lung, ovarian, colorectal, breast, pancreatic and gastric tumours (25, 27, 95, 118, 122, 123). Of high importance to this study was the identification of T_{reg} cells in human MM biopsies by immunohistochemistry (32). Only a few of these studies have however, characterized changes in the intra-tumoural T_{reg} cell population. In a mouse fibrosarcoma model it was most recently found that although there is no change in the $CD4^+CD25^+$ T_{reg} cell population within the spleen and draining-LN of tumour-bearing mice, there is an increase in the $CD4^+CD25^+$ T_{reg} cells in tumours between day 7 and day 16 post tumour challenge (from approximately 30% to approximately 65%) (28). Curiel *et al* (2004) found a much larger percentage of T_{reg} cells in late stage human ovarian carcinomas where $CD4^+CD25^+$ T_{reg} cells represented approximately 30% of total intra-tumoural $CD4^+$ T cells compared to the percentage found in early stage tumours

($CD4^+CD25^+$ T_{reg} cells represented approximately 12% of total tumour-located $CD4^+$ T cells). As a final comparison it was shown that $CD4^+CD25^+$ T_{reg} cells were undetectable in normal ovarian tissue.

Although there were varying methods for the quantification of intra-tumoural T_{reg} cells used in the above studies, it is clear that different tumours have different intra-tumoural percentages of T_{reg} cells. When B16 melanomas were examined in this chapter a similar trend of intra-tumoural T_{reg} cell percentage increases between small and large tumours was found. However, overall in both the B16 melanoma model and EL4 lymphoma model a much lower percentage of intra-tumoural $CD4^+$ T cells and $CD4^+CD25^+Foxp3^+$ T_{reg} cells were observed (in large mesotheliomas approximately 60% of $CD4^+$ T cells were CD25 expressing while only 20% and 40% of $CD4^+$ cells were $CD25^+$ in melanomas and lymphomas respectively). These lower percentages of intra-tumoural T_{reg} cells observed in both murine melanoma and lymphoma tumours may suggest that B16 melanomas and EL4 lymphomas rely less on T_{reg} cells for immune evasion. In fact, several tumour immune evasion mechanisms, other than the upregulation of T_{reg} cells, have been described (201, 202). In a recent review of immune evasion mechanisms in melanoma, T-cell anergy, the expression of inhibitory ligands such as programmed cell death-ligand 1 (PD-L1), the activity of nutrient–catabolising enzymes such as indoleamine 2,3-dioxygenase (IDO) and T_{reg} cells were all suggested to be involved in tumours escaping the immune response (203).

Finally, the correlation between the substantial intra-tumoural increase in T_{reg} cells and tumour size is not a direct proof of their role as T_{reg} cells. Although the Foxp3 expression data presented in this chapter confirmed the regulatory phenotype of the intra-tumoural $CD4^+CD25^+$ T cells, an analysis of the suppressive function of these cells *in vivo* was still required. To demonstrate the functional role of intra-tumoural T_{reg} cells in murine mesothelioma a method for the intra-tumoural inactivation of T_{reg} cells was developed and is presented in the next chapter.

Chapter 5:
Intra-tumoural T_{reg} cell inactivation

5.1 Introduction

Chapter 4 showed for the first time that murine AE17 mesotheliomas can be a site of T_{reg} cell activity in that a large upregulation of intra-tumoural $CD4^+CD25^+Foxp3^+$ T_{reg} cells occurs with tumour development. This finding coupled with the fact that the efficacy of anti-CD25 mAb administered systemically as an anti-tumour therapy (Chapter 3, Section 3.2.3) was limited by the tumour burden and non-specificity encouraged the examination of the specific intra-tumoural inactivation of T_{reg} cells as a therapy for mesothelioma.

There were now several published protocols for the systemic inactivation of T_{reg} cells via the administration of monoclonal antibodies such as anti-CD25 mAb and anti-CTLA-4 mAb (87, 156, 157). However, at this time, only one other published attempt had been made to intra-tumourally modulate T_{reg} cells. T_{reg} cell function was successfully modulated by the intra-tumoural administration of anti-IL-10 mAb (53). IL-10 is an immunosuppressive cytokine and is accepted as one of the mechanisms by which T_{reg} cells exert their suppression (50, 204-206).

CD25 is a critical marker of T_{reg} cells as it is the IL-2 receptor alpha chain. IL-2 is critical for the development and peripheral expansion of $CD4^+CD25^+$ T_{reg} cells (41, 207-209). Although there is some controversy as to whether the administration of anti-CD25 mAb (PC61) results in the depletion or inactivation (shedding of the CD25 molecule) of T_{reg} cells it is clear that this monoclonal antibody has the ability to disrupt T_{reg} cell function (132, 210). This chapter reveals the novel suppressive *in vivo* functioning of $CD4^+CD25^+Foxp3^+$ T_{reg} cells within murine mesotheliomas by demonstrating that the intra-tumoural inactivation of these cells using anti-CD25 mAb results in the marked inhibition of established tumour growth.

To further understand the mechanism of action of anti-CD25 mAb treatment tumour infiltrating lymphocyte (TIL) populations were examined post treatment. As this treatment regime appeared promising, it was studied intensely to identify any limitations or improvement that could be made.

5.2 Results

The murine model of mesothelioma was used to examine the effect of the intra-tumoural inactivation of T_{reg} cells using the anti-CD25 mAb (PC61) in a novel treatment regime involving intra-tumoural injections of the antibody.

5.2.1 Intra-tumoural inactivation of T_{reg} cells.

The effect of intra-tumoural anti-CD25 mAb administration on intra-tumoural T_{reg} cell inactivation, the subsequent release of $CD8^+$ CTLs from immunosuppression and the effect of this treatment on tumour growth were investigated.

5.2.1.1 Intra-tumoural anti-CD25 mAb treatment inactivates intra-tumoural T_{reg} cells and releases anti-tumour $CD8^+$ CTLs from immunosuppression.

Mice were implanted s.c. with 1 x 10^7 AE17 tumour cells. For intra-tumoural (i.t.) T_{reg} cell inactivations, mice received a total of 0.15 mg of anti-CD25 mAb in 40 µl PBS administered to tumours once they had reached 9 mm^2 size. 10 µl of mAb was injected directly into the tumour followed by injections of 10 µl s.c. at 120° intervals around the base of the tumour. Tumours were then removed 1 day, 3 days or 10 days post intra-tumoural anti-CD25 mAb treatment and analysed by flow cytometry by secondary staining with a mAb directed against a different CD25 epitope (7D4 clone) and compared to untreated control tumours (day 0). The percentage of intra-tumoural $CD4^+CD25^+$ T_{reg} cells remaining after the treatment was determined as a percentage of total $CD4^+$ T cells (Fig. 5.1A). The percentage of these $CD4^+CD25^+$ T cells co-expressing Foxp3 was also determined (Fig. 5.1B). At the same time the effect of T_{reg} cell inactivation on the expression of CD25 (activation marker) by intra-tumoural $CD8^+$ T cells was also determined (Fig. 5.1C). As can be seen in figure 5.1A only approximately one third of the original $CD4^+CD25^+$ T_{reg} cells remained 1 day post intra-tumoural anti-CD25 mAb treatment (11.5 ± 4.9% compared to 30.2 ± 6.1%). It appeared that by day 3, and certainly by day 10, that the $CD4^+CD25^+$ T_{reg} cells had largely recovered. On closer examination of the T_{reg} cell subset by way of intra-cellular staining for Foxp3 it was revealed that the $CD4^+CD25^+$ T cells that had recovered by day 3 were not in fact $Foxp3^+$ T_{reg} cells but may have represented a population of activated ($CD25^+$) $CD4^+$ helper T cells (Fig. 5.1B). In support of day 3 being an

important day for activated effector cells, such as $CD4^+$ helper T cells, it was also on day 3 that a significant increase in activated $CD8^+$ CTLs was observed (Fig. 5.1C). By day 10 however, when it was seen that the true $CD4^+CD25^+Foxp3^+$ T_{reg} cells had recovered, these activated $CD8^+CD25^+$ CTLs were again immuno-suppressed (characterised by a drop in expression of CD25 from $82.8 \pm 1.3\%$ to $21.7 \pm 7.3\%$). These figures represent the combined data from two independent experiments.

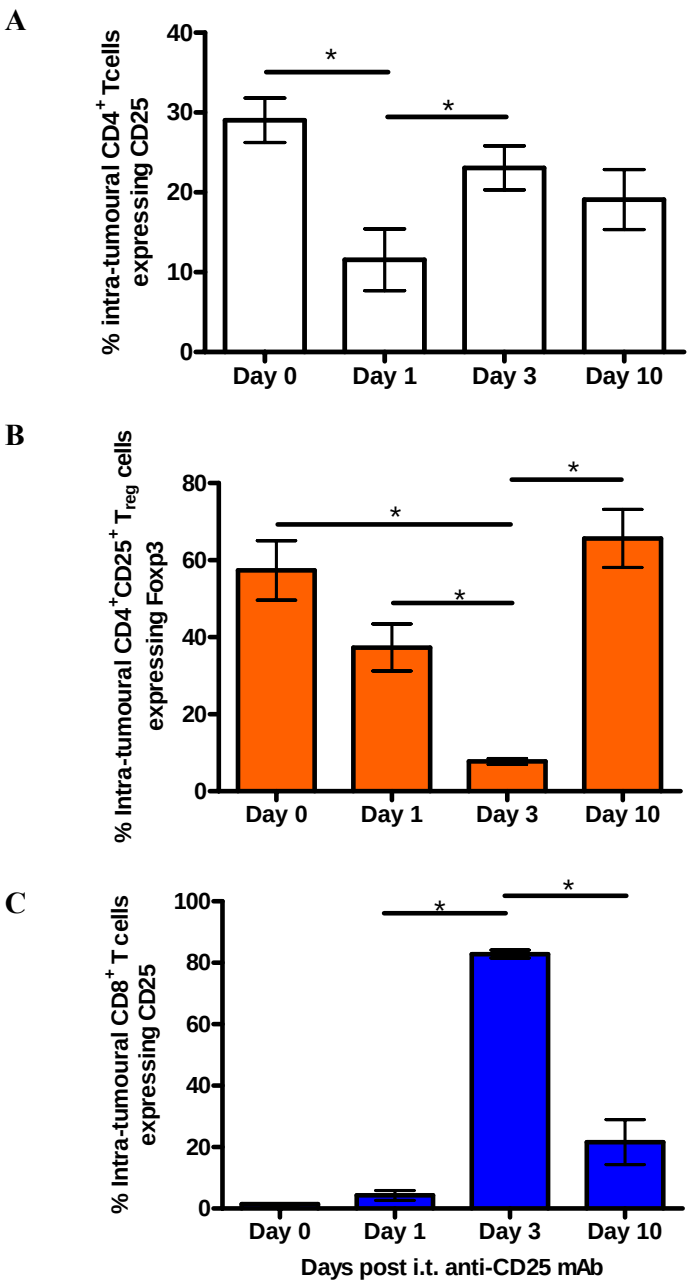

Figure 5.1: Intra-tumoural (i.t.) anti-CD25 mAb treatment inactivates intra-tumoural T_{reg} cells and releases intra-tumoural $CD8^+$ CTLs from immunosuppression.

Mice were implanted s.c. with 1 x 10^7 AE17 cells. Once tumours reached 9 mm^2 a single, intra-tumoural treatment with anti-CD25 mAb was administered. Tumours were removed 1, 3 and 10 days post treatment and compared to untreated (day 0) control tumours. Flow cytometry was used to determine (A) the intra-tumoural percentage of $CD4^+$ T cells co-expressing CD25, (B) the intra-tumoural percentage of $CD4^+CD25^+$ T cells co-expressing Foxp3 and (C) the intra-tumoural percentage of $CD8^+$ T cells co-expressing CD25. Data are the mean ± SEM for 6 tumours removed at day 0 prior to treatment, 3 tumours removed on days 1 and 3 post treatment and 6 tumours removed on day 10 post treatment. A single asterisk represents a p-value < 0.05.

5.2.1.2 Single intra-tumoural anti-CD25 mAb inactivation inhibits tumour growth.

The effect of T_{reg} inactivation and the subsequent activation of $CD8^+$ CTLs on tumour development was examined in two intra-tumoural anti-CD25 mAb inactivation experiments. The data from these two independent experiments is combined in this section. Tumours were grown to 9 mm^2 prior to initiating intra-tumoural anti-CD25 mAb injections. Tumour-bearing mice were treated with a single dose of 0.15 mg anti-CD25 mAb administered directly into the established, 9 mm^2 tumours. Tumours had taken between 3 and 6 days to reach the treatment size of 9 mm^2. Anti-CD25 mAb treatment administered directly into 9 mm^2 tumours resulted in both the significant inactivation of tumour-located T_{reg} cells (Fig. 5.1) and 10 days of significant tumour growth inhibition in the 10 mice treated with the anti-CD25 mAb ($p < 0.05$ at day 10 post treatment) (Fig. 5.2). As a control, 10 tumour-bearing mice were treated in the same manner with an equivalent dose of an unrelated isotype-matched mAb (anti-Ross River Virus (RRV) IgG1 mAb). All isotype-matched mAb treated mice were significantly faster at developing tumours when compared to anti-CD25 mAb treated mice up to 13 days post-treatment. The same tumour growth rate observed in the mice treated with the isotype control mAb was also observed in mice left untreated or treated with PBS (data not shown).

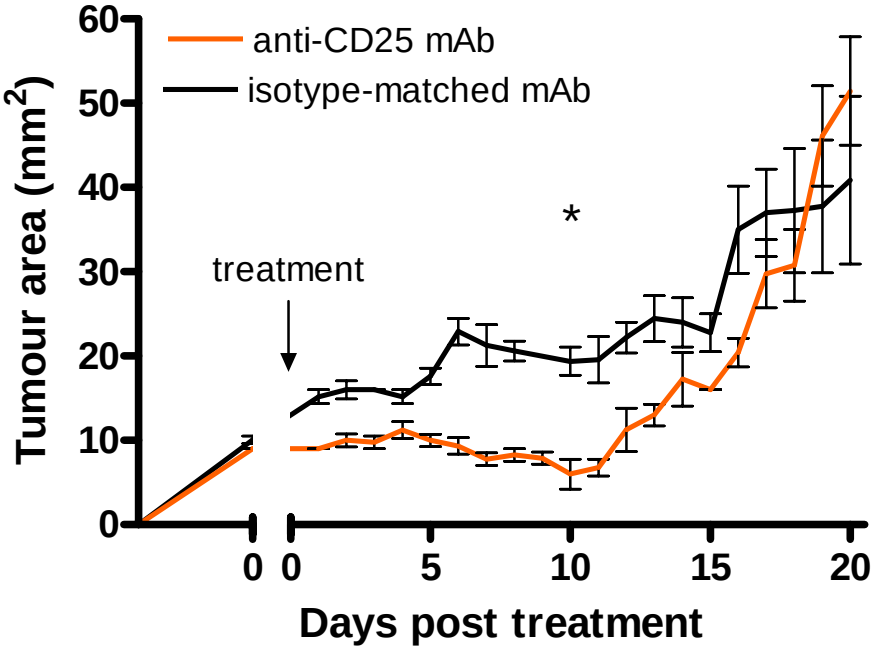

Figure 5.2: Inhibition of tumour development by a single intra-tumoural administration of anti-CD25 mAb.

20 mice were implanted s.c. with 1 x 10^7 AE17 cells. Tumour areas were calculated by multiplying two, right-angled tumour diameters measured using micro-callipers and is presented on the vertical axis. Once tumours reached 9 mm^2 a single, intra-tumoural treatment with anti-CD25 mAb was administered to ten mice (—). This treatment time-point is designated on the horizontal axis as day 0 and labelled "treatment". Ten control mice were treated in the same manner with a single 0.3 mg dose of an isotype-matched mAb solution (anti-IgG1 RRV) (—). The higher dose of isotype matched mAb solution was used as the isotype matched mAb was purified from serum-positive tissue culture media while anti-CD25 mAb was purified from serum free CD Hybridoma media. Data are the mean ± SEM for 10 mice per group per time-point. A single asterisk represents a p-value < 0.05.

5.2.1.3 Multiple, intra-tumoural anti-CD25 mAb treatments prolong tumour growth inhibition.

To test whether the period of tumour growth inhibition could be extended past 10 days, multiple intra-tumoural administrations of anti-CD25 mAb at 10 day intervals were trialled. The combined results of two experiments showed all 12 treated mice to undergo 10 days of tumour growth inhibition following the intra-tumoural administration of anti-CD25 mAb into the 9 mm^2 tumours (Fig. 5.3). Following the second intra-tumoural treatment 10 of the 12 treated mice showed tumour growth inhibition out to day 20. The remaining 2 mice "escaped" tumour growth inhibition and their tumours resumed rapid growth despite the continued administration of the anti-CD25 mAb at 10 day intervals. The resumption of tumour growth in these 2 mice was initiated after the second anti-CD25 mAb treatment and hence they are termed "escapes after T2". After the third treatment (T3), 3 further mice escaped anti-CD25 mAb induced tumour growth inhibition. Figure 5.4 presents the full data for this study, particularly the fate of the final 7 mice inhibited in tumour development in Figure 5.3. Mice were treated in total with up to 6 intra-tumoural doses of anti-CD25 mAb at 10 day intervals. As a result of each treatment the majority of mice were inhibited for a further 10 days while a small proportion resumed tumour growth. After T6 the tumour in one mouse completely regressed and was undetectable out to day 70 post tumour challenge when the experiment was terminated. Control mice were treated with multiple doses of the isotype matched mAb at 10 day intervals (data not shown). Control mice developed tumours at a much faster rate and reached the humane end-point of 100 mm^2 by approximately day 25 post treatment 1.

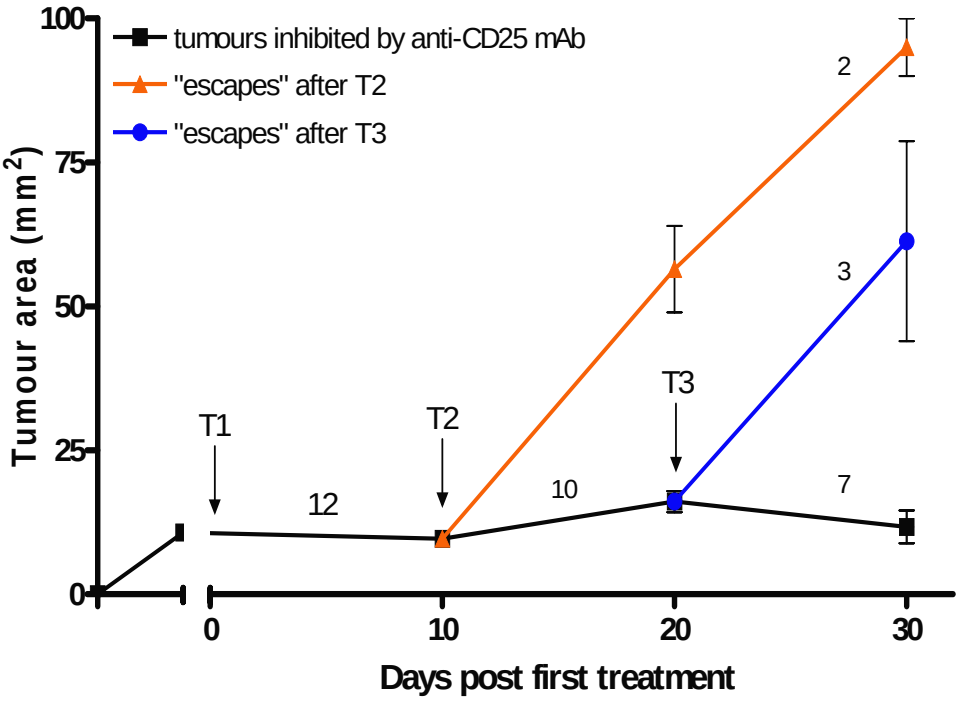

Figure 5.3: Prolonged inhibition of tumour development by multiple intra-tumoural administrations of anti-CD25 mAb.

Mice were implanted s.c. with 1 x 10^7 AE17 cells. Tumour areas were calculated by multiplying two, right-angled tumour diameters measured using micro-callipers and is presented on the vertical axis. Once tumours reached 9 mm^2 the first intra-tumoural treatment with anti-CD25 mAb was administered. To extend the period of tumour growth inhibition, a further 12 tumour-bearing mice were treated with multiple doses (3 in total) of anti-CD25 mAb at 10 day intervals and compared to control mice treated with the isotype-matched mAb (data not shown). The first treatment was administered to tumours of 9 mm^2 and designated day 0 on the horizontal axis with an arrow labelled "T1". Subsequent treatments were given at 10 day intervals and labelled "T2" and "T3". Mice that remained inhibited in tumour development were grouped as "tumours inhibited by anti-CD25 mAb" (■). For some of the mice, tumour development was not further inhibited by subsequent treatments. Mice which "escaped" tumour growth inhibition after one of the treatments are plotted separately and termed "escapes after T2" (▲) and "escapes after T3" (●). The number of mice with either inhibited tumour growth or "escaping" tumours after each treatment are indicated within the figure. Data are the mean tumour area ± SEM per time-point.

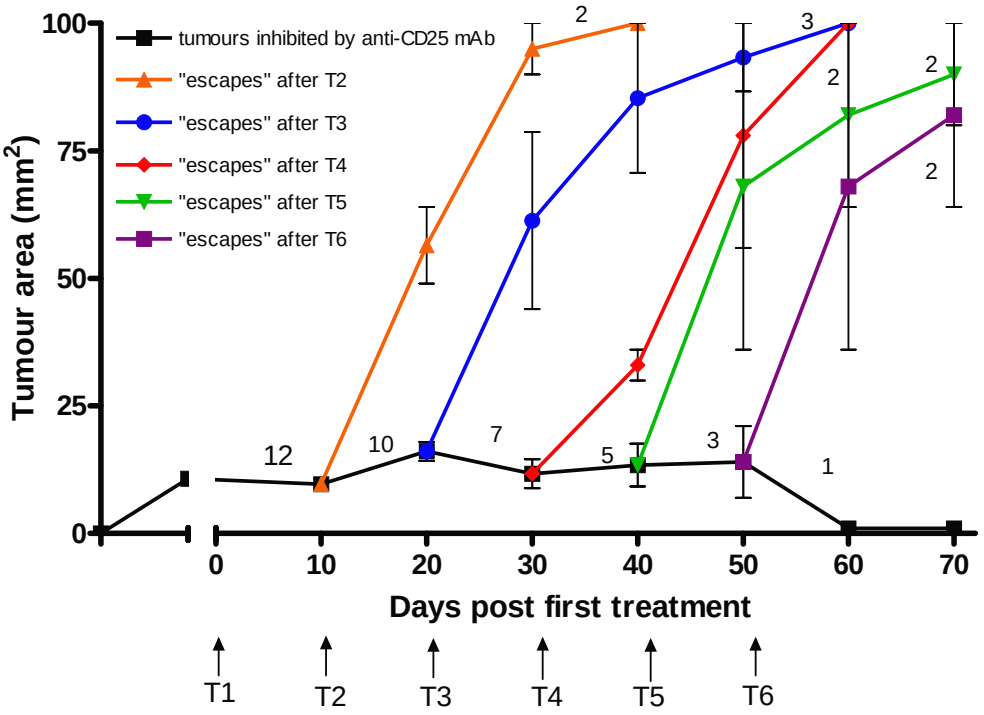

Figure 5.4: Prolonged inhibition of tumour development by multiple intra-tumoural administrations of anti-CD25 mAb.

Mice were implanted s.c. with 1 x 10^7 AE17 cells. Tumour areas were calculated by multiplying two, right-angled tumour diameters measured using micro-callipers and is presented on the vertical axis. Once tumours reached 9 mm^2 the first intra-tumoural treatment with anti-CD25 mAb was administered. To extend the period of tumour growth inhibition, a further 12 tumour-bearing mice were treated with multiple doses (6 in total) of anti-CD25 mAb at 10 day intervals and compared to control mice treated with the isotype-matched mAb (data not shown). The first treatment was administered to tumours of 9 mm^2 and designated day 0 on the horizontal axis with an arrow labelled "T1". Subsequent treatments were given at 10 day intervals and labelled "T2", "T3" etc. Mice that remained inhibited in tumour development were grouped as "tumours inhibited by anti-CD25 mAb" (■). For some of the mice, tumour development was not further inhibited by subsequent treatments. Mice which "escaped" tumour growth inhibition after one of the treatments are plotted separately and termed "escapes after T2" and "escapes after T3" etc. The number of mice with either inhibited tumour growth or escaping tumours after each treatment are indicated within the figure. Data are the mean tumour area ± SEM per time-point

5.2.2 Analysis of "escape" tumours.

The intra-tumoural administration of anti-CD25 mAb every 10 days is highly effective at inhibiting tumour development in the majority of mice. This treatment regime is limited however by the fact that some mice resume tumour growth after multiple treatments as if the antibody treatment had ceased. The failure to inhibit tumour growth over time in the remaining mice may be due to several reasons including (i) the loss of mAb bioactivity (107, 156, 157), (ii) a non-$CD25^+$ T_{reg} cell assuming the immunosuppressive role over time (106, 107), (iii) the development of neutralizing antibodies against the rat anti-mouse CD25 mAb (28, 29, 211), (iv) the depletion of activated effector T cells (28, 29, 87, 156, 211), (v) poor timing of subsequent doses of mAb (107, 156, 157) or (vi) a mutation in the tumour such that the TCR specificity is altered (201, 212). Studies aimed at investigating these potential mechanisms of "escape" from tumour growth inhibition have been conducted and are presented below.

5.2.2.1 Loss of antibody bioactivity.

To confirm the anti-CD25 mAb used in the above experiments had not degraded in storage and was hence still active *in vivo* it was retested for the ability to inactivate intra-tumoural T_{reg} cells. Two mice with 40 mm^2 tumours were treated i.t. with a single dose of anti-CD25 mAb. Two tumours of the same size were left untreated. 24 hours post anti-CD25 mAb treatment (PC61 clone) the treated and untreated tumours were removed, dissociated and analysed by flow cytometry to determine the percentage of tumour-located $CD4^+$ T cells expressing CD25 by secondary staining with a mAb directed against a different CD25 epitope (7D4 clone). 24 hours post anti-CD25 mAb treatment there was a 92.3 ± 3.7% reduction in the expression of CD25 by intra-tumoural $CD4^+$ T cells confirming the antibody was still active *in vivo* and that degradation of the anti-CD25 mAb in storage could not explain the resumption of tumour growth in some mice treated multiple times with anti-CD25 mAb.

5.2.2.2 Induction of a non-$CD25^+$ T_{reg} cell.

Although $CD4^+CD25^+$ T_{reg} cells are most often implicated in tumour immunity $CD4^+CD69^+CD25^-$ T cells have also been proposed as T_{reg} cells in both retroviral

infection models and a murine tumour model (personal communication: A. van der Vuurst de Vries, Amgen, USA and (106, 107)). In order to determine whether a second non-$CD25^+$ T_{reg} cell population was assuming the immunosuppressive role in tumours treated multiple times with anti-CD25 mAb the expression of CD69 by intra-tumoural $CD4^+CD25^-$ T cells was determined. Six untreated tumours were compared to 6 tumours treated once with anti-CD25 mAb and 6 tumours treated multiple times with the anti-CD25 mAb. The flow cytometric analysis of CD69 expression by intra-tumoural $CD4^+CD25^-$ T cells revealed no significant difference in the expression of CD69 by intra-tumoural $CD4^+CD25^-$ T cells despite treatment status of the tumours (Fig. 5.5). These data suggest that $CD4^+CD25^-CD69^+$ T_{reg} cells are not induced in tumours that have resumed tumour growth following multiple treatments with anti-CD25 mAb.

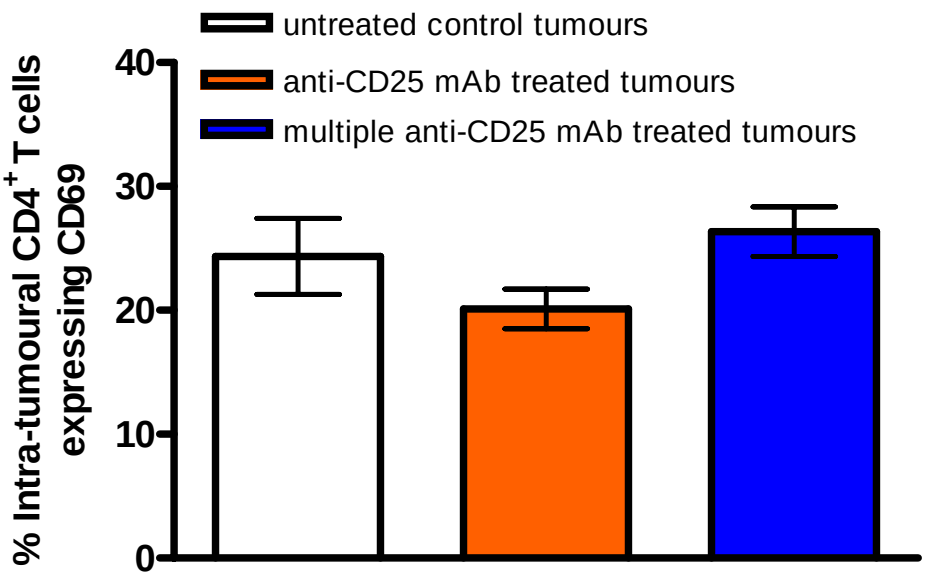

Figure 5.5: Expression of CD69 by intra-tumoural $CD4^+CD25^-$ T cells is not increased following multiple treatments with anti-CD25 mAb.

Mice were implanted s.c. with 1 x 10^7 AE17 cells. Tumour areas were calculated by multiplying two, right-angled tumour diameters measured using micro-callipers and is presented on the vertical axis. Tumours of 9 mm^2 were treated intra-tumourally with 0.15 mg anti-CD25 mAb or left untreated as controls. 24 hours post anti-CD25 mAb treatment both untreated mice and the mice treated once with anti-CD25 mAb were culled, tumours removed and dissociated for flow cytometric analysis of the percentage of intra-tumoural $CD4^+CD25^-$ T cells co-expressing CD69. The same methods were used to examine tumours treated five times with the same dosage of anti-CD25 mAb at 10 day intervals. Data are the mean ± SEM of 6 mice per group.

5.2.2.3 Depletion of activated effector T cells

CD25 is also an activation marker and may therefore be expressed by other cells including activated $CD4^+Foxp3^-$ helper T cells and activated $CD8^+$ CTLs. Section 5.2.1.1 describes the low level of CD25 expression by intra-tumoural $CD8^+$ CTLs while T_{reg} cells are co-resident in tumours. It was only once T_{reg} cells were removed by the specific inactivation of T_{reg} cells with anti-CD25 mAb that CD25 expression by $CD8^+$ CTLs was seen to increase above 20%. To examine whether a second dose of anti-CD25 mAb administered 10 days post the first might now specifically target $CD8^+CD25^+$ CTLs, tumours were removed and examined by flow cytometry by secondary staining with a mAb directed against a different CD25 epitope (7D4 clone). The percentage of intra-tumoural $CD8^+$ CTLs co-expressing CD25 on day 10 post T1 (pre-T2) was compared to the percentage of intra-tumoural $CD8^+$ CTLs expressing CD25 in tumours removed on day 11 post T1 (1 day post-T2). No significant difference in the expression of CD25 by intra-tumoural $CD8^+$ CTLs was observed (21.6 ± 7.3% compared to 20.8 ± 3.9% respectively, n=6).

5.2.2.4 Poor timing of subsequent anti-CD25 mAb treatments: SAA as a marker of T_{reg} cell activity.

Although it appeared from both the tumour growth inhibition experiments and the analysis of the efficacy of T_{reg} cell inactivation (Section 5.2.1) that 10 day intervals between anti-CD25 mAb treatments were effective in most mice at prolonging tumour growth inhibition, some mice resumed tumour growth. A further reason for this "escape" may be inter-mouse differences in the timing of T_{reg} cell expansion in response to tumour challenge and effector cell priming (137). T_{reg} cells are suggested to live in homeostatic relationship with effector T cells. That is, when effector T cells are highly active, T_{reg} cells must be low in activity but then once effectors have completed the task of tumour clearance the T_{reg} cells are upregulated and act to suppress the effector cell response before any over action of the effector cells could result in self harm (see Figure 3.1). A predictive serum marker for T_{reg} cell cycling in response to tumour challenge could therefore be useful in targeting the anti-CD25 mAb treatments more specifically in individuals. Serum Amyloid A (SAA) is an acute phase protein which was analysed alongside C-reactive protein (CRP) for use in post transplant monitoring

of renal allograft rejection (213). Although the specific link was not made in the renal allograft rejection paper, the rejection of transplants has also been linked to T_{reg} cell activity (116). In the cases of renal graft rejection reported by Maury and Teppo (1984), SAA levels were significantly elevated when graft rejection was occurring with the time between rejection episodes shown to be 14 days (213). Elevated SAA levels were suggested to be a result of the host's response to cellular injury (graft rejection) which corresponds to a time at which T_{reg} cells are inactive. This finding of a 14 day cycle in SAA levels in response to an immune challenge was also noted in a study looking at SAA levels in response to juvenile chronic arthritis, another immune disease also associated with T_{reg} cell activity (214, 215).

A commercial ELISA kit (TriDelta, Ireland) was used to measure SAA levels in mice challenged with mesothelioma in order to determine any peaks in SAA levels (associated with an anti-tumour effector response) or low SAA (associated with T_{reg} cell suppression of the anti-tumour immune response) in the hope of determining the appropriate time interval between subsequent intra-tumoural anti-CD25 mAb treatments. A preliminary study to assess the effect of murine mesothelioma development on SAA levels was conducted. This study measured SAA levels in the serum of mice implanted s.c. with 1 x 10^6 AE17 cells. Five mice were bled at d0 (prior to tumour challenge) and then again on days 14, 21, 28 and 35 post tumour challenge. The SAA level at each of the weekly time points was determined using the murine SAA ELISA kit and found to be very low in both the tumour-challenged and naïve mice (Fig. 5.6). In fact, the level of SAA detected in all mice of this experiment, despite the size of the tumours, was considered "normal" (<20 µg/ml) according to the manufacturer's protocol.

The subcutaneous tumours developed in the murine model of mesothelioma are encapsulated and have not been found to be prone to metastasis when kept below the humane end-point size of 100 mm^2. The tumours may therefore not have resulted in a high enough systemic inflammatory immune response to result in elevated SAA levels (13, 216). An extended study was therefore conducted in mice challenged with i.p. mesothelioma tumours which are known to be more aggressive (15). Three groups of 10 mice were implanted i.p. with 1 x 10^6 AE17 cells. Blood samples (<200 µl) were collected from the three groups of tumour-bearing mice on a 3 day rotation and

compared to blood collected from naïve, tumour-free mice. After collection, blood was allowed to clot in tubes containing no additive before serum collection and analysis of SAA using the murine SAA ELISA kit. One microlitre from each of the ten serum samples per time point were pooled together and analysed on the same assay plate in order to generate an average SAA reading per time-point post tumour challenge. For the first 20 days only a low level of SAA was detectable and the concentration of SAA for both naïve mice and tumour challenged mice was within the normal range (<20 μg/ml) (Fig. 5.7). As at day 20 the mice in this experiment had not yet succumbed to their tumours, 6 mice were culled to confirm tumours had in fact developed in these mice. Small i.p. tumour nodules were identified in all mice. The remaining mice (8 per group) were monitored out to day 38 when the majority of mice had begun to succumb to large (palpable) intra-peritoneal tumours. Even at these later time-points post tumour challenge SAA levels were within the normal range. It was only at very late time-points (day 38-55) that the SAA results exceeded the normal level. There was no evidence for regular SAA "cycling" in the murine mesothelioma model.

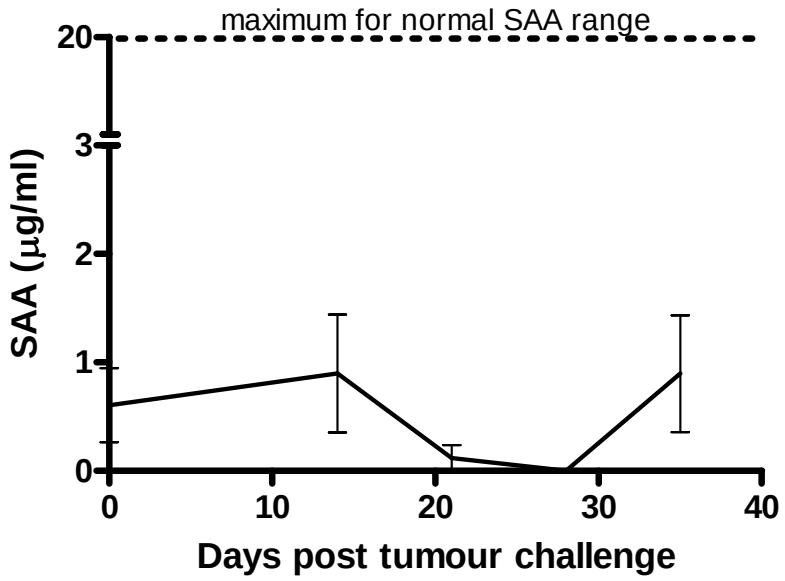

Figure 5.6: SAA levels in mice challenged s.c. with 1 x 10^6 mesothelioma cells.

Mice were implanted s.c. with 1 x 10^6 AE17 cells. Mice were bled on days 14, 21, 28 and 35 post tumour challenge and blood collected for serum separation. The sera were analysed for the presence of SAA by ELISA following the manufacturer's protocol (Tridelta, Ireland). SAA levels were calculated by comparison to an SAA standard and are presented on the vertical axis. The maximum of the normal range is represented by a dashed line. Data are the mean ± SEM of triplicate wells per serum sample.

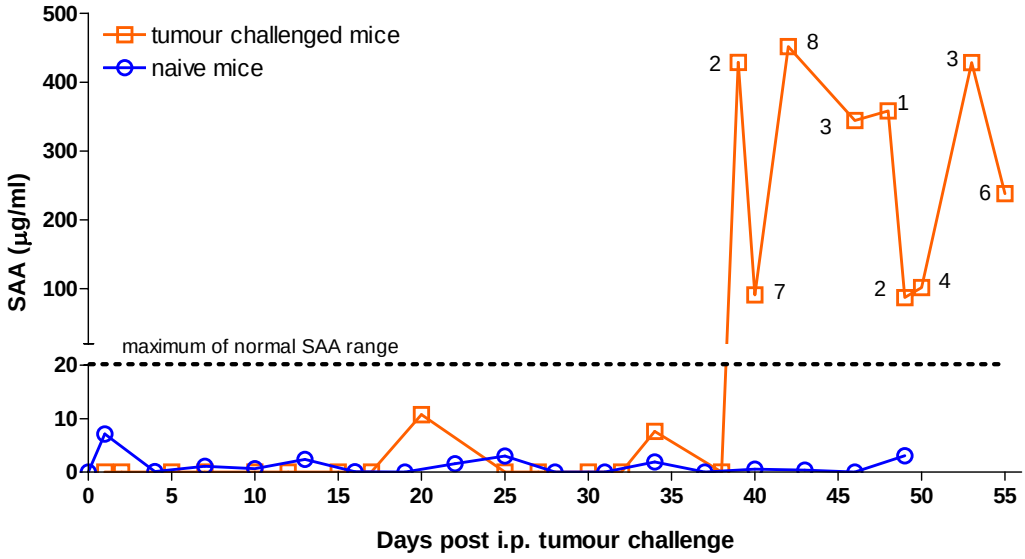

Figure 5.7: SAA levels in mice challenged i.p. with murine mesothelioma.

Mice were implanted i.p. with 1 x 10^6 AE17 cells. Mice were placed in three groups and bled on alternate days on a 3 day rotation for 55 days. Blood was collected for serum separation and the sera from all mice of the group bled on a particular day pooled together and analysed for the presence of SAA by ELISA. SAA levels were calculated by comparison to an SAA standard and compared to SAA levels in naïve mice. Data are the mean ± SEM of triplicate wells per serum sample made up of 2 pooled serum samples for naïve mice and 10 pooled serum samples for 10 tumour-bearing mice up to day 20 and 8 tumour-bearing mice from day 21 to day 38. From day 38 onwards, the number of tumour challenged mice pooled for SAA analysis is presented in the figure. The maximum of the normal range of SAA is represented by the dashed line.

5.2.2.5 Development of a neutralising antibody to the rat-derived anti-CD25 mAb.

PC61 is a rat anti-mouse CD25 mAb and its repeated administration and therefore the prolonged exposure of mice to the rat derived antibody may result in the development of anti-rat antibodies. The immunogenicity of monoclonal antibodies used in therapy is a recognised problem and the development of humanised antibodies for use in cancer patients is a direct result of this (211). An ELISA was developed to determine whether neutralising antibodies were being made by mice treated with multiple doses of anti-CD25 mAb. The PC61 anti-CD25 mAb itself was used as the capture antibody in the ELISA. Should the mice have developed neutralising antibodies to the rat anti-mouse CD25 mAb, the neutralising antibodies would be mouse anti-rat specific and would therefore bind to the PC61 capture antibody. The test samples were sera from untreated tumour-bearing mice and sera from mice treated once with anti-CD25 mAb or multiple times with the anti-CD25 mAb. Mice were bled by cardiac puncture or tail vein bleed and blood was collected into sterile uncoated blood tubes for serum preparation. Sera were diluted in mouse osmolarity buffered saline (MOBS) prior to addition to the ELISA plate. The detection antibody in the ELISA was an alkaline phosphatase-conjugated anti-mouse IgG. The average OD readings (each serum sample was plated in triplicate) for absorbances measured at 405 nm are presented in Figure 5.8. This figure represents a single ELISA and was confirmed by a second ELISA assay (data not shown). MOBS was used as the blank reagent while goat anti-rat serum reacted with an alkaline phosphatase-conjugated anti-goat IgG was used as a positive control. The sera from untreated tumour-bearing mice gave an average absorbance reading of 0.10 ± 0.001 which was not significantly different from the absorbance of sera prepared from mice 3 days after a single treatment with anti-CD25 mAb (0.12 ± 0.005). The absorbance readings for sera prepared from mice treated once with anti-CD25 mAb did not increase even with time since exposure to the mAb (0.12 ± 0.005 at day 3 compared to 0.13 ± 0.02 at day 10 post treatment). The sera prepared from mice treated twice with anti-CD25 mAb gave the first significant increase in absorbance reading when compared to the sera of untreated, tumour-bearing mice ($p < 0.01$). This suggested the development of neutralising antibodies can occur after as little as two treatments at 10 day intervals with anti-CD25 mAb. The sera from "escape" mice (mice with tumours that had resumed growth despite having being treated either 3 or 5 times with anti-CD25 mAb) gave an even higher average

absorbance reading when compared to naïve mouse serum (0.3 ± 0.01 and 0.7 ± 0.03 respectively) suggesting that over time and after multiple treatments with anti-CD25 mAb, more neutralising antibodies are made which could block the *in vivo* functioning of the anti-CD25 mAb.

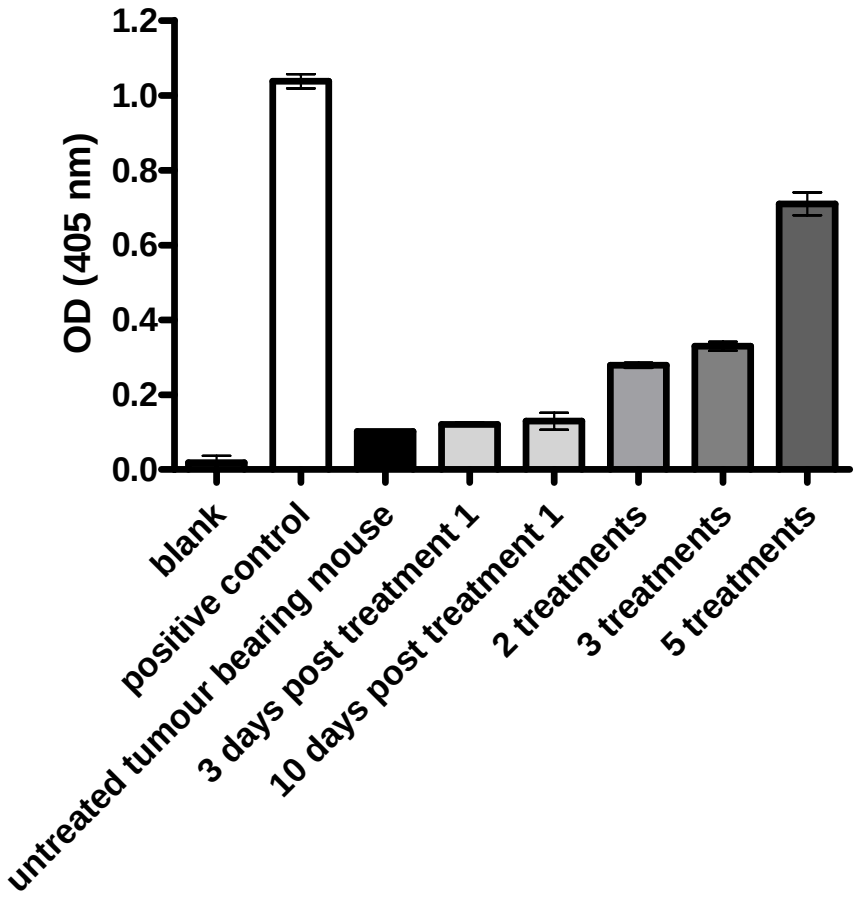

Figure 5.8: Development of neutralising antibodies in mice treated multiple times with anti-CD25 mAb, representative data.

Mice were implanted s.c. with 1 x 10^7 AE17 cells. Tumours of 9 mm^2 were treated intra-tumourally with 0.15 mg anti-CD25 mAb or left untreated as controls. Subsequent treatments with anti-CD25 mAb were administered a 10 day intervals. 24 hours post the first anti-CD25 mAb treatment both treated and untreated mice were bled for serum separation. The same methods were used to collect serum from mice 3 and 10 days post the first anti-CD25 mAb treatment and from mice treated 2, 3 and 5 times with anti-CD25 mAb. The sera were diluted 1/2 and analysed for the presence of mouse anti-rat neutralising antibodies by ELISA using a 1/50 dilution of anti-CD25 mAb (PC61) as the capture antibody and 1/1000 dilution of alkaline phosphatase-conjugated anti-mouse IgG to as the detection antibody. Absorbances were read at 405 nm. Data are the mean ± SEM of triplicate wells per serum sample.

5.3 Discussion

Anti-CD25 mAb treatment was shown to inactivate intra-tumoural T_{reg} cells and as a consequence release activated $CD8^+CD25^+$ CTLs from immunosuppression allowing them to begin tumour clearance. Although a single intra-tumoural treatment with anti-CD25 mAb has proven successful at inhibiting tumours in 100% of the cases, this effect was limited to 10 days, presumably reflecting the loss of antibody from the site. Extended intra-tumoural anti-CD25 mAb treatments demonstrated second and subsequent treatments were only effective in a major proportion of the mice. This novel observation formed the majority of our recent publication in Biochemical and Biophysical Research Communications (196). The success of intra-tumoural anti-CD25 mAb treatment for murine mesotheliomas was, however, limited by the fact that in some mice tumours "escape" or resume tumour growth despite repeated anti-CD25 mAb treatments. No comments have been made in the published literature about a lack of anti-CD25 mAb activity over time and so the final part of this chapter examined the reasons behind the resumption of tumour growth in some of the treated mice. Several reasons were proposed to explain the resumption of tumour growth in some mice treated multiple times with anti-CD25 mAb including (i) poor timing of anti-CD25 mAb (107, 156, 157), (ii) a non-$CD25^+$ T_{reg} cell assuming the immunosuppressive role over time (106, 107), (iii) the development of neutralizing antibodies against the rat anti-mouse CD25 mAb (28, 29, 211), (iv) the depletion of activated effector T cells (28, 29, 87, 156, 211), (v) a mutation in the tumour such that the TCR specificity is altered (201, 212) or (vi) loss of anti-CD25 mAb bioactivity *in vivo* (107, 156, 157).

The analysis of the targeting of anti-CD25 mAb to activated effector T cells was inconclusive. The data in section 5.2.1.1 suggested that the first dose of anti-CD25 mAb administered intra-tumourally preferentially targets intra-tumoural T_{reg} cells and not intra-tumoural activated $CD8^+CD25^+$ CTLs but also suggested that the most appropriate day for the analysis of the effect of intra-tumoural anti-CD25 mAb treatment on intra-tumoural $CD8^+$ T cells was day 3 post treatment. It can not therefore be concluded that multiple intra-tumoural anti-CD25 mAb treatments had no effect on intra-tumoural $CD8^+$ CTLs and hence that this was the reason for resumption of tumour growth in some mice treated multiple times with anti-CD25 mAb. To confirm the role

of $CD8^+$ CTLs in the anti-tumour immune response, co-depletions of T_{reg} cells and $CD8^+$ CTLs using an anti-CD8 mAb could be conducted. It would be expected if $CD8^+$ CTLs were important in this anti-tumour immune response that co-depletion of the $CD8^+$ CTLs with the T_{reg} cells would result in normal tumour growth kinetics as no anti-tumour immune response could be mounted.

At this stage, no studies had been conducted to investigate tumour antigen mutation as a mechanism of "escape" from tumour growth inhibition. To investigate this further in the future, "escape" tumours could be removed from mice and primary cell cultures made. By the process of clonal dilution, individual tumour cells from the "escape" tumours could be used to generate new tumour cells lines that could be compared to the original AE17 cells both *in vitro* and *in vivo* for changes in gene expression by global genechip analysis for common tumour associated antigens (217). Also in terms of tumour antigen mutation, changes in the TCRs expressed by effector T cells in the original AE17 and the "escape" tumours may indicate tumour antigen mutation or loss of effector T cell tumour specificity. V_α or V_β expression by purified effector T cells could be determined and followed by an investigation for oligoclonality as a measure of a changed response to tumour antigens in escapes (218). Differences in tumour growth kinetics between the newly derived tumour cell lines from the "escape" tumours and the original AE17 cells could be determined both *in vivo* and *in vitro* and indicate mutations while differences in the response of the newly derived tumour cell lines from the "escape" tumours to the original AE17 tumour cells to anti-CD25 mAb treatment may confirm any direct changes in the tumour cells themselves resulting in the generation of "escape" tumours.

Although some further studies could be conducted to investigate the role of tumour antigen mutation or CTL responses in "escape" tumours, it was clearly shown that neutralising antibodies to the rat-derived anti-mouse CD25 mAb were being induced in this tumour model in response to multiple treatments with anti-CD25 mAb. In humans, the administration of mouse monoclonal antibodies can lead to the development of a human anti-mouse antibody immune response (211). The T_{reg} cell inactivation therapy presented in this chapter is therefore still clinically relevant as humanised anti-CD25 mAbs (e.g. basiliximab and daclizumab) are now part of well-established clinical immunosuppressive regimens after it was confirmed that they could prevent acute graft

rejection in clinical phase III studies (5, 219). Intra-tumoural T_{reg} cell inactivation could be utilized as a secondary treatment of residual tumour deposits following surgical debulking of tumours as it is believed that combining surgery with other forms of therapy may result in significant increases in survival for some mesothelioma patients (5, 220). More specifically, it has been shown in a mouse model of mesothelioma that partial, but not complete, tumour-debulking surgery promotes protective anti-tumour memory when combined with both chemotherapy and immunotherapy (162). Although, our work has been conducted in a murine model of mesothelioma, this treatment strategy is designed to release the anti-tumour immune response from suppression rather than to target the cancer cells specifically and is therefore potentially applicable to all solid tumours which use T_{reg} cells as a significant immune evasion strategy. This site targeted treatment to eliminate T_{reg} cells based on CD25 expression has several other advantages over systemic treatments. Intra-tumoural treatment may avoid side effects associated with the systemic inactivation of T_{reg} cells, such as the induction of autoimmunity, by reducing the dosage of mAb required (28, 221) and is easier to translate into the clinical situation in which patients present with established tumours.

Since this work was conducted, two further attempts to intra-tumourally inactivate T_{reg} cells have been published. Anti-CD4 mAb was administered intra-tumourally at day 14 post tumour challenge and resulted in the regression of established tumours in a murine fibrosarcoma model (28). Although this treatment was effective, in the long term, treatment may be inhibited by the non-specific targeting of other important $CD4^+$ T cell populations such as helper T cells. Ko *et al* (2005) trialled the administration of intra-tumoural anti-GITR mAb to more specifically target the functioning of T_{reg} cells and to thereby treat mice with Meth A fibrosarcomas. Glucocorticoid induced tumour necrosis factor receptor (GITR) has been associated with T_{reg} cell function and intra-tumoural treatment with this antibody gave good results (222).

Improvements can still be made to the intra-tumoural anti-CD25 mAb therapy. Further studies within the tumour microenvironment of both the T_{reg} cell and CTL anti-tumour immune responses could be conducted in order to more specifically time the administration of subsequent (repeated) anti-CD25 mAb treatment to coincide with T_{reg} cell upregulation. The ability to monitor T_{reg} cell activity via a serum marker of

inflammation (SAA) was examined but it was concluded that SAA was not a reliable predictor of T_{reg} cell activity even in the intra-peritoneal tumour model which is known to induce a more severe inflammatory response. No cycling of T_{reg} cell and CTL activity was evident and SAA levels remained within the normal range except at very late time-points when mice were succumbing to their tumour burden. In this case the elevated SAA levels may not represent a lack of T_{reg} cells and hence an active effector immune response but may simply reflect the overall state of inflammation or immune dysfunction at the time of death.

In a very recent study, a time-course of T_{reg} cell inactivation following anti-CD25 mAb administration was shown. The injection of 500 mg anti-CD25 mAb (7D4) intra-peritoneally was shown to result in the rapid but short lived inactivation of T_{reg} cells with T_{reg} cells recovering to a normal level by days 10-14 post treatment (223). In a similar study by the same authors this 10 day time-frame from inactivation to recovery of T_{reg} cell function was confirmed (132). These two works support the decision in this study to administer anti-CD25 mAb treatments intra-tumourally at 10 day intervals. In addition, the current findings of the Kohm group suggest that increased effector cell function following anti-CD25 mAb treatment decreased the level of cell surface CD25 expression without altering the level of intracellular CD25 protein or CD25 mRNA expression suggesting that CD25 is in fact shed form the surface of the T_{reg} cells and not internalised. In agreement with this, IL-2 binding is well known to result in the shedding of CD25 (224, 225). This effect of IL-2 on CD25 expression and hence function or development of T_{reg} cells may also help explain the observations made in a similar murine mesothelioma study where recombinant IL-2 was administered intra-tumourally to murine mesotheliomas (14). In this study small tumours treated with IL-2 underwent tumour regression while large tumours treated with IL-2 failed to respond. Timing experiments showed that the IL-2 mediated responses were dependent upon tumour size, not on the duration of disease which correlated with the intra-tumoural T_{reg} cell increases observed in chapter 4. It was shown that although intra-tumoural IL-2 did not alter tumour antigen presentation in draining lymph nodes, it did enhance a previously primed, endogenous, tumour-specific *in vivo* CTL response that coincided with regressing tumours. Based on the studies presented in this chapter it may be the case that IL-2 treatment in this model did not directly "boost" anti-tumour effector cells as planned but may have targeted intra-tumoural T_{reg} cells resulting in the shedding of

the CD25 molecule, inactivation of T_{reg} cells and hence and the release of the anti-tumour immune response from suppression. The finding that tumour-infiltrating $CD8^+$ T cells but not $CD4^+$ T cells increased in association with the IL-2 therapy would support this.

Finally, future studies could focus on adapting this intra-tumoural anti-CD25 mAb therapy to the treatment of larger tumours as is often the case in the clinic. Preliminary studies in this laboratory found that the treatment of AE17 tumours larger than 50 mm^2 with a single 0.15 mg dose (40 µl) of anti-CD25 mAb did not result in the significant inactivation of intra-tumoural T_{reg} cells and hence no tumour growth inhibition. The correct dose of anti-CD25 mAb for the treatment of larger tumours should be titrated with careful consideration for any spill over effect of the mAb into the periphery and hence the induction of a non-specific systemic response. The treatment of larger tumours with many agents is often hindered by a decrease in uptake/penetration of the drug/treatment into large tumours (226). This decrease in uptake/penetration may be dependent on poor vasculature or increased areas of necrosis. Although the ability to treat larger tumours would be ideal, in animal models it is limited by rapid tumour growth kinetics with tumours often reaching humane endpoint sizes quickly before any delayed drug/treatment induced toxicity of tumour growth inhibition may be evident.

Whilst further definition of T_{reg} cell anti-tumour immunosuppression mechanisms are still required, we conclude that this new strategy of delivering anti-CD25 mAb directly into the tumour is potentially viable and is in line with current thinking that T_{reg} cells are active at the site of immune regulation. Attempts to modulate the effects of these T_{reg} cells should be targeted to these sites of action. The next chapter presents experiments further characterising intra-tumoural T_{reg} cells in the hope of determining more specific targets for T_{reg} cell inactivation and hints also as to the origin and lineage of these cells. Further to this, cytokines and costimulatory molecules were investigated as potential mechanisms of T_{reg} cell action.

Chapter 6:
Characterisation, origin and potential mechanisms of action of intra-tumoural T_{reg} cells

6.1 Introduction

There is a history in the field of T_{reg} cell immunology to want to identify T_{reg} cells based on characteristics such as cell surface marker expression or cytokine secretion profile. Naturally occurring T_{reg} cells originate in the thymus and have been described to have an antigen specificity for self-antigens (227). Tr1/Th3 cells are generally foreign antigen-specific and may be derived in the periphery from conventional naïve $CD4^+CD25^-$ T cell precursors following exposure to antigen and primarily secrete IL-10 and TGF-β (228). While $CD4^+CD25^+Foxp3^+$ T_{reg} cells are most commonly implicated in cancer studies of both mice and humans (25-27, 53, 94, 95, 118, 156, 179), there is increasing evidence that T_{reg} cells are in fact a heterogenous population (66, 67).

In this chapter, the expression of several proposed T_{reg} cell surface markers, including cytotoxic T lymphocyte associated antigen-4 (CTLA-4), Neuropilin-1 (Nrp-1) and CD69 by intra-tumoural T_{reg} cells were examined. The expression of CTLA-4 has been shown to distinguish recently activated T cells from $CD4^+CD25^+$ T_{reg} cells (87, 88). CTLA-4 and CD28 are both homologues that can bind to B7 with opposing functions. CD28 co-stimulates T cells while CTLA-4 inhibits T cell activation (229). CD69 is an accepted activation marker of T cells but has also been suggested as a marker of T_{reg} cells in both retroviral models and a cancer model (personal communication A. van der Vuurst de Vries, Amgen, USA and (106, 107)). Nrp-1, a receptor involved in axon guidance, angiogenesis, and the activation of T cells, was identified in 2004 by global genechip analysis to be a novel marker of T_{reg} cells with the ability to differentiate T_{reg} cells from activated $CD4^+$ T cells (86). Although CTLA-4 has been linked directly to T_{reg} cell function the roles of CD69 and Nrp-1 are less well understood.

Beyond cell-to-cell contact dependent mechanisms of immunosuppression involving CTLA-4, $CD4^+CD25^+$ T_{reg} cells have also been shown to act via the secretion of immunosuppressive cytokines to induce immunosuppression. Secretion of an elevated level of either IL-10 and/or TGF-β together with some IL-5 and no IL-4 is currently the best indicator of induced TCR-specific T_{reg} cells (personal communication K Mills, Trinity College, Ireland). This chapter presents data on the cytokine secretion profile of intra-tumoural T_{reg} cells in an attempt to further characterise these cells and to understand their mechanisms of action. With the development of techniques to make

single cell suspensions from tumours and the ability to isolate T_{reg} cells from tumours at a reasonably high level of purity cytokine experiments were also conducted to specifically analyse the intra-cellular cytokine expression by T_{reg} cells together with direct *ex vivo* cytokine secretion profiles. As the secretion of both or either of IL-10 and TGF-β are potential mechanisms of action of intra-tumoural T_{reg} cells both molecules were blocked *in vivo* in order to assess the requirement of either or both cytokines for T_{reg} cell function.

Following the thorough characterisation of intra-tumoural T_{reg} cells in the murine model of mesothelioma based on cell surface marker expression and cytokine secretion profiles the question: "Where do intra-tumoural T_{reg} cells come from?" still remained. Both the traditionally-defined natural, thymically derived T_{reg} cells and peripherally-induced T_{reg} cells have been implicated in tumour immunity (67, 230). Beyond this characterisation of T_{reg} cells based on thymic or peripheral selection, there are further hypotheses about the origin and movement of intra-tumoural T_{reg} cells *in vivo* in response to tumour challenge. The first theory is that T_{reg} cells preferentially move to and accumulate in tumours as they progress. At the time this work was being conducted it had been hypothesised that the intra-tumoural accumulation of T_{reg} cells resulted from a migration of peripheral $CD4^+$ T cells consistent with the findings of Curiel *et al* (2004). The chemokine CCL22 was implicated in this migration of T_{reg} cells and was shown to be secreted both by tumour cells themselves but also by tumour-located macrophages (27). Others suggested CD62L and CD103 as markers of T_{reg} cell migration that could be useful in addressing migration questions. CD62L is suggested to be involved in the homing of lymphocytes to the lymph nodes (73) while CD103 is suggested to be involved in the migration of lymphocytes to inflamed sites (47). The role of CCL22 and the cell surface markers CD62L and CD103 on the migration of T_{reg} cells into murine mesotheliomas is investigated in this chapter.

A second explanation for the intra-tumoural presence and activity of T_{reg} cells is that T_{reg} cells are induced within tumours via the immunosuppressive cytokine TGF-β (127, 128). It has been suggested that TGF-β within tumours can induce the conversion of $CD4^+CD25^-$ T cells into $CD4^+CD25^+Foxp3^+$ T_{reg} cells (127, 128). As it was known that mesothelioma tumour cells are secretors of TGF-β (129) it was further hypothesised

that TGF-β secreted by the tumour cells themselves may induce the conversion of naïve $CD4^+$ T cells into T_{reg} cells in order to provide an environment of immunosuppression thus allowing unrestrained tumour growth. Finally, it has been proposed that the accumulation of intra-tumoural T_{reg} cells could result from the selective proliferation of naturally occurring $CD4^+CD25^+Foxp3^+$ T_{reg} cells requiring signalling through the TGF-β receptor II (130). Two rodent tumour models were used to show that during tumour development tumour cells themselves convert a population of immature dendritic cells into a regulatory type DC that secrete TGF-β. These DCs are then recruited to tumour draining LN where they selectively promote the proliferation of T_{reg} cells in a TGF-β dependent manner.

While examining the role of TGF-β in inhibiting tumour development the conversion or proliferation of intra-tumoural T_{reg} cells by TGF-β was also investigated. Finally, a global genechip analysis was specifically designed to compare the mRNA expression levels of T_{reg} cells active at a tumour site compared to naïve spleen derived natural T_{reg} cells. A comparison of active tumour-located T_{reg} cells to naïve T_{reg} cells was directed finding a number of genes specifically upregulated in the tumour derived cells which could then be associated to T_{reg} cell recruitment, induction or selection during the activation process.

6.2 Results

This section describes a further characterisation of intra-tumoural T_{reg} cells based on cell surface marker expression and cytokine secretion profiles. Following this, experiments examining both the hypotheses for T_{reg} cell increases within tumours were investigated in this chapter.

6.2.1 Cell surface markers

Flow cytometry was used to analyse the expression by intra-tumoural T_{reg} cells of 3 potential T_{reg} cell surface markers, CD69, Nrp-1 and CTLA-4. The expression of CD69, Nrp-1 and CTLA-4 by intra-tumoural $CD4^+CD25^+$ T_{reg} cells was examined in small (<25 mm^2) and large (>80 mm^2) tumours. Mice were implanted with 1 x 10^7 AE17 tumours cells and tumours allowed to grow to the appropriate size before the

animals were humanely culled and tumours removed for flow cytometric analysis. Three tumours in the small size range were analysed by flow cytometry for the percentage of $CD4^+CD25^+$ T_{reg} cells co-expressing CD69 (Fig. 6.1A), Nrp-1 (Fig. 6.1B) or CTLA-4 (Fig. 6.1C). Twelve large tumours were also analysed by flow cytometry for the percentage of $CD4^+CD25^+$ T_{reg} cells co-expressing CD69 (Fig. 6.1A), Nrp-1 (Fig. 6.1B) and CTLA-4 (Fig. 6.1C) and are presented alongside the small tumour data. A statistically significant increase was found in the expression of both CD69 and Nrp-1 ($p < 0.01$ and $p < 0.01$ respectively) by intra-tumoural $CD4^+CD25^+$ T_{reg} cells as the tumours increased in size. Figure 6.1C shows that a low level of expression of CTLA-4 by intra-tumoural $CD4^+CD25^+$ T_{reg} cells in both small and large tumours. Unlike Nrp-1 and CD69 there is no upregulation of CTLA-4 by intra-tumoural T_{reg} cells as tumours grow.

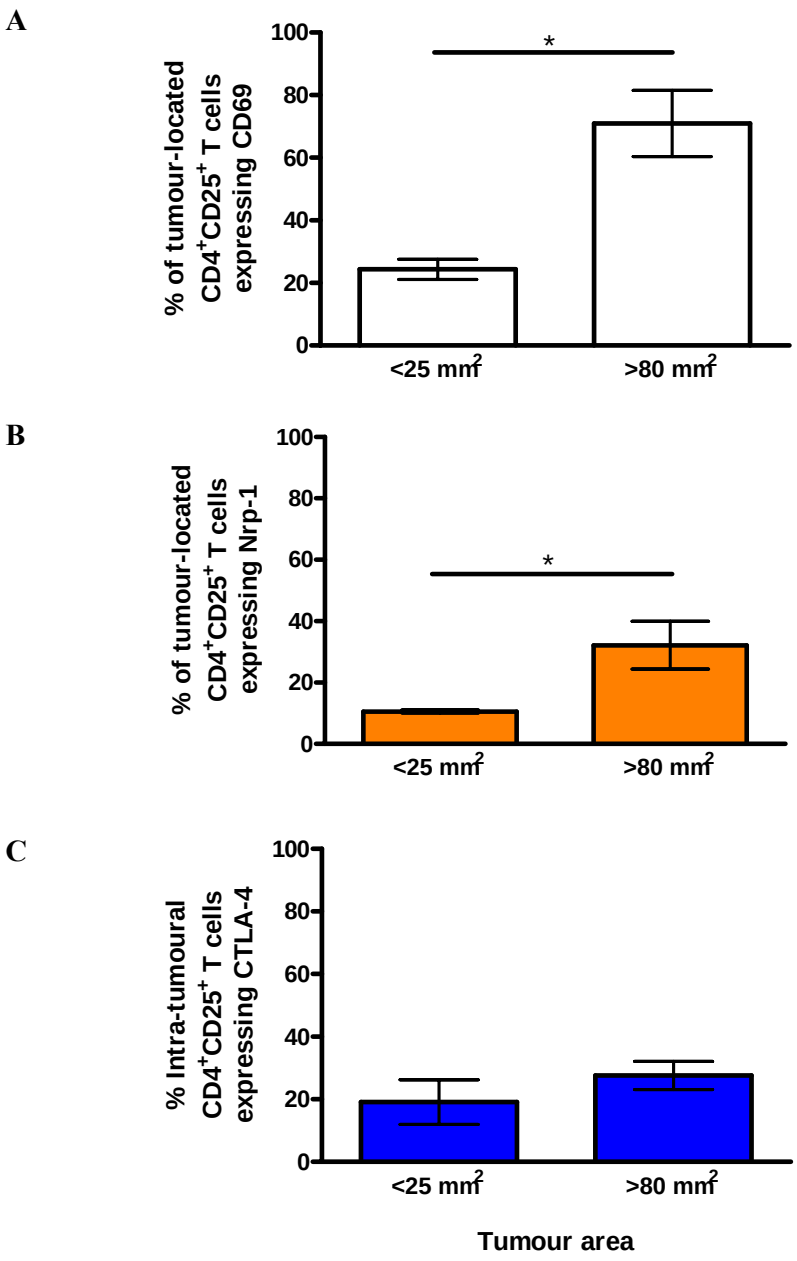

Figure 6.1: Expression of proposed T_{reg} cell markers by intra-tumoural T_{reg} cells.

Mice were implanted with 1 x 10^7 AE17 tumours cells. Tumours < 25 mm^2 or > 80 mm^2 were then removed and dissociated for flow cytometric analysis of cell surface markers. The percentage of intra-tumoural $CD4^+CD25^+$ T_{reg} cells co-expressing (A) CD69, (B) Nrp-1 and (C) CTLA-4 was calculated in small versus large tumours. Data are the mean ± SEM for 3 small tumours and 12 large tumours. A single asterisk represents a p-value < 0.05.

6.2.2 Cytokine secretion profile

Much work has been conducted to profile T_{reg} cells based on cytokine secretion. Tr1 cells are defined by the secretion of IL-10 (231) while Th3 cells are defined on the basis of TGF-β secretion (49). Without assigning labels to specific cell populations, others have proposed that T_{reg} cells should secrete IL-10 and/or TGF-β, little IL-5 and no IL-4 (personal communication: K Mills, Trinity College, Ireland). In our laboratory's previous T_{reg} cell work using the MAIDS model, some serum cytokine changes were seen in response to progressing retroviral disease (107). While studying the murine model of mesothelioma, no detectable changes in serum IL-4 or IL-10 was found as tumours progress (data not shown). TGF-β was however detectable in the serum of both naïve control mice and tumour-bearing test mice but levels did not increase with tumour growth (data not shown). In the MAIDS model, the most clear cytokine data was generated when specifically analysing intra-cellular cytokine levels and secreted cytokine levels by T_{reg} cells directly *ex vivo*. This section therefore provides an analysis of the intra-cellular and secreted cytokine profile of directly *ex vivo* (unstimulated) intra-tumoural T_{reg} cells in order to better define and understand this cell population.

6.2.2.1 T_{reg} cell associated cytokines

Serum cytokine levels in tumour-bearing mice did not provide any evidence for the role of cytokines in tumour development. Using the previously described protocol for tumour dissociation and the preparation of single cell suspensions intra-tumoural T_{reg} cells themselves were analysed directly *ex vivo* for intra-cellular cytokine levels and secreted cytokine levels. For intra-cellular cytokine analyses mice were implanted s.c. with 1 x 10^7 AE17 tumour cells. Tumours were removed at either 25 mm^2 or 100 mm^2 and dissociated for flow cytometric analysis. First tumour cell suspensions were stained for the CD4 and CD25 cell surface markers of T_{reg} cells. The stained tumour cell suspensions were then permeabilised and fixed prior to intra-cellular staining for IL-4 and IL-10. Mick-2 IL-10 and IL-4 positive control cells were stained in the same manner and used to set the gating criteria for flow cytometric analysis. Mick-2 positive control cells are prepared by the manufacturer to be 11% positive for IL-4 and 40.8% positive for IL-10. By intra-cellular flow cytometry, only very low levels of IL-10 and IL-4 could be detected to be expressed by tumour-located T_{reg} cells in small tumours. In large tumours, a higher level of expression of both IL-10 and IL-4 was observed

(19.6 ± 3.1% and 22.9 ± 3.8% of tumour located $CD4^+CD25^+$ T_{reg} cells respectively) (Fig. 6.2).

A final, direct method for the analysis of T_{reg} cell cytokine secretion was trialled. In this case, T_{reg} cells were isolated from 100 mm^2 tumours by magnetic bead selection using the Imag system (BD Pharmingen) for $CD4^+CD25^+$ T_{reg} cells. Cells were then plated into a 96 well tissue culture plate at a concentration of 1 x 10^5 cells in 200 µl supplemented RPMI-1640 tissue culture media per well. Cells were incubated overnight (without further stimulation) and the next morning the supernatant was separated from the cells and used in cytokine ELISA assays for IL-10, IL-4 and TGF-β. The supernatant for TGF-β ELISA analysis required acidification prior to analysis to activate the TGF-β for detection. $CD4^+CD25^+$ T_{reg} cells isolated from tumours were compared to their $CD4^+CD25^-$ T cell counterparts in these immunoassays. Using these *ex vivo* ELISA immunoassays it was more clearly shown that tumour-isolated T_{reg} cells specifically secrete only a low level of IL-4 (no significant difference between $CD25^-$ and $CD25^+$ T cell secretion, $p = 0.92$), a higher level of IL-10 (but not significantly different to $CD25^-$ T cells, $p = 0.25$) and significantly higher levels of TGF-β (significant difference between $CD25^-$ and $CD25^+$ T cell secretion, $p = 0.05$) (Fig. 6.3). In comparison, IL-10 and TGF-β, are not secreted by tumour derived $CD4^+CD25^-$ T cells suggesting these cytokines may be involved in the suppressive function of intra-tumoural T_{reg} cells.

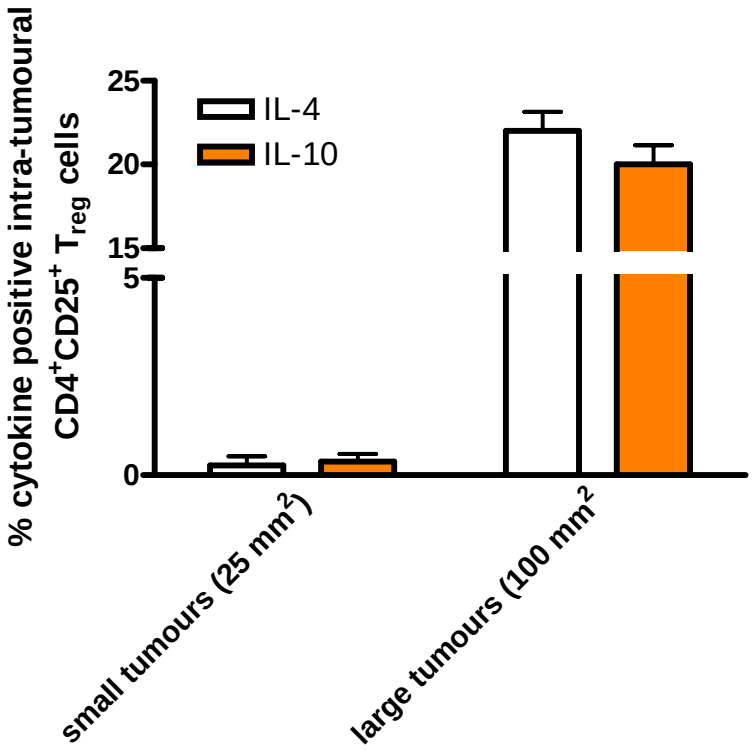

Figure 6.2: Intracellular flow cytometric analysis of cytokine expression by intra-tumoural T_{reg} cells.

Mice were implanted s.c. with 1 x 10^7 AE17 tumour cells. 3 tumours were removed once they reached 25 mm^2 and 3 tumours removed once they reached 100 mm^2. Tumours were dissociated and cell surface stained for CD4 and CD25 prior to fixation and permeabilisation. Cells were then stained for intra-cellular IL-4 or IL-10. Mick-2 IL-4 and IL-10 positive control cells were used to set the gating criteria. Data are the percentage of intra-tumoural $CD4^+CD25^+$ T_{reg} cells expressing intracellular cytokine. Data are the mean ± SEM of 3 tumours per size range.

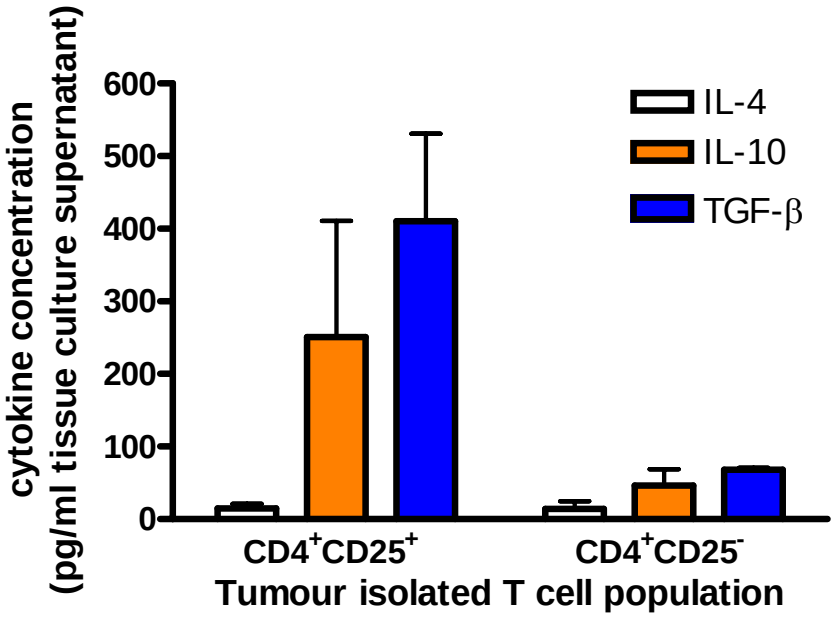

Figure 6.3: Cytokine secretion levels of sorted intra-tumoural T_{reg} cells.

T_{reg} cells and $CD4^+CD25^-$ T cells were sorted by Imag magnetic bead selection from 100 mm^2 tumours. Cells were then incubated without extra stimulation in supplemented RPMI-1640 tissue culture media overnight in a 96 well tissue culture plate with 1 x 10^5 cells in 200 µl media per well. Cytokine secretion levels in supernatant were calculated by ELISA by comparison to recombinant cytokine standards. Data are the mean concentration ± SEM for 6 samples per cytokine per cell type.

6.2.2.2 T_{reg} cell inactivation by anti-IL-10 mAb treatment.

The cytokine secretion experiments presented above, particularly the supernatant ELISAs, suggested that IL-10 and TGF-β may be important cytokines in the immunosuppressive response mediated by intra-tumoural T_{reg} cells. An anti-IL-10 mAb was therefore used to block the effect of secreted IL-10 within tumours to determine the importance of this cytokine for the *in vivo* T_{reg} cell response. Mice were implanted s.c. with 1 x 10^7 AE17 murine mesothelioma tumour cells. Once tumours reached 9 mm^2 a single intra-tumoural 0.3 mg dose of anti-IL-10 mAb solution was administered. A single 0.3 mg dose of anti-IL-10 mAb solution was based on the administration protocol of Seo *et al* 2001 (53). Tumours were monitored regularly for tumour growth inhibition as a result of IL-10 blockade and potentially the blockade of T_{reg} cell function (Fig. 6.4A). No tumour growth inhibition was observed as a result of this single intra-tumoural treatment.

The blockade of IL-10 and hence T_{reg} cell function has been shown in the past to be effective at inducing tumour growth inhibition (53). This type of treatment is complicated by the fact that IL-10 is a secreted cytokine and so the effect of anti-IL-10 mAb may be transient. In order to prolong the IL-10 blockade multiple intra-tumoural doses of the same amount of anti-IL-10 mAb (0.3 mg) were administered intra-tumourally at 3 to 4 day intervals (i.e. on days 0 and then days 4, 7 and 11 post initial treatment). Again no significant differences in tumour growth was seen between the anti-IL-10 mAb treated mice and the untreated control animals (Fig. 6.4B).

The intra-tumoural blockade of TGF-β was also undertaken and is fully described in Section 6.2.4 below.

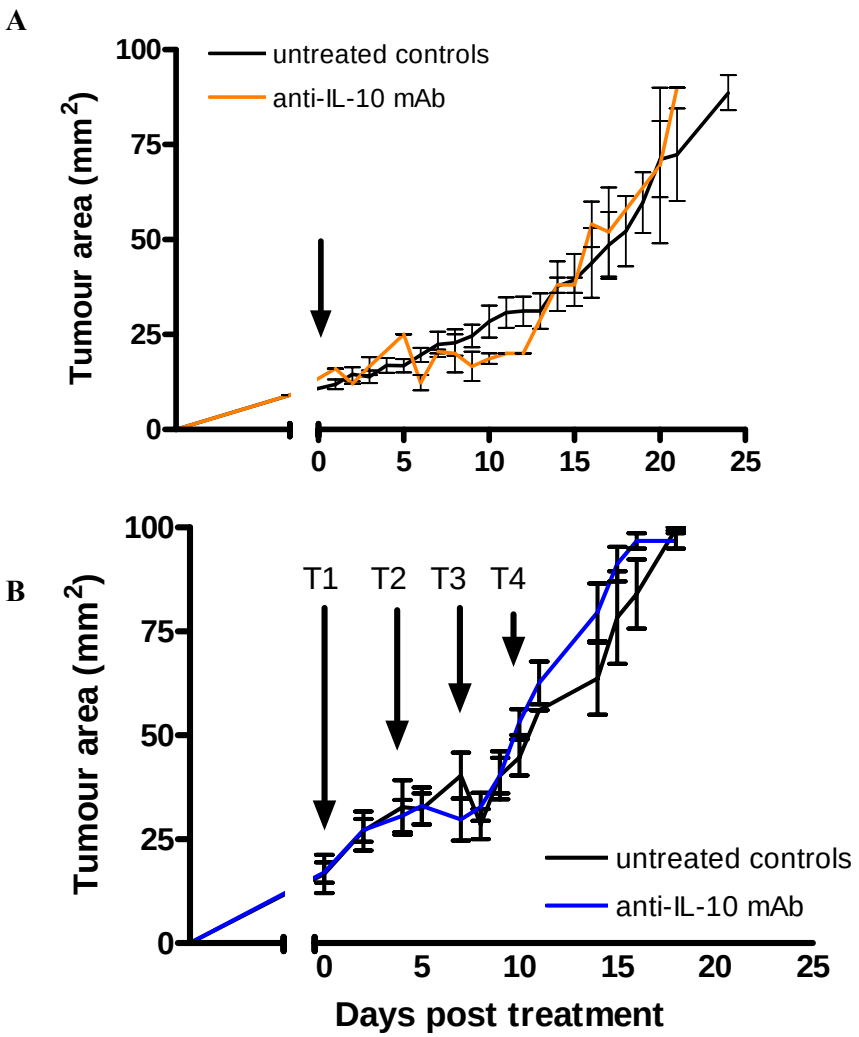

Figure 6.4: Blocking T_{reg} cell function with intra-tumoural anti-IL-10 mAb treatment

Mice were implanted s.c. with 1 x 10^7 AE17 tumour cells. Tumours were allowed to grow to 9 mm^2 prior to the initiation of treatment. (A) Mice were treated with a single, intra-tumoural 0.3 mg dose of anti-IL-10 mAb solution in a 40 µl volume. Control mice were left untreated. (B) Mice were treated with a single dose of 0.3 mg anti-IL-10 mAb solution intra-tumourally. Subsequent treatments were also of a 0.3 mg dosage on days 4, 7 and 11 post initial treatment. All mice were monitored regularly and tumour areas calculated. Data are the mean ± SEM for (A) 3 anti-IL-10 mAb treated mice and 9 untreated control mice and (B) 3 untreated control mice and 5 mice treated with the multiple doses of anti-IL-10 mAb.

6.2.3 T_{reg} cell recruitment from the periphery

The question "where do intra-tumoural T_{reg} cells come from still remained"? If T_{reg} cells were being recruited from the periphery, potentially via the tumoural secretion of the chemokine CCL22 as proposed by Curiel *et al* (2004), a decrease in the peripheral T_{reg} cell population should result.

6.2.3.1 Early T_{reg} cell recruitment from the periphery

Although the relative expression of CD25 by $CD4^+$ T cells in the periphery of tumour-bearing mice was analysed in chapter 3 and only a small increase in CD25 expression was observed in the blood, the percentage of $CD4^+$ T cells with respect to total cells in the peripheral lymphoid organs (spleen, blood and LNs) was not examined. A reanalysis of the data presented in Figures 3.2A and 3.2B revealed a significant and early (day 14 post tumour challenge) decrease in $CD4^+$ T cells in the spleen ($p < 0.05$) and LNs ($p < 0.01$) of tumour bearing mice when calculated as a percentage of total cells (Fig. 6.5A and 6.5B respectively). This same decrease was not seen in the blood (Fig. 6.5C). In a similar analysis, the actual number of $CD4^+CD25^+$ T_{reg} cells in the peripheral lymphoid organs were calculated over the same 5 week time-course of tumour development by multiplying total cell counts with the percentage of $CD4^+CD25^+$ T_{reg} cells identified by flow cytometry (Fig. 6.6). Again an early drop in T_{reg} cells was seen from the time of tumour implantation to approximately 14 days post tumour challenge with a gradual recovery in the $CD4^+CD25^+$ T_{reg} cell population by day 28 in both the spleen and draining LN of the mesothelioma-bearing mice (Fig. 6.6A and Fig 6.6B respectively). Interestingly, the opposite was seen in the blood, that is, an increase in peripheral T_{reg} cells with tumour development (Fig 6.6C) perhaps suggesting a role for the blood in the transportation of peripheral T_{reg} cells to the tumour. Together, the data suggests that the low levels of $CD4^+CD25^+$ T_{reg} cells seen inside small tumours may result from the recruitment of natural T_{reg} cells from the periphery.

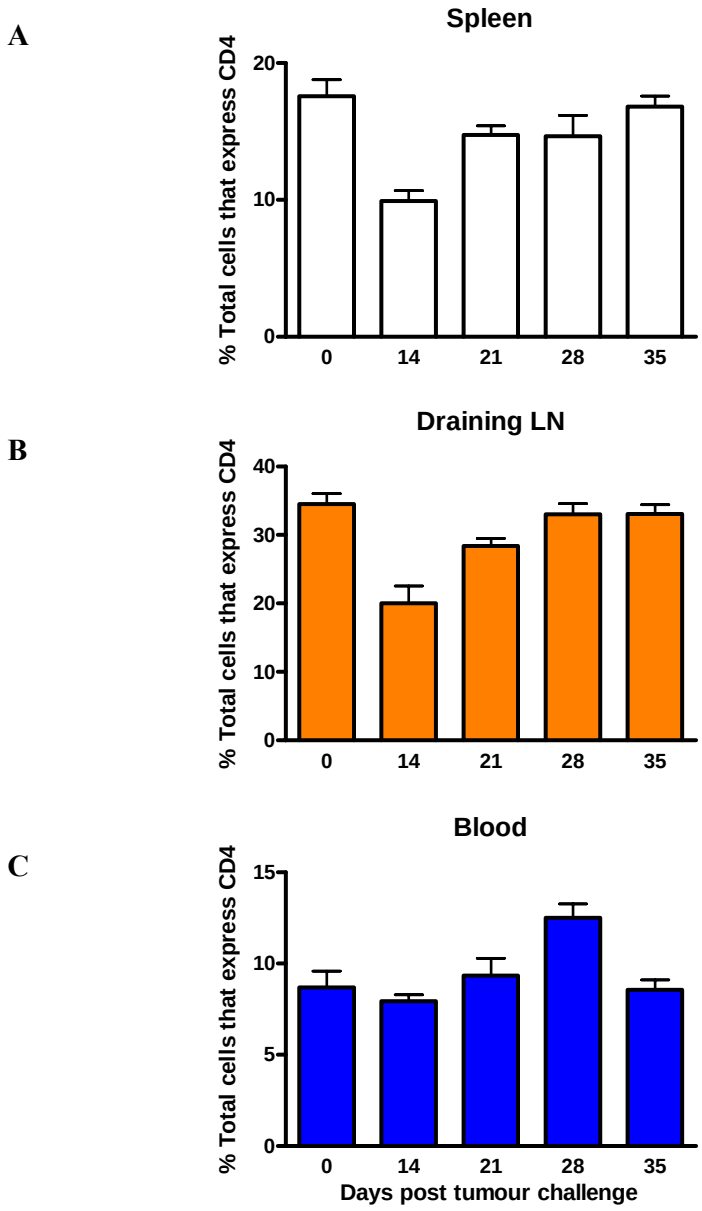

Figure 6.5: Percentage of $CD4^+$ T cells in the periphery of mesothelioma-bearing mice.
Mice were implanted s.c. at day 0 with 1 x 10^6 AE17 tumour cells. Mice were culled at days 14, 21, 28 and 35 post tumour challenge and single cell suspensions made from (A) spleens, (B) draining LN and (C) blood for analysis by flow cytometry for the presence of $CD4^+$ T cells. $CD4^+$ T cells were calculated as a percentage of the total cells over a 5 week time-course of tumour development and compared to the percentage seen in naïve, tumour free mice (day 0). Data are the mean ± SEM of 8 mice per time-point.

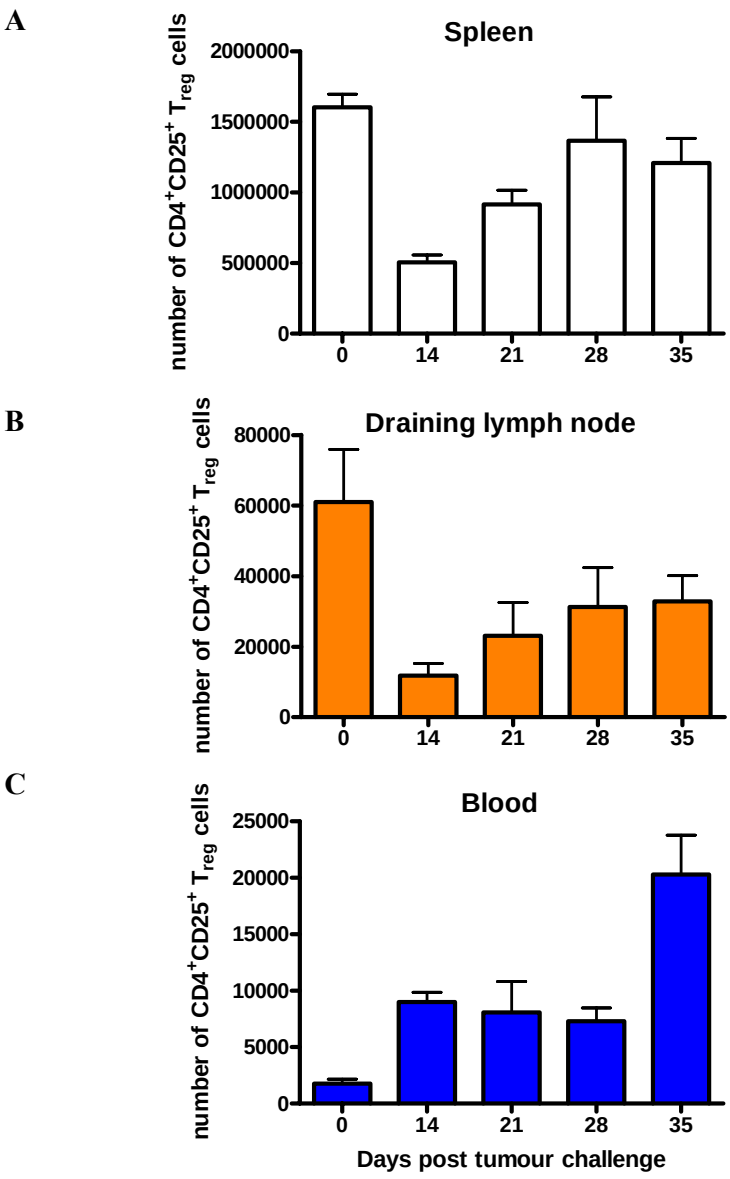

Figure 6.6: Total number of $CD4^+CD25^+$ T_{reg} cells in the periphery of mesothelioma-bearing mice. Mice were implanted s.c. at day 0 with 1 x 10^6 AE17 tumour cells. Mice were culled at days 14, 21, 28 and 35 post tumour challenge and single cell suspensions made from (A) spleens, (B) draining LN and (C) blood for analysis by flow cytometry for the presence of $CD4^+CD25^+$ T_{reg} cells. Total cell numbers were calculated by multiplying the percentage of cells identified by flow cytometry with cell counts made by counting total live cells using a neubauer chamber and the trypan blue exclusion method over a 5 week time-course of tumour development and compared to the number seen in naïve, tumour free mice (day 0). Data are the mean ± SEM of 5 mice per time-point.

6.2.3.2 T_{reg} cells express cell surface markers of T cell migration

It was clear from Section 6.2.4.1 that the T_{reg} cells observed with tumours may represent a population of T_{reg} cells recruited from the periphery of the tumour-bearing mouse. To further examine this recruitment, $CD4^+CD25^+$ T_{reg} cells in the spleen, blood, draining LN and tumours of mice were examined for the expression of CD62L and CD103 by flow cytometry. A total of 12 mice were examined in 3 independent experiments and the data pooled for presentation in Figure 6.7. It was revealed that a significant expression of CD62L exists on T_{reg} cells in the blood of tumour-bearing mice suggesting blood located T_{reg} cells are homing to LN. As these T_{reg} cells make it to the LN, CD62L expression significantly drops (Fig 6.7A). An opposite trend was noted when investigating the expression of CD103 by T_{reg} cells in the periphery and tumours of mice. A low expression of CD103 is observed in the blood, with intermediate expression in the LN and a high expression in the tumour (Fig 6.7B).

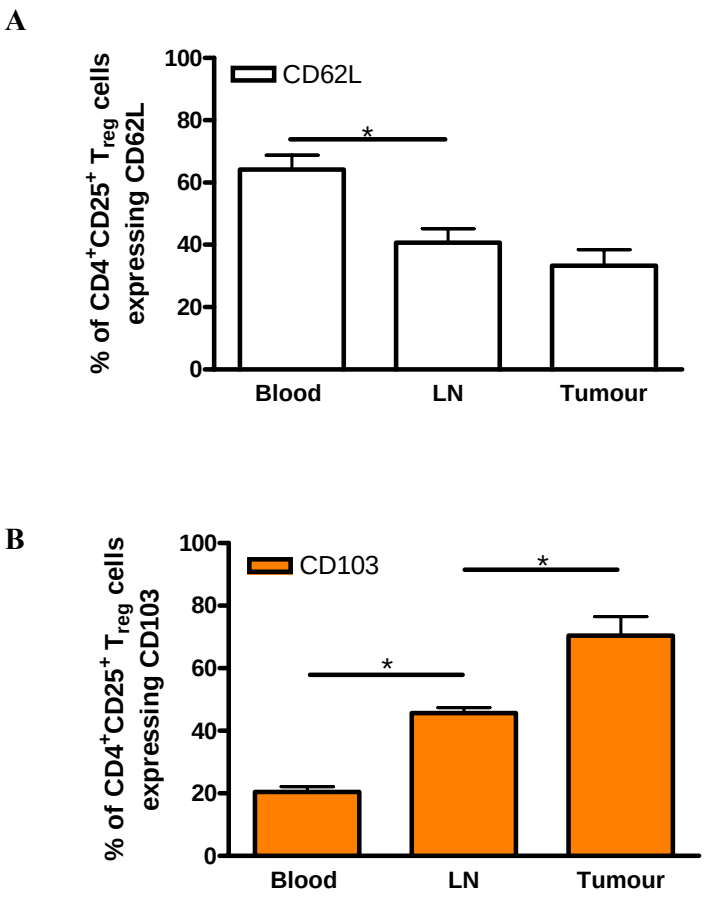

Figure 6.7: Markers of T_{reg} cell migration

Mice were implanted s.c. at day 0 with 1 x 10^7 AE17 tumour cells. Mice were culled when tumours had reached the humane endpoint of 100 mm^2 and single cell suspensions made from draining LN and tumours and lymphocytes prepared from blood for analysis by flow cytometry for the percentage of $CD4^+CD25^+$ T_{reg} cells co-expressing (A) CD62L and (B) CD103. Data are the mean ± SEM of 12 mice per tissue type. A single asterisk represents a p-value < 0.05.

6.2.3.3 CCL22 as an inducer of T_{reg} cell migration.

There was accumulating evidence that T_{reg} cells were migrating to the tumours from the periphery. This supported the finding of a murine ovarian cancer model that T_{reg} cells were recruited to tumours from the periphery via the secretion of the chemokine CCL22 by tumours (27). The administration of an anti-CCL22 mAb in this murine ovarian cancer model was shown during adoptive transfer experiments to block the migration of transferred T_{reg} cells. Rather than using an artificial adoptive transfer model, it was proposed in this murine mesothelioma study that if CCL22 was important in the migration of T_{reg} cells from the periphery to the tumour, the blockade of this migration by the administration of anti-CCL22 mAb would result in tumour growth inhibition as the T_{reg} cells would not make it to the tumour to exert their suppression over the anti-tumour CTLs. Initially, experiments were conducted to investigate the effect of blocking CCL22 intra-tumourally as it has been found that CCL22 is secreted by both tumour cells and tumour-located macrophages. 0.2 mg of anti-CCL22 mAb (in a 40 µl volume) was administered once, intra-tumourally, to AE17 tumours of 9 mm^2. Tumour growth was monitored and compared to untreated control mice (Fig 6.8A). The combined data from two independent experiments and hence a total of nine mice per treatment group is presented. Intra-tumoural treatment with a single dose of intra-tumoural anti-CCL22 mAb did not inhibit tumour development.

As it was proposed that CCL22 was inducing the migration of T_{reg} cells from the periphery, systemic administration of anti-CCL22 mAb was trialled to block the migration of all peripheral T_{reg} cells. A single 0.5 mg dose of anti-CCL22 mAb was administered i.p. (in a 100µl volume) to mice bearing 9 mm^2 AE17 tumours. Control mice were left untreated. Again the combined results of 2 independent experiments utilising 9 mice per group are presented in Figure 6.8B. A single, systemic treatment with anti-CCL22 mAb was also ineffective at inhibiting tumour development in the murine model of mesothelioma demonstrated by the similar tumour growth kinetics in both groups of mice. To examine whether anti-CCL22 mAb treatment was having an effect on T cell populations within the tumour which was not evident by a change in tumour growth rate, tumours that had been treated with anti-CCL22 mAb were investigated for intra-tumoural T_{reg} cell and CTL population differences compared to untreated control tumours. In this experiment mice were implanted s.c. with 1 x 10^7

AE17 tumour cells and then treated with an i.p. dose of 0.5 mg anti-CCL22 mAb when tumours reached 9 mm^2. In order to maximise the potential effect of the antibody on tumour located cells, 4 follow-up doses with the same amount of anti-CCL22 mAb were administered i.p. at 3 day intervals until day 15 post treatment 1. At day 15 post treatment 1 (and after a total of 5 treatments with anti-CCL22 mAb had been administered to mice) the average tumour size for the 3 mice left untreated was 26.6 ± 4.4 mm^2 while the tumours from mice treated multiple times with the mAb were in fact larger and averaged 45.5 ± 5.3 mm^2 ($p=0.05$). Flow cytometric analysis was conducted on the tumours (both untreated and anti-CCL22 mAb treated tumours) in order to examine the effect of CCL22 blockade on the migration of T_{reg} cells into tumours. The same percentage of $CD4^+$ T cells was observed within the treated and untreated tumours ($1.4 \pm 0.3\%$ of total tumour cells and $1.4 \pm 0.5\%$ of total tumour cells respectively). Of these tumour located $CD4^+$ T cells a similar percentage co-expressed CD25 in both CCL22 mAb treated tumours ($49.8 \pm 2.8\%$) and untreated tumours ($40.7 \pm 5.1\%$). The observation that the tumours of the anti-CCL22 mAb treated mice were larger than the untreated tumours suggested that perhaps the intra-tumoural $CD8^+$ CTLs may have been blocked resulting in an inability of the anti-tumour immune response to keep tumour growth under control. Upon flow cytometric analysis of intra-tumoural $CD8^+$ CTLs it was found that again both the treated and untreated tumours comprised the same percentage of $CD8^+$ CTLs ($1.8 \pm 0.5\%$ of total tumour cells and $0.8 \pm 0.2\%$ of total tumour cells respectively) and of these $CD8^+$ CTLs a similarly low percentage were activated ($6.8 \pm 0.2\%$ coexpressed CD25 in untreated tumours while $5.1 \pm 0.4\%$ coexpressed CD25 in anti-CCL22 mAb treated tumours) most likely due to the high proportion of T_{reg} cells remaining in both the treated and untreated tumours.

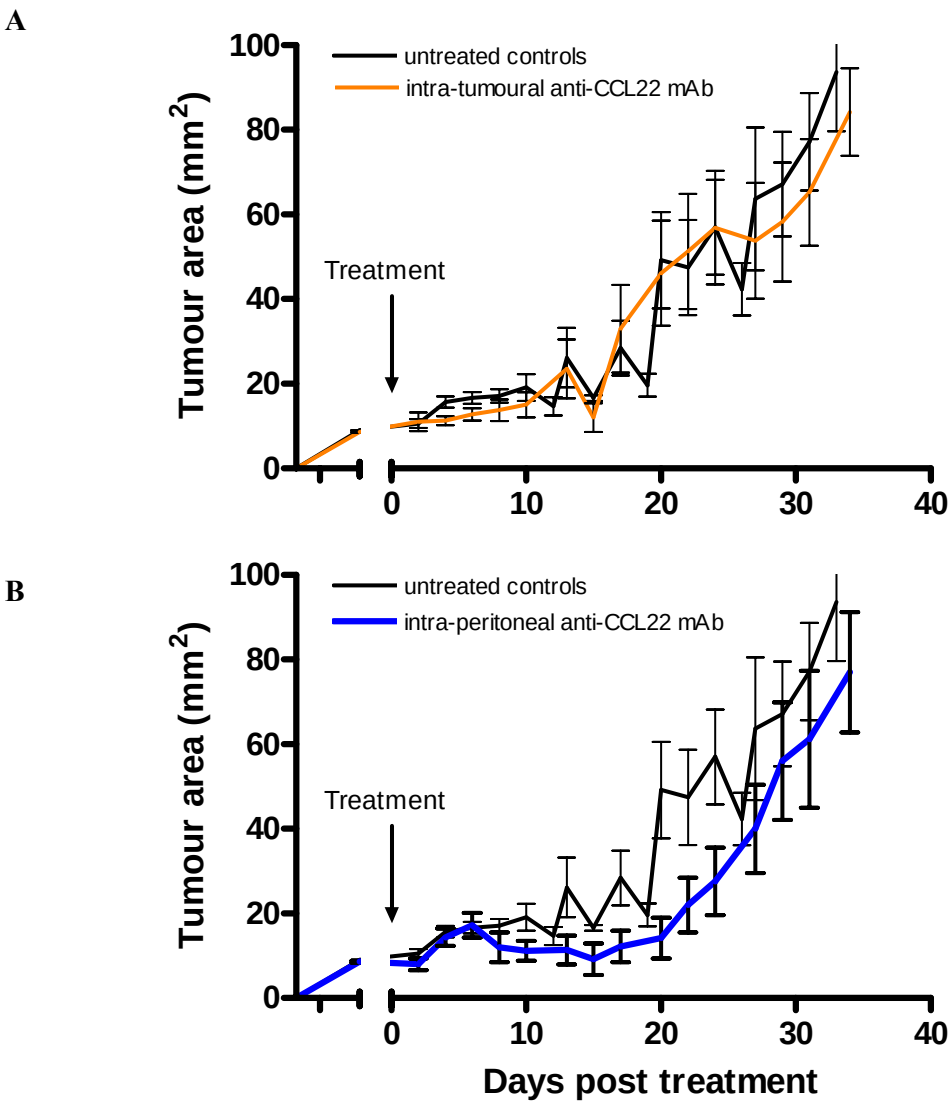

Figure 6.8: Blocking T_{reg} cell migration by intra-tumoural and intra-peritoneal administration of anti-CCL22 mAb

Mice were implanted s.c. with 1 x 10^7 AE17 tumour cells. At day 0, or when tumours had reached 9 mm^2 (A) a single 0.2 mg dose of anti-CCL22 mAb was administered intra-tumourally or (B) a single 0.5 mg dose of anti-CCL22 mAb was administered intra-peritoneally. Control mice were left untreated. Tumour growth was monitored daily and tumour areas calculated by multiplying two, right-angled tumour diameters measured using microcallipers. Data are the mean ± SEM of 9 mice per treatment group.

6.2.4 The role of TGF-β in T_{reg} cell conversion

Data in this chapter has shown that $CD4^+$ T cells appear to remain at a constant percentage in tumours (approximately 2%) despite tumour growth. Obviously, the total number of $CD4^+$ T cells increases as the tumour grows and is comprised of more cells, but $CD4^+$ T cells remain at an overall constant percentage. Within this $CD4^+$ T cell compartment the percentage of cells expressing CD25 increases significantly with tumour size and consequently the percentage of cells that are $CD25^-$ decreases. This change in $CD4^+$ T cell phenotype could be explained by the selective recruitment of T_{reg} cells from the periphery into growing tumours or a second mechanism of T_{reg} cell conversion from naïve T cell may also be occurring within tumours. This potential second mechanism of $CD4^+CD25^+$ T_{reg} cell conversion from naïve $CD4^+CD25^-$ T cells was also worthy of investigation and is presented in this section.

6.2.4.1 TGF-β blockade inhibits murine mesothelioma tumour development

Several groups have now proposed that TGF-β may induce the conversion of $CD4^+CD25^-$ T cells into $CD4^+CD25^+Foxp3^+$ T_{reg} cells most likely via immature/semi-mature DCs (127, 128, 232). It was therefore hypothesised that TGF-β may be inducing the conversion of $CD4^+CD25^-$ T cells into T_{reg} cells within tumours themselves resulting in immunosuppression. To investigate the effect of the neutralisation of tumour located TGF-β on murine mesothelioma tumour growth, murine AE17 tumours of 9 mm^2 were treated intra-tumourally with 500 ng TGF-β soluble receptor every 3 days for 15 days (Fig 6.9A). Although control tumours grew quite rapidly, the three tumours treated with TGF-β soluble receptor were significantly smaller at day 15 post treatment 1. These tumours were analysed for the intra-tumoural percentage of $CD8^+$ CTLs compared to untreated tumours. As can be seen in the representative flow cytometric plots of Figure 6.9 there is a similar percentage of $CD4^+CD25^+Foxp3^+$ T cells in both untreated (Fig. 6.9Bi and 6.9Bii) and TGF-β soluble receptor treated tumours (Fig. 6.9Ci and 6.9Cii). On the other hand, there is a large increase in the expression of CD25 by intra-tumoural $CD8^+$ CTLs in tumours treated with the TGF-β soluble receptor (represented by Fig. 6.9Ciii) compared to untreated tumours (represented by Fig 6.9Biii). This increase from 5.2 ± 0.4% of intra-tumoural $CD8^+$ T cells co-expressing CD25 in untreated tumours to 74.6 ± 2.3% in TGF-β

soluble receptor treated tumours is likely to represent CTL activation as a result of the inactivation of T_{reg} cells.

A similar experiment was conducted to confirm these results and also to examine the efficacy of a lowered dose of TGF-β soluble receptor to block T_{reg} cell function. Mice were again implanted with 1 x 10^7 AE17 tumour cells and treatment initiated once tumours reached 9 mm^2. Tumours were treated intra-tumourally with 100 ng TGF-β soluble receptor on day 0 and then every 3 days. It became clear early into the treatments with the TGF-β soluble receptor at the 100 ng dosage that some tumours were responding to the treatment and were inhibited in tumour growth (2/5) while other tumours continued tumour growth at a similar rate to untreated controls (3/5). Figure 6.10A depicts the growth kinetics of tumours that appeared to respond to the TGF-β blocking treatment compared to tumours that appeared not to respond to the treatment and also untreated control tumours. In confirmation of previous experiments T_{reg} cell percentages within tumours treated with the TGF-β soluble receptor were determined. Again treated tumours comprised a normal percentage of T_{reg} cells when compared to untreated control tumours whether the tumours had responded to TGF-β blockade or not (Fig. 6.10Bi and 6.10Ci are representative figures for the responding and non-responding treatment groups). It was predicted from the original TGF-β experiments (using a 500 ng dose of TGF-β soluble receptor) that the percentage of intra-tumoural $CD8^+$ T cells that were activated (co-expressing CD25) would be increased in tumours responding to the TGF-β soluble receptor and hence T_{reg} cell blockade. It was in fact the case in this experiment that a significantly greater percentage of activated $CD8^+$ CTLs was observed in tumours responding to TGF-β treatment ($p < 0.01$) as represented by figures 6.10Bii and 6.10Cii. It was also clear from an ELISA analysis of intra-tumoural TGF-β concentration in tumours responding or not responding to treatment with the TGF-β soluble receptor that in those tumours which had responded the intra-tumoural concentration of TGF-β was lower (20.3 ± 1.1 pg/g tumour) compared to those tumours that had not responded to treatment (38.1 ± 7.5 pg/g tumour).

6.2.4.2 AE17 cells are TGF-β positive.

TGF-β is a master cytokine of the T_{reg} cell response. Not only is it involved in T_{reg} cell function as shown in the previous section but it may also be involved in the conversion of naïve T cells into T_{reg} cells or the selective proliferation of T_{reg} cells within tumours. The reduced tumour growth kinetics seen in the above experiments as a result of the intra-tumoural treatment of tumours with a soluble TGF-β receptor may be a result of the blockade of intra-tumoural T_{reg} cell conversion from naïve T cells. AE17 cells were demonstrated to be TGF-β positive by RT-PCR. RNA was extracted from AE17 cells prior to reverse transcription and real-time PCR for the expression of TGF-β mRNA compared to the house keeping gene hypoxanthine -phosphoribosyl transferase (HPRT). The PCR products were analysed by electrophoresis for single products (Fig 6.11). Only single products for both TGF-β and HPRT were observed. Both products were of the correct size when compared to a 100 bp ladder (TGF-β product is 141 bp, HPRT product is 179 bp). TGF-β secretion by AE17 cells was confirmed by ELISA (data not shown) suggesting the conversion of the $CD4^+CD25^-$ T cells into $CD4^+CD25^+Foxp3^+$ T_{reg} cells may be occurring within the tumour by a TGF-β mediated mechanism.

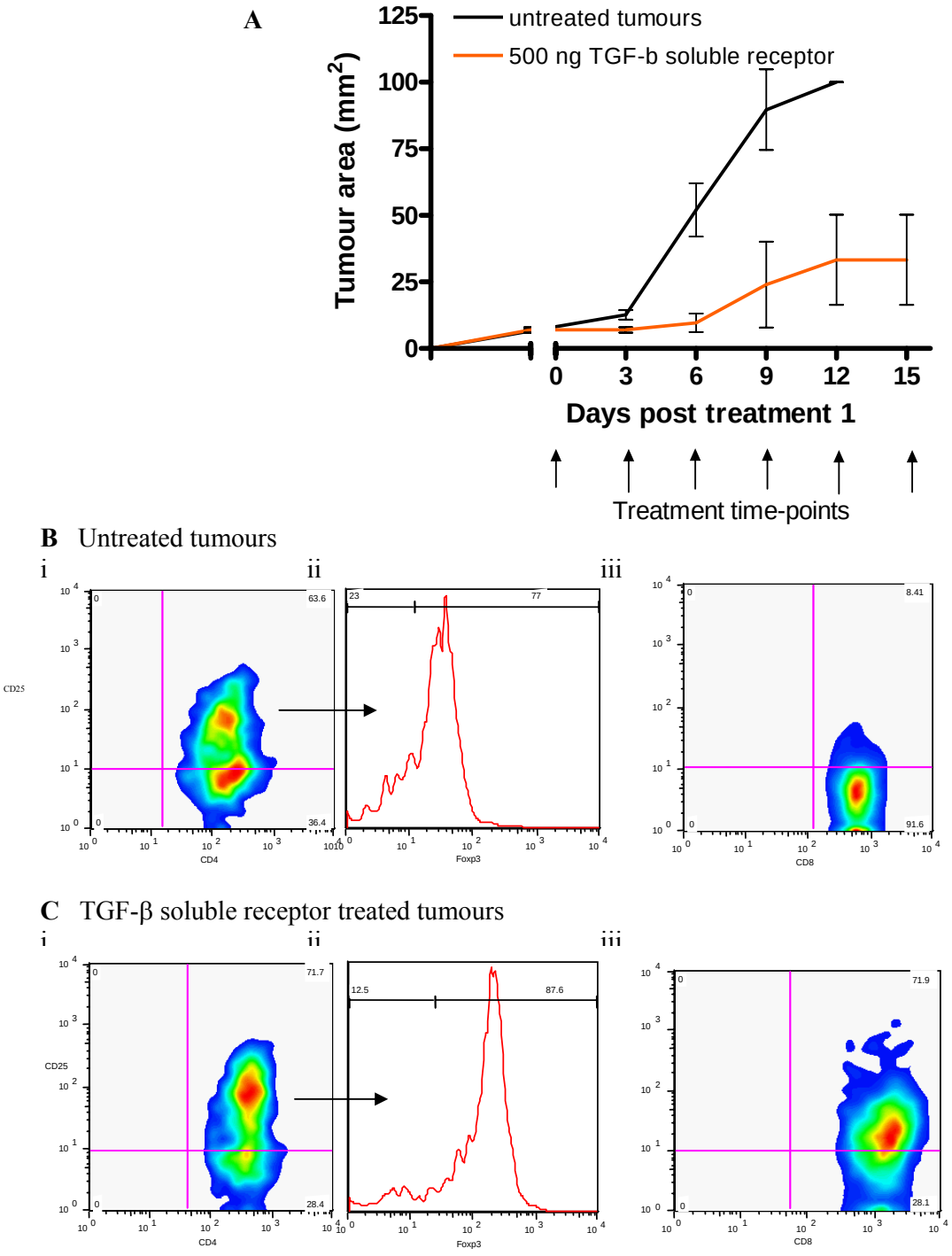
A
untreated tumours
500 ng TGF-b soluble receptor
Tumour area (mm2)
125
100
75
50
25
0
0
3
6
9
12
15
Days post treatment 1
Treatment time-points
B Untreated tumours
i
ii
iii
CD25
CD4
Foxp3
CD8
63.6
36.4
23
77
8.41
91.6
C TGF-β soluble receptor treated tumours
71.7
28.4
12.5
87.6
71.9
28.1

Figure 6.9: Treatment with TGF-β soluble receptor inhibits murine mesothelioma tumour growth by blocking T_{reg} cell function.

Mice were implanted s.c. with 1 x 10^7 AE17 tumour cells. Treatment with TGF-β soluble receptor was initiated once tumours reached 9 mm^2. Treatment involved the administration of 500 ng TGF-β soluble receptor intra-tumourally every 3 days. Control tumours were left untreated. (A) Tumour growth was monitored regularly and tumour areas calculated. Tumours were removed from mice at day 15 and dissociated for flow cytometric analysis. Representative flow cytometric graphs are presented for (B) untreated tumours and (C) TGF-β soluble receptor treated tumours with (i) $CD4^+CD25^+$ T_{reg} cells shown as a percentage of tumour-located $CD4^+$ T cells, (ii) Foxp3 expression shown by intra-tumoural $CD4^+CD25^+$ T_{reg} cells and (iii) $CD8^+CD25^+$ T cells as a percentage of total tumour-located $CD8^+$ T cells. Data are the mean ± SEM for 3 untreated control tumours and 5 TGF-β soluble receptor treated tumours.

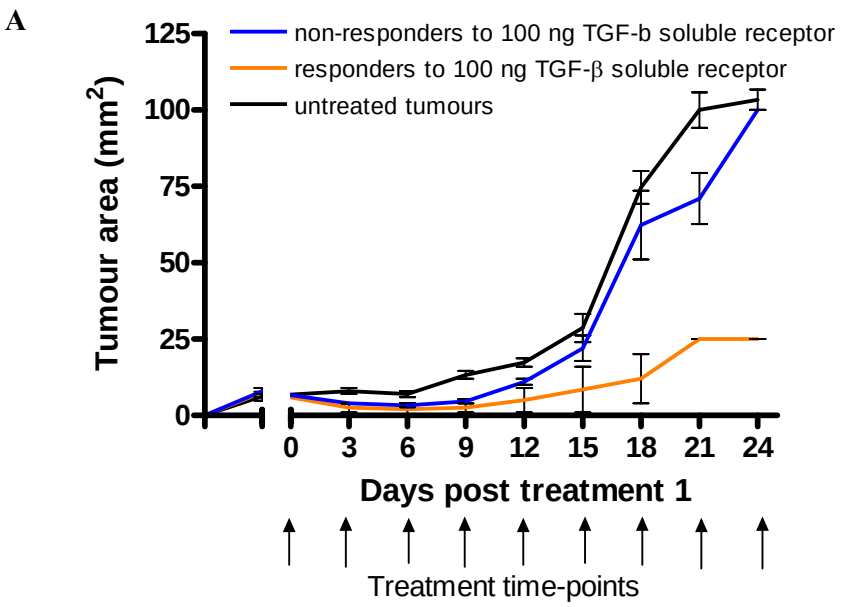
A
non-responders to 100 ng TGF-b soluble receptor
responders to 100 ng TGF-β soluble receptor
untreated tumours
Tumour area (mm2)
125
100
75
50
25
0
0 3 6 9 12 15 18 21 24
Days post treatment 1
Treatment time-points

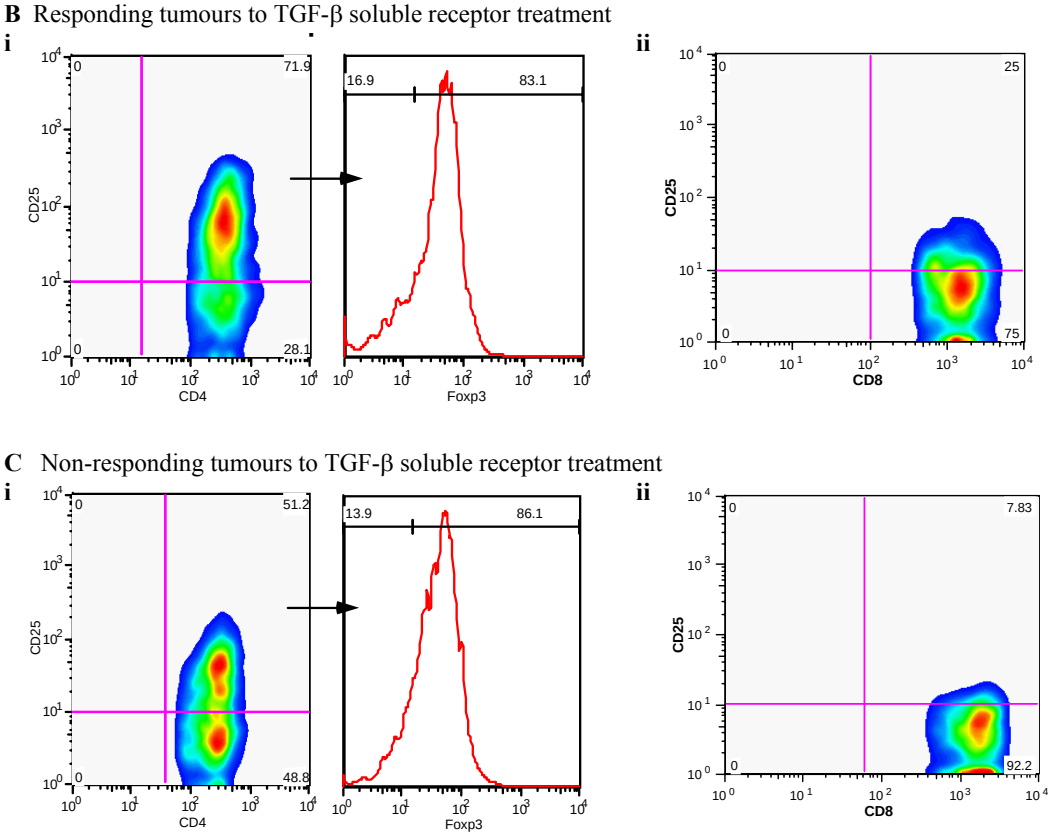
B Responding tumours to TGF-β soluble receptor treatment
i
ii
71.9
28.1
16.9
83.1
CD25
CD4
Foxp3
25
75
CD8
C Non-responding tumours to TGF-β soluble receptor treatment
i
ii
51.2
48.8
13.9
86.1
7.83
92.2

Figure 6.10: Inhibition of tumour growth by treatment with TGF-β soluble receptor is dependent on the activation of intra-tumoural CTLs.

Mice were implanted s.c. with 1 x 10^7 AE17 tumour cells. Treatment with TGF-β soluble receptor was initiated once tumours reached 9 mm^2. Treatment involved the administration of 100 ng TGF-β soluble receptor intra-tumourally every 3 days. Control tumours were left untreated. (A) Tumour growth was monitored regularly and tumour areas calculated. Tumours were removed from mice at day 24 and dissociated for flow cytometric analysis. Representative flow cytometric graphs are presented for (B) tumours that responded to TGF-β soluble receptor treatment and (C) Tumours that did not respond to TGF-β soluble receptor treatment with (i) $CD4^+CD25^+$ T_{reg} cells shown as a percentage of tumour-located $CD4^+$ T cells together with Foxp3 expression shown by intra-tumoural $CD4^+CD25^+$ T_{reg} cells and (ii) $CD8^+CD25^+$ T cells as a percentage of total tumour-located $CD8^+$ T cells. Data are the mean ± SEM for 3 untreated control tumours, 2 tumours that responded to TGF-β soluble receptor treatment and 3 tumours that did not respond to TGF-β soluble receptor treatment.

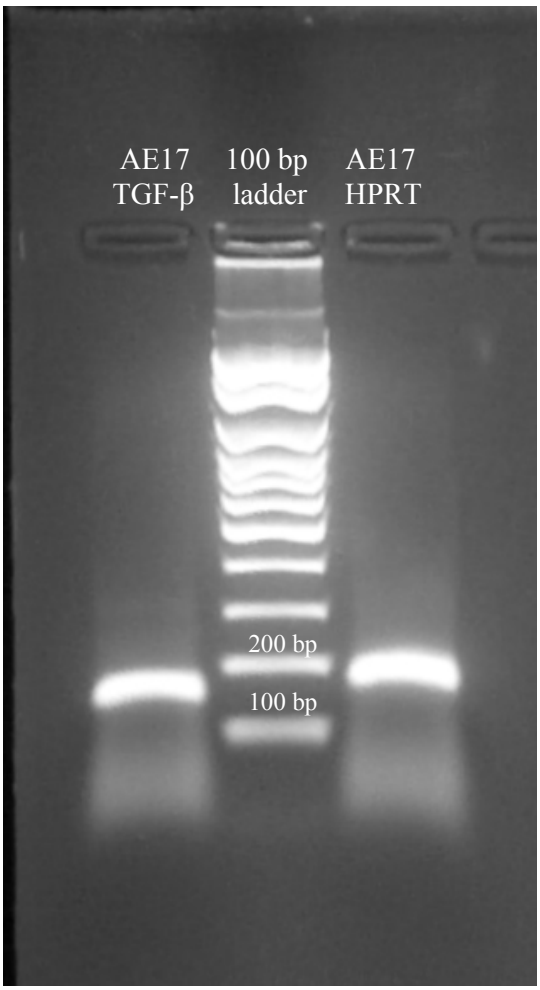

Figure 6.11: Agarose gel electrophoresis of AE17 tumour cell PCR products.

RNA was extracted from 1 x 10^7 AE17 cells prior to reverse transcription and PCR analysis for TGF-β and the HPRT house keeping gene. 10 µl of PCR product was mixed with 5 µl SEB dye and ran on a 2% agarose gel at 100 V for 30 min. A 100 bp DNA ladder was used to confirm product sizes.

6.2.4.3 Blockade of TGF-β does not prevent intra-tumoural T_{reg} cell conversion

In the previous experiment it was shown that the treatment of tumours with a TGF-β soluble receptor results in the release of anti-tumour $CD8^+$ CTLs from immunosuppression and subsequently, tumour growth inhibition. Murine AE17 tumours of 9 mm^2 treated intra-tumourally with 500 ng TGF-β soluble receptor every 3 days for 15 days were also analysed to determine the intra-tumoural percentage of $CD4^+$ T cells co-expressing CD25. Although the TGF-β soluble receptor had neutralised the majority of TGF-β naturally found within tumours, as determined by ELISA of fresh tumour lysates (Fig 6.12A), there was no difference in the intra-tumoural T_{reg} cell percentage between TGF-β soluble receptor treated and untreated tumours (Fig 6.12B). It therefore appeared that TGF-β was not required for the intra-tumoural conversion of T_{reg} cells in murine mesothelioma.

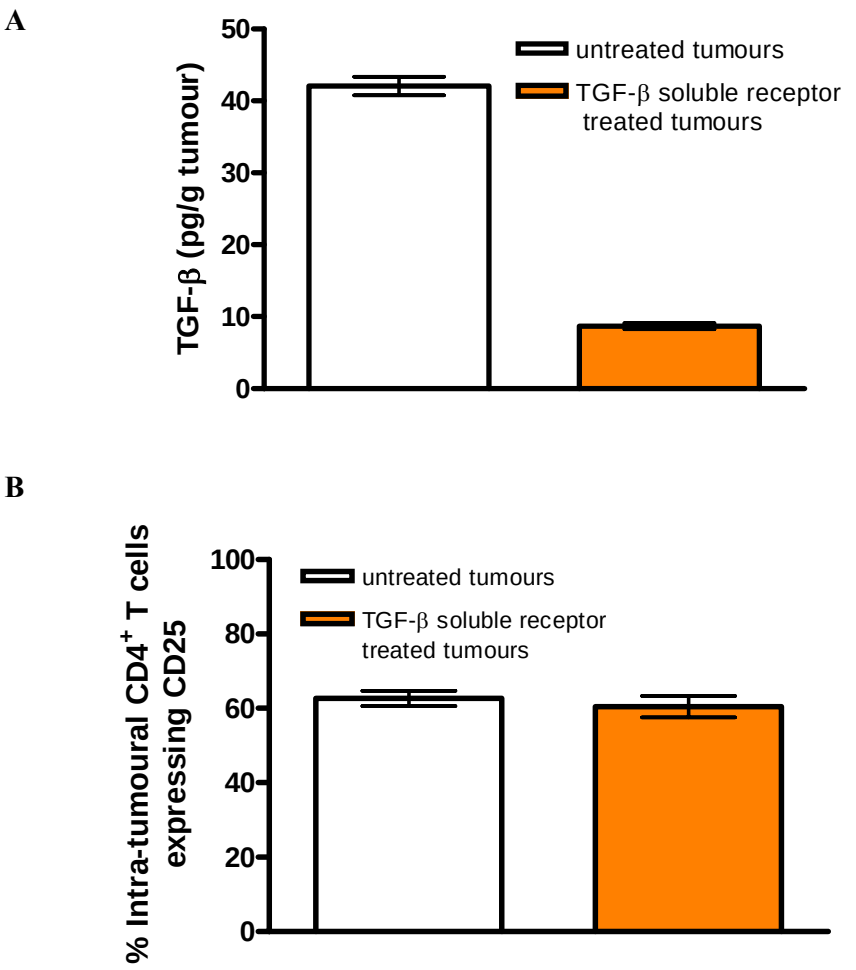

Figure 6.12: TGF-β blockade does not block the conversion of intra-tumoural T_{reg} cells.

Mice were implanted s.c. with 1 x 10^7 AE17 tumour cells. Tumours of 9 mm^2 were treated intra-tumourally with 500 ng TGF-β soluble receptor every 3 days for 15 days. Control tumours were left untreated. Tumours were then removed and samples taken from each tumour for (A) ELISA analysis of TGF-β concentration in tumour lysates and (B) flow cytometric analysis for the intra-tumoural percentage of $CD4^+$ T cells expressing CD25. Data are the mean ± SEM for 3 mice per treatment group.

6.2.5 Gene-chip analysis of novel markers

So far intra-tumoural T_{reg} cells had been demonstrated to be $CD4^+CD25^+Foxp3^+CD103^+CD69^{hi}CD62L^{lo}CTLA\text{-}4^{lo}Nrp\text{-}1^{lo}$ and had been shown to secrete high levels of IL-10 and TGF-β but little to no IL-4. Some mechanisms of action were beginning to be elucidated as anti-CD25 mAb treatment resulted in T_{reg} cell inactivation and the blockade of TGF-β did result in the release of $CD8^+$ CTLs from immunosuppression and tumour growth inhibition. To further understand the mechanism of action of intra-tumoural T_{reg} cells specifically, a global genechip analysis was conducted comparing natural T_{reg} cells isolated from the spleens of naïve mice to tumour-isolated, active T_{reg} cells. Thus any genes that were identified to be upregulated within the tumour T_{reg} cell subset would reflect the recruitment, selection or activation process of T_{reg} cells that were active at a tumour site. Any upregulated genes may then in the future be studied as more specific targets for therapies which will selectively target active tumour located T_{reg} cells rather than T_{reg} cells generally.

T_{reg} cells ($CD4^+CD25^+$) and their $CD4^+CD25^-$ T cell counterparts isolated by flow cytometric cell sorting from end-point (100 mm^2) murine mesotheliomas together with T_{reg} cells and their $CD4^+CD25^-$ T cell counterparts isolated from naïve spleens were shipped in RNAlater to the Mater Medical Research Institute, Qld, Australia, for gene expression profiling. Affymetrix GeneChip Mouse Genome 430 2.0 Arrays were used to profile the cells. The genechips allow for the analysis of over 39,000 transcripts, with two genechip analyses performed for each of the 4 samples.

6.2.5.1 Purity of cell populations and RNA extraction efficiencies

The cell populations analysed by genechip are outlined in Table 6.1 along with the cell numbers and purity following flow cytometric isolation. Figure 6.13 is a representative flow cytometric plot of the pre- and post-isolation percentage of T_{reg} cells from tumour samples. Pre-sort, R2 or the $CD4^+CD25^+$ T_{reg} cells represented only 1.86% of the total tumour cells (Fig. 6.13A). Post-sorting, the $CD4^+CD25^+$ T_{reg} cells represented 87.16% of the total cells in the sample (6.13B). Spectrophotometric amounts of total RNA were detected for three of the four samples (tumour isolated $CD4^+CD25^+$, tumour isolated $CD4^+CD25^-$ and spleen isolated $CD4^+CD25^+$. The amount of total RNA from the $CD4^+CD25^-$ from naive mice was undetectable. All samples were processed using

Affymetrix Two-Cycle Labelling Kit. Each sample was analysed on the multi-species Test3 genechip to confirm sample integrity and labelling efficiency prior to analysis using the Mouse Genome 430 2.0 Arrays.

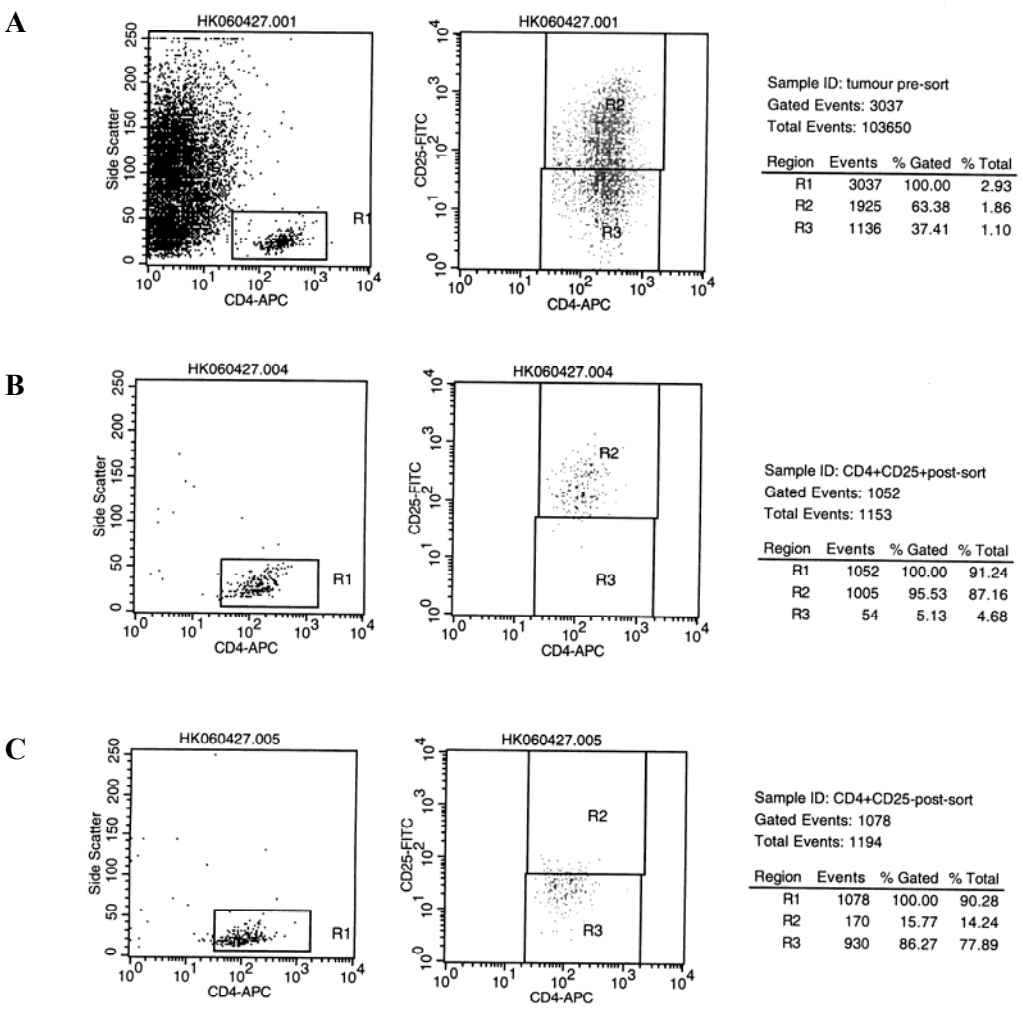

Figure 6.13: Representative FACS plot of T_{reg} cell purity pre- and post- flow cytometric sorting for T_{reg} cells from within murine mesotheliomas.

Mice were implanted s.c. with 1 x 10^7 AE17 tumour cells. Once tumours reached 100 mm^2 5 mice were sacrificed and tumours removed and pooled. (A) Tumours were dissociated and stained for cell surface CD4 (APC) and CD25 (FITC). The tumour cell homogenate was then sorted by flow cytometry and (B) the $CD4^+CD25^+$ and (C) the $CD4^+CD25^-$ populations collected. The collected populations were then analysed for purity and compared to1 (A) the pre-sort cell preparation. R1 represents the $CD4^+$ population with respect to total cells. R2 is the proportion of R1 ($CD4^+$ cells) that co-express CD25. R3 is the proportion of R1 that do not co-express CD25.

Table 6.1: Cell subsets analysed by genechip microarray along with corresponding purity.

Cell source	**Cell type**	**Cell number** (at 1 x 10^6/ml in RNAlater)	**Cell purity**
Naïve spleen	$CD4^+CD25^+$	3 x 10^5 cells	86%
	$CD4^+CD25^-$	1 x 10^6 cells	95%
Murine mesothelioma	$CD4^+CD25^+$	1 x 10^5 cells	95%
	$CD4^+CD25^-$	1x 10^5 cells	99%

6.2.5.2 Number of genes present and technical repeat capacity.

Naïve $CD4^+CD25^+$ T cells were chosen to demonstrate technical repeat capacity with the Affymetrix system. All four samples were subject to two independent labelling events from total RNA starting material. Labelled cRNA derived from naïve $CD4^+CD25^+$ T cells was also hybridised to two separate Mouse Genome 430 2.0 Arrays and considered as technical repeats. The R squared correlation between the two arrays, using only transcripts considered PRESENT, was 0.9643. Table 6.2 presents the genechip operating software call rates for gene presence detection. Naive $CD4^+CD25^-$ T cells had an elevated ABSENT call rate. This reflected the absence of detectable starting material. These samples were considered outliers and not included in the data analysis.

6.2.5.3 Differentially expressed genes between naïve and tumour-isolated T_{reg} cells

When comparing the gene expression between naïve $CD4^+CD25^+$ T_{reg} cells and tumour-isolated $CD4^+CD25^+$ T_{reg} cells it was found that several genes were very highly upregulated (Table 6.3). Interestingly, the most upregulated gene expressed differentially by tumour-located T_{reg} cells compared to naïve $CD4^+CD25^+$ T_{reg} cells was TGF-β (relative expression greater than 5). Other highly upregulated genes include the chemokine receptor CCR2 (relative expression of 4.6), the effector molecule Granzyme B (relative expression of 3.4) and CD103 the marker of T cell migration to inflamed sites (relative expression of 3.3). The most down-regulated genes between naïve $CD4^+CD25^+$ T cells and tumour isolated T_{reg} cells are heavy chain immunoglobulins (relative expression less than -7) (Table 6.4). Other down-regulated genes included CD62L/Sell (relative expression of -3.4) and Nrp-1 (relative expression of -2.5).

The 45101 Affymetrix probes were filtered for detectable expression in both $CD4^+CD25^+$ T cells isolated from naïve spleens and murine mesotheliomas and for greater than a four-fold difference in expression between the two sources. A total of 214 Affymetrix probes passed the filtering process, some probes targeted the same gene giving a total gene number under 214. One hundred probes showed a decrease in expression when extracted from murine mesotheliomas c.f. naïve spleens, 114 probes showed an increase. Probes were ranked by their gene ontology classifications of

biological process, molecular function and cellular component after a manual reduction of complexity in naming (i.e. "regulation of transcription, DNA-dependent" and "transcription" were both defined as "Transcription"). Some evidence exists for a bias gene ontology classification between the decreased and increased probe sets (data not shown). This suggests that $CD4^+CD25^+$ T cells extracted from murine mesotheliomas are actively communicating with surrounding cells, whilst simultaneously changing their profile of expression involving genes in the cell cycle and transcriptional activity.

In order to confirm the above gene-lists the T_{reg} cell populations were prepared again, sent to the MMRI and analysed. Despite some minor technical difficulties in the second run, the data sets produced in the first run and the biological repeat showed a high-degree of similarity (data not shown). Therefore the differential gene-list generated in the first run can be considered robust and indicative of the changes $CD4^+CD25^+$ T_{reg} cells undergo when changing from a naïve state to a stimulated state by exposure to tumour antigens.

Table 6.2: Genechip operating software call rates for gene presence detection

	Naive $CD4^+CD25^+$	Naive $CD4^+CD25^-$	Tumour $CD4^+CD25^+$	Tumour $CD4^+CD25^-$
#Probe Sets	45101	45101	45101	45101
#Present	15438	4289	13430	12171
#Absent	28992	40408	30981	32316
#Marginal	672	405	691	615

Table 6.3: Up-regulated genes differentially expressed by tumour-isolated T_{reg} cells compared to naïve T cells

Genes up-regulated greater than a relative expression of 2 were included in this table. Relative expression is equal to the $\log_2$(tumour expression/naïve expression). Unknown genes (e.g. RIKEN DNA) were excluded from this table but included in overall gene expression calculations.

Gene	Naive $CD4^+CD25^+$ Expression level	Tumour $CD4^+CD25^+$ Expression level	Relative expression	Public ID
TGF-β, induced	180.35	8281.7	5.5	BB533460
TGF-β, induced	160.6	5860.1	5.2	BB532080
CCR2	284.2	6934.75	4.6	BB148128
Lzp-s	418.85	7346.3	4.1	AV058500
Fgl2	381.95	6245.55	4.0	BF136544
CTLA-2a	1002.5	13100.15	3.7	NM_007796
Lgals3	643.85	8030.6	3.6	X16834
Lyzs	204.75	2426.55	3.5	AW208566
Lzp-s	1668.9	19633.4	3.5	AV066625
Maf	139.3	1579.1	3.5	AV284857
Pls3	107.5	1176.15	3.4	BC005459
GrzB	647.9	6784.8	3.4	NM_013542
Integrin αE (CD103)	1935.05	19741.15	3.3	AV210813
Gja1	506.3	4992.2	3.3	BB039269
Gja1	227.85	2213.2	3.3	BB142324
S100a4	4610.1	43564.05	3.2	D00208
S100a6	1631.85	14563.55	3.1	NM_011313
Iigp1	390.8	3297.9	3.1	BM239828
CCR5	201.25	1660.55	3.0	D83648
Iigp1	1043.6	8596.95	3.0	BM239828
CTLA-2a ///CTLA-2b	521.9	4212.75	3.0	NM_007796
Cul4a	515.65	4058.15	3.0	BC007159
CTLA-2b	462.15	3504.95	2.9	BG064656
Mrc1	96.65	731.1	2.9	NM_008625
Klrg1	2261.2	16994	2.9	NM_016970
Lmna	526.6	3879.5	2.9	NM_019390
Ifit1	377.6	2751.15	2.8	NM_008331
Anxa1	782.95	5565.15	2.8	NM_010730
Rai17	192.75	1330.75	2.8	BB164673
Glrx1	642.4	4411.45	2.8	AF276917
Kif2c	311.05	2092.25	2.7	BB104669
Sh3d19	89.1	597.8	2.7	NM_012059
Incenp	3349.65	21765.55	2.7	BB418702
Cul4a	684.6	4395.25	2.7	BC007159
Cpe	477.35	3047.4	2.7	BC010197
Runx2	415.05	2644.8	2.6	D14636
Lck	354.35	2242.6	2.6	AA867167
Dab2	144.7	891.5	2.6	NM_023118
Arl5	2702.4	16493.15	2.6	BG064956

Gene	Naive $CD4^+CD25^+$ Expression level	Tumour $CD4^+CD25^+$ Expression level	Relative expression	Public ID
Plec1	1877.6	10652.35	2.5	AW123286
Gcnt1	170.5	959.05	2.5	AK017462
Ccnb1-rs1 /// Ccnb1	617.3	3430.1	2.5	NM_007629
Cldn12	160.7	891.35	2.4	AW554231
CXCR3	1780.25	9720.05	2.4	NM_009910
Tcra	150.25	790.6	2.4	BB032962
Iigp2	677.45	3480.35	2.3	NM_019440
Lgals1	6687.35	34250.3	2.3	NM_008495
Osbpl3	494.25	2511.25	2.3	AK004768
Dgat1	1232.2	6240.4	2.3	BC003717
Tnfaip1	917.65	4645.95	2.3	AK004593
St3gal2	90.3	453.85	2.3	BB750118
Lmnb1	609.6	3043.05	2.3	BB152209
Lgals1	20005.95	99690.5	2.3	AI642438
CD151	448.6	2201.8	2.3	BB113673
Ddit4	6653.6	3174.95	2.3	AK017926
CCL5	2998.65	14403.9	2.2	NM_013653
Gja1	233.65	1119.85	2.2	AV330726
Ehd1	1799.05	8607.8	2.2	NM_010119
Gda	169.05	808.8	2.2	AW911807
Mx1	190.95	908.55	2.2	M21039
Anxa2	1767.95	8360.55	2.2	NM_007585
Arnt2	197.25	928.4	2.2	BQ174321
Icos	2452.9	11515.8	2.2	AB023132
Itgae	717.85	3368.05	2.2	NM_008399
Slc2a1	454.1	2127.45	2.2	BM209618
Cdc20	2549.8	11878	2.2	BB041150
Vim	5564	25633.45	2.2	AV147875
Gsn	1352.1	6208.8	2.2	AV025559
Atp13a2	611.7	2799.55	2.2	BM944122
Ifit3	483.55	2209.15	2.2	NM_010501
Thap7	484.15	2201.95	2.2	BM210680
Sca1	302.75	1363.4	2.1	BE852876
Neb	101.15	454.05	2.1	AI595938
Capza2	6124.3	27348.95	2.1	BI102231
Padi2	247.65	1094.95	2.1	NM_008812
Ifi205 /// Mnda	1425.4	6298	2.1	AI481797
Gsn	1205.9	5321.15	2.1	AV025667
Maf	3016.45	13287.5	2.1	AV323441
Ect2	252	1098.2	2.1	NM_007900
Tpi1	2121.7	9243.75	2.1	AA153477
Arl5	1136	4925.9	2.1	BB811124
Diap1	387.4	1678.05	2.1	BB408240
Ms4a11	460.65	1986.6	2.1	NM_026835
Trpv2	910	3873.65	2.1	NM_011706
Nfix	723.65	3056.25	2.1	AW049660

Gene	Naive $CD4^+CD25^+$ Expression level	Tumour $CD4^+CD25^+$ Expression level	Relative expression	Public ID
Entpd1	153.4	647.35	2.1	AV117919
Calmbp1	272.2	1135.5	2.0	NM_009791
Parp11	323	1342.7	2.0	BB026163
Mpa2l	2912.25	12097.4	2.0	BG092512
CD68	105.15	434	2.0	BC021637
Dnajc1	1161.35	4737.6	2.0	NM_007869
Incenp	144.95	590.4	2.0	AV301185

Table 6.4: Down-regulated genes between naïve and tumour-isolated T_{reg} cells

Genes down-regulated more than a relative expression of -2 were included in this table. Relative expression is equal to the $\log_2$(tumour expression/naïve expression). Unknown genes (e.g. RIKEN DNA) were excluded from this table but included in overall gene expression calculations.

Gene	Naive $CD4^+CD25^+$ Expression level	Tumour $CD4^+CD25^+$ Expression level	Relative expression	Public ID
Igh-VJ558	56650.95	315.45	-7.5	AK007826
Igh-VJ558	88212.5	549.9	-7.3	BC019425
Igh-VJ558	82499.85	600.6	-7.1	NM_134051
Igk-C /// Igk-V28 ///	83688.25	940.1	-6.5	BI107286
CD24a	8430.45	177.3	-5.6	NM_009846
Klf2	17593.95	458.25	-5.3	NM_008452
Igh-6	78123.8	2144.4	-5.2	AI326478
Rhob	6046.3	278	-4.5	BC018275
Tsc22d3	8498.5	493.95	-4.1	AF201289
Dusp10	3729	307.85	-3.6	NM_022019
Igk-C /// Igk-V28 ///	45282.8	4159.85	-3.5	BC013496
Btg2	3162.1	308.65	-3.4	NM_007570
Sell	8854.55	876.65	-3.4	M36005
CD83	7106.35	812.65	-3.2	NM_009856
Myd116	5777.05	702.05	-3.1	NM_008654
Dnajb9	7875.55	1034.75	-3.0	NM_013760
Btg2	4412.95	543.6	-3.0	NM_007570
CXCR4	6257.1	792.45	-3.0	D87747
Rnu22	7269.75	949.7	-3.0	BQ177137
Ssbp2	3138.35	438.8	-2.9	NM_024186
Rnu22	2073.55	296	-2.8	BQ177137
Rab3ip	1936.6	281.4	-2.8	BF319015
Igk-C /// Igk-V28 ///	26767.85	3957.4	-2.8	AV057155
CD96	6015.4	939.5	-2.7	NM_032465
Ifrd1	7244.9	1170.9	-2.7	NM_013562
Klf6	1390.35	210.05	-2.7	NM_011803
Klf4	8265.1	1250	-2.7	BG069413
Igk-V8	3728	576.85	-2.7	BF159226
Lef1	2609.25	417.5	-2.7	AV156352
Xbp1	4540.5	767.8	-2.6	NM_013842
Ctse	3365.6	571.35	-2.6	NM_007799
Sell	5983.7	1008.35	-2.6	M36005
Irf2bp2	8438.05	1431.1	-2.6	BB183385
Plac8	9608.6	1560.75	-2.6	AF263458
Tagap1	6278.9	1121.15	-2.5	BM220475
Itm2a	6198.45	1081.55	-2.5	BI966443
Sfrs7	2189.15	392.85	-2.5	BE825013
Wdr56	2348.65	414.15	-2.5	BC013814
Ptp4a1	6310.25	1120.95	-2.5	BC003761
Igh-6	95326.1	17145.85	-2.5	BB226392

Gene	Naive $CD4^+CD25^+$ Expression level	Tumour $CD4^+CD25^+$ Expression level	Relative expression	Public ID
Centd1	3656.5	669.35	-2.5	AV375176
Copeb	9091.65	1665.9	-2.5	AV025472
Pde7a	1865.75	341.35	-2.5	AU015378
Nrp-1	6346.15	1157.45	-2.5	AK011144
CD79b	2060.75	409.15	-2.4	NM_008339
Emb	2688.9	522.5	-2.4	BG064842
Txndc5	3027.95	563.7	-2.4	BC016252
Nme1	11171.55	2124.5	-2.4	AV156640
CD69	10916.5	2137.85	-2.4	AK017979
Jun	9196.7	1846.95	-2.3	NM_010591
CD1d1	3668.1	738.15	-2.3	NM_007639
Ier5	7937.45	1687.7	-2.3	BF147705
Ga17	3669.75	759.45	-2.3	BC005598
Hist1h1c	18703.7	4086	-2.2	NM_015786
Xbp1	2887.45	644.35	-2.2	C77390
Dnajb1	1057	237.1	-2.2	AK002290
Prkcq	4209.2	943.4	-2.2	AB062122
Bhlhb2	5649.55	1323.65	-2.1	NM_011498
CD1d1	1065.1	254.5	-2.1	NM_007639
Atf4	4374.05	1069.1	-2.1	M94087
Etv3	1544.95	356.4	-2.1	BI456953
Bcl2l11	6884.95	1676.6	-2.1	BB667581
Bteb1	1955.55	452.8	-2.1	AW488885
Zfhx1a	2180.65	500	-2.1	AV363000
Slc25a30	724.8	176.35	-2.1	AV000840
Txnip	9638.9	2250.25	-2.1	AF173681
Rnf19	3673.65	845.55	-2.1	AF120206
TNFαip3	28977.4	7343.2	-2.0	BM241351
Foxp1	2840.45	719.9	-2.0	BM220880
Axud1	5090.5	1264.3	-2.0	BG070296
Dnaja1	4889.45	1211.25	-2.0	BF141076
Ets2	3632	903.8	-2.0	BC005486
Pim3	12415.8	3124.6	-2.0	BB206220

6.3 Discussion

CTLA-4 has been shown to be constitutively expressed by T_{reg} cells but varying frequencies of CTLA-4 expression have been reported. Intensities of staining are generally quite low and may reflect the varying staining protocols (cell surface or intracellular) used by different research groups. By flow cytometry, the expression of CTLA-4 in this tumour model was shown to remain consistent perhaps implicating its involvement in both early and late stage tumours. Nrp-1 and CD69 were both shown to increase in expression on intra-tumoural T_{reg} cells as tumours grow. Although Nrp-1 and CD69 both appear to be expressed on freshly isolated T_{reg} cells the utility of Nrp-1 or CD69 for the isolation of T_{reg} cells from activated T cells has not been ascertained (62). *In vivo* CTL assays may be used in the future to determine the importance of each of these molecules for T_{reg} cell function in the murine model of mesothelioma.

One of the biggest factors negatively affecting T_{reg} cell research and T_{reg} cell functional analysis such as *in vivo* CTL assays is the difficulty in obtaining pure populations of sorted T_{reg} cells. The work of Raimondi *et al* (2006) may improve this in the future. They discovered a marker, PD1, almost exclusively expressed on activated T cells and absent from T_{reg} cells. This could be used during purification of T_{reg} cells by negative selection if determined to be appropriate in this tumour model. The bonus of negative selection/specific removal of activated $CD4^+$ T cells from the total $CD4^+CD25^+$ T_{reg} cell population is that it minimises the risk of altering T_{reg} cell function by direct manipulation. Foxp3 has already been ruled out for the positive selection of T_{reg} cells due to its nuclear location. CD62L and CD103 have been shown in this study to be useful and specific T_{reg} cell markers of migration and so the binding of antibodies to these markers on T_{reg} cells for T_{reg} cell isolation for use in downstream *in vivo* CTL assays may adversely affect T_{reg} cell function (62). In conjunction with PD-1, LAG-3 may be used to improve the purification of T_{reg} cells for further functional and phenotypic analysis such as gene-chip. LAG-3 is known to be expressed by stimulated T_{reg} cells but not resting/quiescent T_{reg} cells (233, 234). Isolation of T_{reg} cells based on the expression of CD4, CD25, PD-1 and LAG-3 could be appropriate to elucidate three important populations: resting T_{reg} cells ($PD\text{-}1^-$), activated T_{reg} cells ($PD\text{-}1^+LAG\text{-}3^+$) and activated T cells ($PD\text{-}1^+LAG\text{-}3^-$).

Other issues with a functional analysis of T_{reg} cells is the complexity of the T_{reg} cell response as evident by this research. T_{reg} cells do not work in isolation when suppressing effector cells but undergo important interactions with dendritic cells at multiple sites of immune activity such as lymph nodes and in the tumours themselves. These interactions can not be easily replicated in *in vitro* systems. Lastly with regards to functional analyses in the case of mesothelioma the specific tumour antigens, be that self antigens or a tumour-associated antigens are unknown. This makes analysing tumour specificity of T_{reg} cells difficult. To overcome this, several neo-tumour antigen expressing murine mesothelioma models have been developed including AE17-sOVA (ovalbumin) and AB1-HA (haemagglutinin). These models could be employed to investigate the tumour specificity of T_{reg} cells but they are based on the expression of a highly dominant immuno-peptide. Studies in our lab (data not shown) using the AE17-sOVA model showed that the OVA peptide is perhaps both too dominant and too foreign to mount an immune response similar to that seen in the original AE17 cells and effector T cells against OVA can not be suppressed by T_{reg} cells from AE17-sOVA tumours in *in vivo* CTL assays.

Should a specific marker of mesothelioma be identified in the future and hence the antigen of T_{reg} cell specificity, there is increasing new evidence that *in vivo* CTL assays can be performed. Mesothelin is a differentiation antigen which has been shown to be present on normal mesothelial cells and over-expressed in several human tumours, including mesothelioma, may be a useful starting marker for future CTL studies in this model (235). At present the determination of mesothelin levels in serum is being used as a marker for the diagnosis of mesothelioma and to monitor disease progression (6). Interestingly, mesothelin has been identified in pancreatic cancers where it has been shown that $CD8^+$ T cell responses can be induced to multiple HLA-A2, A3, and A24 restricted mesothelin epitopes (236). In a recent study it was found that T_{reg} cells need to be transferred two days prior to effector cells in order to allow them enough time to become activated and antigen specific so they are actively able to suppress the transferred effector T cells (personal communication: Diego Silva, ANU, Australia). This research group also showed that tumour specific T_{reg} cells may not need to be required for transfer but that naive T_{reg} cells put into a tumour bearing mouse may become educated and activated in the periphery to be antigen specific. An interesting Nature paper published earlier this year also importantly showed that T_{reg} cells must

stably interact with DCs in order to become suppressive (required in those extra two days *in vivo*) by the two-photon scanning laser microscopic analysis of transferred T_{reg} cells and resident DCs (237). There is therefore a future for *in vivo* functional assays of T_{reg} cells but they need to be carefully designed.

As expected, cytokine profiling demonstrated T_{reg} cells located intra-tumourally secrete high levels of IL-10 and TGF-β but low levels of IL-4. The importance of TGF-β to active intra-tumoural T_{reg} cells was confirmed by both global genechip analysis and the TGF-β neutralising experiments discussed later. Global genechip analysis did not suggest an up- or down-regulation of IL-10 or IL-4 by intra-tumoural T_{reg} cells. This could suggest an equivalent level of mRNA expression between tumour-located T_{reg} cells and naïve splenic T cells of the same phenotype and that IL-4 and IL-10 are not required for the action of T_{reg} cells at a tumour site. The attempts to block IL-10 intra-tumourally did not appear to block T_{reg} cell function and hence did not result in tumour growth inhibition as expected by the work of Seo *et al* 2001. This may suggest that there is some redundancy in the T_{reg} cell system. T_{reg} cells have multiple mechanisms of activation and suppression depending on the environment and disease situation they are in. It may be the case that if one such mechanism is interrupted another is employed. This complexity would also not be evident if studying T_{reg} cells within an *in vitro* system. The potential redundancy of T_{reg} cell mechanisms of action is discussed further in the next chapter.

While attempting to answer the question "where do the intra-tumoural T_{reg} cells come from?" it was discovered that there is an initial drop (as a percentage of total cells) in $CD4^+$ T cells in the spleen and lymph nodes of tumour bearing mice 14 days post tumour challenge. This drop in peripheral $CD4^+$ T cells is also matched by a drop in peripheral $CD4^+CD25^+$ T_{reg} cell numbers at this early stage of tumour development. 14 days post tumour challenge is the time at which tumours become palpable and when a distinct population of $CD4^+CD25^+$ T_{reg} cells becomes resident within tumours suggesting a recruitment of T_{reg} cells from the periphery.

The observed drop in the peripheral $CD4^+$ T cell percentage at day 14 post tumour challenge was also accompanied by an observed change in the phenotype of T_{reg} cells. There was a change in phenotype of T_{reg} cells from $CD62L^+CD103^{lo}$ in the blood to

$CD62L^{lo}CD103^{lo}$ in the LN to $CD103^{+}CD62L^{lo}$ in tumours suggestive of a change in expression levels with location and hence migration of T_{reg} cells from the periphery to the tumour and hence to the site of immune regulation. Several groups have subdivided $CD4^{+}CD25^{+}$ T_{reg} cells into two groups based on the expression of L-selectin/CD62L. Those cells found to express high levels of CD62L were shown to be more suppressive *in vivo* (68-70) and to have a superior capacity to home to lymph nodes (71, 72). CD62L has now also been suggested as a marker capable of delineating activated effector cells from T_{reg} cells in tumour-draining lymph nodes (73). Integrin $\alpha_E\beta_7$/CD103 on the other hand was shown to divide the $CD4^{+}CD25^{+}$ T_{reg} cells into two subsets the $CD103^{+}$ and $CD103^{-}$ (47). A subsequent global gene expression study found that the $CD25^{+}CD103^{-}$ T_{reg} cells displayed a naïve-like phenotype with high expression of CD62L while the $CD103^{+}$ T_{reg} cells showed an activated phenotype as they expressed lower levels of CD62L and high levels of CD44 (72). In terms of migratory ability, the expression of CD103 was necessary for the homing of T_{reg} cells to the site of *Leishmania major* infection in mice (80). Studies of the inactivation of T_{reg} cells based on the expression of CD62L or CD103 by monoclonal antibody treatment could be performed in the future to further study the roles of CD62L and CD103 in the recruitment or trafficking of T_{reg} cells into tumours. A further marker of T_{reg} cell trafficking/migration, CD44, has also been suggested as a means of subtyping $CD4^{+}CD25^{+}$ T_{reg} cells and may also be useful in future studies of intra-tumoural T_{reg} cell recruitment. An inactive form of CD44 is highly expressed on resting lymphocytes but after being conformationally activated ($CD44^{act}$) can bind to its ligand (hyaluronan) on microvascular endothelium and result in extravasation (82). Further examination of $CD4^{+}CD25^{+}$ T_{reg} cells expressing the $CD44^{act}$ has found them to be more suppressive compared to $CD4^{+}CD25^{+}$ T_{reg} cells expressing CD44 in the unactivated form (81).

This observed drop in peripheral total $CD4^{+}$ T cells and $CD4^{+}CD25^{+}$ T_{reg} cells at the same time as the recruitment of $CD4^{+}CD25^{+}$ T cells into murine mesotheliomas correlated well with the findings of Curiel *et al* (2004) that T_{reg} cells preferentially move to and accumulate in tumours as they progress as a result of the secretion of the chemokine CCL22 by tumour cells and/or tumour-derived macrophages. Although recruitment of T_{reg} cells from the periphery seemed clear, the stimulus for recruitment was still unknown. The fact that intra-tumoural treatment with multiple doses of anti-CCL22 mAb significantly increased the tumour growth rate of murine

mesotheliomas suggested that the mAb treatment may in fact be targeting anti-tumour effector cells hence allowing for uncontrolled tumour growth. It is important to note that since experiments with anti-CCL22 mAb were conducted for this chapter it was revealed that CCL22 is also a chemokine that induces the migration of activated $CD8^+$ T cells (58). This revelation was reported by members of Curiel's own group and certainly complicated the interpretation of Curiel's work and the studies presented here that were based on the initial Curiel *et al* (2004) publication.

At the early time-points of tumour development only a low percentage of intra-tumoural $CD4^+$ T cells were found to be $CD25^+$. Over time and as tumours grow a higher proportion of intra-tumoural $CD4^+$ T cells coexpressed CD25. It may be the case that as tumours grow $CD4^+CD25^+$ T_{reg} cells are selectively recruited to tumours. Alternatively, based on the studies of Ghiringhelli *et al* (2005) it could be postulated that this initially small population of intra-tumoural T_{reg} cells selectively proliferates due to TGF-β secretion by tumour induced DCs to result in the much larger population observed in larger, late stage tumours (130). Finally, the large increase in CD25 expression by intra-tumoural T_{reg} cells as tumours grow may result from the combination of initial recruitment of T_{reg} cells followed by the conversion of $CD4^+CD25^-$ T cells into T_{reg} cells within the tumour.

From earlier studies it seemed that CD103 was important in the function or T_{reg} cells at the site of immune regulation. Interestingly, CD103 is a TGF-β inducible surface integrin (238). As CD103 appeared to be important in the murine mesothelioma tumours it was proposed that TGF-β may play an important role in the recruitment or induction of $CD103^+$ T_{reg} cells in tumours but may also be mediating the conversion of naïve $CD4^+CD25^-$ T cells into T_{reg} cells. Although only preliminary and requiring confirmation it was initially shown by utilising a TGF-β soluble receptor that TGF-β does not induce the conversion of T_{reg} cells within murine mesothelioma tumours as evident by no change in the intra-tumoural T_{reg} cell compartment following treatment with the TGF-β soluble receptor. The failure to observe the role of TGF-β in intra-tumoural T_{reg} cell conversion may be attributed to (a) only measuring T_{reg} cell conversion at a single time-point at the end of the experiment, (b) the peripheral recruitment of T_{reg} cells into tumours as they grow may be a sufficient mechanism to

induce tumour immune evasion in the absence of conversion or (c) a more complex interaction between the tumour, DCs and T_{reg} cells may be occurring that was not examined in these experiments.

It is becoming increasingly clear that T_{reg} cells can not be studied in isolation as their interactions are complex and hence the induction of immunosuppression is also complex. To this end, it has been shown that the promotion of T_{reg} cell conversion from naïve T cells might involve other factors including TCR costimulation, the IL-2R and DCs (232). Specifically, TGF-β may be important for the differentiation of tolerogenic (Tol)-DCs most likely in tumour-draining LNs where antigen is presented. The effect of TGF-β on T_{reg} cell conversion may not be evident by the analysis of intra-tumoural T_{reg} cells and future studies should examine populations of T_{reg} cells in tumour-draining LNs and also examine the role of TGF-β on Tol-DC differentiation.

The maintenance of DCs in an immature or tolerogenic state by tumour induced T_{reg} cells may constitute an additional mechanism of tumour immune evasion (130, 239). Murine $BCR^{-}ABL^{+}$ leukaemia derived T_{reg} cells can suppress bone marrow-derived DC maturation and function by down-regulating the activation of NFκB in DCs. This inhibitory mechanism requires cell-to-cell contact and involves both TGF-β and IL-10 and is associated with the induction of the Smad intracellular signalling pathway and the activation of the signal transducer and activator of transcription 3 (STAT3) transcription factor. The inhibited DCs lose their ability to stimulate anti-tumour T cells. Fully differentiated and mature DCs are insensitive to the suppressive effects of T_{reg} cells. It is becoming clear that T_{reg} cells from tumour bearing mice are capable of maintaining DCs in an immature/tolerogenic state during the early stages of the induction of an anti-tumour immune response (240-242). These Tol-DCs can induce effector T cell anergy but more interestingly are involved in the generation of more T_{reg} cells. Such a positive feed-back loop by which Tol-DCs induce T_{reg} cells that in turn enhance immunosuppression could contribute to the persistence of tumour induced tolerance and hence tumour immune evasion.

What was clear from the studies utilising the TGF-β soluble receptor was that TGF-β is necessary for T_{reg} cell function as the blockade of this cytokine lead to reduced tumour

growth and the activation of $CD8^+$ CTLs. The neutralisation of TGF-β in these experiments did not result in the direct depletion of the intra-tumoural T_{reg} cells as seen post anti-CD25 mAb treatment. In fact, the treatment with the TGF-β soluble receptor appeared to increase the expression of Foxp3 by intra-tumoural T_{reg} cells. This is likely to be the result of the increase in intra-tumoural IL-2 within tumours after the activation of $CD8^+$ CTLs with this treatment. IL-2 is required to maintain activated anti-tumour effector T cells but has also been shown to maintain the survival and suppressive function of T_{reg} cells within mice (243).

100 ng of the TGF-β soluble receptor was however shown to be only marginally effective at inhibiting tumour development. 100 ng is likely to be the lower threshold of the effective dose and depending on slight variations in tumour growth kinetics may not quite be enough to induce the neutralisation of TGF-β and hence tumour growth inhibition (responders). TGF-β receptor type II (the membrane bound form of the soluble TGF-β receptor II used in this study) has been detected at elevated levels on effector T cells once they have been activated through their TCR (244). Although confirmation of this experiment is still required, it is likely that the soluble receptor used in this experiment mops up the TGF-β secreted by T_{reg} cells or has saturated the T_{reg} cell membrane-bound TGF-β thereby blocking the immunosuppression of effector T cells. Also in confirmation of the effect of TGF-β blockade on activated effector T cells, it has been found in mice with T cell restricted expression of a dominant negative form of the TGF-β receptor II that there is an accumulation of activated T cells and these mice succumb to autoimmune disease by 12 weeks of age (245). But how does TGF-β directly effect anti-tumour $CD8^+$ effector T cells such that they can still accumulate in tumours but fail to exert a CTL function? There is now evidence that T_{reg} cells interfere with $CD8^+$ CTL responses relatively early in tumour development (246). It was found that T_{reg} cells neither influenced $CD8^+$ T cell proliferation nor the commitment of recently activated CTLs to secrete inflammatory cytokines but that $CD8^+$ CTLs failed to undergo normal functional maturation when in the presence of T_{reg} cells. The expression of the TGF-β receptor by $CD8^+$ CTLs was required for their cytotoxicity and as such there may be a specific role for TGF-β signalling in the inhibition of cytotoxicity. Although TGF-β blockade did result in tumour growth inhibition in most mice and did release anti-tumour $CD8^+$ CTLs from

immunosuppression, not all mice were protected and complete tumour regression did not occur suggesting TGF-β may not be the sole mediator of T_{reg} cell function. Future experiments will need to be conducted to optimise the most effective dose and treatment regime for TGF-β soluble receptor treatments. These future experiments must address the direct effect of TGF-β neutralisation on tumour cells. Autocrine TGF-β signalling is operative in some tumour cells and can contribute to tumour invasiveness and metastases (247). TGF-β blockade on its own is reasonably effective at inhibiting tumour development but like anti-CD25 mAb administration alone did not result in complete tumour regression. A combination therapy of TGF-β blockade and anti-CD25 mAb inactivation should be trialled in the future and may improve treatment efficacy.

It was clear that $CD4^+CD25^+$ T_{reg} cells were active within tumours and their intra-tumoural inactivation via anti-CD25 mAb or TGF-β soluble receptor treatment resulted in the release of anti-tumour CTLs from immunosuppression. There was still an interest in the identification of further activation markers of tumour-specific activated T_{reg} cells. By global genechip analysis several expected genes were found to be upregulated including TGF-β and CD103. Several novel markers which could be associated with T_{reg} cell function were also identified to be upregulated.

Granzyme B (GrzB) has been identified as a potentially key component of T_{reg} cell mediated immunosuppression as the induction of regulatory activity has been correlated with the up-regulation of GrzB expression by T_{reg} cells and the subsequent induction of apoptosis in $CD4^+CD25^-$ effector T cells (134). Proof of a functional involvement of GrzB in contact-mediated suppression by T_{reg} cells was shown by the reduced ability of T_{reg} cells from $GrzB^{-/-}$ mice to suppress as efficiently as T_{reg} cells from WT mice. In a separate study designed to identify genes that were specifically expressed by T_{reg} cells in a Foxp3-dependent or independent manner DNA microarray analysis found that natural $CD4^+CD25^+$ T_{reg} cells expressed GrzB but that $CD4^+CD25^-$ T cells retrovirally induced to express Foxp3 did not express GrzB (248). A recent review by Sakaguchi and Yamaguchi commented that GrzB may be an important mediator of the tumour specific T_{reg} cell response but that the role of GrzB had not yet been confirmed in tumour models (249). Future studies in the murine model of mesothelioma could utilize a soluble receptor for GrzB to confirm its role in tumour immunosuppression.

Lymphocyte protein tyrosine kinase (Lck) is another potential T_{reg} cell activation marker. It is becoming increasingly clear that the efficient generation of T_{reg} cells in the thymus requires CD28 costimulation. In a study which investigated the molecular mapping of CD28 costimulation it was shown that T_{reg} cell generation requires a motif that binds Lck (250). This motif is precisely the same motif that is required for CD28 costimulation of IL-2 production. Future analysis of the chemokine (C-C motif) receptor 2 (CCR2) may also reveal interesting insights into the function of intra-tumoural T_{reg} cells. CCR2 has been shown to be expressed on T_{reg} cells in mice with collagen induced arthritis (251). Purified $CCR2^+$ T_{reg} cells were found to be fully anergic toward polyclonal and collagen-specific activation and could potentially suppress activation of other T and B cells. This subpopulation of $CCR2^+CD25^+$ T_{reg} cells were shown to increase ~5-fold in the progression phase of the disease, while CCR2 expression on other leukocyte populations remained unchanged. Finally, $Foxp3^+$ T_{reg} cells have been shown to express high levels of fibrinogen-like protein 2 (Fgl2) mRNA. Recombinant fibrinogen-like protein 2 has been shown to be capable of suppressing *in vitro* T cell responses and may be an important molecule for T_{reg} cell function in tumours (252).

The last molecules of interest identified in the global genechip analysis performed here have not yet been shown to have any direct link to T_{reg} cells. They are however linked to activated T cells and hence may be important molecules for future studies. Cytotoxic T lymphocyte associated protein-2 alpha (CTLA-2α) is expressed by activated T cells (253). Galectin-3 (lectin, galactose binding, soluble 3, Lgals3) is a member of a large family of B-galactoside-binding animal lectins and has been shown to be upregulated in proliferating cells, suggesting a possible role for this lectin in regulation of cell growth (254). Finally, several lysozyme genes including soluble lysozyme (Lyzs) and p-structural lysozyme (Lzp-3s) were identified to be unregulated. It has been suggested that polysaccharides, glycoproteins and glycolipids of the cell membrane can be bound to lysozyme in a substrate-specific way. This has led to the hypothesis that lysozyme has a regulatory function in membrane-dependent cellular processes and in protection against membrane abnormalities associated with neoplastic transformation (255, 256).

To confirm the differential expression of these genes found to be specifically upregulated by intra-tumoural T_{reg} cells compared to naïve, splenic T cells of the same

phenotype a real-time RT-PCR could be developed with specific primers for each of the genes of interest and HPRT as a house keeping gene. Alternatively, flow cytometry could be used to confirm the expression of these genes at the protein level. Finally, the effects of these genes *in vivo* can be analysed. Blocking antibodies could be used against the CD103 marker, or a soluble receptor could be used to mop up the effect of GrzB. Real-time RT-PCR validated genes could also be targeted by gene-specific, anti-sense, morpholinos oligonucleotides. These morpholinos anti-sense oligonucleotides are stable in intra-peritoneal delivery to mice, disperse widely via the lymphatics and represent a new approach to anti-sense oligonucleotide inhibition of specific genes (257, 258).

Although it was now clear that T_{reg} cells were involved in tumour immune evasion, neither T_{reg} cell inactivation via anti-CD25 mAb treatment alone or the blockade of T_{reg} cell function via TGF-β soluble receptor treatment alone were able to completely inhibit tumour growth or result in complete tumour regression. The final chapter of this thesis undertook an initial examination of a multi-modality cancer treatment as a potentially more effective therapy as it is becoming increasingly clear that T_{reg} cells do not act in isolation and perhaps simply inactivating T_{reg} cells may not be sufficient to mount an effective anti-tumour immune response. Indeed in this context the lower percentages of intra-tumoural T_{reg} cells found in B16 melanomas and EL4 lymphomas would suggest that the extent to which T_{reg} cells contribute to tumour immune evasion will vary from tumour to tumour (opcit Chapter 4, Section 4.2.2).

Chapter 7:
The development of multi-targeted approaches for the treatment of murine mesothelioma

7.1 Introduction

The early, successful attempts to inactivate $CD4^+CD25^+$ T_{reg} cells resulted in the failure of tumours to grow and involved the systemic administration of anti-CD25 mAb prior to tumour challenge (29, 156, 157). On several occasions it was found that the anti-tumour effect of anti-CD25 mAb administered before tumour inoculation was no longer seen if the treatment was given on day 0 (the day of tumour implantation) or thereafter. This thesis has provided evidence that the intra-tumoural recruitment, selective proliferation and/or conversion of $CD4^+CD25^+Foxp3^+$ T_{reg} cells constitutes an immune evasion mechanism in the murine model of mesothelioma. The work has demonstrated a strong correlation between tumour size and percentage of $CD4^+CD25^+Foxp3^+$ T cells within the murine mesotheliomas. It is suggested that the increase in T_{reg} cells within the small murine mesotheliomas allows the evasion of the host anti-tumour effector immune response leading to increased tumour growth. In addition, it has been shown in this thesis that tumours of the same size have similar percentages of T_{reg} cells regardless of the initial inoculum used to create the tumours. Together these results suggest that as a tumour reaches a particular size (~9 mm^2) T_{reg} cells are recruited, selectively proliferated and/or converted and the anti-tumour immune response is suppressed resulting in rapid tumour growth. It followed therefore, that if T_{reg} cells are intra-tumourally suppressing effector cells targeted against the tumour, their intra-tumoural inactivation should lead to increased anti-tumour immunity. The suppressive *in vivo* functioning of $CD4^+CD25^+Foxp3^+$ T_{reg} cells within murine mesotheliomas was demonstrated by the intra-tumoural inactivation of these cells using anti-CD25 mAb (or a soluble TGF-β receptor) resulting in marked inhibition of established tumour growth.

Neither the anti-CD25 mAb nor TGF-β soluble receptor treatment experiments presented in the previous chapters resulted in complete tumour regression. It appeared that the efficient targeting of tumours and hence the induction of tumour regression may require a multi-targeted approach to overcome the complexity of the T_{reg} cell response and the potential redundancy in the system. A combination of the removal of suppression on anti-tumour effector cells combined with effector cell "boosting" may provide a more effective treatment for solid tumours. In this chapter, preliminary work focusing on (i) T_{reg} cell inactivation combined with the blockade of T cell costimulation

and (ii) T_{reg} cell inactivation combined with the induction of apoptosis in tumour cells is presented.

Combinations of mAb therapies targeted at multiple aspects of the anti-tumour immune response, and specifically the T_{reg} cell response have been trialled in the past but often involved the pre-treatment of mice prior to tumour challenge. The major costimulatory molecule on T cells is CD28. CTLA-4 is a costimulatory molecule which shares the ligands of CD28 (CD80 and CD86) and down-regulates T cell responsiveness (87). Several mechanisms have been proposed to account for the inhibitory effect of CTLA-4 and were recently reviewed by Zheng *et al* 2006 (259). Because the affinity of CTLA-4 for B7 is greater than the affinity of CD28 for B7, CTLA-4 may out compete CD28 for B7 binding sites on APCs. Tryptophan catabolic products that inhibit T cell activation are induced by CTLA-4 along with TGF-β production which is specifically induced by the cross-linking of cell surface CTLA-4. Intra-cellular CTLA-4, on the other hand, can localise to the immunological synapse and interfere with TCR signalling. It follows therefore that if CTLA-4 can act as a negative regulator of the immune response, the blockade of CTLA-4 should release the immune response from immunosuppression. In a study of the efficacy of a whole tumour cell based vaccine in B16-BL6 murine melanoma development it was found that there was improved efficacy in the vaccine when coupled with the disruption of immune regulation (87). Specifically it was found that there is synergy between CTLA-4 blockade using an anti-CTLA-4 mAb and T_{reg} cell inactivation via the administration of anti-CD25 mAb when combined with vaccination. In this study however, treatment with the anti-CD25 mAb was administered 4 days prior to tumour challenge and is hence not a realistic treatment for human disease.

In a second tumour study, it was found that a combination of anti-GITR mAb combined with anti-CD25 mAb administered i.v. at day 8 post tumour challenge resulted in a reduced efficacy to inhibit tumour development compared to the anti-GITR mAb alone (29). Like CTLA-4, glucocorticoid induced tumour necrosis factor receptor (GITR) is considered to be constitutively expressed by T_{reg} cells but can be expressed by other T cells at a high level upon activation. The physiologic role of GITR is to control T cell activation (reviewed by (260)). GITR is activated by GITR-L on APC with costimulation of effector T cells and partial abrogation of T_{reg} cell activity. The

mechanism underlying T_{reg} cell suppression may however not directly involve GITR and GITR-L but may modulate APC functional status. When GITR is activated by agonistic anti-GITR mAb costimulation of responder cells is enhanced while the suppressor function of T_{reg} cell is completely abrogated resulting in a more efficient anti-tumour response (89). It may therefore be the case that pathologically low levels of GITR-L on APC or high levels of soluble GITR protein might result in an under stimulation of GITR and underlie the decreased immune responses seen in tumours. The anti-GITR mAb results in the cross-linking/agonism of the GITR molecule and abrogates T_{reg} cell suppression (131). Interestingly, a combination of anti-GITR mAb with anti-CTLA-4 mAb administered i.v. 12 days post tumour challenge resulted in increased tumour growth inhibition compared to either antibody alone at this later treatment time-point. Similar to these studies, it was found by our own laboratory that an improved disease outcome results during MAIDS infection when mice are treated i.p. with a combination of anti-CD25 mAb, anti-CTLA-4 mAb and anti-GITR mAb (107). Although in this study the combination of mAbs resulted in a better outcome than either mAb administered alone, treatment was begun 2 days prior to viral challenge. The efficacy of the intra-tumoural administration of a combination of anti-CD25 mAb, anti-CTLA-4 mAb and anti-GITR mAb into small but established tumours in tumour growth inhibition of murine mesotheliomas was investigated in this chapter.

Finally, the potential combination of T_{reg} cell inactivation with apoptosis induction in tumour cells was explored. The anti-neoplastic and pro-apoptotic effects of alpha-tocopheryl succinate (α-TOS), an analogue of vitamin E (VitE), have been shown in numerous studies both *in vitro* and *in vivo* (163, 164, 261-266). Interestingly, α-TOS has been reported to specifically target tumour cells, including mesothelioma cells, while remaining mostly non-toxic to other cells of the host (163, 262, 266, 267). α-TOS has a detergent like property which results in lysosomal destabilisation and release of pro-apoptotic proteins particularly at low pH (265). Although the exact reason behind the cancer cell specificity is still unknown, it is believed that the low internal pH of cancer cells and the higher than normal generation of reactive oxygen species (ROS) by cancer cells may increase the membrane destabilising properties of α-TOS (268). The Beilharz laboratory therefore proposed a potentially synergistic approach to the treatment of established malignant mesothelioma tumours based on increasing the

anti-tumour effector immune response by the inactivation of intra-tumoural T_{reg} cells using the anti-CD25 mAb coupled with the induction of apoptosis of the tumour cells via systemic treatment with α-TOS. Unlike the anti-CD25 mAb treatments investigated in this thesis, the intra-tumoural administration of α-TOS is not possible. α-TOS is suggested to only be effective as an anti-cancer agent when administered i.p. due to the specific effects of its metabolism on its efficacy (reviewed in (269)). In fact, the intra-tumoural delivery of α-TOS was suggested to result in the precipitation of α-TOS out of solution (personal communication: Assoc. Prof. Jiri Neuzil, Griffith University, Australia). As such, the approach taken in this chapter is the established i.p. route of delivery.

7.2 Results

7.2.1 Multi-targeted approach to blocking T_{reg} cell function

A combined approach to blocking T_{reg} cell function by directly targeting the T_{reg} cells with anti-CD25 mAb but also disrupting costimulation via the treatment with anti-CTLA-4 and anti-GITR mAbs was trialled.

7.2.1.1 The efficacy of blocking a single T_{reg} cell functional marker.

T_{reg} cells are considered to constitutively express CTLA-4 although often at a low level. This was also confirmed by our own data in this murine model of mesothelioma presented in Chapter 6. This constitutive expression suggests CTLA-4 is important for T_{reg} cell function at both early and late time-points of tumour development. Direct cell-to-cell contact between T_{reg} cells and effector cells has been suggested to be mediated by CTLA-4 as CTLA-4 and CD28 are both homologues that can bind to B7 with opposing functions. CD28 co stimulates T cells while CTLA-4 inhibits T cell activation (229). The blockade of CTLA-4 by anti-CTLA-4 mAb should therefore block T_{reg} cell function and result in tumour growth inhibition. Eight mice were implanted with 1 x 10^7 AE17 tumour cells. Once tumours reached 9 mm^2 5 mice were treated intra-tumourally with 0.03 mg anti-CTLA-4 mAb solution (38 µl of a 0.1 mg/120 µl stock). This intra-tumoural dose of anti-CTLA-4 mAb solution was

estimated to represent approximately 1/3 of the published systemic doses of the mAb (87, 270). Tumour growth was then monitored daily and tumours areas calculated in comparison to 3 untreated control tumours. The treatment of tumours with a single intra-tumoural dose of anti-CTLA-4 mAb did not result in tumour growth inhibition (Fig. 7.1).

A similar result was also found when tumours were treated with an anti-GITR mAb. GITR controls T cell activation and so the activation of GITR by an agonistic anti-GITR mAb should abrogate T_{reg} cell function. Again 8 mice were implanted with 1 x 10^7 AE17 tumour cells prior to treatment with 0.1 mg anti-GITR mAb (42.5 µl of a 1 mg/425 µl stock) administered intra-tumourally to tumours of 9 mm^2. This antibody dose was also estimated to be equivalent to approximately 1/3 of the published doses used for systemic treatment of mice with a protein G purified mAb solution (29, 271). Again no inhibitory effect on tumour growth was observed as a result of anti-GITR mAb treatment (n = 5) when compared to untreated control tumours (n = 3) (Fig. 7.2).

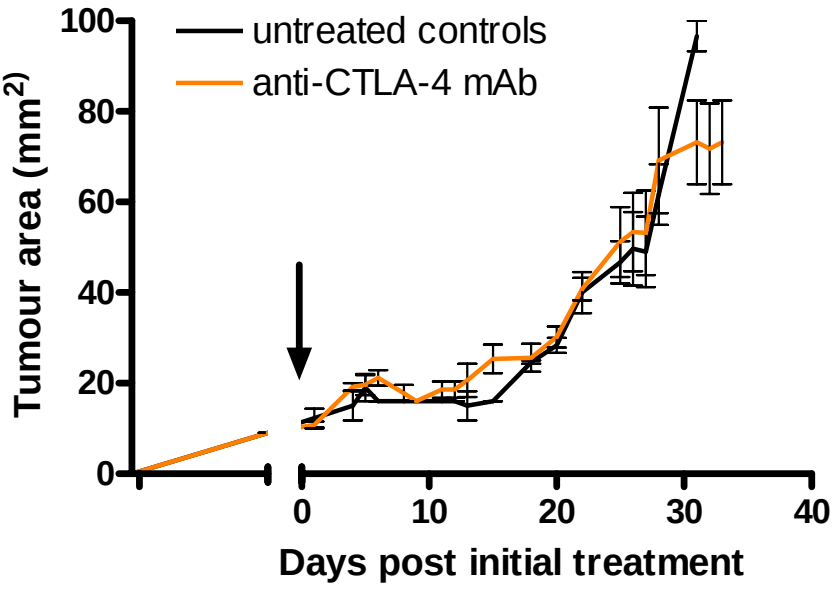

Figure 7.1: Blocking T_{reg} cell function by intra-tumoural anti-CTLA-4 mAb treatment

Mice were implanted with 1 x 10^7 AE17 murine mesothelioma cells. Mice were treated with a single intra-tumoural 0.03 mg dose of anti-CTLA-4 mAb solution when tumours reached 9 mm^2. Control tumours were left untreated. Tumour growth was monitored regularly and tumour areas calculated by multiplying two, right-angled tumour diameters measured using microcallipers. Data are the mean ± SEM of 5 treated tumours and 3 untreated tumours.

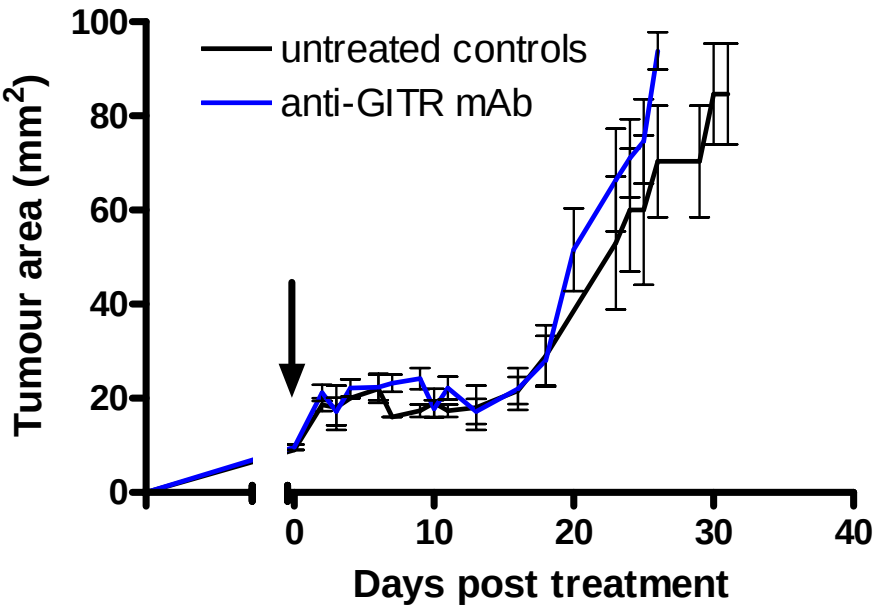

Figure 7.2: Blocking T_{reg} cell function by intra-tumoural anti-GITR mAb treatment

Mice were implanted with 1 x 10^7 AE17 murine mesothelioma cells. Mice were treated with a single intra-tumoural 0.1 mg dose of anti-GITR mAb solution when tumours reached 9 mm^2. Control tumours were left untreated. Tumour growth was monitored regularly and tumour areas calculated by multiplying two, right-angled tumour diameters measured using microcallipers. Data are the mean ± SEM of 5 treated tumours and 3 untreated tumours.

7.2.1.2 Combined anti-CD25 mAb, anti-CTLA-4 mAb and anti-GITR mAb treatments.

The individual mAbs against CD25, CTLA-4 and GITR were mixed at the appropriate ratio such that after concentration using microconcentrator columns a 40 µl intra-tumoural delivery volume would comprise 0.15 mg of anti-CD25 mAb, 0.1 mg of anti-GITR mAb and 0.03 mg of anti-CTLA-4 mAb. Mice were then implanted with 1×10^7 AE17 tumour cells. Mice were treated intra-tumourally with a single 40 µl volume of the concentrated mixed mAb solution when tumours reached 9 mm^2. Control mice were left untreated. Figure 7.3 is the combined results of two individual experiments comprising a total of 8 mice treated with the mAb combination and 8 untreated controls. Up to day 10 post treatment there was no obvious effect of the mAb combination on tumour development such that there was no increase or decrease in tumour growth kinetics. From day 10 onwards however it became clear that some mice (4/8) were responding very well to the treatment with almost complete tumour regression observed by day 15 post treatment while the remaining 50% of the treated animals had tumour growth kinetics matching the untreated controls. The mice that responded positively to the treatment had regressed tumours which remained virtually non-palpable for the entire period of experimentation (38 days for the one mouse with a tumour reduced to approximately 2 mm^2 in size and almost 4 months for the remaining 3 mice with completely regressed tumours).

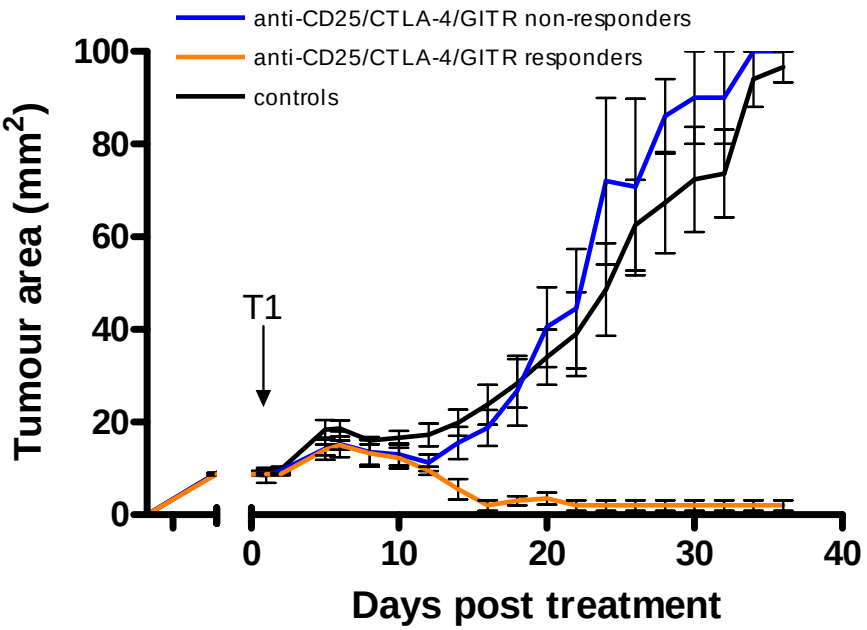

Figure 7.3: Combined approach to blockade of T_{reg} cell function.

Mice were then implanted with 1 x 10^7 AE17 tumour cells. Mice were treated intra-tumourally with a single 40 µl volume of the concentrated mAb solution comprising 0.15 mg of anti-CD25 mAb, 0.1 mg of anti-GITR mAb and 0.03 mg of anti-CTLA-4 mAb when tumours reached 9 mm^2. Control mice were left untreated. Tumour growth was monitored regularly and tumour areas calculated. Data are the mean ± SEM of 8 untreated control mice, 4 mice which responded to treatment with the combination of mAbs and 4 mice which did not respond to the same treatment.

7.2.2 A bimodal approach to tumour growth inhibition – apoptosis induction combined with T_{reg} cell inactivation.

Currently, there is a lack of *in vivo* studies of the anti-neoplastic effects of α-TOS in immuno-competent tumour models. In a study of intra-peritoneal human malignant mesothelioma (MM) xenografts in nude mice, mice treated with α-TOS were found to survive three times longer than control mice which succumbed to tumour burden between 5 and 7 weeks post tumour inoculation (164). This same study also confirmed the ability of α-TOS to specifically target malignant cells by showing non-malignant mesothelial cells to not undergo apoptosis when challenged with α-TOS. Later investigations of α-TOS found an additional effect of this substance to down-regulate fibroblast growth factor receptor-1 (FGFR1) on the surface of human MM cells (163). This receptor has been shown to be involved in cancer cell proliferation and tumourigenesis and the effect of α-TOS on FGFR1 offers an additional mechanism α-TOS may use to inhibit MM progression. Based on current evidence, α-TOS seemed worthy of further investigation (32). However, it must be recognised that these studies promoting the anti-neoplastic effects of α-TOS were carried out using immuno-compromised animal models and xenografted tumours that are not representative of the clinical situation. For this reason, we first investigated the anti-tumour efficacy of α-TOS on established AE17 murine mesotheliomas in immuno-competent, syngeneic hosts.

7.2.2.1 α-TOS induces apoptosis in murine mesothelioma cells in vitro.

Apoptosis induction in AE17 cells was determined by Annexin V staining as previously described (164). α-TOS concentrations of 25 or 50 μM α-TOS added as an ethanol solution to cells that were 60-70% confluent resulted in a dose dependent induction of apoptosis that increased with the length of time the cells were exposed to the drug (personal communication, Assoc. Prof J. Neuzil, Griffith University, Australia) Apoptosis was induced in the murine mesothelioma cells by α-TOS (Fig. 7.4). It was therefore concluded that α-TOS should be tested *in vivo* for its ability to inhibit established murine mesothelioma growth in syngeneic and immuno-competent C57BL/6J mice.

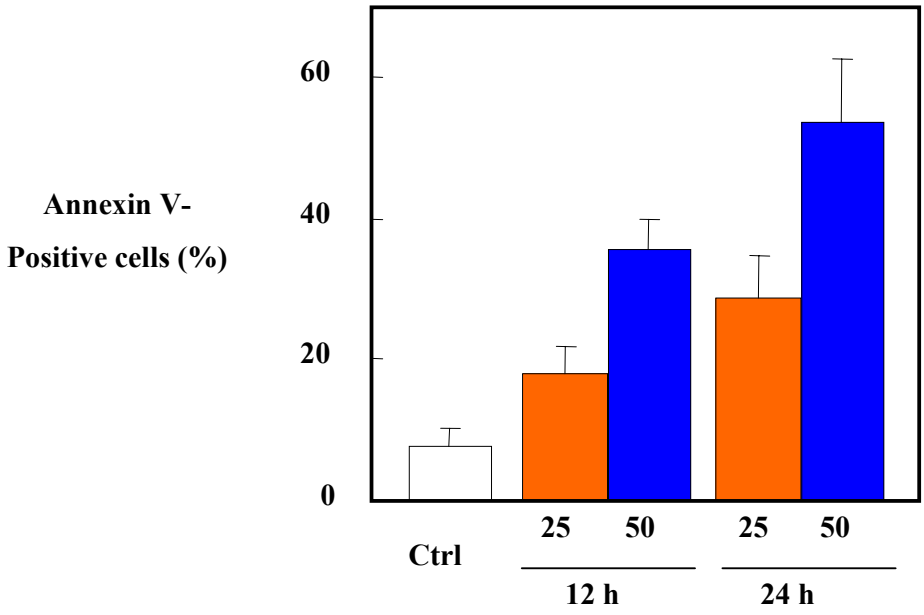

Figure 7.4: Apoptosis induction in AE17 cells by α-TOS *in vitro*.

α-TOS concentrations of 25 or 50 μM α-TOS were added as an ethanol solution to AE17 cells that were 60-70% confluent in tissue culture. Apoptosis induction was determined by Annexin V binding at 12 and 24 hrs post treatment with α-TOS and compared to cells treated with ethanol alone.

7.2.2.2 The toxic effect of 100 µl of a 200 mM solution of α-TOS in C57BL/6J mice.

The survival of athymic nude mice implanted with human mesothelioma cells was significantly increased by i.p. treatment of the mice every third day with 100 µl of a 200 mM solution of α-TOS resuspended in DMSO (164). We therefore sought to investigate the effects of α-TOS within the AE17 model system which is significantly closer to human application. Eight 10 week old C57BL/6J mice were implanted sub-cutaneously (s.c) with 1 x 10^7 AE17 mesothelioma cells. Tumour growth was monitored daily and treatment with α-TOS initiated once tumours reached 9 mm^2. α-TOS was resuspended in DMSO at a concentration of 200 mM α-TOS and stored at 4°C. α-TOS was thawed and vortexed to ensure resuspension prior to treatment. Four mice received 100 µL of the 200 mM α-TOS solution intra-peritoneally (i.p) while 4 control mice received 100 µL i.p. of DMSO only. This initial treatment with the previously published dose of α-TOS (164) was poorly tolerated by all mice, while the mice treated with DMSO alone showed no effects. The mice treated with α-TOS were noted to suffer immediate ataxia in the hind limbs, drowsiness and were hunched and ruffled for up to 24 hours post treatment. The mice seemed to recover and resumed close to normal behaviour by day 3 post treatment. A second treatment was administered three days post the first and was again detrimental to the mice. Indeed, the paralysing effects were so severe that all mice required humane culling within 30 min of this second α-TOS treatment due to a complete loss of condition as regulated by our institutional Animal Ethics Committee. No tumour growth data could therefore be collected for this experiment. As severe side effects had been noted in this first experiment using the previously published dose of α-TOS, we tested lower doses of α-TOS in order to achieve a dose which could be tolerated by immuno-competent mice.

Tumour-free C57BL/6J mice were used to test the toxicity of both a 50 mM and 100 mM solution of α-TOS in 100 µl DMSO administered i.p every 3rd day. One mouse each was used to test a 100 µl dose of the 50 mM and 100 mM α-TOS solutions. The mice again showed immediate ataxia which was more noticeable in the hind-leg on the side of the peritoneum into which the α-TOS solution was injected. Within 1 hour this seemed to settle, but both mice were slowed and often sat huddled and ruffled for up to 24 hours. The mice then seemed to recover and resumed close to normal behaviour before the next treatment was administered 3 days later. It was found that

subsequent treatments did not affect mice as negatively as the first, but were increasingly well tolerated with time and multiple treatments such that both mice began to resume close to normal movement within 4 hours of treatment. As a result of this experiment it was decided to test the efficacies of both the 50mM and 100 mM solutions of α-TOS resuspended in DMSO to inhibit tumour growth in the murine model of mesothelioma.

7.2.2.3 100 µl of 100 mM and 50 mM α-TOS solution has little effect on murine mesothelioma development and is limited by severe side effects.

C57BL/6J mice were again implanted s.c with 1 x 10^7 AE17 mesothelioma cells. Treatment with α-TOS was initiated once tumours reached 9 mm^2. 5 mice received 100 µl of 100 mM α-TOS in DMSO i.p while 3 control mice received 100 µl of DMSO only. Tumour areas were calculated daily. Subsequent treatments were administered in the same manner every 3rd day. One α-TOS treated mouse was culled as a result of an adverse reaction to this first treatment. Only 4 mice treated with α-TOS tolerated the treatments and were hence included in the analysis of the effect of α-TOS on tumour development. Again ataxia and drowsiness were observed in the α-TOS treated mice while no adverse effects were noted in the DMSO treated control mice. Figure 7.5A depicts the tumour growth inhibition observed as a result of α-TOS treatment compared to DMSO only. No difference in the tumour growth rate was observed between the α-TOS and DMSO treated groups until after treatment 4 was administered 9 days post treatment initiation. Tumour regression was not observed as a result of the α-TOS treatment, however, some slowing of tumour growth was observed as α-TOS treated animals reached the humane endpoint of 100 mm^2 at day 27 post treatment 1 compared to day 15 post treatment 1 in the DMSO treated control group.

Interestingly, it was again observed that mice receiving α-TOS treatment became tolerant over the course of the experiment to the α-TOS with a reduction in post injection effects. As some inhibitory effect on tumour growth was seen, it was decided to repeat the experiment and include a 50 mM dosage and to treat at 2 day intervals. The reduction from 3 day treatment intervals to 2 days was reasoned to maintain a more constant level of α-TOS exposure. C57BL/6J mice were implanted s.c. with 1 x 10^7 AE17 tumour cells. Treatment with α-TOS was initiated once tumours reached 9 mm^2.

5 mice received 100 µl of 100 mM α-TOS i.p. every second day while 5 mice received 100 µl of a 50 mM solution of α-TOS administered in the same way. 3 control mice were treated with 100 µl of DMSO only. Figure 7.5B shows that in this experiment neither of the treatment regimes tested had any inhibitory effect of tumour growth. In addition to this, severe toxicity of α-TOS was again noted for a minority of mice (2/5 for each treatment group) at both of the tested concentrations.

The mice affected most severely by α-TOS treatment in the above experiment (n = 4, 2 from each treatment group) were further examined post humane culling and compared to 2 control mice treated with DMSO alone. α-TOS treated mice which showed adverse effects to the treatment had a white, sticky substance between the skin and peritoneum at the location of the injections. DMSO mice did not have this same deposition suggesting it represented an effect of α-TOS. When the peritoneum was opened, the organs of α-TOS treated mice were observed to be fused together and to the inner surface of the peritoneum. This fusion of organs was dose dependent with greater fusion observed in mice treated with the 100 mM solution compared to the 50 mM solution of α-TOS. This pathology was not observed in mice treated with DMSO alone. Also, upon autopsy, it was found that the spleens of these severely effected α-TOS treated mice were enlarged to approximately twice the size and also seemed to have lost structural integrity compared to the spleens of the DMSO treated mice. The ill health of the mice treated with α-TOS was also characterised by their loss of appetite correlated with the emptiness of their stomachs and intestines. DMSO treated mice appeared to have normal appetites as their stomachs were observed to be full.

Finally, the only clear difference between this study and the studies published in the past examining the effect of α-TOS on tumour development is our use of a syngeneic tumour cell line and its implantation into fully immuno-competent mice. We therefore examined the splenic population of total T cells within murine mesothelioma-bearing mice in our model and investigated whether α-TOS had any effects on them. 3 spleens from mice treated with DMSO only, 3 spleens from mice treated with the 50 mM α-TOS solution and 3 spleens from mice treated with the 100 mM α-TOS solution were compared for total T cell percentages by flow cytometry. Figure 7.6 shows that there is a dose dependent loss of total T cells ($CD3^+$) in the spleens of mice treated with α-TOS. Given these severe effects on treated mice coupled to a lack of tumour growth

inhibition, the plans to combine α-TOS treatment with intra-tumoural T_{reg} cell inactivation were abandoned.

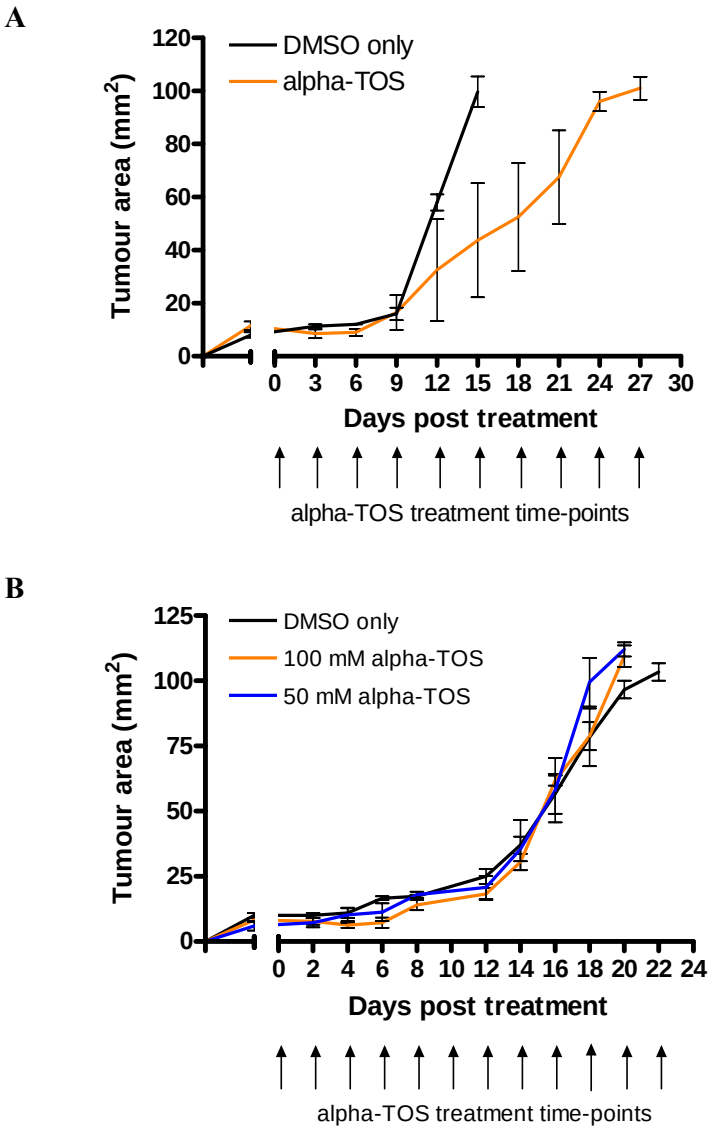

Figure 7.5: The effect of α-TOS on murine mesothelioma development *in vivo*.

C57BL/6J mice were implanted s.c with 1 x 10^7 AE17 mesothelioma cells. Treatments were initiated once tumours reached 9 mm^2 (day 0). Tumour areas were calculated by multiplying two, right-angled tumour diameters measured using micro-callipers. (A) Mice received 100 µl of 100 mM α-TOS i.p or 100 µl of DMSO only every three days. (B) Mice received 100 µl of 50 mM or 100 mM α-TOS i.p or 100 µl of DMSO alone every two days. Data are the mean ± SEM of (A) 4 α-TOS treated mice and 3 DMSO treated control mice and (B) 5 α-TOS treated mice per group and 3 DMSO treated control mice.

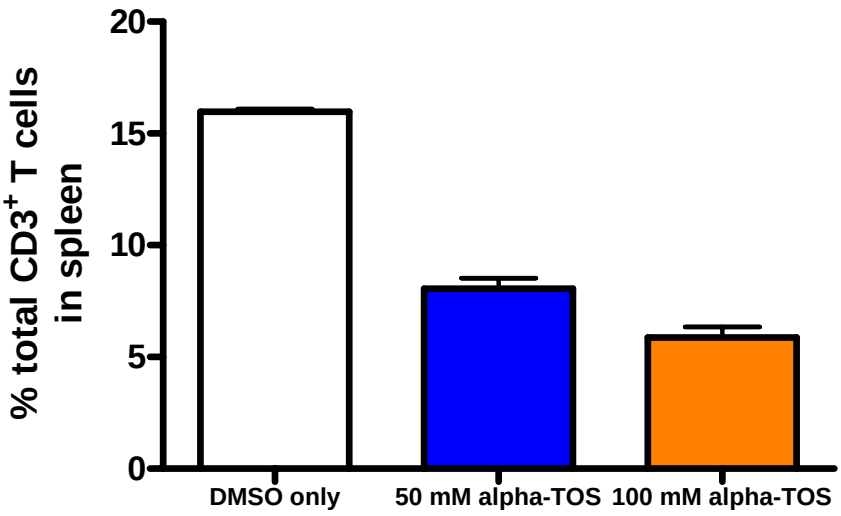

Figure 7.6: Effects of α-TOS on T cells in immuno-competent mice.

Spleens were removed from α-TOS treated and DMSO only treated mice, dissociated and stained for flow cytometric analysis of total T cells ($CD3^+$). Data are the mean ± SEM of 3 mice per group.

7.3 Discussion

It is clear from published literature that multi-targeted approaches to T_{reg} cell inactivation and effector cell boosting can not only be effective but may also be optimal. Initial experiments in this chapter investigated the efficacy of combining anti-CD25 mAb treatment with anti-CTLA-4 and anti-GITR mAb treatments.

In terms of T_{reg} cell development and function it has now been shown that TGF-β can induce the expression of CTLA-4 by $CD4^+CD25^-$ T cells. CTLA-4 ligation of CD80 is hence needed along with TGF-β early after T cell activation to induce the conversion of $CD4^+CD25^-$ T cells into $CD4^+CD25^+Foxp3^+$ T_{reg} cells (259). Specifically, it has been shown that the blockade of CTLA-4 function during the first 24 hours post T cell stimulation can also block the ability of TGF-β to induce Foxp3 expression (259). This may explain the inability to inhibit tumour development when anti-CTLA-4 mAb was used to treat 9 mm^2 murine mesothelioma tumours in this experiment at approximately 5-7 days post tumour implantation. Similarly no effect on tumour growth was seen when tumours were treated intra-tumourally with a single dose of anti-GITR mAb alone. GITR is strongly up-regulated for several days in both $CD4^+$ T cells and $CD8^+$ T cells following T cell activation but is expressed constitutively at high levels by T_{reg} cells (92). The fact that the single anti-GITR mAb treatment used in this chapter was administered only 4-7 days post tumour challenge may mean that the mAb had also targeted important anti-tumour effector cells that had recently upregulated GITR following T cell activation in response to tumour challenge. This should have however had a positive result on the anti-tumour response as the treatment should have stimulated the GITR expressing effector T cells to render them resistant to immunosuppression. Future treatments with either of these mAbs may need to be timed more appropriately to target and block T_{reg} cells specifically or to target effector T cells in a positive manner. Alternatively, like the lack of anti-tumour effect seen in mice treated with intra-tumoural anti-IL-10 mAb, it may be the case that the blockade of CTLA-4 or GITR alone may not be sufficient to block T_{reg} cell function. Some level of redundancy may exist where a second mechanism of T_{reg} cell suppression is employed if another is blocked. By combining anti-CD25 mAb with anti-CTLA-4 and anti-GITR mAb treatments multiple pathways of Treg cell suppression may be inactivated resulting in an improved therapy and tumour regression.

The intra-tumoural combined treatment of tumours in the murine model of mesothelioma with anti-CD25 mAb, anti-GITR mAb and anti-CTLA-4 mAbs showed much promise and requires further investigation. The fact that tumours completely regressed in 50% of treated mice after only one treatment while other tumours were not affected at all is intriguing. As discussed above it was recently suggested that the most appropriate time for the blockade of CTLA-4 function is within 24 hours of T cell activation. Perhaps the later treatment time-point used in this experiment (approximately day 5-7 post tumour challenge) resulted in the inconsistent results such that some mice are fully protected and others are not (259). GITR is strongly up-regulated for several days in both $CD4^+$ T cells and $CD8^+$ T cells following T cell activation but is expressed constitutively at high levels by T_{reg} cells (92). The fact that the combined mAb treatment used in this chapter was administered only 4-7 days post tumour challenge may mean that the mAb had also targeted important anti-tumour effector cells that had recently upregulated GITR following T cell activation in response to tumour challenge. The mAbs used in these experiments were ammonium sulphate precipitated only. As such their concentrations in these experiments may not be sufficiently high. That is, it might be the case that the mAb concentrations used in these experiments were at the lower end of the efficacy threshold. The varying tumour growth kinetics known to occur in individual mice in this murine mesothelioma model may mean that the doses were not quite sufficient in each case to induce tumour regression. The fact that some mice were protected from tumour growth and in fact showed regression from 9 mm^2 to impalpable, or at least too small to be measured using accurately with the micro-callipers, following the combined mAb treatment suggests that a multi-targeted approach maybe effective. In fact, this combined mAb treatment resulted in the complete regression of tumours for up to four months at which time the experiment was terminated and all mice humanely culled. Future experiments could therefore focus on the delivery of a larger and more sustained amount of mAb, for example at 3 day intervals. It was interestingly noted by Ko *et al* (2005) that the combination of anti-GITR mAb with anti-CD25 mAb had a reduced effect on tumour growth inhibition compared to treatment with either mAb alone. Future work should also determine the level of systemic versus local effect of this combined treatment efficacy as Ko and colleagues suggests the anti-CD25 mAb delivered in his system (which was systemic) resulted in the inactivation of effector T cells also (29).

Finally the potential of combination of T_{reg} cell inactivation and apoptosis induction was explored. Apoptosis was induced in the murine mesothelioma cells by α-TOS as expected by published studies examining the effect of α-TOS on human mesothelioma cells lines. It was therefore concluded that α-TOS should be tested *in vivo* for its ability to inhibit established murine mesothelioma growth in syngeneic and immuno-competent C57BL/6J mice. The α-TOS dosage employed in these experiments was derived from published work examining the effect of α-TOS on human mesotheliomas or colon cancers xenografted onto athymic nude mice (164). Neither of these studies commented on toxicity, in fact, the authors comment "that α-TOS is a non-toxic anti-neoplastic". *In vitro* studies published by the same group reported that while α-TOS is a potent inducer of apoptosis in malignant mesothelial cells it is largely non-toxic to normal cells and tissues (163, 164, 261, 262). It has been proposed that the resistance of non-malignant cells to the toxic effects of α-TOS may be due to their lower capacity to generate ROS and/or their more efficient anti-oxidant system (262).

The side effects observed in the α-TOS treated mice (ataxia, sluggishness) were very similar to symptoms observed in mice treated by our laboratory with a related compound, terpinen-4-ol, the major component of tea tree oil (data not shown). Tea tree oil, and other natural products such as geranium oil, are known to be toxic *in vivo* (272-275) with symptoms including drowsiness, ataxia, "fussiness" and un-coordinated gait. The fusion of organs to each other and the peritoneum seemed to suggest some destruction of cell membranes. The similar side effects observed between mice treated with α-TOS and terpinen-4-ol prompted further investigation of the published side effects of terpinen-4-ol further and revealed a recently published study describing the destruction of plasma membranes as a major result of the treatment of melanoma cells with terpinen-4-ol (276, 277). Both terpinen-4-ol and α-TOS have terpenoid structures which may explain their similar side-effects in immuno-competent mice.

Finally, the only clear difference between this study and the studies published in the past examining the effect of α-TOS on tumour development is the use of a syngeneic tumour cell line and its implantation into fully immuno-competent mice. α-TOS was shown to destroy total $CD3^+$ T cells in our fully immuno-competent murine model of mesothelioma. Athymic nude mice lack T cells, have a normal complement of bone marrow-dependent B cells but elevated levels of both macrophages and NK cells (278).

The macrophages from these athymic nude mice are also more potent than those from mice with a normal functioning thymus. Athymic nude mice are hence unable to mount a normal immune response to both the tumour xenografts used in the previous study but perhaps also to the α-TOS treatment. The negative effect of α-TOS may not have been evident in studies using athymic nude mice but was particularly important for this study as it was hoped that apoptosis induction via α-TOS treatment could be combined with the inactivation of T_{reg} cells (196).

From these results we have concluded that α-TOS is not a suitable treatment for syngeneic mesothelioma in immuno-competent mice. The discovery of negative side effects coupled with the lack of efficacy in this immuno-competent model of murine mesothelioma suggests that systemic α-TOS administration in immuno-competent hosts needs careful evaluation. Certainly, safer routes of administration will need to be considered. More importantly, the reason behind the lack of *in vivo* efficacy of α-TOS in an immuno-competent host needs to be evaluated. It had been hoped to combine apoptosis induction by α-TOS treatment with T_{reg} cell inactivation in order to develop a more effective, multi-targeted therapy for mesothelioma (196). The obvious destruction of host lymphocytes by α-TOS strongly limits its ability to be combined with an immunotherapy.

Future work into analogues of VitE as anti-cancer treatments will need to consider the effect of these agents on the natural host immune response. α-TOS was delivered as a suspension in DMSO for this study as it was based on previous *in vivo* work. Should this work proceed in the future realistic delivery methods must be examined. DMSO and other vehicles such as Tweens may not be suitable for man. Considerable advances have been made in the development of biocompatible formulations for poorly water soluble compounds such as betacyclodextrin-based systems (226). The only other available study to date using immuno-competent mice was in fact focussed on developing a more appropriate method for the delivery of α-TOS. The vesiculated form of α-TOS is more soluble and hence more relevant for clinical use in that it is easier to administer with a potentially lower risk of toxicity (269, 279). It has been suggested that α-TOS delivered in liposomes via the tail vein may be suitable for this purpose (personal communication: Assoc. Prof. Jiri Neuzil). The use of liposomes for the

delivery of anti-cancer drugs for cancers such as breast cancer is currently an actively pursued field of drug development (280).

The values and liabilities of using athymic nude mice in xenograft cancer studies of novel drugs were recently reviewed by Kelland in 2004 (226). The author mentioned that although these models have been in use for the past 25 years or so, significant consideration needs to be taken when deciding to use such a model. There are many variables that need to be considered such as the site of tumour implantation, growth properties of the tumour, the size of the tumour at the time of treatment, the formulation of the drug, the mode of delivery, dose and treatment regime and the endpoint for assessing efficacy. The author argued that murine syngeneic models which have often been dismissed since the development of human to mouse xenograft models may be more appropriate to use than human subcutaneously planted xenografts in immunodeficient mice. Kelland also pointed out in his review that an easy mistake to make during preclinical studies using athymic nude and other models is that early time-points for the analysis of drug efficacy are used before any drug induced toxicity such as body weight loss, lethargy and even death is evident. The final limitation for the use of xenograft models in a athymic mice is when the drug/treatment of interest is one which relies on factors of or the whole immune response. Beyond the fact that athymic mice are lacking a fully functional immune response, the vasculature of human grafted tumours will be murine and may not be conducive to the transportation or the extravasation of the required cells in the mice.

Other potentially synergistic approaches to boost both effector T cells and eliminate immuno-suppression could be trialled in the future. For example, in several murine tumour models, bacterial unmethylated cytosine-phosphorothioate-guanine (CpG)-rich oligodeoxynucleotides (CpG-ODN) have been shown to result in the local activation of NK cells through induction of cytokines and priming of tumour-specific $CD8^+$ T cells resulting in tumour growth suppression and rejection of established tumours (281). The repeated peri-tumoural administration of CpG-ODN does not directly target activated T cells but exerts its effect indirectly via DCs. It appears that peri-tumoural treatment with CpG-ODN activates APCs that have taken up tumour derived material enhancing their maturation and migration to local lymph nodes where tumour-specific T cells are primed. It follows that this boosting of DC and effector cell function could only be

enhanced by the combination of this therapy with T_{reg} cell inactivation. Effective tumour therapy however, requires a proinflammatory microenvironment within or around the tumour that permits effector cells to extravasate and reject the tumour. A further benefit of CpG-ODN is that the systemic (i.v.) administration of CpG-ODN induces a large increase in ICAM and VCAM in the tumour vasculature (282). CpG-ODN therapy, when administered systemically, synergises with adoptively transferred antigen-specific $CD8^+$ CTLs for improved tumour rejection emphasising the complex nature of the anti-tumour immune response. CpG-ODN is most effective as a pro-inflammatory factor in T cell based immunotherapy. Future experiments could therefore investigate the potentially synergistic approach to the treatment of solid, established tumours based on the notion that CpG-ODN treatment works best when combined with effector cell "boosting". This discussion proposes to "boost" effector cells by releasing them from immunosuppression by inactivating tumour-located T_{reg} cells.

Similarly promising inhibitions of tumour growth have been achieved with various vaccination strategies designed to boost effector cell responses. Ralph and colleagues have shown that combined interferon (IFN)-γ and -β treatment of murine melanoma B16-F10 cells results in the concurrent increased expression of B7-1, MHC Class I and ICAM-1 (283). When these IFN treated tumour cells are inactivated by lethal irradiation, they provide a highly effective immunotherapeutic vaccine for murine melanoma. The combination of effector cell "boosting" by whole tumour cell vaccination with T_{reg} cell inactivation could also be potentially synergistic and so future experiments could focus on the development of a whole tumour cell vaccine for murine mesothelioma. As mentioned previously, Sutmuller *et al* (2001) demonstrated the synergy between the inactivation of T_{reg} cells using anti-CTLA-4 and anti-CD25 mAbs combined with whole tumour cell vaccination. Cesares *et al* (2003) and Elia *et al* (2006) also combined T_{reg} cell inactivation with a vaccination strategy but like the work of Sutmuller T_{reg} cell inactivation was performed either several days prior to tumour challenge or only one day after tumour challenge (210, 284). A further American study also confirmed the ability to successfully combine T_{reg} cell inactivation of established tumours with vaccination using a recombinant poxviral vector that contained the transgenes for a carcinoembryonic antigen and a triad of the T cell costimulatory molecules B7-1, ICAM-1 and LFA-3 (285). It was found that neither vaccination alone

administered at day 8 post tumour challenge, anti-CD25 mAb administered alone or external beam radiation administered alone at day 8 could improve tumour outcome. It was only when a combination of vaccination, T_{reg} inactivation and radiation treatment were administered to established tumours that a positive effect on tumour growth inhibition was observed including complete tumour regression. This multi-modalilty approach resulted in the vaccine inducing an antigen specific T cell response, the external beam radiation upregulating Fas on tumour cells making them more susceptible to T cell killing and anti-CD25 mAb eliminating suppression.

In the last 30 years the incidence of MM has increased dramatically throughout the industrialised world, particularly in Australia (286). MM is a uniformly fatal cancer for which there is no effective treatment (5). In the past, scientific and clinical assessments of the cancer have been severely hindered by the relatively low incidence of patients at any particular institution at the one time and by the lack of experimental models. The development of a murine model of MM has significantly advanced our understanding of the pathogenesis, progression and potential treatments of this disease (13).

Although the asbestos induced models of murine mesothelioma such as the AE17 model have been studied in depth and are considered on both the ultrastructural and histological level to be a good representation of human mesothelioma, there are still some significant differences between the human disease and the murine model (13, 15). Human MM tumours accumulate multiple somatic genetic mutations including the inactivation of the *NF2* and *CDKN2A/ARF* tumour suppressor genes (287). The recent development of a murine tumour model which combines asbestos induced mesothelioma with a mouse with a genetic knockout of *NF2* may be useful for future studies to more closely recapitulate the human disease (288, 289). MM usually develops as a cancer of the pleura, pericardium, peritoneum or tunica vaginalis. Primarily, the s.c. murine models are used but can be adapted to induce intra-peritoneal tumours. Murine mesothelioma, as presented in chapter 5, can be implanted i.p. to develop peritoneal tumours, but this is experimentally harder to analyse. Modern imaging technology can however be implemented in the future to aid in the daily measurement of tumour growth. This could both be beneficial over the sometimes difficult and subjective calliper measurement and can be appropriate to intra-peritoneal tumours.

A major hurdle of human cancer treatment is the removal of residual disease. Combination therapies are likely to be the most effective strategies to inhibit tumour development with debulking surgery often the first procedure. We propose potentially synergistic treatment regimes as a method to remove residual tumour masses. T_{reg} cell inactivating mAbs or soluble receptors can be delivered directly into the tumour at the time of tumour debulking or with the development of stereotactic injection techniques, mAbs and soluble receptors can be delivered at any time directly into the tumour. As mice are alive under the modern imaging techniques the intra-tumoural delivery of anti-CD25 mAb presented in Chapter 5 could still be conducted by injection during imaging of the tumours to better mirror the true course of the cancer and the suggested clinical utilisation of stereotactic injection delivery of the humanised anti-CD25 mAb to mesothelioma patients.

The inactivation of T_{reg} cells as a therapy for malignant mesothelioma and in fact many other cancers, shows much promise and is confirmed by the multiple studies demonstrating the high intra-tumoural presence of T_{reg} cells in cancers. There are several issues when translating this work to the clinic, but there are also several reasons for the sooner rather than later move to higher animal or clinical trials. Issues when moving to the clinic include the translation of the intra-tumoural delivery. For s.c. tumours, as in the murine model, this is easy as tumours are palpable and accessible. Skin cancers such as basal cell carcinoma, melanoma may be good places to start for clinical trials. For other tumours located further inside the body delivery is more difficult. Again imaging and stereotactic injection may be the answer. In terms of moving to the clinic sooner than later, it is important to demonstrate that this form of T_{reg} cell inactivation by anti-CD25 mAb is applicable to humans. Anti-CD25 mAbs are already in use in the clinic primarily to aid in the induction of transplantation tolerance where they are used to limit effector T cell activation which leads to graft rejection. The clinical transition to using the anti-CD25 mAb intra-tumourally to treat cancers by inactivating T_{reg} cells should be straight forward and in fact an anti-CD25 mAb (Ontak) has already been given systemically to ovarian cancer patients to this effect (290).

Side effects of systemic delivery of T_{reg} cell inactivating drugs such as autoimmunity may result and so the change to intra-tumoural delivery should be of benefit both to the patient physically but also financially as lower doses could be used. Although this

antibody (Ontak) is in use already in the clinic, the translation to a novel delivery regime or perhaps even the future development of additional T_{reg} cell inactivating drugs should be done with much care as evidenced by the recent disastrous phase one clinical trial of the anti-CD28 mAb in six human volunteers (291).

References

1. Wang NS. Anatomy and physiology of the pleural space. Clin Chest Med 1985;6(1):3-16.

2. Berry G, de Klerk NH, Reid A, Ambrosini GL, Fritschi L, Olsen NJ, et al. Malignant pleural and peritoneal mesotheliomas in former miners and millers of crocidolite at Wittenoom, Western Australia. Occup Environ Med 2004;61(4):e14.
3. Hirano H, Maeda T, Tsuji M, Ito Y, Kizaki T, Yoshii Y, et al. Malignant mesothelioma of the pericardium: case reports and immunohistochemical studies including Ki-67 expression. Pathol Int 2002;52(10):669-76.
4. Abe K, Kato N, Miki K, Nimura S, Suzuki M, Kiyota H, et al. Malignant mesothelioma of testicular tunica vaginalis. Int J Urol 2002;9(10):602-3.
5. Robinson BW, Musk AW, Lake RA. Malignant mesothelioma. Lancet 2005;366(9483):397-408.
6. Robinson BW, Creaney J, Lake R, Nowak A, Musk AW, de Klerk N, et al. Mesothelin-family proteins and diagnosis of mesothelioma. Lancet 2003;362(9396):1612-6.
7. Ismail-Khan R, Robinson LA, Williams CC, Jr., Garrett CR, Bepler G, Simon GR. Malignant pleural mesothelioma: a comprehensive review. Cancer Control 2006;13(4):255-63.
8. Fingerhut M, Nelson DI, Driscoll T, Concha-Barrientos M, Steenland K, Punnett L, et al. The contribution of occupational risks to the global burden of disease: summary and next steps. Med Lav 2006;97(2):313-21.
9. Kazan-Allen L. Asbestos and mesothelioma: worldwide trends. Lung Cancer 2005;49 Suppl 1:S3-8.
10. Sterman DH, Treat J, Litzky LA, Amin KM, Coonrod L, Molnar-Kimber K, et al. Adenovirus-mediated herpes simplex virus thymidine kinase/ganciclovir gene therapy in patients with localized malignancy: results of a phase I clinical trial in malignant mesothelioma. Hum Gene Ther 1998;9(7):1083-92.
11. Robinson BW, Robinson C, Lake RA. Localised spontaneous regression in mesothelioma -- possible immunological mechanism. Lung Cancer 2001;32(2):197-201.
12. Robinson C, Callow M, Stevenson S, Scott B, Robinson BW, Lake RA. Serologic responses in patients with malignant mesothelioma: evidence for both public and private specificities. Am J Respir Cell Mol Biol 2000;22(5):550-6.
13. Davis MR, Manning LS, Whitaker D, Garlepp MJ, Robinson BW. Establishment of a murine model of malignant mesothelioma. Int J Cancer 1992;52(6):881-6.
14. Jackaman C, Bundell CS, Kinnear BF, Smith AM, Filion P, van Hagen D, et al. IL-2 intratumoral immunotherapy enhances CD8+ T cells that mediate destruction of tumor cells and tumor-associated vasculature: a novel mechanism for IL-2. J Immunol 2003;171(10):5051-63.
15. Bielefeldt-Ohmann H, Fitzpatrick DR, Marzo AL, Jarnicki AG, Himbeck RP, Davis MR, et al. Patho- and immunobiology of malignant mesothelioma: characterisation of tumour infiltrating leucocytes and cytokine production in a murine model. Cancer Immunol Immunother 1994;39(6):347-59.
16. Nowell PC. The clonal evolution of tumor cell populations. Science 1976;194(4260):23-8.
17. Wicha MS, Liu S, Dontu G. Cancer stem cells: an old idea--a paradigm shift. Cancer Res 2006;66(4):1883-90; discussion 1895-6.

18. Duesberg P, Li R, Fabarius A, Hehlmann R. The chromosomal basis of cancer. Cell Oncol 2005;27(5-6):293-318.
19. Loeb KR, Loeb LA. Significance of multiple mutations in cancer. Carcinogenesis 2000;21(3):379-85.
20. Smyth MJ, Godfrey DI, Trapani JA. A fresh look at tumor immunosurveillance and immunotherapy. Nat Immunol 2001;2(4):293-9.
21. Bielefeldt-Ohmann H, Jarnicki AG, Fitzpatrick DR. Molecular pathobiology and immunology of malignant mesothelioma. J Pathol 1996;178(4):369-78.
22. Upham JW, Garlepp MJ, Musk AW, Robinson BW. Malignant mesothelioma: new insights into tumour biology and immunology as a basis for new treatment approaches. Thorax 1995;50(8):887-93.
23. Dunn GP, Old LJ, Schreiber RD. The immunobiology of cancer immunosurveillance and immunoediting. Immunity 2004;21(2):137-48.
24. Pawelec G. Tumour escape: antitumour effectors too much of a good thing? Cancer Immunol Immunother 2004;53(3):262-74.
25. Woo EY, Chu CS, Goletz TJ, Schlienger K, Yeh H, Coukos G, et al. Regulatory CD4(+)CD25(+) T cells in tumors from patients with early-stage non-small cell lung cancer and late-stage ovarian cancer. Cancer Res 2001;61(12):4766-72.
26. Liyanage UK, Moore TT, Joo HG, Tanaka Yi, Herrmann V, Doherty G, et al. Prevalence of regulatory T cells is increased in peripheral blood and tumor microenvironment of patients with pancreas or breast adenocarcinoma. J Immunol 2002;169(5):2756-61.
27. Curiel TJ, Coukos G, Zou L, Alvarez X, Cheng P, Mottram P, et al. Specific recruitment of regulatory T cells in ovarian carcinoma fosters immune privilege and predicts reduced survival. Nat Med 2004;10(9):942-9.
28. Yu P, Lee Y, Liu W, Krausz T, Chong A, Schreiber H, et al. Intratumor depletion of CD4+ cells unmasks tumor immunogenicity leading to the rejection of late-stage tumors. J Exp Med 2005;201(5):779-91.
29. Ko K, Yamazaki S, Nakamura K, Nishioka T, Hirota K, Yamaguchi T, et al. Treatment of advanced tumors with agonistic anti-GITR mAb and its effects on tumor-infiltrating Foxp3+CD25+CD4+ regulatory T cells. J Exp Med 2005;202(7):885-91.
30. Fitzpatrick DR, Bielefeldt-Ohmann H, Himbeck RP, Jarnicki AG, Marzo AL, Robinson BWS. Transforming growth factor-beta: Antisense RNA-mediated inhibition affects anchorage-independent growth, tumorigenicity and tumour-infiltrating T-cells in malignant mesothelioma. Growth Factors 1994;11:29-44.
31. Delong P, Carroll RG, Henry AC, Tanaka T, Ahmad S, Leibowitz MS, et al. Regulatory T Cells and Cytokines in Malignant Pleural Effusions Secondary to Mesothelioma and Carcinoma. Cancer Biol Ther 2005;4(3).
32. Hegmans JP, Hemmes A, Hammad H, Boon L, Hoogsteden HC, Lambrecht BN. Mesothelioma environment comprises cytokines and T-regulatory cells that suppress immune responses. Eur Respir J 2006;27(6):1086-95.
33. Christmas TI, Manning LS, Davis MR, Robinson BWS, Garlepp MJ. HLa antigen expression and malignant mesothelioma. Am J Respir Cell Mol Biol 1991;5:213-220.
34. Manning LS, Bowman RV, Darby SB, Robinson BWS. Lysis of human malignant mesothelioma cells by natural killer (NK) and lymphokine-activated killer (LAK) cells. Am Rev Respir Dis 1989;139:1369-1374.
35. Meloni F, Morosini M, Solari N, Passadore I, Nascimbene C, Novo M, et al. Foxp3 expressing CD4+ CD25+ and CD8+CD28- T regulatory cells in the peripheral

blood of patients with lung cancer and pleural mesothelioma. Hum Immunol 2006;67(1-2):1-12.
36. Nishizuka Y, Sakakura T. Thymus and reproduction: sex-linked dysgenesia of the gonad after neonatal thymectomy in mice. Science 1969;166(906):753-5.
37. Gershon RK, Kondo K. Infectious immunological tolerance. Immunology 1971;21(6):903-14.
38. North RJ. Down-regulation of the antitumor immune response. Adv Cancer Res 1985;45:1-43.
39. Sakaguchi S, Sakaguchi N, Asano M, Itoh M, Toda M. Immunologic self-tolerance maintained by activated T cells expressing IL-2 receptor alpha-chains (CD25). Breakdown of a single mechanism of self-tolerance causes various autoimmune diseases. J Immunol 1995;155(3):1151-64.
40. Shevach EM. Certified professionals: CD4(+)CD25(+) suppressor T cells. Journal of Experimental Medicine 2001;193(11):F41-6.
41. Thornton AM. Signal transduction in CD4+CD25+ regulatory T cells: CD25 and IL-2. Front Biosci 2006;11:921-7.
42. Shevach EM. CD4+ CD25+ suppressor T cells: more questions than answers. Nat Rev Immunol 2002;2(6):389-400.
43. Bluestone JA, Abbas AK. Natural versus adaptive regulatory T cells. Nat Rev Immunol 2003;3(3):253-7.
44. Groux H, O'Garra A, Bigler M, Rouleau M, Antonenko S, de Vries JE, et al. A CD4+ T-cell subset inhibits antigen-specific T-cell responses and prevents colitis. Nature 1997;389(6652):737-42.
45. Zhang X, Izikson L, Liu L, Weiner HL. Activation of CD25(+)CD4(+) regulatory T cells by oral antigen administration. J Immunol 2001;167(8):4245-53.
46. Jonuleit H, Schmitt E, Schuler G, Knop J, Enk AH. Induction of interleukin 10-producing, nonproliferating CD4(+) T cells with regulatory properties by repetitive stimulation with allogeneic immature human dendritic cells. Journal of Experimental Medicine 2000;192(9):1213-22.
47. Lehmann J, Huehn J, de la Rosa M, Maszyna F, Kretschmer U, Krenn V, et al. Expression of the integrin alpha Ebeta 7 identifies unique subsets of CD25+ as well as CD25- regulatory T cells. Proc Natl Acad Sci U S A 2002;99(20):13031-6.
48. Kalams SA, Walker BD. The critical need for CD4 help in maintaining effective cytotoxic T lymphocyte responses. J Exp Med 1998;188(12):2199-204.
49. Weiner HL. Induction and mechanism of action of transforming growth factor-beta-secreting Th3 regulatory cells. Immunol Rev 2001;182:207-14.
50. Segal BM, Glass DD, Shevach EM. Cutting Edge: IL-10-producing CD4+ T cells mediate tumor rejection. J Immunol 2002;168(1):1-4.
51. Fukaura H, Kent SC, Pietrusewicz MJ, Khoury SJ, Weiner HL, Hafler DA. Induction of circulating myelin basic protein and proteolipid protein-specific transforming growth factor-beta1-secreting Th3 T cells by oral administration of myelin in multiple sclerosis patients. J Clin Invest 1996;98(1):70-7.
52. Chen Y, Kuchroo VK, Inobe J, Hafler DA, Weiner HL. Regulatory T cell clones induced by oral tolerance: suppression of autoimmune encephalomyelitis. Science 1994;265(5176):1237-40.
53. Seo N, Hayakawa S, Takigawa M, Tokura Y. Interleukin-10 expressed at early tumour sites induces subsequent generation of CD4(+) T-regulatory cells and systemic collapse of antitumour immunity. Immunology 2001;103(4):449-57.
54. Thornton AM, Shevach EM. Suppressor effector function of CD4+CD25+ immunoregulatory T cells is antigen nonspecific. J Immunol 2000;164(1):183-90.

55. Read S, Malmstrom V, Powrie F. Cytotoxic T lymphocyte-associated antigen 4 plays an essential role in the function of CD25(+)CD4(+) regulatory cells that control intestinal inflammation. Journal of Experimental Medicine 2000;192(2):295-302.
56. Nakamura K, Kitani A, Strober W. Cell contact-dependent immunosuppression by CD4(+)CD25(+) regulatory T cells is mediated by cell surface-bound transforming growth factor beta. Journal of Experimental Medicine 2001;194(5):629-44.
57. Jonuleit H, Schmitt E, Kakirman H, Stassen M, Knop J, Enk AH. Infectious tolerance: human CD25(+) regulatory T cells convey suppressor activity to conventional CD4(+) T helper cells. J Exp Med 2002;196(2):255-60.
58. Wei S, Kryczek I, Zou L, Daniel B, Cheng P, Mottram P, et al. Plasmacytoid dendritic cells induce CD8+ regulatory T cells in human ovarian carcinoma. Cancer Res 2005;65(12):5020-6.
59. Zheng SG, Wang JH, Koss MN, Quismorio F, Jr., Gray JD, Horwitz DA. CD4+ and CD8+ regulatory T cells generated ex vivo with IL-2 and TGF-beta suppress a stimulatory graft-versus-host disease with a lupus-like syndrome. J Immunol 2004;172(3):1531-9.
60. Brisslert M, Bokarewa M, Larsson P, Wing K, Collins LV, Tarkowski A. Phenotypic and functional characterization of human CD25+ B cells. Immunology 2006;117(4):548-57.
61. Maloy KJ, Powrie F. Regulatory T cells in the control of immune pathology. Nat Immunol 2001;2(9):816-22.
62. Raimondi G, Shufesky WJ, Tokita D, Morelli AE, Thomson AW. Regulated compartmentalization of programmed cell death-1 discriminates CD4+CD25+ resting regulatory T cells from activated T cells. J Immunol 2006;176(5):2808-16.
63. Suri-Payer E, Amar AZ, Thornton AM, Shevach EM. CD4+CD25+ T cells inhibit both the induction and effector function of autoreactive T cells and represent a unique lineage of immunoregulatory cells. Journal of Immunology 1998;160(3):1212-8.
64. Fontenot JD, Gavin MA, Rudensky AY. Foxp3 programs the development and function of CD4+CD25+ regulatory T cells. Nat Immunol 2003;4(4):330-6.
65. Ziegler SF. FOXP3: of mice and men. Annu Rev Immunol 2006;24:209-26.
66. Huehn JaH, A. Regulatory T cell migration: suppressors find their way. Regulatory T cells and Immunoregulation Newsletter 2005(1):3-5.
67. Zou W. Regulatory T cells, tumour immunity and immunotherapy. Nat Rev Immunol 2006;6(4):295-307.
68. Fisson S, Darrasse-Jeze G, Litvinova E, Septier F, Klatzmann D, Liblau R, et al. Continuous activation of autoreactive CD4+ CD25+ regulatory T cells in the steady state. J Exp Med 2003;198(5):737-46.
69. Cohen JL, Trenado A, Vasey D, Klatzmann D, Salomon BL. CD4(+)CD25(+) immunoregulatory T Cells: new therapeutics for graft-versus-host disease. J Exp Med 2002;196(3):401-6.
70. Szanya V, Ermann J, Taylor C, Holness C, Fathman CG. The subpopulation of CD4+CD25+ splenocytes that delays adoptive transfer of diabetes expresses L-selectin and high levels of CCR7. J Immunol 2002;169(5):2461-5.
71. Jung TM, Gallatin WM, Weissman IL, Dailey MO. Down-regulation of homing receptors after T cell activation. J Immunol 1988;141(12):4110-7.
72. Huehn J, Siegmund K, Lehmann JC, Siewert C, Haubold U, Feuerer M, et al. Developmental stage, phenotype, and migration distinguish naive- and effector/memory-like CD4+ regulatory T cells. J Exp Med 2004;199(3):303-13.

73. Hiura T, Kagamu H, Miura S, Ishida A, Tanaka H, Tanaka J, et al. Both regulatory T cells and antitumor effector T cells are primed in the same draining lymph nodes during tumor progression. J Immunol 2005;175(8):5058-66.
74. Cerf-Bensussan N, Jarry A, Brousse N, Lisowska-Grospierre B, Guy-Grand D, Griscelli C. A monoclonal antibody (HML-1) defining a novel membrane molecule present on human intestinal lymphocytes. Eur J Immunol 1987;17(9):1279-85.
75. Kilshaw PJ. Expression of the mucosal T cell integrin alpha M290 beta 7 by a major subpopulation of dendritic cells in mice. Eur J Immunol 1993;23(12):3365-8.
76. Cepek KL, Shaw SK, Parker CM, Russell GJ, Morrow JS, Rimm DL, et al. Adhesion between epithelial cells and T lymphocytes mediated by E-cadherin and the alpha E beta 7 integrin. Nature 1994;372(6502):190-3.
77. Shieh CC, Sadasivan BK, Russell GJ, Schon MP, Parker CM, Brenner MB. Lymphocyte adhesion to epithelia and endothelia mediated by the lymphocyte endothelial-epithelial cell adhesion molecule glycoprotein. J Immunol 1999;163(3):1592-601.
78. Gavin MA, Clarke SR, Negrou E, Gallegos A, Rudensky A. Homeostasis and anergy of CD4(+)CD25(+) suppressor T cells in vivo. Nat Immunol 2002;3(1):33-41.
79. Schon MP, Arya A, Murphy EA, Adams CM, Strauch UG, Agace WW, et al. Mucosal T lymphocyte numbers are selectively reduced in integrin alpha E (CD103)-deficient mice. J Immunol 1999;162(11):6641-9.
80. Suffia I, Reckling SK, Salay G, Belkaid Y. A role for CD103 in the retention of CD4+CD25+ Treg and control of Leishmania major infection. J Immunol 2005;174(9):5444-55.
81. Firan M, Dhillon S, Estess P, Siegelman MH. Suppressor activity and potency among regulatory T cells is discriminated by functionally active CD44. Blood 2006;107(2):619-27.
82. DeGrendele HC, Estess P, Siegelman MH. Requirement for CD44 in activated T cell extravasation into an inflammatory site. Science 1997;278(5338):672-5.
83. Lesley J, Hyman R. CD44 can be activated to function as an hyaluronic acid receptor in normal murine T cells. Eur J Immunol 1992;22(10):2719-23.
84. Miyake K, Underhill CB, Lesley J, Kincade PW. Hyaluronate can function as a cell adhesion molecule and CD44 participates in hyaluronate recognition. J Exp Med 1990;172(1):69-75.
85. Estess P, DeGrendele HC, Pascual V, Siegelman MH. Functional activation of lymphocyte CD44 in peripheral blood is a marker of autoimmune disease activity. J Clin Invest 1998;102(6):1173-82.
86. Bruder D, Probst-Kepper M, Westendorf AM, Geffers R, Beissert S, Loser K, et al. Neuropilin-1: a surface marker of regulatory T cells. Eur J Immunol 2004;34(3):623-30.
87. Sutmuller RP, van Duivenvoorde LM, van Elsas A, Schumacher TN, Wildenberg ME, Allison JP, et al. Synergism of cytotoxic T lymphocyte-associated antigen 4 blockade and depletion of CD25(+) regulatory T cells in antitumor therapy reveals alternative pathways for suppression of autoreactive cytotoxic T lymphocyte responses. J Exp Med 2001;194(6):823-32.
88. Phan GQ, Yang JC, Sherry RM, Hwu P, Topalian SL, Schwartzentruber DJ, et al. Cancer regression and autoimmunity induced by cytotoxic T lymphocyte-associated antigen 4 blockade in patients with metastatic melanoma. Proc Natl Acad Sci U S A 2003;100(14):8372-7.

89. Wang HY, Lee DA, Peng G, Guo Z, Li Y, Kiniwa Y, et al. Tumor-specific human CD4+ regulatory T cells and their ligands: implications for immunotherapy. Immunity 2004;20(1):107-18.
90. Salomon B, Bluestone JA. Complexities of CD28/B7: CTLA-4 costimulatory pathways in autoimmunity and transplantation. Annual Review of Immunology 2001;19:225-52.
91. Takahashi T, Tagami T, Yamazaki S, Uede T, Shimizu J, Sakaguchi N, et al. Immunologic self-tolerance maintained by CD25(+)CD4(+) regulatory T cells constitutively expressing cytotoxic T lymphocyte-associated antigen 4. Journal of Experimental Medicine 2000;192(2):303-10.
92. Shimizu J, Yamazaki S, Takahashi T, Ishida Y, Sakaguchi S. Stimulation of CD25(+)CD4(+) regulatory T cells through GITR breaks immunological self-tolerance. Nat Immunol 2002;3(2):135-42.
93. McHugh RS, Whitters MJ, Piccirillo CA, Young DA, Shevach EM, Collins M, et al. CD4(+)CD25(+) immunoregulatory T cells: gene expression analysis reveals a functional role for the glucocorticoid-induced TNF receptor. Immunity 2002;16(2):311-23.
94. Wolf AM, Wolf D, Steurer M, Gastl G, Gunsilius E, Grubeck-Loebenstein B. Increase of regulatory T cells in the peripheral blood of cancer patients. Clin Cancer Res 2003;9(2):606-12.
95. Ichihara F, Kono K, Takahashi A, Kawaida H, Sugai H, Fujii H. Increased populations of regulatory T cells in peripheral blood and tumor-infiltrating lymphocytes in patients with gastric and esophageal cancers. Clin Cancer Res 2003;9(12):4404-8.
96. Sakaguchi S. Regulatory T cells: key controllers of immunologic self-tolerance. Cell 2000;101(5):455-8.
97. Roncarolo MG, Levings MK. The role of different subsets of T regulatory cells in controlling autoimmunity. Curr Opin Immunol 2000;12(6):676-83.
98. Powrie F, Leach MW, Mauze S, Menon S, Caddle LB, Coffman RL. Inhibition of Th1 responses prevents inflammatory bowel disease in scid mice reconstituted with CD45RBhi CD4+ T cells. Immunity 1994;1(7):553-62.
99. Allez M, Mayer L. Regulatory T cells: peace keepers in the gut. Inflamm Bowel Dis 2004;10(5):666-76.
100. Tsuji NM, Mizumachi K, Kurisaki J. Antigen-specific, CD4+CD25+ regulatory T cell clones induced in Peyer's patches. Int Immunol 2003;15(4):525-34.
101. Hori S, Carvalho TL, Demengeot J. CD25+CD4+ regulatory T cells suppress CD4+ T cell-mediated pulmonary hyperinflammation driven by Pneumocystis carinii in immunodeficient mice. Eur J Immunol 2002;32(5):1282-91.
102. McGuirk P, McCann C, Mills KH. Pathogen-specific T regulatory 1 cells induced in the respiratory tract by a bacterial molecule that stimulates interleukin 10 production by dendritic cells: a novel strategy for evasion of protective T helper type 1 responses by Bordetella pertussis. J Exp Med 2002;195(2):221-31.
103. Akbari O, Freeman GJ, Meyer EH, Greenfield EA, Chang TT, Sharpe AH, et al. Antigen-specific regulatory T cells develop via the ICOS-ICOS-ligand pathway and inhibit allergen-induced airway hyperreactivity. Nat Med 2002;8(9):1024-32.
104. Shi HZ, Qin XJ. CD4CD25 regulatory T lymphocytes in allergy and asthma. Allergy 2005;60(8):986-95.
105. Zuany-Amorim C, Sawicka E, Manlius C, Le Moine A, Brunet LR, Kemeny DM, et al. Suppression of airway eosinophilia by killed Mycobacterium vaccae-induced allergen-specific regulatory T-cells. Nat Med 2002;8(6):625-9.

106. Iwashiro M, Messer RJ, Peterson KE, Stromnes IM, Sugie T, Hasenkrug KJ. Immunosuppression by CD4+ regulatory T cells induced by chronic retroviral infection. Proc Natl Acad Sci U S A 2001;98(16):9226-30.
107. Beilharz MW, Sammels LM, Paun A, Shaw K, van Eeden P, Watson MW, et al. Timed ablation of regulatory CD4+ T cells can prevent murine AIDS progression. J Immunol 2004;172(8):4917-25.
108. Lim AY, Price P, Beilharz MW, French MA. Cell surface markers of regulatory T cells are not associated with increased forkhead box p3 expression in blood CD4 T cells from HIV-infected patients responding to antiretroviral therapy*. Immunol Cell Biol 2006;84(6):530-6.
109. Andersson J, Boasso A, Nilsson J, Zhang R, Shire NJ, Lindback S, et al. The prevalence of regulatory T cells in lymphoid tissue is correlated with viral load in HIV-infected patients. J Immunol 2005;174(6):3143-7.
110. Cao D, Malmstrom V, Baecher-Allan C, Hafler D, Klareskog L, Trollmo C. Isolation and functional characterization of regulatory CD25brightCD4+ T cells from the target organ of patients with rheumatoid arthritis. Eur J Immunol 2003;33(1):215-23.
111. Ruprecht CR, Gattorno M, Ferlito F, Gregorio A, Martini A, Lanzavecchia A, et al. Coexpression of CD25 and CD27 identifies FoxP3+ regulatory T cells in inflamed synovia. J Exp Med 2005;201(11):1793-803.
112. Green EA, Choi Y, Flavell RA. Pancreatic lymph node-derived CD4(+)CD25(+) Treg cells: highly potent regulators of diabetes that require TRANCE-RANK signals. Immunity 2002;16(2):183-91.
113. Herman AE, Freeman GJ, Mathis D, Benoist C. CD4+CD25+ T regulatory cells dependent on ICOS promote regulation of effector cells in the prediabetic lesion. J Exp Med 2004;199(11):1479-89.
114. Lepault F, Gagnerault MC. Characterization of peripheral regulatory CD4+ T cells that prevent diabetes onset in nonobese diabetic mice. Journal of Immunology 2000;164(1):240-7.
115. Aluvihare VR, Kallikourdis M, Betz AG. Regulatory T cells mediate maternal tolerance to the fetus. Nat Immunol 2004;5(3):266-71.
116. Graca L, Cobbold SP, Waldmann H. Identification of regulatory T cells in tolerated allografts. J Exp Med 2002;195(12):1641-6.
117. Nakajima T, Ueki-Maruyama K, Oda T, Ohsawa Y, Ito H, Seymour GJ, et al. Regulatory T-cells infiltrate periodontal disease tissues. J Dent Res 2005;84(7):639-43.
118. Diederichsen AC, Zeuthen J, Christensen PB, Kristensen T. Characterisation of tumour infiltrating lymphocytes and correlations with immunological surface molecules in colorectal cancer. Eur J Cancer 1999;35(5):721-6.
119. Sasada T, Kimura M, Yoshida Y, Kanai M, Takabayashi A. CD4+CD25+ regulatory T cells in patients with gastrointestinal malignancies: possible involvement of regulatory T cells in disease progression. Cancer 2003;98(5):1089-99.
120. Seo N, Hayakawa S, Tokura Y. Mechanisms of immune privilege for tumor cells by regulatory cytokines produced by innate and acquired immune cells. Semin Cancer Biol 2002;12(4):291-300.
121. Reome JB, Hylind JC, Dutton RW, Dobrzanski MJ. Type 1 and type 2 tumor infiltrating effector cell subpopulations in progressive breast cancer. Clin Immunol 2004;111(1):69-81.
122. Liyanage UK, Moore TT, Joo HG, Tanaka Y, Herrmann V, Doherty G, et al. Prevalence of regulatory T cells is increased in peripheral blood and tumor

microenvironment of patients with pancreas or breast adenocarcinoma. J Immunol 2002;169(5):2756-61.
123. Woo EY, Yeh H, Chu CS, Schlienger K, Carroll RG, Riley JL, et al. Cutting edge: Regulatory T cells from lung cancer patients directly inhibit autologous T cell proliferation. J Immunol 2002;168(9):4272-6.
124. Yamagiwa S, Gray JD, Hashimoto S, Horwitz DA. A role for TGF-beta in the generation and expansion of CD4+CD25+ regulatory T cells from human peripheral blood. J Immunol 2001;166(12):7282-9.
125. Levings MK, Sangregorio R, Galbiati F, Squadrone S, de Waal Malefyt R, Roncarolo MG. IFN-alpha and IL-10 induce the differentiation of human type 1 T regulatory cells. J Immunol 2001;166(9):5530-9.
126. McGuirk P, Mills K. Pathogen-specific regulatory T cells provoke a shift in the Th1/Th2 paradigm in immunity to infectious diseases. Trends in Immunology 2002;23(9):450-5.
127. Chen W, Jin W, Hardegen N, Lei KJ, Li L, Marinos N, et al. Conversion of peripheral CD4+CD25- naive T cells to CD4+CD25+ regulatory T cells by TGF-beta induction of transcription factor Foxp3. J Exp Med 2003;198(12):1875-86.
128. Valzasina B, Piconese S, Guiducci C, Colombo MP. Tumor-induced expansion of regulatory T cells by conversion of CD4+CD25- lymphocytes is thymus and proliferation independent. Cancer Res 2006;66(8):4488-95.
129. Suzuki E, Kapoor V, Cheung HK, Ling LE, DeLong PA, Kaiser LR, et al. Soluble type II transforming growth factor-beta receptor inhibits established murine malignant mesothelioma tumor growth by augmenting host antitumor immunity. Clin Cancer Res 2004;10(17):5907-18.
130. Ghiringhelli F, Puig PE, Roux S, Parcellier A, Schmitt E, Solary E, et al. Tumor cells convert immature myeloid dendritic cells into TGF-beta-secreting cells inducing CD4+CD25+ regulatory T cell proliferation. J Exp Med 2005;202(7):919-29.
131. Ji HB, Liao G, Faubion WA, Abadia-Molina AC, Cozzo C, Laroux FS, et al. Cutting edge: the natural ligand for glucocorticoid-induced TNF receptor-related protein abrogates regulatory T cell suppression. J Immunol 2004;172(10):5823-7.
132. Kohm AP, McMahon JS, Podojil JR, Begolka WS, Degutes M, Kasprowicz DJ, et al. Cutting Edge: Anti-CD25 Monoclonal Antibody Injection Results in the Functional Inactivation, Not Depletion, of CD4+CD25+ T Regulatory Cells. J Immunol 2006;176(6):3301-5.
133. Thornton AM, Donovan EE, Piccirillo CA, Shevach EM. Cutting edge: IL-2 is critically required for the in vitro activation of CD4+CD25+ T cell suppressor function. J Immunol 2004;172(11):6519-23.
134. Gondek DC, Lu LF, Quezada SA, Sakaguchi S, Noelle RJ. Cutting edge: contact-mediated suppression by CD4+CD25+ regulatory cells involves a granzyme B-dependent, perforin-independent mechanism. J Immunol 2005;174(4):1783-6.
135. Thornton AM, Shevach EM. CD4+CD25+ immunoregulatory T cells suppress polyclonal T cell activation in vitro by inhibiting interleukin 2 production. Journal of Experimental Medicine 1998;188(2):287-96.
136. Baecher-Allan C, Viglietta V, Hafler DA. Inhibition of human CD4(+)CD25(+high) regulatory T cell function. J Immunol 2002;169(11):6210-7.
137. North RJ, Awwad M, Dunn PL. The immune response to tumors. Transplant Proc 1989;21(1 Pt 1):575-7.
138. Papiernik M, Banz A. Natural regulatory CD4 T cells expressing CD25. Microbes Infect 2001;3(11):937-45.

139. Takahashi T, Kuniyasu Y, Toda M, Sakaguchi N, Itoh M, Iwata M, et al. Immunologic self-tolerance maintained by CD25+CD4+ naturally anergic and suppressive T cells: induction of autoimmune disease by breaking their anergic/suppressive state. International Immunology 1998;10(12):1969-80.
140. Lord SJ, Rajotte RV, Korbutt GS, Bleackley RC. Granzyme B: a natural born killer. Immunol Rev 2003;193:31-8.
141. Appay V, Zaunders JJ, Papagno L, Sutton J, Jaramillo A, Waters A, et al. Characterization of CD4(+) CTLs ex vivo. J Immunol 2002;168(11):5954-8.
142. van Leeuwen EM, Remmerswaal EB, Vossen MT, Rowshani AT, Wertheim-van Dillen PM, van Lier RA, et al. Emergence of a CD4+CD28- granzyme B+, cytomegalovirus-specific T cell subset after recovery of primary cytomegalovirus infection. J Immunol 2004;173(3):1834-41.
143. Kemper C, Chan AC, Green JM, Brett KA, Murphy KM, Atkinson JP. Activation of human CD4+ cells with CD3 and CD46 induces a T-regulatory cell 1 phenotype. Nature 2003;421(6921):388-92.
144. Grossman WJ, Verbsky JW, Tollefsen BL, Kemper C, Atkinson JP, Ley TJ. Differential expression of granzymes A and B in human cytotoxic lymphocyte subsets and T regulatory cells. Blood 2004;104(9):2840-8.
145. Seddon B, Mason D. Peripheral autoantigen induces regulatory T cells that prevent autoimmunity. Journal of Experimental Medicine 1999;189(5):877-82.
146. Hsieh CS, Liang Y, Tyznik AJ, Self SG, Liggitt D, Rudensky AY. Recognition of the peripheral self by naturally arising CD25+ CD4+ T cell receptors. Immunity 2004;21(2):267-77.
147. Kullberg MC, Jankovic D, Gorelick PL, Caspar P, Letterio JJ, Cheever AW, et al. Bacteria-triggered CD4(+) T regulatory cells suppress Helicobacter hepaticus-induced colitis. J Exp Med 2002;196(4):505-15.
148. Belkaid Y, Piccirillo CA, Mendez S, Shevach EM, Sacks DL. CD4+CD25+ regulatory T cells control Leishmania major persistence and immunity. Nature 2002;420(6915):502-7.
149. Wang HY, Peng G, Guo Z, Shevach EM, Wang RF. Recognition of a new ARTC1 peptide ligand uniquely expressed in tumor cells by antigen-specific CD4+ regulatory T cells. J Immunol 2005;174(5):2661-70.
150. Awwad M, North RJ. Cyclophosphamide-induced immunologically mediated regression of a cyclophosphamide-resistant murine tumor: a consequence of eliminating precursor L3T4+ suppressor T-cells. Cancer Res 1989;49(7):1649-54.
151. Awwad M, North RJ. Sublethal, whole-body ionizing irradiation can be tumor promotive or tumor destructive depending on the stage of development of underlying antitumor immunity. Cancer Immunol Immunother 1988;26(1):55-60.
152. North RJ. Radiation-induced, immunologically mediated regression of an established tumor as an example of successful therapeutic immunomanipulation. Preferential elimination of suppressor T cells allows sustained production of effector T cells. J Exp Med 1986;164(5):1652-66.
153. Awwad M, North RJ. Immunologically mediated regression of a murine lymphoma after treatment with anti-L3T4 antibody. A consequence of removing L3T4+ suppressor T cells from a host generating predominantly Lyt-2+ T cell-mediated immunity. J Exp Med 1988;168(6):2193-206.
154. North RJ, Awwad M. Elimination of cycling CD4+ suppressor T cells with an anti-mitotic drug releases non-cycling CD8+ T cells to cause regression of an advanced lymphoma. Immunology 1990;71(1):90-5.

155. Shimizu J, Yamazaki S, Sakaguchi S. Induction of tumor immunity by removing CD25+CD4+ T cells: a common basis between tumor immunity and autoimmunity. Journal of Immunology 1999;163(10):5211-8.
156. Onizuka S, Tawara I, Shimizu J, Sakaguchi S, Fujita T, Nakayama E. Tumor rejection by in vivo administration of anti-CD25 (interleukin-2 receptor alpha) monoclonal antibody. Cancer Res 1999;59(13):3128-33.
157. Jones E, Dahm-Vicker M, Simon AK, Green A, Powrie F, Cerundolo V, et al. Depletion of CD25+ regulatory cells results in suppression of melanoma growth and induction of autoreactivity in mice. Cancer Immun 2002;2:1-12.
158. Yee C, Thompson JA, Roche P, Byrd DR, Lee PP, Piepkorn M, et al. Melanocyte destruction after antigen-specific immunotherapy of melanoma: direct evidence of t cell-mediated vitiligo. J Exp Med 2000;192(11):1637-44.
159. Ludewig B, Ochsenbein AF, Odermatt B, Paulin D, Hengartner H, Zinkernagel RM. Immunotherapy with dendritic cells directed against tumor antigens shared with normal host cells results in severe autoimmune disease. J Exp Med 2000;191(5):795-804.
160. Hara I, Takechi Y, Houghton AN. Implicating a role for immune recognition of self in tumor rejection: passive immunization against the brown locus protein. J Exp Med 1995;182(5):1609-14.
161. McHugh RS, Shevach EM. Cutting edge: depletion of CD4+CD25+ regulatory T cells is necessary, but not sufficient, for induction of organ-specific autoimmune disease. J Immunol 2002;168(12):5979-83.
162. Broomfield S, Currie A, van der Most RG, Brown M, van Bruggen I, Robinson BW, et al. Partial, but not complete, tumor-debulking surgery promotes protective antitumor memory when combined with chemotherapy and adjuvant immunotherapy. Cancer Res 2005;65(17):7580-4.
163. Stapelberg M, Tomasetti M, Alleva R, Gellert N, Procopio A, Neuzil J. alpha-Tocopheryl succinate inhibits proliferation of mesothelioma cells by selective down-regulation of fibroblast growth factor receptors. Biochem Biophys Res Commun 2004;318(3):636-41.
164. Tomasetti M, Gellert N, Procopio A, Neuzil J. A vitamin E analogue suppresses malignant mesothelioma in a preclinical model: a future drug against a fatal neoplastic disease? Int J Cancer 2004;109(5):641-2.
165. Dalen H, Neuzil J. Alpha-tocopheryl succinate sensitises a T lymphoma cell line to TRAIL-induced apoptosis by suppressing NF-kappaB activation. Br J Cancer 2003;88(1):153-8.
166. Lian H, Jin N, Li X, Mi Z, Zhang J, Sun L, et al. Induction of an effective anti-tumor immune response and tumor regression by combined administration of IL-18 and Apoptin. Cancer Immunol Immunother 2007;56(2):181-192.
167. Sammels LM, Bosio E, Fragall CT, Grounds MD, van Rooijen N, Beilharz MW. Innate inflammatory cells are not responsible for early death of donor myoblasts after myoblast transfer therapy. Transplantation 2004;77(12):1790-7.
168. North RJ, Bursuker I. Generation and decay of the immune response to a progressive fibrosarcoma. I. Ly-1+2- suppressor T cells down-regulate the generation of Ly-1-2+ effector T cells. J Exp Med 1984;159(5):1295-311.
169. Bursuker I, North RJ. Generation and decay of the immune response to a progressive fibrosarcoma. II. Failure to demonstrate postexcision immunity after the onset of T cell-mediated suppression of immunity. J Exp Med 1984;159(5):1312-21.

170. Lobert S, Fahy J, Hill BT, Duflos A, Etievant C, Correia JJ. Vinca alkaloid-induced tubulin spiral formation correlates with cytotoxicity in the leukemic L1210 cell line. Biochemistry 2000;39(39):12053-62.
171. Bass P. Chemotherapy for Malignant Mesothelioma: From Doxorubicin to Vinorelbine. Seminars in Oncology 2002;29(1):62-69.
172. Berghmans T, Paesmans M, Lalami Y, Louviaux I, Luce S, Mascaux C, et al. Activity of chemotherapy and immunotherapy on malignant mesothelioma: a systematic review of the literature with meta-analysis. Lung Cancer 2002;38(2):111-21.
173. Leigh J, Hendrie L, Berry D. The Incidence of Mesothelioma in Australia 1995 to 1997: Australian Mesothelioma Register Report 2000. Canberra: National Occupational Health and Safety Commission; 2000 December 2000.
174. Sikic BI. Antineoplastic Agents. In: Vraig CR, Stitzel RE, editors. Modern Pharmacology. 3 ed. Boston: Little, Brown and Compnay; 1990. p. 809-811.
175. Ferguson PJ, Phillips JR, Selner M, Cass CE. Differential activity of vincristine and vinblastine against cultured cells. Cancer Res 1984;44(8):3307-12.
176. Gout PW, Noble RL, Bruchovsky N, Beer CT. Vinblastine and vincristine--growth-inhibitory effects correlate with their retention by cultured Nb 2 node lymphoma cells. Int J Cancer 1984;34(2):245-8.
177. Li WW, Cordon-Cardo C, Chen Q, Jhanwar SC, Bertino JR. Establishment, characterization and drug sensitivity of four new human soft tissue sarcoma cell lines. Int J Cancer 1996;68(4):514-9.
178. Rivera-Fillat MP, Pallares-Trujillo J, Domenech C, Grau-Oliete MR. Comparative uptake, retention and action of vincristine, vinblastine and vindesine on murine leukaemic lymphoblasts sensitive and resistant to vincristine. Br J Pharmacol 1988;93(4):902-8.
179. Jones E, Dahm-Vicker, M., Simon, A.K., Green, A., Powrie, F., Cerundolo, V., Gallimore, A. Depletion of CD25+ regulatory cells results in suppression of melanoma growth and induction of autoreactivity in mice. Cancer Immunity 2002;2(1):12 pages.
180. Carmichael J, Mitchell JB, DeGraff WG, Gamson J, Gazdar AF, Johnson BE, et al. Chemosensitivity testing of human lung cancer cell lines using the MTT assay. Br J Cancer 1988;57(6):540-7.
181. Tarnowski GS, Ralph P, Stock CC. Sensitivity to chemotherapeutic and immunomodulating agents of two mouse lymphomas and of a macrophage tumor. Cancer Res 1979;39(10):3964-7.
182. O'Gorman MR, Bianchi L, Zaas D, Corrochano V, Pachman LM. Decreased levels of CD54 (ICAM-1)-positive lymphocytes in the peripheral blood in untreated patients with active juvenile dermatomyositis. Clin Diagn Lab Immunol 2000;7(4):693-7.
183. Ladanyi A, Somlai B, Gilde K, Fejos Z, Gaudi I, Timar J. T-cell activation marker expression on tumor-infiltrating lymphocytes as prognostic factor in cutaneous malignant melanoma. Clin Cancer Res 2004;10(2):521-30.
184. Dixon GL, Newton PJ, Chain BM, Katz D, Andersen SR, Wong S, et al. Dendritic cell activation and cytokine production induced by group B Neisseria meningitidis: interleukin-12 production depends on lipopolysaccharide expression in intact bacteria. Infect Immun 2001;69(7):4351-7.
185. Khattri R, Cox T, Yasayko SA, Ramsdell F. An essential role for Scurfin in CD4+CD25+ T regulatory cells. Nat Immunol 2003;4(4):337-42.
186. Hori S, Nomura T, Sakaguchi S. Control of regulatory T cell development by the transcription factor Foxp3. Science 2003;299(5609):1057-61.

187. Fontenot JD, Rudensky AY. A well adapted regulatory contrivance: regulatory T cell development and the forkhead family transcription factor Foxp3. Nat Immunol 2005;6(4):331-7.
188. DeLong P, Tanaka T, Kruklitis R, Henry AC, Kapoor V, Kaiser LR, et al. Use of cyclooxygenase-2 inhibition to enhance the efficacy of immunotherapy. Cancer Res 2003;63(22):7845-52.
189. Bundell CS, Jackaman C, Suhrbier A, Robinson BW, Nelson DJ. Functional endogenous cytotoxic T lymphocytes are generated to multiple antigens co-expressed by progressing tumors; after intra-tumoral IL-2 therapy these effector cells eradicate established tumors. Cancer Immunol Immunother 2005:1-15.
190. Stumbles PA, Himbeck R, Frelinger JA, Collins EJ, Lake RA, Robinson BW. Cutting edge: tumor-specific CTL are constitutively cross-armed in draining lymph nodes and transiently disseminate to mediate tumor regression following systemic CD40 activation. J Immunol 2004;173(10):5923-8.
191. Caminschi I, Venetsanakos E, Leong CC, Garlepp MJ, Robinson BW, Scott B. Cytokine gene therapy of mesothelioma. Immune and antitumor effects of transfected interleukin-12. Am J Respir Cell Mol Biol 1999;21(3):347-56.
192. Leong CC, Marley JV, Loh S, Milech N, Robinson BW, Garlepp MJ. Transfection of the gene for B7-1 but not B7-2 can induce immunity to murine malignant mesothelioma. Int J Cancer 1997;71(3):476-82.
193. Caminschi I, Venetsanakos E, Leong CC, Garlepp MJ, Scott B, Robinson BW. Interleukin-12 induces an effective antitumor response in malignant mesothelioma. Am J Respir Cell Mol Biol 1998;19(5):738-46.
194. Nelson DJ, Mukherjee S, Bundell C, Fisher S, van Hagen D, Robinson B. Tumor progression despite efficient tumor antigen cross-presentation and effective "arming" of tumor antigen-specific CTL. J Immunol 2001;166(9):5557-66.
195. Marzo AL, Lake RA, Lo D, Sherman L, McWilliam A, Nelson D, et al. Tumor antigens are constitutively presented in the draining lymph nodes. J Immunol 1999;162(10):5838-45.
196. Needham DJ, Lee JX, Beilharz MW. Intra-tumoural regulatory T cells: A potential new target in cancer immunotherapy. Biochem Biophys Res Commun 2006;343(3):648-691.
197. Jones E, Dahm-Vicker M, Golgher D, Gallimore A. CD25+ regulatory T cells and tumor immunity. Immunol Lett 2003;85(2):141-3.
198. Sakaguchi S, Sakaguchi N, Shimizu J, Yamazaki S, Sakihama T, Itoh M, et al. Immunologic tolerance maintained by CD25+ CD4+ regulatory T cells: their common role in controlling autoimmunity, tumor immunity, and transplantation tolerance. Immunol Rev 2001;182:18-32.
199. Gilboa E. How tumors escape immune destruction and what we can do about it. Cancer Immunol Immunother 1999;48(7):382-5.
200. Finke J, Ferrone S, Frey A, Mufson A, Ochoa A. Where have all the T cells gone? Mechanisms of immune evasion by tumors. Immunol Today 1999;20(4):158-60.
201. Pawelec G. Tumour escape from the immune response. Cancer Immunol Immunother 2004.
202. Pawelec G. Tumour escape from the immune response: the last hurdle for successful immunotherapy of cancer? Cancer Immunol Immunother 1999;48(7):343-5.
203. Gajewski TF. Identifying and overcoming immune resistance mechanisms in the melanoma tumor microenvironment. Clin Cancer Res 2006;12(7 Pt 2):2326s-2330s.

204. Asseman C, Mauze S, Leach MW, Coffman RL, Powrie F. An essential role for interleukin 10 in the function of regulatory T cells that inhibit intestinal inflammation. Journal of Experimental Medicine 1999;190(7):995-1004.
205. Levings MK, Bacchetta R, Schulz U, Roncarolo MG. The role of IL-10 and TGF-beta in the differentiation and effector function of T regulatory cells. Int Arch Allergy Immunol 2002;129(4):263-76.
206. O'Garra A, Vieira PL, Vieira P, Goldfeld AE. IL-10-producing and naturally occurring CD4+ Tregs: limiting collateral damage. J Clin Invest 2004;114(10):1372-8.
207. Nelson BH. IL-2, regulatory T cells, and tolerance. J Immunol 2004;172(7):3983-8.
208. Malek TR. The main function of IL-2 is to promote the development of T regulatory cells. J Leukoc Biol 2003;74(6):961-5.
209. Furtado GC, Curotto de Lafaille MA, Kutchukhidze N, Lafaille JJ. Interleukin 2 signaling is required for CD4(+) regulatory T cell function. J Exp Med 2002;196(6):851-7.
210. Elia L, Aurisicchio L, Facciabene A, Giannetti P, Ciliberto G, La Monica N, et al. CD4(+)CD25(+) regulatory T-cell-inactivation in combination with adenovirus vaccines enhances T-cell responses and protects mice from tumor challenge. Cancer Gene Ther 2006.
211. Khazaeli MB, Conry RM, LoBuglio AF. Human immune response to monoclonal antibodies. J Immunother 1994;15(1):42-52.
212. Kiessling R, Wasserman K, Horiguchi S, Kono K, Sjoberg J, Pisa P, et al. Tumor-induced immune dysfunction. Cancer Immunol Immunother 1999;48(7):353-62.
213. Maury CP, Teppo AM. Comparative study of serum amyloid-related protein SAA, C-reactive protein, and beta 2-microglobulin as markers of renal allograft rejection. Clin Nephrol 1984;22(6):284-92.
214. de Kleer IM, Wedderburn LR, Taams LS, Patel A, Varsani H, Klein M, et al. CD4+CD25bright regulatory T cells actively regulate inflammation in the joints of patients with the remitting form of juvenile idiopathic arthritis. J Immunol 2004;172(10):6435-43.
215. Elliott MJ, Woo P, Charles P, Long-Fox A, Woody JN, Maini RN. Suppression of fever and the acute-phase response in a patient with juvenile chronic arthritis treated with monoclonal antibody to tumour necrosis factor-alpha (cA2). Br J Rheumatol 1997;36(5):589-93.
216. Leong CC, Robinson BW, Garlepp MJ. Generation of an antitumour immune response to a murine mesothelioma cell line by the transfection of allogeneic MHC genes. Int J Cancer 1994;59(2):212-6.
217. Shi YY, Wang HC, Yin YH, Sun WS, Li Y, Zhang CQ, et al. Identification and analysis of tumour-associated antigens in hepatocellular carcinoma. Br J Cancer 2005;92(5):929-34.
218. Ebato M, Nitta T, Yagita H, Sato K, Okumura K. Skewed distribution of TCR V alpha 7-bearing T cells within tumor-infiltrating lymphocytes of HLA-A24(9)-positive patients with malignant glioma. Immunol Lett 1993;39(1):53-64.
219. Buhaescu I, Segall L, Goldsmith D, Covic A. New immunosuppressive therapies in renal transplantation: monoclonal antibodies. J Nephrol 2005;18(5):529-36.
220. Sterman DH, Albelda SM. Advances in the diagnosis, evaluation, and management of malignant pleural mesothelioma. Respirology 2005;10(3):266-83.
221. Dranoff G. The therapeutic implications of intratumoral regulatory T cells. Clin Cancer Res 2005;11(23):8226-9.

222. Kanamaru F, Youngnak P, Hashiguchi M, Nishioka T, Takahashi T, Sakaguchi S, et al. Costimulation via glucocorticoid-induced TNF receptor in both conventional and CD25+ regulatory CD4+ T cells. J Immunol 2004;172(12):7306-14.
223. Kohm AP, Williams JS, Bickford AL, McMahon JS, Chatenoud L, Bach JF, et al. Treatment with nonmitogenic anti-CD3 monoclonal antibody induces CD4+ T cell unresponsiveness and functional reversal of established experimental autoimmune encephalomyelitis. J Immunol 2005;174(8):4525-34.
224. Mullberg J, Rauch CT, Wolfson MF, Castner B, Fitzner JN, Otten-Evans C, et al. Further evidence for a common mechanism for shedding of cell surface proteins. FEBS Lett 1997;401(2-3):235-8.
225. Karlsson H, Nassberger L. Influence of compounds affecting synthesis, modification and transport of proteins on the expression and release of interleukin-2 receptor. Immunol Cell Biol 1995;73(1):81-8.
226. Kelland LR. Of mice and men: values and liabilities of the athymic nude mouse model in anticancer drug development. Eur J Cancer 2004;40(6):827-36.
227. Bluestone JA, Tang Q. Therapeutic vaccination using CD4+CD25+ antigen-specific regulatory T cells. Proc Natl Acad Sci U S A 2004;101 Suppl 2:14622-6.
228. Shevach EM. Regulatory/suppressor T cells in health and disease. Arthritis Rheum 2004;50(9):2721-4.
229. Krummel MF, Allison JP. CD28 and CTLA-4 have opposing effects on the response of T cells to stimulation. J Exp Med 1995;182(2):459-65.
230. Chattopadhyay S, Chakraborty NG, Mukherji B. Regulatory T cells and tumor immunity. Cancer Immunol Immunother 2005.
231. Roncarolo MG, Bacchetta R, Bordignon C, Narula S, Levings MK. Type 1 T regulatory cells. Immunol Rev 2001;182:68-79.
232. Rutella S, Danese S, Leone G. Tolerogenic dendritic cells: Cytokine modulation comes of age. Blood 2006.
233. Probst HC, McCoy K, Okazaki T, Honjo T, van den Broek M. Resting dendritic cells induce peripheral CD8+ T cell tolerance through PD-1 and CTLA-4. Nat Immunol 2005;6(3):280-6.
234. Ito T, Ueno T, Clarkson MR, Yuan X, Jurewicz MM, Yagita H, et al. Analysis of the role of negative T cell costimulatory pathways in CD4 and CD8 T cell-mediated alloimmune responses in vivo. J Immunol 2005;174(11):6648-56.
235. Hassan R, Bera T, Pastan I. Mesothelin: a new target for immunotherapy. Clin Cancer Res 2004;10(12 Pt 1):3937-42.
236. Thomas AM, Santarsiero LM, Lutz ER, Armstrong TD, Chen YC, Huang LQ, et al. Mesothelin-specific CD8(+) T cell responses provide evidence of in vivo cross-priming by antigen-presenting cells in vaccinated pancreatic cancer patients. J Exp Med 2004;200(3):297-306.
237. Tang Q, Adams JY, Tooley AJ, Bi M, Fife BT, Serra P, et al. Visualizing regulatory T cell control of autoimmune responses in nonobese diabetic mice. Nat Immunol 2006;7(1):83-92.
238. Nakamura K, Kitani A, Fuss I, Pedersen A, Harada N, Nawata H, et al. TGF-beta 1 plays an important role in the mechanism of CD4+CD25+ regulatory T cell activity in both humans and mice. J Immunol 2004;172(2):834-42.
239. Larmonier N, Marron M, Zeng Y, Cantrell J, Romanoski A, Sepassi M, et al. Tumor-derived CD4(+)CD25 (+) regulatory T cell suppression of dendritic cell function involves TGF-beta and IL-10. Cancer Immunol Immunother 2006.

240. Mahnke K, Schmitt E, Bonifaz L, Enk AH, Jonuleit H. Immature, but not inactive: the tolerogenic function of immature dendritic cells. Immunology and Cell Biology 2002;80(5):477-83.
241. Mahnke K, Qian Y, Knop J, Enk AH. Induction of CD4+/CD25+ regulatory T cells by targeting of antigens to immature dendritic cells. Blood 2003;101(12):4862-9.
242. Kuwana M. Induction of anergic and regulatory T cells by plasmacytoid dendritic cells and other dendritic cell subsets. Hum Immunol 2002;63(12):1156-63.
243. D'Cruz LM, Klein L. Development and function of agonist-induced CD25+Foxp3+ regulatory T cells in the absence of interleukin 2 signaling. Nat Immunol 2005;6(11):1152-9.
244. Chen W, Wahl SM. TGF-beta: the missing link in CD4+CD25+ regulatory T cell-mediated immunosuppression. Cytokine Growth Factor Rev 2003;14(2):85-9.
245. Lucas PJ, Kim SJ, Melby SJ, Gress RE. Disruption of T cell homeostasis in mice expressing a T cell-specific dominant negative transforming growth factor beta II receptor. J Exp Med 2000;191(7):1187-96.
246. Chen ML, Pittet MJ, Gorelik L, Flavell RA, Weissleder R, von Boehmer H, et al. Regulatory T cells suppress tumor-specific CD8 T cell cytotoxicity through TGF-beta signals in vivo. Proc Natl Acad Sci U S A 2005;102(2):419-24.
247. Dumont N, Arteaga CL. Transforming growth factor-beta and breast cancer: Tumor promoting effects of transforming growth factor-beta. Breast Cancer Res 2000;2(2):125-32.
248. Sugimoto N, Oida T, Hirota K, Nakamura K, Nomura T, Uchiyama T, et al. Foxp3-dependent and -independent molecules specific for CD25+CD4+ natural regulatory T cells revealed by DNA microarray analysis. Int Immunol 2006;18(8):1197-209.
249. Yamaguchi T, Sakaguchi S. Regulatory T cells in immune surveillance and treatment of cancer. Semin Cancer Biol 2005.
250. Tai X, Cowan M, Feigenbaum L, Singer A. CD28 costimulation of developing thymocytes induces Foxp3 expression and regulatory T cell differentiation independently of interleukin 2. Nat Immunol 2005;6(2):152-62.
251. Bruhl H, Cihak J, Schneider MA, Plachy J, Rupp T, Wenzel I, et al. Dual role of CCR2 during initiation and progression of collagen-induced arthritis: evidence for regulatory activity of CCR2+ T cells. J Immunol 2004;172(2):890-8.
252. Chan CW, Kay LS, Khadaroo RG, Chan MW, Lakatoo S, Young KJ, et al. Soluble fibrinogen-like protein 2/fibroleukin exhibits immunosuppressive properties: suppressing T cell proliferation and inhibiting maturation of bone marrow-derived dendritic cells. J Immunol 2003;170(8):4036-44.
253. Denizot F, Brunet JF, Roustan P, Harper K, Suzan M, Luciani MF, et al. Novel structures CTLA-2 alpha and CTLA-2 beta expressed in mouse activated T cells and mast cells and homologous to cysteine proteinase proregions. Eur J Immunol 1989;19(4):631-5.
254. Yang RY, Hsu DK, Liu FT. Expression of galectin-3 modulates T-cell growth and apoptosis. Proc Natl Acad Sci U S A 1996;93(13):6737-42.
255. Bregant F, Ceschia V, Pacor S, Sava G. Reduction of MCa mammary carcinoma in mice fed with egg-white lysozyme. Pharmacol Res 1990;22 Suppl 3:95-6.
256. Sava G, Benetti A, Ceschia V, Pacor S. Lysozyme and cancer: role of exogenous lysozyme as anticancer agent (review). Anticancer Res 1989;9(3):583-91.
257. Fletcher S, Honeyman K, Fall AM, Harding PL, Johnsen RD, Wilton SD. Dystrophin expression in the mdx mouse after localised and systemic administration of a morpholino antisense oligonucleotide. J Gene Med 2006;8(2):207-16.

258. Moulton HM, Nelson MH, Hatlevig SA, Reddy MT, Iversen PL. Cellular uptake of antisense morpholino oligomers conjugated to arginine-rich peptides. Bioconjug Chem 2004;15(2):290-9.
259. Zheng SG, Wang JH, Stohl W, Kim KS, Gray JD, Horwitz DA. TGF-beta requires CTLA-4 early after T cell activation to induce FoxP3 and generate adaptive CD4+CD25+ regulatory cells. J Immunol 2006;176(6):3321-9.
260. Nocentini G, Riccardi C. GITR: a multifaceted regulator of immunity belonging to the tumor necrosis factor receptor superfamily. Eur J Immunol 2005;35(4):1016-22.
261. Weber T, Lu M, Andera L, Lahm H, Gellert N, Fariss MW, et al. Vitamin E succinate is a potent novel antineoplastic agent with high selectivity and cooperativity with tumor necrosis factor-related apoptosis-inducing ligand (Apo2 ligand) in vivo. Clin Cancer Res 2002;8(3):863-9.
262. Stapelberg M, Gellert N, Swettenham E, Tomasetti M, Witting PK, Procopio A, et al. Alpha-tocopheryl succinate inhibits malignant mesothelioma by disrupting the fibroblast growth factor autocrine loop: mechanism and the role of oxidative stress. J Biol Chem 2005;280(27):25369-76.
263. Neuzil J, Tomasetti M, Mellick AS, Alleva R, Salvatore BA, Birringer M, et al. Vitamin E analogues: a new class of inducers of apoptosis with selective anti-cancer effects. Curr Cancer Drug Targets 2004;4(4):355-72.
264. Neuzil J, Swettenham E, Gellert N. Sensitization of mesothelioma to TRAIL apoptosis by inhibition of histone deacetylase: role of Bcl-xL down-regulation. Biochem Biophys Res Commun 2004;314(1):186-91.
265. Neuzil J, Zhao M, Ostermann G, Sticha M, Gellert N, Weber C, et al. Alpha-tocopheryl succinate, an agent with in vivo anti-tumour activity, induces apoptosis by causing lysosomal instability. Biochem J 2002;362(Pt 3):709-15.
266. Neuzil J, Weber T, Schroder A, Lu M, Ostermann G, Gellert N, et al. Induction of cancer cell apoptosis by alpha-tocopheryl succinate: molecular pathways and structural requirements. Faseb J 2001;15(2):403-15.
267. Weber T, Dalen H, Andera L, Negre-Salvayre A, Auge N, Sticha M, et al. Mitochondria play a central role in apoptosis induced by alpha-tocopheryl succinate, an agent with antineoplastic activity: comparison with receptor-mediated pro-apoptotic signaling. Biochemistry 2003;42(14):4277-91.
268. Quillet-Mary A, Jaffrezou JP, Mansat V, Bordier C, Naval J, Laurent G. Implication of mitochondrial hydrogen peroxide generation in ceramide-induced apoptosis. J Biol Chem 1997;272(34):21388-95.
269. Wang XF, Dong L, Zhao Y, Tomasetti M, Wu K, Neuzil J. Vitamin E analogues as anticancer agents: lessons from studies with alpha-tocopheryl succinate. Mol Nutr Food Res 2006;50(8):675-85.
270. Sotomayor EM, Borrello I, Tubb E, Allison JP, Levitsky HI. In vivo blockade of CTLA-4 enhances the priming of responsive T cells but fails to prevent the induction of tumor antigen-specific tolerance. Proc Natl Acad Sci U S A 1999;96(20):11476-81.
271. Uraushihara K, Kanai T, Ko K, Totsuka T, Makita S, Iiyama R, et al. Regulation of murine inflammatory bowel disease by CD25+ and CD25- CD4+ glucocorticoid-induced TNF receptor family-related gene+ regulatory T cells. J Immunol 2003;171(2):708-16.
272. Jacobs MR, Hornfeldt CS. Melaleuca oil poisoning. J Toxicol Clin Toxicol 1994;32(4):461-4.
273. Abe S, Maruyama N, Hayama K, Inouye S, Oshima H, Yamaguchi H. Suppression of neutrophil recruitment in mice by geranium essential oil. Mediators Inflamm 2004;13(1):21-4.

274. Del Beccaro MA. Melaleuca oil poisoning in a 17-month-old. Vet Hum Toxicol 1995;37(6):557-8.
275. Morris MC, Donoghue A, Markowitz JA, Osterhoudt KC. Ingestion of tea tree oil (Melaleuca oil) by a 4-year-old boy. Pediatr Emerg Care 2003;19(3):169-71.
276. Calcabrini A, Stringaro A, Toccacieli L, Meschini S, Marra M, Colone M, et al. Terpinen-4-ol, the main component of Melaleuca alternifolia (tea tree) oil inhibits the in vitro growth of human melanoma cells. J Invest Dermatol 2004;122(2):349-60.
277. Giordani C, Molinari A, Toccacieli L, Calcabrini A, Stringaro A, Chistolini P, et al. Interaction of tea tree oil with model and cellular membranes. J Med Chem 2006;49(15):4581-8.
278. Pelleitier M, Montplaisir S. The nude mouse: a model of deficient T-cell function. Methods Achiev Exp Pathol 1975;7:149-66.
279. Ramanathapuram LV, Hahn T, Graner MW, Katsanis E, Akporiaye ET. Vesiculated alpha-tocopheryl succinate enhances the anti-tumor effect of dendritic cell vaccines. Cancer Immunol Immunother 2006;55(2):166-77.
280. Sharma G, Anabousi S, Ehrhardt C, Ravi Kumar MN. Liposomes as targeted drug delivery systems in the treatment of breast cancer. J Drug Target 2006;14(5):301-10.
281. Kawarada Y, Ganss R, Garbi N, Sacher T, Arnold B, Hammerling GJ. NK- and CD8(+) T cell-mediated eradication of established tumors by peritumoral injection of CpG-containing oligodeoxynucleotides. J Immunol 2001;167(9):5247-53.
282. Garbi N, Arnold B, Gordon S, Hammerling GJ, Ganss R. CpG motifs as proinflammatory factors render autochthonous tumors permissive for infiltration and destruction. J Immunol 2004;172(10):5861-9.
283. Dezfouli S, Hatzinisiriou I, Ralph SJ. Enhancing CTL responses to melanoma cell vaccines in vivo: synergistic increases obtained using IFNgamma primed and IFNbeta treated B7-1+ B16-F10 melanoma cells. Immunol Cell Biol 2003;81(6):459-71.
284. Casares N, Arribillaga L, Sarobe P, Dotor J, Lopez-Diaz de Cerio A, Melero I, et al. CD4+/CD25+ regulatory cells inhibit activation of tumor-primed CD4+ T cells with IFN-gamma-dependent antiangiogenic activity, as well as long-lasting tumor immunity elicited by peptide vaccination. J Immunol 2003;171(11):5931-9.
285. Kudo-Saito C, Schlom J, Camphausen K, Coleman CN, Hodge JW. The requirement of multimodal therapy (vaccine, local tumor radiation, and reduction of suppressor cells) to eliminate established tumors. Clin Cancer Res 2005;11(12):4533-44.
286. Leigh J, Davidson P. Malignant Mesothelioma in Australia, 1945-2000. Am J Ind Med 2002;41(3):188-201.
287. Murthy SS, Testa JR. Asbestos, chromosomal deletions, and tumor suppressor gene alterations in human malignant mesothelioma. J Cell Physiol 1999;180(2):150-7.
288. Altomare DA, Vaslet CA, Skele KL, De Rienzo A, Devarajan K, Jhanwar SC, et al. A mouse model recapitulating molecular features of human mesothelioma. Cancer Res 2005;65(18):8090-5.
289. Kane AB. Animal models of malignant mesothelioma. Inhal Toxicol 2006;18(12):1001-4.
290. Barnett B, Kryczek I, Cheng P, Zou W, Curiel TJ. Regulatory T cells in ovarian cancer: biology and therapeutic potential. Am J Reprod Immunol 2005;54(6):369-77.
291. Suntharalingam G, Perry MR, Ward S, Brett SJ, Castello-Cortes A, Brunner MD, et al. Cytokine storm in a phase 1 trial of the anti-CD28 monoclonal antibody TGN1412. N Engl J Med 2006;355(10):1018-28.